Development of New Therapeutic Strategies for Sporadic Inclusion Body Myositis

A thesis submitted to the University of London
For the degree of Doctor of Philosophy

By

Dr Adrian Dimitri Miller
MA (Cantab) MB BChir MRCP

MRC Centre for Neuromuscular Diseases
Institute of Neurology
University College London

2015

Declaration

I, Adrian Miller, confirm that the work presented in this thesis is my own. Where information has been derived from other sources, I confirm that this has been indicated in the thesis.

Acknowledgements

I am indebted to numerous people who provided various types of assistance during the conduct of this work. First and foremost, I am indebted to the patients who devoted considerable time and courage to participate in the clinical work described in this thesis. Throughout the period of this project, I was struck by the selfless determination and enthusiasm of the patients attending the IBM clinic at Queen Square to furthering our understanding of this disabling and incurable disease.

I am particularly grateful for the patient guidance and encouragement of my supervisors, Linda Greensmith and Mike Hanna throughout this work. I thank my friends and colleagues in Linda's laboratory, who were consistently entertaining, helpful and extremely tolerant of the limitations of a clinician in the scientific environment.

The establishment of the Arimoclomol clinical trial was a highly informative and challenging task, which would not have been possible without the energetic help of Gisela Barreto, Pedro Machado, the biomedical research unit at UCL and the trial team at the US site in Kansas City. I am also grateful to the staff of the department of neuropathology at NHNN, particularly Janice Holton, who assisted greatly with ensuring expert handling and interpretation of the trial tissue.

I thank Aarti, who became my wife during the course of this work and whose incredible energy I rely upon so heavily. Finally, I thank our daughter Amari, who represents the greatest happiness and inspiration I could imagine.

Abstract

Sporadic inclusion body myositis (IBM) is the commonest myopathy acquired after 50 years of age and causes significant disability. No effective treatment exists despite several clinical trials of immunotherapies. This reflects a lack of pre-clinical disease models. The work described in this thesis began with development of such a system, in which disease relevant pathological outcome measures were characterised *in vitro* using primary satellite cell cultures. Through over-expression of β-Amyloid Precursor Protein or exposure to inflammatory mediators IL1β and TNFα, IBM-like pathology was induced. Myotubes demonstrated ubiquinated intracellular aggregates, increased expression of MHC Class I, cytoplasmic translocation of TDP-43, ER stress, calcium dyshomeostasis and activation of NFκB. As some of these are proposed to be central pathogenic mechanisms in IBM, they provide a panel of tools on which to assess new IBM treatment strategies.

The effects of heat shock response augmentation were examined using Arimoclomol, a co-inducer of the transcription factor HSF-1 that drives expression of key endogenous Heat Shock Proteins. Arimoclomol treatment ameliorated several IBM-relevant features, represented by improved cell viability, reduced ER stress, inhibition of NFκB and reduced cytoplasmic translocation of TDP-43.

These data supported further evaluation of HSR manipulation as a potential therapy for IBM. Therefore, Arimoclomol was advanced into a randomised, placebo-controlled clinical trial involving 24 patients with IBM over one year. The primary outcome measure was safety and tolerability. Muscle biopsy was performed before and after the treatment phase to evaluate HSP expression and histopathological changes.

Together, this *in vitro* model and clinical trial represent a novel translational research pathway in IBM, the lack of which has hampered the development of effective treatments for this disease.

Table of Contents

List of Figures

List of Tables

Abbreviations

ACTN3	Alpha-actinin skeletal muscle isoform 3
AE	Adverse Event
ALS	Amyotrophic lateral sclerosis
ANOVA	Analysis of variance
APP	Amyloid precursor protein
ATF	Activating transcription factor
ATP	Adenosine triphosphate
Aβ40/42	Amyloid-β 40/42
BACE	Beta-secretase 1
BiP	Binding immunoglobulin protein
C5N1A	Cytosolic 5'-nucleotidase 1A
C9orf72	Chromosome 9 open reading frame 72
Ca^{2+}	Calcium
Ca^{2+}_{Cyto}	Cytosolic Calcium concentration
Ca^{2+}_{ER}	ER Calcium Concentration
CCL	Chemokine 'CC-motif' ligand
CD	Cluster of differentiation
CHOP	CCAAT/enhancer-binding protein homologous protein
CK	Creatine kinase
CMT	Charcot Marie Tooth disease
COX	Cytochrome c oxidase
CXCL	Chemokine 'CXC-motif' ligand
DAPI	4',6-diamidino-2-phenylindole
DEXA	Dual energy X-ray absorptiometry
DM	Dermatomyositis
DMEM	Dulbecco's modified eagle medium
DNA	Deoxyribonucleic acid
ECG	Electrocardiography
eIF2	Eukaryotic initiation factor 2
ELISA	Enzyme linked immunosorbence assay
EMG	Electromyography

ENMC	European Neuromuscular Centre
EOR	Endoplasmic reticulum overload response
ER	Endoplasmic reticulum
ERAD	Endoplasmic reticulum associated degradation
EV	Empty vector (transfection)
FACS	Fluorescence activated cell sorting
FCS	Fetal calf serum
FDP	Flexor digitorum profundus
FDS	Flexor digitorum sublimis
FSHD	Faciascapulohumeral dystrophy
FTD	Frontotemporal dementia
GADD	Growth arrest and DNA-damage-inducible protein
GAPDH	Glyceraldehyde 3-phosphate dehydrogenase
GRP	Glucose regulated protein
hIBM	Hereditary inclusion body myositis
HLA	Human leukocyte antigen
HRP	Horseradish peroxidase
HS	Horse serum
HSF	Heat shock factor
HSP	Heat shock protein
HSR	Heat shock response
HTLV	Human T-lymphocytic virus
IBM	Sporadic inclusion body myositis
IBMFRS	Inclusion Body Myositis Functional Rating Scale
IBMPFTD	Inclusion body myositis with Paget's disease and Frontotemporal dementia
IFN	Interferon
IKK	Inhibitor of nuclear factor kappa-B kinase
IL1	Interleukin 1
IMP	Investigational Medicinal Product
IP3	Inositol trisphosphate
IRE	Inositol-requiring enzyme
LBM	Lean body mass

LDH	Lactate dehydrogenase
MFM	Myofibrillar myopathy
MHC	Major histocompatibility complex
MHRA	Medicines and Healthcare Regulatory Agency
MMT	Manual muscle testing
MND	Motor neuron disease
MRC	Medical Research Council
MRI	Magnetic resonance imaging
mtDNA	Mitochondrial deoxyribonucleic acid
MTT	3-(4,5-Dimethylthiazol-2-yl)-2,5-diphenyltetrazolium bromide
MVICT	Maximal voluntary isometric contraction testing
MYBPC	Myosin-binding protein-C
NCAM	Neural cell adhesion molecule
NFκB	Nuclear factor kappa-B
NHNN	National Hospital for Neurology and Neurosurgery
NOS	Nitric oxide synthase
PBS	Phosphate buffered saline
PE	Phycoerythrin
PERK	Pancreatic endoplasmic reticulum kinase
PI	Propidium iodide
PM	Polymyositis
POLG	Polymerase gamma
RNA	Ribonucleic acid
RNP	Ribonucleoprotein
ROI	Region of interest
ROS	Reactive oxygen species
RyR	Ryanodine Receptor
SAE	Serious Adverse Event
SD	Standard deviation
SDS	Sodium dodecyl sulfate
SEM	Standard error of the mean
SERCA	Sarco/endoplasmic reticulum ATPase

SNAP	Sural nerve action potential
SOD	Superoxide dismutase
SR	Sarcoplasmic reticulum
STIM1	Stromal interacting molecule 1
TDP-43	Tar dna binding protein 43
TGF	Transforming growth factor
TMB	Tetramethylbenzidine
TMRM	Tetramethylrhodamine, methyl ester
TNF	Tumour necrosis factor
TRIS	Tris(hydroxymethyl)aminomethane
UCL	University College London
UPR	Unfolded protein response
VCP	Valosin containing protein
XBP	X-box binding protein
ZASP	Z-disc associated protein

Chapter 1: General Introduction

1.1 Preface

Sporadic Inclusion Body Myositis (IBM) represents a host of clinical and scientific challenges in the field of neuromuscular diseases. Despite being the commonest myopathy acquired after the age of fifty years, the condition remains without effective management. As a result, most patients suffer progressive limb weakness and significant disability (Dalakas 2006). Traditionally classified with the primary myositides, Polymyositis (PM) and Dermatomyositis (DM), yet appearing clinically more similar to degenerative conditions such as Motor Neuron Disease (MND), IBM's mystery is represented by a divided literature.

The lack of treatment for IBM reflects several deficiencies in our understanding of and approach to the disease. Most fundamentally, the pathogenesis of IBM is enigmatic, comprising a plethora of interlinking processes and cascades, the initial trigger of which remains elusive. Even the significance of individual downstream pathological elements is debated and it follows that no coordinated translational research programme in IBM has yet been established. Rather, a series of small, typically underpowered, clinical trials represents the unsuccessful effort to develop a therapeutic strategy. A more robust foundation requires a panel of preclinical models in which a selection of relevant pathological outcome measures are characterised, on which potential treatments can be evaluated. To advance promising agents towards the clinic, a large and well characterised patient population, diagnosed according to widely accepted criteria, is essential. Validated clinical outcome measures are then required to determine the number of participants and duration required of future clinical trials.

This thesis represents one theme in such a proposed framework of translational research in IBM. It is introduced by a consideration of existing IBM literature, through which various pathogenic and clinical priorities were determined and applied to the subsequent experiments. Throughout the process, the overriding

focus was to achieve the most efficient and effective programme for translation of the basic science towards meaningful clinical differences for patients.

1.2 Clinical description of IBM

1.2.1 Epidemiology

In clinical practice, IBM remains an undefined entity since the two generally accepted diagnostic criteria are not consistently applied and do not reflect all advances in histopathological findings during the past ten years. For example, the most commonly used Griggs' criteria frequently require the application of electron microscopy, which is not routinely performed in even specialist clinical neuropathology departments in Europe, or electromyography, which is not routinely performed on suspected IBM cases in most countries. Therefore, it can be difficult to distinguish IBM from other myopathies that display an inflammatory infiltrate, notably PM. This may prevent refinement of a descriptive diagnosis of 'myositis', particularly in cases without a stereotypical clinical presentation. Furthermore, the reasonable histological characterisation of IBM as a 'Polymyositis-plus' condition means that misdiagnosis of PM is extremely common where insufficiently detailed analysis of the biopsy has been performed. Indeed, it has been estimated that IBM is the initial diagnosis in only 16% of subsequently confirmed IBM cases, with the most frequent first diagnosis being PM in 18% (Badrising et al. 2000). The outdated Bohan and Peter criteria, which do not exclude IBM, are still employed to diagnose PM (Bohan et al. 1975). This contributes to the likely underestimation of the true prevalence of IBM. There is further ascertainment bias from the unstructured distribution of patients with myositis among primary care physicians, rheumatologists and neurologists, the delay between presentation and diagnosis and the potential overlap of the mild end of the IBM disease spectrum with weakness attributed to the sarcopenia of ageing. Conversely, factors that may contribute towards overestimation of the prevalence of IBM include the lack of routine screening for myofibrillar myopathies (MFMs) and other genetic causes, in addition to the lack of routine neurophysiology, precluding detection

of slowly progressive motor neuron disease (MND). Overall, however, it appears most likely that IBM remains under diagnosed.

There have been relatively few large epidemiological studies of IBM. Nevertheless, these suggest IBM is the commonest muscle disease acquired after the age of 50 years and represents at least 28% of all inflammatory myopathies (Lotz et al. 1989). One national study of IBM epidemiology in the Netherlands estimated a prevalence of 16 x 10^{-6} among inhabitants aged over 50 years, and 4.9 x 10^{-6} among the general population (Badrising et al. 2000). However, this estimation was based on a sample of only 76 living patients, of which a small alteration would have produced a substantial difference in the final estimate. Indeed, the variation between 0 and 9.3 per million of the population in the twelve provinces of the Netherlands reveals the magnitude of the potential sampling error. Wilson and colleagues estimate the prevalence of IBM in Olmsted County, Minnesota at 71 x 10^{-6} and PM at 34.5 x 10^{-6} (Wilson et al. 2008). This reflects an IBM sample of only 9 patients, using the stricter Griggs' diagnostic criteria. A further regional study in Western Australia also included patients meeting Griggs' criteria and identified 17 patients, giving an overall prevalence of 9.3 x 10^{-6}, adjusted to 35.3 x 10^{-6} among those aged over 50 years (Phillips et al. 2000). In summary, previous epidemiological studies of IBM have been small and yielded substantially different estimations of the true disease prevalence. In a large part, this reflects the use of diagnostic criteria that are likely to exclude a significant number of patients whose biopsy did not fulfill a considerable set of histological features. This may have excluded patients in the early stages of the disease, where such features have not yet developed.

A consistent finding in epidemiological studies of IBM is a male preponderance, the magnitude of which may be between two and four male cases for each female case (Cox et al. 2011). The increased prevalence of IBM with greater age, particularly over 50 years, is also consistent (Dalakas 2006). Together, the apparent susceptibility of elderly males to IBM is notably inconsistent with the young female population typical affected by autoimmune conditions, and more in keeping with a degenerative disease.

Finally, considerable time typically separates symptoms at onset and a biopsy-confirmed diagnosis. Engel's study of 64 patients reported this delay as 5.9 years (SD ±4.4) (Chahin et al. 2008). This is likely to reflect a combination of the slow progression of the disease, initial misdiagnosis and limitations of ability to apply diagnostic criteria.

1.2.2 Clinical features

The hallmark of IBM is slowly progressive weakness of forearm flexor and quadriceps muscles. This clinical pattern, reflecting involvement of the distal upper limbs and proximal lower limbs, is a relatively unusual one for other neuromuscular conditions and represents an important early indicator to the diagnosis (Hilton-Jones et al. 2010). Specifically, this contrasts with PM, in which patients typically demonstrate predominantly proximal weakness (Chahin et al. 2008). The deep tendon reflexes are frequently reduced or absent, which is consistent with a chronic myopathy.

There have been relatively few phenotypic studies of IBM and these are discrepant, reflecting the use of different diagnostic inclusion criteria and the inter- or intra-investigator variability of the Medical Research Council (MRC) score of limb power.

Until 2008, the largest single centre natural history study of IBM was that by Lotz, in 1989, of forty consecutive patients with electromicroscopically confirmed diagnosis (Lotz et al. 1989). All patients described weakness at onset and at diagnosis. The second commonest symptom was dysphagia, affecting four patients at onset and sixteen by the point of diagnosis. Fatigue, muscle pain and paraesthesia were less common. Interestingly, contrasting with the phenotypic stereotype, this study describes biceps and triceps as the predominantly affected muscles, in which weakness was detected in approximately half of all patients.

In 2008, Chahin and Engel described a cohort of 64 patients with IBM, 27 patients with PM and 16 patients in whom either diagnosis remained a possibility. 55 of the 64 IBM patients displayed selective weakness of

quadriceps and finger flexors. Of the remaining 9 patients, 8 had selective quadriceps weakness and one had selective finger flexor weakness. Tellingly, 14 of the 16 indeterminate cases resembled IBM clinically from the beginning of their illness and the remaining two developed an IBM phenotype within two years of onset (Chahin et al. 2008). This concept of a clinically defined population, who may not yet demonstrate sufficient pathological features to achieve a pathologically defined diagnosis, has been highlighted as potentially important subgroup with respect to understanding IBM and planning of clinical trials since these patients may be the most likely to respond to treatment (Hilton-Jones et al. 2010).

35 patients were described in a study by Felice (Felice et al. 2001), which also confirmed weakness as the commonest symptom, with 54% also suffering dysphagia. Interestingly, 43% of patients were felt to have facial weakness, which is considered an atypical feature. All patients demonstrated atrophy of the anterior thigh and 91% of the forearm flexor compartment. This corresponded with the characteristic features of this population being weakness of quadriceps, long finger flexors and ankle extensors.

Badrising and colleagues reported a national population of 64 IBM patients from the Netherlands (Badrising et al. 2000). This largely supports the findings of the others studies, with 63% of patients describing quadriceps weakness as their first symptom, followed by 14% who first noted finger flexion weakness. The authors provided a detailed and interesting breakdown of MRC strength scores on examination of all muscle groups (Fig 1.1). This confirmed that knee extension was the commonest region of weakness and, importantly, was normal in only a fraction of patients. Elbow flexors and the deep finger flexors were the next commonest affected respectively. Examination of these data supports the notion that the combination of weak knee extension (quadriceps), which exceeds weakness of hip flexion (iliopsoas), and weak grip is highly consistent with a diagnosis of IBM. Similar to the study by Felice, 41% of patients demonstrated mild symmetrical facial weakness. Outside these muscles, it is evident that weakness does extend considerably; IBM is not specific to certain muscles, rather some muscles appear to be more severely affected than others.

Primary muscle disorders are often characterised by a symmetrical severity and IBM is again atypical in this respect, with the majority of patients demonstrating asymmetrical weakness (Felice et al. 2001).

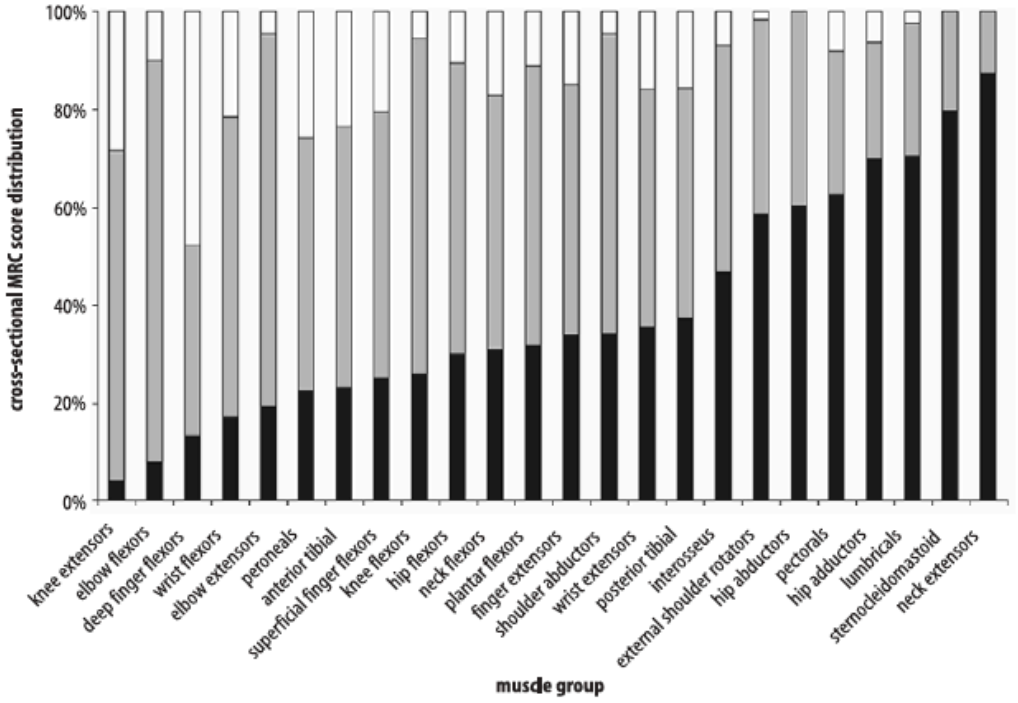

Figure 1.1 Distribution of weakness in IBM by MRC score

From (Badrising et al. 2005). Examination of the distribution of weakness in this cohort of 64 patients supports the stereotypical description of IBM's predilection for knee extensors and deep finger flexors, although a small number of patients demonstrate normal power in these groups. The data highlight that the differential involvement of muscles occurs along a fairly smooth spectrum rather than a binary fashion. In notable contrast to the clinically similar condition, Amyotrophic Lateral Sclerosis, the neck extensors were not weak in any patient. Black = MRC grade 5 (full power), Grey = MRC grade 4 (weakness when resistance is applied), White = MRC grades ≤3 (marked weakness, evident without resistance).

The steadily progressive nature of symptoms is a consistent feature of IBM and this typically leads to the accumulation of disability. In one representative natural history study, 63% could not ambulate independently after 7 years and

mean duration until wheelchair dependency was approximately 15 years (Cortese et al. 2013). This reflects an annual decline of muscle strength, as estimated over a period of 12 years in the longest examined single cohort, of 3.5% by manual muscle testing or 5.4% by quantitative muscle testing (Cox et al. 2011).

Neuromuscular respiratory insufficiency is not a typical feature of IBM, differentiating it from MND (Hardiman et al. 2011). Respiratory symptoms are more likely to represent aspiration consequent to dysphagia which explains why pneumonia is the commonest cause of death in IBM (Felice et al. 2001). Life expectancy *per se* does not appear to be significantly reduced (Cox et al. 2011).

1.2.3 Associated conditions

In keeping with the aetiological hypothesis that IBM is an autoimmune condition, considerable attention has focused on its associations with other autoimmune disorders. The epidemiological study by Lotz observed autoimmune diseases in 6 of the 40, or 15% of patients (Lotz et al. 1989). However, one of these conditions was Dermatomyositis, implying lack of diagnostic clarity, and two were idiopathic interstitial pneumonitis, of which the possible primary causes include many non-immune conditions. Of note were the 11 patients who demonstrated evidence of peripheral neuropathy. In 3 patients, this was attributed to diabetes mellitus. The study by Felice did not suggest strong associations between IBM and other conditions. The commonest concurrent medical problem was hypertension, affecting 37% of patients, consistent with the expected prevalence in this age group. Autoimmune conditions were rare, affecting only 4 patients (Felice et al. 2001). Chahin and Engel's cohort detected coexistent autoimmune disease in 8 of 64 IBM patients, or 12.5%, compared with 4 of 27 PM patients, or 14.8%. These included Hashimoto thyroiditis, coeliac disease, Sjögren's syndrome, rheumatoid arthritis and ocular myasthenia gravis (Chahin et al. 2008). Contrasting with adult onset DM, in which associated malignancy must be assumed until disproven, no clear association exists between malignancy and IBM (Lotz et al. 1989).

There are also reported cases in which IBM has been proposed to arise from the presence of another immune condition. A potential viral trigger has long been considered, with one case adenovirus type 2 being detected in the muscle a patient with IBM and further case of mumps virus antigen (Mikol et al. 1982; Chou 1986). Indeed, Chou suggested that the cytoplasmic and intranuclear inclusion bodies of IBM represent nucleocapsids of mumps viral infection. Interestingly, he also noted the similarity of these intranuclear bodies with those observed in osteoclasts affected by Paget's disease of bone. This condition can be caused by mutations of Valosin-containing-protein (VCP) in which it coexists with Frontotemporal dementia and an inclusion body myopathy. A viral hypothesis for sporadic IBM is also supported by Dalakas, who described four cases of IBM that appeared to follow infection with human immunodeficiency virus in which there viral specific clonal expansion of cytotoxic $CD8^+$ T-cells (Dalakas et al. 2007). However, the potential contribution of antiretroviral mediated mitochondrial toxicity should also be borne in mind. Similar rare observations of an IBM-like myopathy have been made in cases of human T-lymphocytic virus type 1 (HTLV-1) infection (Ozden et al. 2001).

1.2.4 Genetic predisposition

To date, no large exome sequencing or genome wide association studies have been undertaken in sporadic IBM. Smaller studies have revealed genetic associations with inflammatory and degenerative connotations. HLA genes represent the most widely studied area, revealing association with the DRβ1*0301 and DQβ1*0201 alleles (Koffman et al. 1998). The B8-DR3-DR52-DQ2 haplotype is detected in a similar proportion of patients with IBM and the autoimmune condition myasthenia gravis and correlates with earlier disease onset (Badrising et al. 2004). Apolipoprotein E4, which has strong links with susceptibility to Alzheimer's disease, also appears to associate with IBM (Garlepp et al. 1995).

A distinct group of conditions termed hereditary IBMs (hIBMs), demonstrate considerable phenotypic or histological distinction from sporadic IBM. Nonaka

or 'GNE' myopathy (hIBM2) follows mutations of UDP-N-Acetylglucosamine 2-Epimerase/N-Acetylmannosamine kinase (GNE) on chromosome 9. Patients tend not to display quadriceps weakness, which is almost uniform in sporadic IBM. The condition originally referred to as hIBM1, which is a vacuolar myopathy that does manifest with quadriceps weakness has since been reclassified as a myofibrillar myopathy (MFM) due to mutations of desmin.

Autosomal dominant mutations of VCP/p97 on chromosome 9 produce IBM with Paget's disease of bone and Frontotemporal dementia (IBMPFD). This disorder demonstrates some similar pathological characteristics to sporadic IBM, including formation of cytoplasmic proteinaceous aggregates and upregulation of NFκB. However, it lacks a pronounced endomysial inflammatory infiltrate. Furthermore, the clinical phenotype, in addition to its earlier age of onset, is typically different to sporadic IBM; that cranial nerve territories are often significantly affected, individual limb weakness is typically proximal and distal, and mortality is far higher (Watts et al. 2007).

The myofibrillar myopathies (MFMs) are, anecdotally, the commonest group of genetic myopathies that mimic IBM. This highlights the importance of including a minimum age of onset within diagnostic criteria, until the spectrum of genes causing MFM is fully determined. The MFMs are currently known to reflect mutations of desmin, αB-cystallin, myotillin, ZASP, filamin C and BAG-3 genes, referred to as MFM 1-6 respectively. None has been routinely detected in a cohort of sporadic IBM patients.

1.2.5 Laboratory abnormalities

Any rise in creatine kinase is conspicuously moderate in IBM cases, contrasting with several other myopathies, notably PM (Machado et al. 2009). Indeed, even a normal CK value is consistent with a diagnosis of IBM. Interpretation of particular values is limited due to variability in normal ranges between laboratories and ethnic groups. One study of 40 cases of IBM described a range between 23 and 605 IU/ml, with a mean value of 199.7 IU/ml for males and 189.6 IU/ml for females (Lotz et al. 1989). In a further cohort, 17 of 63 patients with IBM were found to have a normal CK and the mean CK at diagnosis was

three to four times greater among patients with PM than those with IBM (Chahin et al. 2008).

1.2.6 Neurophysiology

There is anecdotal evidence in the field that IBM patients display abnormal neurophysiological readings in addition to the short duration motor unit potentials and polyphasic potentials that are demonstrated in various inflammatory myopathies. One study of 35 patients described abnormal nerve conduction studies in 43%, reflecting 23% with sensorimotor axonal polyneuropathy and 20% with absent lower extremity SNAPs (Felice et al. 2001). Although some of this may reflect age related changes, the consistency of abnormal neurophysiology in IBM is notable and could indicate a neuropathic element that has not yet been fully characterised.

1.2.7 Imaging

Relative to diseases of the central nervous system, the role of imaging in neuromuscular conditions is limited. Indeed, radiological investigations are not yet routinely performed in the diagnosis or evaluation of IBM. The basis of the particular distribution of IBM, and indeed other myopathies, remains unclear. The detailed anatomical description afforded by MRI can directly indicate which muscles appear more susceptible to the pathological processes involved. Studies of magnetic resonance imaging (MRI) in IBM have yielded interesting results and largely support the phenotypic distribution suggested clinically, including asymmetrical muscle involvement.

Muscles affected by IBM demonstrate signal hyperintensity on T1-weighted sequences and T2-weighted sequences with fat suppression, such as short tau inversion recovery (STIR). This is thought to represent intramuscular fat accumulation and the presence of fluid, as inflammatory oedema, respectively (Machado et al. 2014). In contrast, cases of PM tend to demonstrate purely muscle oedema, which is typically restricted to more proximal groups (Dion et

al. 2002; Cantwell et al. 2005). In DM, unlike either PM or IBM, inflammation is apparent in fascia and subcutaneous fat (Garcia 2000).

Phillips reported a study of 9 patients with IBM, in whom there appeared a strong correlation between clinical weakness and changes of proton-density images or mean T2 relaxation time of the quadriceps and hamstring muscles (Phillips et al. 2001). Radiologically, quadriceps was the most commonly severely affected muscle group, often asymmetrically, and was abnormal in 7 of 9 patients. Further, in keeping with the clinical findings, flexor digitorum profundus (FDP) was radiologically abnormal in the same number of patients, three of whom showed no coexistent involvement of adjacent muscle flexor digitorum sublimis (FDS). This pattern is consistent with the findings of Sekul and colleagues who found MRI of the forearm to reveal marbled brightness of FDP in 20 of 21 subjects, again with sparing of FDS even late in the disease course (Sekul et al. 1997).

The largest single study of MRI in IBM to date was reported by Cox and colleagues. Here, 32 patients with IBM were evaluated, all of whose imaging demonstrated abnormalities, the commonest of which was fatty infiltration of muscle. This number of muscles displaying this feature correlated with the clinical duration of the disease. In the forearm, FDP was preferentially affected, sometimes in isolation, and was abnormal in three quarters of patients. In the lower limb, and overall, vastus lateralis and the medial head of gastrocnemius were the most consistently abnormal muscles. There was relative sparing of rectus femoris, hamstrings and adductor muscles (Cox et al. 2011).

Interestingly, the majority of previous MRI studies in IBM also detected signal abnormalities of the medial head of gastrocnemius. This does not typically manifest clinically, presumably due to the lack of involvement of other muscles responsible for ankle plantarflexion such as soleus and the lateral head of gastrocnemius. However, this muscle can appear radiologically abnormal in a range of neuropathic and myopathic conditions (Wattjes et al. 2010; Sinclair et al. 2012). Two studies demonstrated relative sparing of the quadriceps muscle rectus femoris

MRI offers considerable practical advantages over muscle strength testing and tissue biopsy as a potential outcome measure in clinical trials. Quantitative methods of muscle MRI are, accordingly, being explored in this context and have been validated in populations of healthy volunteers (Morrow et al. 2014). Intramuscular fat accumulation, for example, can be quantified using the three-point Dixon sequence (Glover et al. 1991) and appears to correlate inversely with strength of knee extension in IBM patients (Morrow 2011).

1.3 Pathological abnormalities

The formal diagnosis of IBM continues to rest upon on histological evidence and, indeed, it is histology that provided the first insight into the range of pathological processes IBM represents (Fig 1.2). Biopsy remains particularly useful in distinguishing IBM from PM. The histopathological changes may be broadly divided into those with represent either inflammatory or degenerative processes, a divide which reflects the debate on the underlying aetiology of IBM.

1.3.1 Inflammation

IBM's traditional classification alongside PM and DM as an inflammatory myositis rests upon the frequent demonstration of endomysial infiltration by immune cells. This pattern largely mimics that observed in PM rather than DM, in which the inflammation is predominantly perivascular. There is widespread upregulation of MHC Class I, which is not normally expressed by skeletal muscle, along with infiltration of non-necrotic fibres by predominantly $CD8^+$ cytotoxic T-cells, which are clonally expanded. This contrasts with the chiefly $CD4^+$ T-cell infiltrate that characterise DM (Dalakas 2006). It is proposed that myofibres may act as antigen presenting cells. Costimulatory molecules BB1 and inducible costimulator ligand are upregulated and there is colocalisation of such molecule with cytotoxic T-cells (Murata et al. 1999; Schmidt et al. 2004). The secretion by myofibres of proinflammatory cytokines, such as IL1β, and chemokines, such as CXCL-9, likely attract and perpetuate the T-cell response (De Bleecker et al. 2002).

The upregulation of MHCI in IBM, detectable by immunohistochemistry, extends to fibres that appear otherwise normal and the absence of this feature raises

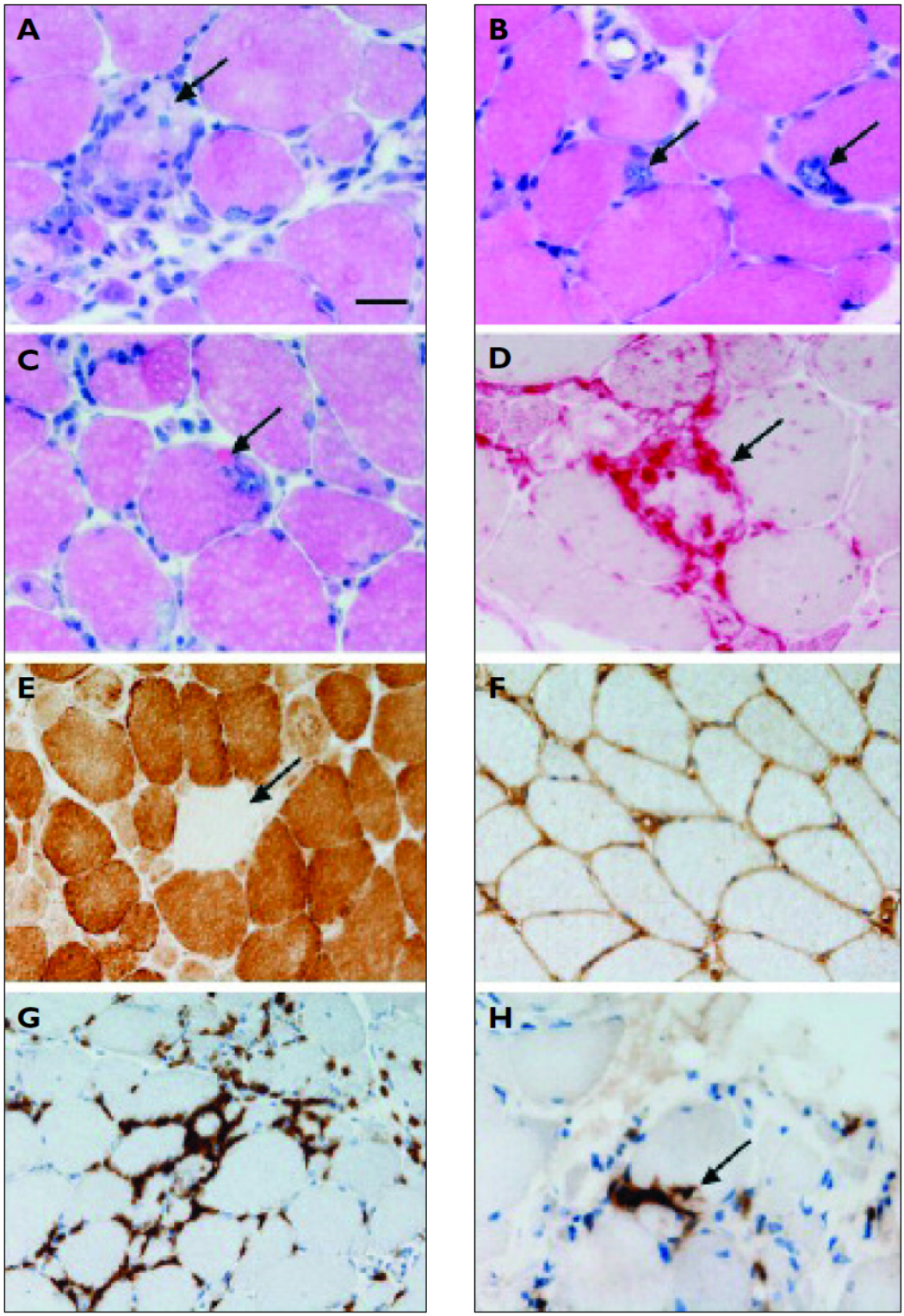

Figure 1.2 Histopathological features of IBM

In haematoxylin and eosin stained sections there may be variation in fibre diameter (A) and fibre necrosis (arrow in A). Vacuoles rimmed by basophilic

granular material are seen (arrows in B) and are sometimes associated with hyalinised eosinophilic inclusions (arrow in C). Fibre necrosis can be confirmed using the acid phosphatase histochemical preparation (D). Fibres lacking cytochrome oxidase activity may be present (arrow in E). There is widespread expression of MHC Class I at the sarcolemma (F). Lymphocytic infiltrates are largely endomysial and are composed predominantly of CD8 expressing cells (G) which infiltrate into intact myofibres (arrow in H). A-C: haematoxylin and eosin; D: acid phosphatase histochemistry; E: cytochrome oxidase histochemistry; F: MHC class I immunohistochemistry; G-H CD8 immunohistochemistry. Bar in A represents 25μm in A-D & H, and 50μm in E-G. From (Machado et al. 2009)

diagnostic doubt, since it is observed in 96% of cases. Its upregulation does not appear to be affected by short-term use of immunosuppressive agents (van der Pas et al. 2004). Whilst the sensitivity of MHCI expression appears high, it is not specific to IBM or the established primary inflammatory myositides and has been demonstrated in cases of Duchenne muscular dystrophy and dysferlinopathy. Endomysial inflammation is additionally seen in FSHD, statin myopathy, caveolinopathy, calpainopathy and merosinopathy. In each of these,

MHCI expression is presumed to be a secondary response to the underling primary genetic or toxic insult (van der Pas et al. 2004). Indeed, both MHCI expression and lymphocytic infiltration of muscle can be observed in neurogenic atrophy (Troost et al. 1992).

The evidence of humoral immunity in IBM is less well defined. Those antibodies associated with autoimmune myositides, such as anti-signal recognition peptide (SRP), Jo-1 or Mi-2, are absent in IBM. Microarray studies suggest immunoglobulin genes are among the most abundantly differentially transcribed genes in IBM muscle, accounting for a greater proportion of those upregulated more than 20-fold than in PM muscle (Greenberg et al. 2005). There is immunohistochemical evidence of CD19 and CD20 B-cells, outnumbered by CD138 differentiated plasma cells. Myeloid dendritic cells, with the potential for antigen presentation and production of interferons, are also detected in IBM muscle (Greenberg et al. 2007).

The identification of antibodies to a 43kDa antigen, subsequently determined as cytosolic 5'-nucleotidase 1A (C5N1A), provides the best evidence of humoral immunity in IBM. Although it is not clear that these antibodies are pathogenic, a dot blot assay has demonstrated up to 70% sensitivity and 92% specificity for IBM in one group of 165 patients with neuromuscular disease. In keeping with the known location of the target antigen, C5N1A immunohistochemistry localises to the perinuclear region and to rimmed vacuoles, supporting the hypothesis that these represent myonuclear degeneration in IBM (Larman et al. 2013).

1.3.2 Degenerative features

1.3.2.1 Rimmed vacuoles

Sarcoplasmic vacuoles are a feature of several myopathies in addition to IBM, including hereditary Inclusion Body Myopathies, oculopharyngeal muscular dystrophy, Emery-Dreifuss muscular dystrophy, Becker's muscular dystrophy and also chronic neuropathies including poliomyelitis and spinal muscular atrophy (Villanova et al. 1993; Semino-Mora et al. 1998; Paradas et al. 2005; Malicdan et al. 2007; Momma et al. 2012). In IBM, these vacuoles are typically detected in those fibres not invaded by lymphocytes and the overwhelming majority are 'rimmed' by basophilic granular deposits at their peripheries (Greenberg et al. 2006). A relatively small proportion of fibres demonstrate rimmed vacuoles, with estimates ranging between less than 1 and 6% (Mhiri et al. 1990; Mendell et al. 1991).

The origin of rimmed vacuoles is unclear but autophagic lysosomal degradation or myonuclear breakdown have been proposed (Villanova et al. 1993). The latter hypothesis is supported by detection of nuclear membrane proteins emerin and lamin A/C by immunohistochemistry in the vacuolar lining along with electron microscopic evidence of nuclear membrane rupture. An association of vacuoles, 15-21nm tubulofilaments and nuclear abnormalities has been proposed since these features are shared by Paget's disease, IBMPDFTD, hIBM due to GNE mutations and OPMD (Greenberg et al. 2006).

1.3.2.2 Intracellular protein deposition

IBM tissue is further characterised, and distinguished from PM, by proteinaceous nuclear and cytoplasmic aggregates. These contain a variety of proteins commonly associated with neurodegenerative diseases, including βamyloid species, phosphorylated tau, presenelin, α-synuclein, TDP-43 and p62 (Nogalska et al. 2009; Salajegheh et al. 2009; Askanas et al. 2012). These are typically detected on histological examination by immunohistochemistry. Electron microscopy demonstrates 15-21nm tubulofilamentous inclusions and cytoplasmic collections of 6-10nm amyloid-like filaments. Some myonuclei contain 7nm filaments (Fig 1.3). The particular pathogenic relevance of protein aggregation in IBM is discussed further below (see Chapter 4 Introduction, Sections 4.2 and 4.3).

1.3.2.3 Mitochondrial abnormalities

Mitochondrial dysfunction is evidenced by ragged red fibres on Gomori trichrome staining and by an excessive number of cytochrome-oxidase negative fibres adjusted for patient age (Fig 1.2, Image E). The latter feature is particularly common, affecting 63 of 64 biopsies in one study (Chahin et al. 2008). Mitochondria also display structural abnormalities in IBM, including paracrystalline inclusions (Oldfors et al. 2006).

The accumulation of COX negative fibres with 'normal' ageing appears to reflect focal deficits of oxidative phosphorylation, reflecting clonal expansion of mtDNA mutations. This can be quite marked, affecting up to 15% of fibres and has, accordingly, been hypothesised as contributory in the sarcopenia of ageing (Wallace 1992). Quantification of COX negativity is further complicated by its tendency to affect fibres segmentally, meaning there is a tendency towards underestimation of the number of COX negative fibres through use of standard cross-sectional histological analysis. Nevertheless, mtDNA mutations, predominantly large-scale deletions, have similarly been demonstrated in COX-deficient fibres of IBM patients (Oldfors et al. 1993). Southern blot has implied that the overall amount of mutated mtDNA is low in IBM, consistent with the

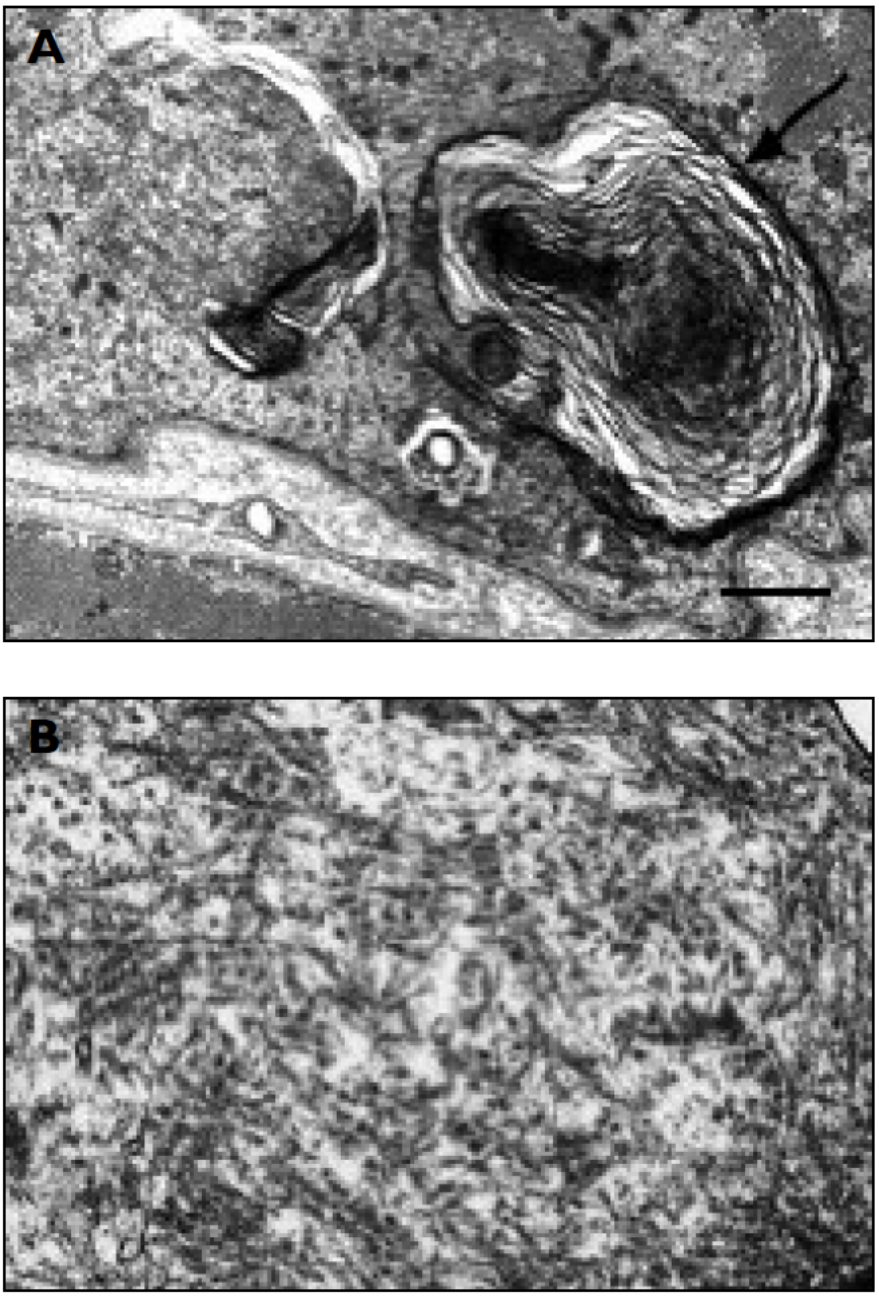

Figure 1.3 Electron microscopic features of IBM

Ultrastructural examination of muscle fibres demonstrates whorled membranous debris (arrow in A) and associated randomly orientated filaments (B). Bar in A represents 700nm in A and 200nm in B. From (Machado et al. 2009)

lack of impaired oxidative metabolism in ^{31}P MR spectroscopy (Santorelli et al. 1996; Lodi et al. 1998). Mutations have not been detected in the nuclear genes, that encode for mitochondrial proteins, such as POLG, in patients with IBM.

A distinct disease entity of 'Polymyositis with mitochondrial pathology in muscle' (PM-Mito) has been proposed (Temiz et al. 2009). This term was applied to patients with a stereotypical IBM phenotype and whose muscle biopsies lack vacuoles but, nevertheless, display similar inflammatory characteristics to those observed in IBM or PM. There appears little evidence to support PM-Mito being anything other than part of the sporadic IBM spectrum. First, the use of the Polymyositis stem is inconsistent with the clinical phenotype being highly distinctive of IBM rather than PM. Secondly, the presence in 'PM-Mito' biopsies of congo-red fluorescent aggregates of βamyloid, phosphorylated tau and TDP-43 is entirely consistent with IBM. Thirdly, the absence of vacuoles is arbitrary since it these represent just one established

feature of IBM muscle biopsies and, conversely, the rare occurrence of vacuoles in DM has not led to creation of a distinct diagnostic entity (Layzer et al. 2009). Therefore, the term IBM-Mito may be more appropriate. To support this, one study has determined significantly greater proportions of COX negative fibres in 'PM-mito' than IBM, along with significantly fewer fibres affected by tau and TDP-43 pathology (Temiz et al. 2009). It is equally likely that these patients represent one element of the extensive IBM histological spectrum. Pragmatically, a significant proportion of this group may represent the 'clinically defined' population who have a milder form of the disease or who less pathologically advanced at the point of biopsy. Definition of this population could prove useful for identification of patients more likely to respond to treatments targeted at degenerative aspects of IBM.

1.3.3 Summary of features of IBM and primary myositides

After considering the various clinical and pathological features of IBM, it is useful to compare these with the primary myositides, PM and DM, with which IBM is traditionally classified (Table 1.1). This highlights that, although some similarities do exist, there are numerous significant differences in both the clinical and pathological domains. Perhaps most notable is the distinct patient population affected by each disorder.

Characteristic	IBM	PM	DM
Pathological	• Endomysial inflammation • $CD8^+$ T-Cells • MHC Class I expression • Intracellular inclusions • TDP-43 translocation • Mitochondrial impairment • Rimmed vacuoles	• Endomysial inflammation • $CD8^+$ T-Cells • MHC Class I expression	• Perivascular inflammation • $CD4^+$ T-Cells • MAC expression
Clinical	• >50 year-old Men • Forearm flexors and quadriceps • Some association with autoimmunity • Mild Increase in CK • Denervation on neurophysiology	• >18 year-old Men and Women • Proximal limb muscles • Strong association with autoimmunity • Large Increase in CK	• Paediatric / strong association with cancer in adults • Rash • Large increase CK

Table 1.1 Basic comparison of IBM and primary myositides

1.4 Diagnostic criteria

After consideration of its clinical and histological phenotype, a number of diagnostic criteria for IBM have emerged. These are of significance in considering the validity of the boundaries such criteria impose between IBM and its differential diagnoses. Indeed, in seeking to formulate a translational research project, it is essential that a defined group of applicable patients can be readily identified. In a sporadic condition, particularly one of uncertain aetiology, the establishment of validated diagnostic criteria is challenging. A review of these criteria was of particular importance in designing the clinical study described in this thesis (described in Chapter 5).

1.4.1 Griggs' criteria

The most commonly applied criteria are those described by Tawil and Griggs (Tawil et al. 2002) which allow diagnosis of *definite* or *probable* IBM. Patients meeting either definition are routinely included in clinical studies, reflecting the high threshold for diagnosis set by these criteria. *Definite* IBM is a histological diagnosis in which invasion of non-necrotic fibres by mononuclear cells, vacuolation and either amyloid deposits or 15-18nm tubulofilaments are required. In this case, the clinical features are not considered. *Probable* IBM refers to the combination of invasion of intact fibres by mononuclear cells and vacuoles but without the other pathological features. In this case, the clinical presentation must be stereotypical, in that there must be at weakness of at least one of finger flexion, wrist flexion or the quadriceps. Furthermore, the serum CK must be <12 times the upper limit of normal and electromyography must be 'consistent with an inflammatory myopathy'. Evidently, even the diagnosis of *probable* IBM requires meeting the majority of the clinical and histological features discussed above. Criticisms of these criteria have included that patients who are clinically stereotypical of IBM but are relatively early in the disease course at the time of muscle biopsy may lack the particular histological features described. Furthermore, the use of 'invasion of intact fibres by mononuclear cells' as a surrogate marker of inflammation may not be demonstrated by all biopsies which nevertheless contain $CD8^+$ lymphocytes and up-regulation of

MHC Class I. Indeed, the widespread expression of MHC Class I appears to be a more reliable segregator of myositis from the secondary inflammation seen in dystrophies (van der Pas et al. 2004). Neither the application of electron microscopy to biopsies nor the use of neurophysiology are routine practices in evaluation of suspected IBM cases, limiting their practical use outside specialised centres. Most importantly, several histological features, such as the presence of p62 and TDP-43 on immunohistochemistry, have emerged in the years succeeding the publication of Griggs' criteria in 2002 (Nogalska et al. 2009; Salajegheh et al. 2009).

It appears likely that these criteria are highly specific for IBM but are of low sensitivity. Some have proposed that those patients, who lack the features required to meet Griggs' criteria, may have the greatest potential benefit from treatment and should be the primary target for recruitment into clinical trials (Hilton-Jones et al. 2010).

1.4.2 European Neuromuscular Centre criteria

The ENMC diagnostic criteria were described in 1997 (Table 1.2). In the single direct comparison with Griggs' criteria, these appear to set a lower threshold for *definite* IBM but do not represent a different level of sensitivity once *probable* cases are included. In this study, 103 patients were identified, of whom 72 were *definite* and 31 *probable* according to ENMC criteria. Applying Griggs' criteria to the same population, 16 cases would have been considered *definite* and 87 *probable* (Badrising et al. 2000). The ENMC criteria place greater onus on the clinical description of the disease.

1.4.3 MRC Centre for Neuromuscular Diseases criteria

Following an international workshop in 2008, a further set of criteria was proposed that contains a 'pathologically defined' group, characterised as per Griggs' criteria, and also a 'clinically defined' group (Table 1.3). Such patients demonstrate disproportionate weakness of finger flexion relative to shoulder abduction and of knee extension relative to hip flexion, reflecting the

European Neuromuscular Centre (ENMC) Criteria for Diagnosis of IBM			
A. Clinical			
1. Presence of muscle weakness			
2. Weakness of forearm muscles, particularly finger flexors, or wrist flexors more than wrist extensors			
3. Slowly progressive course			
4. Sporadic disease			
B. Histopathology			
5. Mononuclear inflammatory infiltrates with invasion of non-necrotic muscle fibres			
6. Rimmed vacuoles			
7. Ultrastructure: tubulofilaments of 16 to 21 nm			
Definite inclusion body myositis:	1, 2, 3, 4, 5, 6	or	1, 3, 4, 5, 6, 7
Probable inclusion body myositis:	1, 2, 3, 4, 5	or	1, 3, 4, 5, 6

Table 1.2 ENMC diagnostic criteria for IBM

MRC Classification	Criteria	Specific Features
Pathologically Defined	Meets Griggs' criteria	• Invasion of non-necrotic fibres my mononuclear cells, rimmed vacuoles and either intracellular amyloid deposits or 15-18nm filaments
Clinically Defined	Clinical Features	• Duration > 12 months • Age > 35 years • Weakness of finger flexion > shoulder abduction AND of knee extension > hip flexion
	Pathological Features	• Invasion of non-necrotic fibres by mononuclear cells or rimmed vacuoles or increased MHC-I but no intracellular amyloid deposits or 15-18nm filaments
Possible IBM	Clinical Features	• Duration > 12 months • Age > 35 years • Weakness of finger flexion > shoulder abduction OR of knee extension > hip flexion
	Pathological Features	• Invasion of non-necrotic fibres by mononuclear cells or rimmed vacuoles or increased MHC-I but no intracellular amyloid deposits or 15-18nm filaments

Table 1.3 MRC Centre criteria for diagnosis of IBM

stereotypical IBM phenotype but biopsy may display only one of mononuclear cell invasion, increased MHCI or rimmed vacuoles (Hilton-Jones et al. 2010). The additional criterion of age being over than 35 years represented the minimum age at which any of an invited panel of experts had observed sporadic IBM. It is hypothesised that these patients may represent the earlier portion of the disease spectrum.

1.4.4 Overall discussion of diagnostic criteria

The principal aim of diagnostic criteria is to distinguish IBM from its differential diagnoses, which incorporate both the primary inflammatory myositides PM and DM, a range of genetic muscular dystrophies and amyotrophic lateral sclerosis (ALS).

Until the aetiological differences between IBM these conditions are fully understood, diagnostic criteria will be of limited accuracy. The pathological differences appear to be of a subtlety not currently incorporated by standard clinical practice, such as the use of detailed immunohistochemical analysis. Therefore, current criteria must maintain a high threshold for diagnosis and hence a high degree of specificity rather than risk the inclusion of non-IBM cases in clinical studies of IBM. The stereotypical clinical phenotype is readily recognised by neuromuscular specialists and the study of a 'clinically defined' population may prove important in identifying subgroups with particular potential for benefit from new treatments. The exclusion of MFM in such cases is particularly important.

1.5 Treatment of IBM

There is no effective pharmacological treatment for IBM. Standard clinical management is to offer only supportive therapies such as physiotherapy, occupational therapy and psychological support. Anecdotally, empirical courses of corticosteroids are common despite lack of supporting trial evidence. A number of small trials, all of which have included immune based drugs, have been undertaken without significant evidence of efficacy. These are considered in detail in Chapter 5 (see Chapter 5 Introduction, Section 5.1.2). Although one inference of the failure of these trials could be that the inflammatory component in IBM is not clinically significant, it is unlikely that these trials were powered to detect realistic clinical changes; therefore this must be done with caution.

1.6 Hypotheses of IBM pathogenesis

Two dominant views have emerged on the pathogenesis of IBM; these are distinguished by the relative importance each attaches to pathological features that can broadly be described as either inflammatory or degenerative. The potential contribution towards overall pathogenesis by individual elements of either of these processes is considered elsewhere in this thesis (see Chapter 3 and 4, Introductions). The general basis of the 'inflammatory' and 'degenerative' hypotheses is described below.

1.6.1 IBM as a primary immune disease

The argument for a primarily inflammatory or autoimmune mechanism, as proposed by Dalakas and colleagues is based upon evidence that degenerative features in IBM are secondary to such inflammation, and has supported IBM's traditional classification as a primary myositis alongside PM and DM. Autoimmunity is implied by an immunogenetic association with HLA haplotypes, the presence of autoantibodies at levels comparable to other autoimmune disorders (Badrising et al. 2004), the expression of paraproteins and the clonal expansion of autoinvasive $CD8^+$ T-cells (Muntzing et al. 2003). If IBM is autoimmune the trigger for breakdown in immune tolerance is not clear. Viral

infection has been postulated due to rare descriptions of an IBM-like myopathy following retroviral infection by HTLV (Ozden et al. 2001) and HIV (Cupler et al. 1996) but viral RNA or DNA has not been consistently detected in cases of sporadic IBM.

More direct evidence has gradually emerged on the mechanisms through which inflammation leads to protein mishandling. Inflammation, induced in skeletal muscle via lipopolysaccharide, has been shown to increase βamyloid concentration and enhance phosphorylation of tau (Kitazawa et al. 2005). Furthermore, exposure of myogenic cells *in vitro* to the inflammatory mediators IL1β and IFNγ increases amyloid load, as assessed by immunostaining and western blotting. A linear relationship has been observed between the concentration of cytokine and chemokine mRNA and the expression of βAPP, tau, and ubiquitin in IBM *in vivo* (Schmidt et al. 2008). Therefore, the local expression of proinflammatory chemokines (including CC- or CXC-chemokine ligands and cytokines such as interleukin-1β (IL1β), tumour necrosis factor alpha (TNFα), interferon gamma (IFNγ) and transforming growth factor-β (TGFβ) could represent an early pathogenic occurrence (Tews et al. 1996; Lundberg et al. 1997; De Bleecker et al. 1999; Confalonieri et al. 2000; Civatte et al. 2005; Raju et al. 2005; De Paepe et al. 2007; Tournadre et al. 2007). The consequent chronic upregulation of MHC Class I (MHCI) may contribute to endoplasmic reticulum stress and, consequent perpetuation of NFκB activation that would generate further pro-inflammatory signalling and create a self-sustaining cycle. However, MHCI upregulation is a feature of other myositides, as well as a non-specific finding in some primary genetic myopathies. Therefore, either the chronicity or magnitude of over-expression would need to be greater in IBM, which has not been established, or additional factors contribute to the downstream effects. Nevertheless, the effect of cytokines (Goldgaber et al. 1989) and NFκB (Grilli et al. 1996) to increase βAPP transcription, and βamyloid translation, may exacerbate endoplasmic reticulum (ER) stress and thereby contribute to proteasome dysfunction and misfolded protein accumulation, in a second self-perpetuating cycle.

1.6.2 IBM as a degenerative disease

Despite the evidence for an inflammatory mechanism, there are fundamental clinical and pathological differences observed between IBM and the established inflammatory myopathies, Polymyositis (PM) and Dermatomyositis (DM). The elderly, predominantly male, population who suffer from IBM, contrasts with the young, female cohort typically affected by autoimmune diseases. Degenerative features, such as intracellular protein aggregates and rimmed vacuoles, are conspicuously absent from PM or DM despite also demonstrating upregulation of MHCI. Moreover, the ER stress induced in transgenic mice over-expressing MHCI, does not translate to intracellular protein aggregation or vacuolation (Nagaraju et al. 2000; Nagaraju et al. 2005). Furthermore, while DM and PM conditions respond clinically to immunotherapy, IBM does not, even when histological inflammation is reduced (Barohn et al. 1995).

In keeping with these criticisms against a purely inflammatory basis for IBM, an alternative hypothesis exists that IBM is primarily degenerative. This was proposed by the work of Askanas and Engel, which also places β-amyloid accumulation as an early upstream event (Askanas et al. 2006). For this reason, IBM has been referred to as 'The Alzheimer's of Muscle'. In this theory, following protein misfolding and accumulation, ER stress and oxidative stress combine to trigger a T-cell response to antigens derived from the accumulating proteins. Amyloid accumulation does induce muscle inflammation *in vivo*; transgenic mice that overexpress βAPP in skeletal muscle develop myositis (Sugarman et al. 2002). Furthermore, when the Aβ42 oligomer is selectively augmented, this inflammation is characterised by $CD8^+$ T-cells, reflecting IBM patient tissue (Kitazawa et al. 2006). This is associated with calcium dyshomeostasis, which reflects the potential for functional impairment of skeletal muscle excitation-contraction coupling by β-amyloid (Moussa et al. 2006).

In addition to a potential role in triggering inflammation, protein accumulation, particularly amyloid oligomers, can induce other key components of IBM pathology *in vitro*. βAPP over-expression, with consequent Aβ42 accumulation in intracellular aggregates, results in a dose-dependent cytopathic effect, impaired innervation by co-cultured neurons and mitochondrial dysfunction

(Askanas et al. 1996; Askanas et al. 1997). It also produces proteasomal dysfunction, a feature of human IBM tissue that appears both to induce and arise from intracellular protein accumulation and is compounded by mutated ubiquitin UBB^{+1} (Bence et al. 2001; Fratta et al. 2005). As is postulated in other conditions, β-amyloid toxicity may not be directly related to that contained in the insoluble aggregates, but rather to its soluble oligomers and protofibrils (Martins et al. 2006). However, among the many neurodegenerative proteins detected in IBM, the particular role of β-amyloid is debated due to the disparity in its rate of detection by different groups and contrasting interpretations of existing evidence (Greenberg 2009; Schmidt et al. 2013). Nevertheless, the majority of the other aggregated proteins demonstrated by IBM-affected tissue, notably TDP-43, have similar associations with ER stress, proteasomal dysfunction and mitochondrial impairment in models of other diseases, as discussed below (see Chapter 4 discussion on ER stress, NFκB and TDP43).

An alternative source of evidence for potential degenerative drivers of secondary inflammation in IBM emerges through comparison with the relatively common neurodegenerative condition amyotrophic lateral sclerosis (ALS), whose lower motor neuron variant is phenotypically more reminiscent of IBM than PM or DM. It shares a predilection for aged male subjects and tendency for distal upper limb muscle wasting, which is rare among all myopathies. Further clinical similarity is found in the frequent, albeit non-specific, neurogenic abnormalities demonstrated on neurophysiology of IBM patients (Askanas 1998). Several myopathological similarities between IBM and ALS have been observed despite a relatively small number of studies of skeletal muscle in patients with ALS. Both conditions demonstrate preferential involvement of fast-fatiguable (Type IIb) muscle fibres that constitute high proportions of the muscle groups typically involved (Atkin et al. 2005) (Parker et al. 2009). Interestingly, the denervated muscle of ALS patients also commonly demonstrates upregulation of MHC Class I (Troost et al. 1992). Indeed, the addition of denervation augments the inflammatory myopathy of SJL mice, which develop a spontaneous myositis, through upregulation of MHCI and significantly increased lymphocytic infiltration by CD8+ T-cells (Kampman et al. 1999). Even the transient MHCI expression that results from peripheral nerve

injury, thought to represent an additional regenerative function, might be sufficient in a given context, to establish a self-perpetuating pathogenic cycle (Maehlen et al. 1989).

Additionally, several degenerative histological features of IBM including rimmed vacuolation, β-amyloid deposits and ubiquinated inclusions can be seen in muscle from patients with chronic denervation (Semino-Mora et al. 1998). Recently, skeletal muscle of a patient with the genetic C9orf72 form of ALS was found to demonstrate p62 and ubiquitin aggregation (Turk et al. 2014). Upregulation of βAPP in skeletal muscle of patients with ALS and the $SOD1^{G93A}$ mouse model of ALS is evident at phenotypic presentation (Koistinen et al. 2006) and, indeed, genetic ablation of βAPP in the $SOD1^{G93A}$ mouse model attenuates disease progression significantly (Bryson et al. 2012).

1.6.3 Unifying mechanisms; contribution of the aged cell environment

It is unclear whether IBM displays a predominantly inflammatory phase in its early stage, before a degenerative 'end stage' emerges. This would be analogous to typical thinking about other conditions that combine these processes, such as multiple sclerosis. It is curious that the chronic inflammation of Polymyositis does not appear to result in those additional features demonstrated by IBM tissue, suggesting that factors additional to MHCI upregulation and inflammatory cell infiltration may be fundamental to IBM pathogenesis. Notably, there have been reports of chronic Dermatomyositis assuming some pathological features of IBM, including rimmed vacuoles (Layzer et al. 2009). If inflammatory factors are indeed the triggers of IBM, it is tempting to propose the vulnerability of the underlying cellular environment as a candidate, on which inflammation is superimposed, for differences observed between IBM and the purely inflammatory myositides. For example, the sarcopenia of normal ageing combines muscle atrophy and reduced contractile force, which reflects a number of degenerative susceptibilities. These would render an elderly patient cohort with significantly impaired ability to counter some of the consequences of chronic inflammation. These susceptibilities are discussed in more detail elsewhere (see Chapter 4, Introduction) but, briefly, include ER 'handicap',

elevated basal calcium concentration, proteasomal dysfunction, deficient protein handling, attenuated cell chaperone responses, elevated production of reactive oxygen species (ROS) and accumulation of mitochondrial DNA mutations.

1.6.4 Overall consideration of pathogenesis

In a condition where the fundamental pathological trigger is unknown, there are two principal strategies with which to prioritise targets for potential treatments. First, is to consider those elements that appear to be particularly characteristic of the disease and differentiate it from other similar conditions. In IBM this would represent inference from its differences with Polymyositis that, in contrast, does respond to immunotherapy. One would focus, therefore, on the degenerative aspects of the condition. Alternatively, is to prioritise those elements that appear to link other components of the pathology, thereby appearing to act as central pathogenic mechanisms. The advantage of this approach in IBM is that it does not rely on a polarised view about whether the upstream events are predominantly inflammatory or degenerative. For example, if one accepts the historical view that IBM is a form of 'Polymyositis-plus', in which an initial inflammatory phase evolves into a degenerative and inflammatory one, these potentially important points of interaction emerge. Equally, they remain relevant if viewing the disease in reverse, where degenerative mechanisms drive secondary inflammation (Fig 1.4). Therefore, regardless of its initial trigger, IBM could best be viewed as an interactive network of self-perpetuating pathological cycles. This view was maintained in the consideration of the specific aims of this thesis, detailed below, which unite towards the overriding hypothesis that through characterisation of certain aspects of IBM pathology, novel potential therapeutic avenues can be explored.

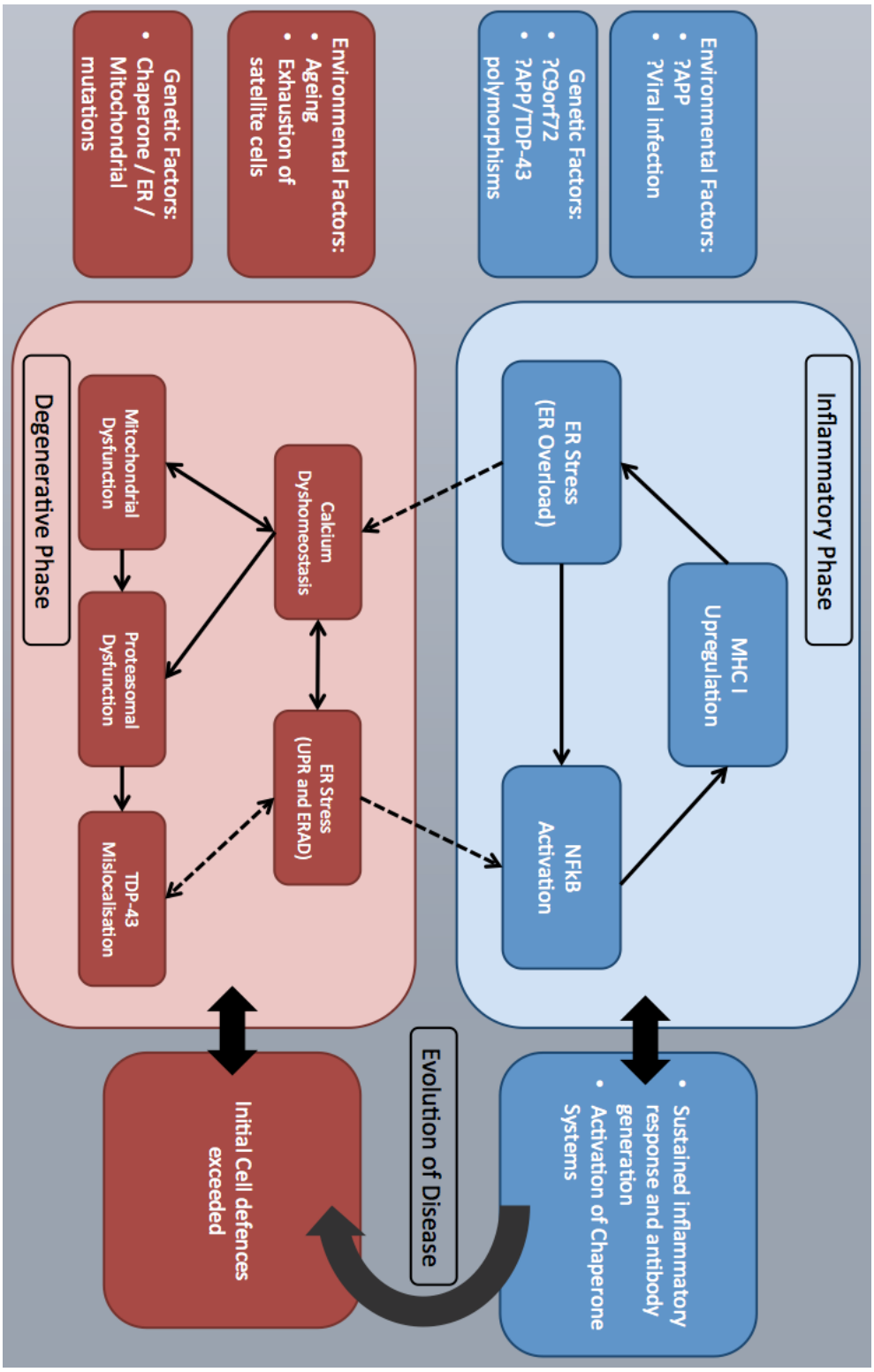

Figure 1.4 Potential mechanism of IBM pathogenesis.

Elements of inflammatory (blue) and degenerative (red) pathology may drive one another, regardless of which occurs first.

1.7 Specific aims of this Thesis:

1. To establish a pre-clinical disease model of salient pathological features of IBM
2. To characterise these features in order to establish a panel of quantifiable IBM-relevant pathological outcome measures
3. To test the effectiveness of novel treatment strategies in this system, determined by consideration of the literature
4. To determine how those treatments could be advanced towards clinical effectiveness in IBM

Chapter 2: General Methods

This Chapter describes the general methods underlying the *in vitro* experiments. Refinement of relevant components of individual techniques and determination of cell-based assays is described in the corresponding sections of the results (throughout Chapters 3 and 4). Composition of solutions and antibody dilutions are provided in the general appendix. Methods specific to the clinical trial are described separately in Chapter 5.

2.1 Myogenic satellite cell culture

The results described in Chapter 3 detail refinement of the cell culture protocol. The basic standard protocol, which represented the starting point for these experiments, is described below.

2.1.1 Standard culture protocol

Wild-type Sprague Dawley rats or C57-B6/SJLF1 mice aged postnatal day 0, 1 or 2 were culled by Schedule 1 methods in accordance with the Animals (Scientific Procedures) Act 1986. Hind limb muscles were retrieved by blunt dissection and washed in Phosphate Buffered Saline (PBS) with 4% Penicillin 100 units/ml and Streptomycin 100µg/ml (PenStrep), at 4°C. All subsequent steps were performed under sterile conditions. Muscle tissue was cut into smaller sections then placed in a shaker within an incubator at 37°C with 3ml 0.1% collagenase II per 0.05g of muscle for 45 minutes, triturating every 15 minutes through a 1ml pipette tip. The resulting solution was filtered through 100µm nylon mesh to remove remaining undigested fragments of tissue and then twice through a 40µm mesh (BD Biosciences™). 5ml of PBS per 5ml of cell suspension was added and the suspension centrifuged at 480g for 10 minutes. Supernatant was removed and the pellet was re-suspended in 1ml of muscle medium: 20% Fetal Calf Serum, 2% PenStrep and 0.5% Chick Embryo Extract in Dulbecco's Modified Eagle Medium (DMEM) GlutaMAX-1 (Invitrogen™). This solution was stored for 20 minutes 'pre-plating' within a plastic container in attempt to remove fibroblasts by means of their greater propensity to adhere to plastic

surfaces. Satellite cells were identified by light microscopy of a 10μL sample, mixed with 10μL Tryphan blue (Sigma Aldrich™) to identify dead cells. The concentration of viable satellite cells was determined with a haemocytometer and the cells were then seeded onto gelatinised cover-slips in a 24-well plate with 500μl of muscle media. Plates were incubated in 5% CO^2 at 37°C. Upon reaching confluency, typically after 24 hours, myotube differentiation was encouraged by substitution of the initial medium by differentiating muscle medium (10% Horse Serum, 2% PenStrep and 0.5% Chick Embryo Extract in DMEM GlutaMAX-1). Muscle medium was subsequently changed at 48 hourly intervals unless otherwise stated. After fixation, myogenicity was determined through demonstration of positive immunocytochemical staining for muscle specific proteins, such as myosin heavy chain or desmin. The absolute then percentage myogenicity was determined through counting the number of nuclei (identified with DAPI staining) present within myogenic cells. As cultures progressed, typically beyond two to three days, myocytes began to fuse to form myotubes, were readily identified by their characteristic long, thin multinucleated morphology. The 'fusion index' was determined by the proportion of nuclei contained within multinucleated myotubes versus myocytes.

All culture protocols, and subsequent experimental cultures, were repeated in full at least 3 times, with each experiment including at least 6 wells for any given culture condition.

2.1.2 Differential centrifugation

A mixed cellular population can be separated into cells of similar type by means of centrifugation through a density gradient medium. This technique, for isolation of the myogenic fraction from a muscle tissue homogenate, was previously described by Mau and colleagues (Mau 2008). Percoll® (GE Healthcare Lifesciences™) is a sterile colloidal suspension comprised of silica particles, 15–30 nm in diameter, coated with polyvinylpyrrolidone (PVP), which spontaneously forms a density gradient when centrifuged. A variety of density gradients were investigated to refine this procedure in our rat cell cultures as

described in Chapter 3. In brief, the cellular suspension produced by the above protocol was carefully pipetted on top of three layered Percoll® suspensions of differing percentages then centrifuged at 1250*g* for 20 minutes. Resulting cellular fractions were collected at the junctions between each Percoll® suspension layer and cultured separately to determine the characteristics of each fraction.

2.1.3 Fluorescence activated cell sorting

Cellular suspensions were obtained according to the above culture protocol. Then cells were incubated for 30 minutes at room temperature with antibody, either NCAM/CD56 conjugated to Phycoerythrin (PE) (BD Biosciences Pharmingen™, 10µl/million cells) or anti-mouse CD34 conjugated to Fluorescein (FITC) (Santa Cruz Biotech™, 5µl/million cells). An unexposed aliquot was kept as a negative control. Surplus antibody was washed off by adding 5ml of PBS and centrifuging at 480*g* for 5 minutes. The cellular pellet was resuspended in 0.5ml 2% fetal calf serum in PBS and transferred to 5ml polystyrene round bottom tubes (BD Falcon™). To indicate cell viability, 1 µg/ml propidium iodide (Invitrogen™) was added. A MoFLo-XPD™ cell sorter (Beckman Coulter™) was calibrated for the fluorescence and light scatter channels following manufacturers guidance. Analyses by light scattering properties and fluorescence were performed, prior to cell sorting into sterile 1ml tubes according to the relevant antibody positivity. As a control, antibody negative cells were sorted by the same criteria.

2.1.4 Fixation of cultured cells

Muscle media was removed from cultured cells and each well washed once with PBS. Either ice-cold 1:1 acetone-methanol solution or paraformaldehyde was added to each well for 10 minutes, at 4°C or room temperature respectively. Fixative was then replaced with PBS, and the samples stored at 4°C.

2.1.5 Homogenisation of cultured cells

When cultured cells were intended for subsequent Western blot analysis, 750 µl of homogenization buffer were added to each well at room temperature. Cells were placed in a shaker at 100rpm for approximately 30 minutes at 37°C. The resulting homogenate was then transferred to a 1.5 ml Eppendorf tube and stored at -20°C.

2.2 Induction of IBM-like pathology *in vitro*

2.2.1 βAPP overexpression

For transfection of βAPP, a DNA construct containing full-length human β-APP gene of 2312bp was cloned into the plasmid pcDNA3.1+. The plasmid pcDNA3.1+ without the βAPP gene was used as an Empty Vector control for transfections. Transfection of the plasmid was achieved using standard Lipofectamine™ 2000 protocol as per manufacturer's instructions (Invitrogen). Differentiating muscle medium was removed and replaced with Optimem™. A transfection solution was prepared in Optimem™, comprising DNA and Lipofectamine™ with the desired ratio of µg DNA to µl Lipofectamine™ (typically 1:3, as detailed in Chapter 3 Results) then incubated at room temperature for 20 minutes. 50µl transfection solution was prepared for each well and mixed with 200µl of Optimem™ before substituting the Optimem™ previously added to each well. Cultures were incubated at 37°C for 5 hours with the transfection solution before this was replaced with standard muscle medium. The cells were maintained in culture for the required length of time before being fixed or other analysis conducted. The timing of transfection and the ratio of DNA to Lipofectamine were optimised to maximise expression of βAPP within cells of myogenic lineage (as described in Chapter 3 Results).

2.2.2 Transfection efficiency

When employing transfection as a means specifically to examine the function of an exogenous protein, commonly a mutated protein, it is necessary to quantify the efficiency of transfection. This either requires the demonstration of the

expressed protein through a specific probe or, more commonly, tagging with an easily visualized marker such as green fluorescent protein (GFP). The purpose of overexpression in this context was, rather, to induce a suitably consistent degree of IBM-representative pathological sequelae, such as the cytoplasmic translocation of TDP-43 or ER stress. Put the other way, the expression of βAPP *per se* was not considered to indicate IBM-like pathology. Therefore, since no particular magnitude of effect was sought, the determination of transfection 'efficiency' in this way was unnecessary. Furthermore, it was noted that GFP tagging can alter the function of the introduced protein (Stevens et al. 2010) so to introduce this step was not justified in this context. To demonstrate that transfection had occurred, the relative expression of βAPP by immunoblot was compared in cultures transfected with the βAPP versus empty vector. In addition, immunocytochemistry was performed to examine inclusions containing βAPP products.

2.2.3 Exposure to other conditions

As indicated, cells in culture were exposed to inflammatory mediators including IL1β (1-20ng/ml), TNFα (1-25ng/ml), IFNγ (1-1000U/ml) and/or to the drug Arimoclomol (1-100μM), all of which were added to the culture medium to achieve the corresponding desired concentration. Where comparison with βAPP over-expressing cultures was made, inflammatory mediators were incorporated in the culture medium from the equivalent time point at which βAPP was transfected.

2.3 Examination of cells

2.3.1 Immunocytochemistry

Following fixation, coverslips were washed three times in PBS (Oxoid Ltd™) for 5 minutes before incubation at room temperature for one hour in blocking solution, which consisted either of 5% milk and 3% serum in PBS-0.1% Triton X-100 (Sigma-Aldrich™) or 10% serum in PBS-0.1% Triton X-100. Serum type was selected according to the secondary antibody host. The blocking solution was aspirated and the coverslips were washed three times with PBS prior to

incubation, either for one hour at room temperature or overnight at 4°C, with primary antibody (listed in Table 2.1) diluted in blocking solution. The primary antibody solution was then removed and the coverslips were washed three times, for 10 minutes, in PBS. The secondary antibody was then applied at its corresponding concentration prior to covering in foil and incubation at room temperature for 2 hours. All antibodies were subject to a negative control, where either the primary or secondary antibodies were omitted to ensure appropriate specificity. Following a further 3 washes in PBS, some coverslips were then incubated with DAPI (Sigma-Aldrich™, 1:2000 in PBS) at room temperature for 10 minutes. The slides were then washed in PBS before being mounted on glass slides with fluorescent mounting medium (DakoCytomation Fluorescent mounting medium S3023). Cells were visualised with a Leica Fluorescent Microscope (DFC420C) at magnifications between 20 and 100x. After determination of the appropriate magnification for the given experiment 3 fields per cover-slip were examined and the cells within those images counted. Unless otherwise stated, each condition was represented by a minimum of 3 cover-slips (*i.e.* cells from 3 culture wells within a plate) and at least 3 plates, representing 3 cultures, were populated for each experimental condition. Throughout this thesis, in reference to immunocytochemical experiments, 'n' refers to the number of cultures.

2.3.2 Western blots

Prior to Western Blotting, the protein concentration in the cellular pellet harvested from cultures was determined by Bio-Rad Protein assay. 100µl homogenising buffer (2% SDS, 2mM EDTA, 2mM EGTA dissolved in 500ml 5mM Tris (5mM TRIS HCL, 5mM Trizma base in dH_2O) pH6.8) was added to each well and cell pellet was triturated three times. BSA standards (Bovine Serum Albumin, Sigma™) were diluted to make a protein concentration gradient (Zero, 0.05, 0.1, 0.25, 0.5, 1, and 2 mg/ml) and 10µl of BSA standards and samples were added to a 96-well plate. The Bio-Rad DC (detergent compatible) Protein Assay contained 3 reagents, A, B and S (Bio-Rad™) which were mixed as per manufacturer's instructions to give 225µl per sample well (200µl reagent B and

	Primary Antibodies			
Target	**Species**	**Manufacturer**	**IHC Concentration**	**WB Concentration**
Desmin	Mouse	Dako	1:100	-
Myosin Heavy Chain	Mouse	DSHB-Iowa	1:20	-
βAPP	Rabbit	Invitrogen	1:250	1:500
Aβ40	Rabbit	Biosource	1:200	1:500
Aβ42	Rabbit	Biosource	1:100	1:500
TDP-43	Rabbit	Proteintech	1:200	1:1000
HSP70	Mouse	Santa Cruz Biotech	1:200	1:500
MHC Class I	Rabbit	Abcam	1:200	1:5000
NFκB	Rabbit	Abcam	1:200	-
Phospho-Tau	Mouse	Pierce Endogen	1:500	-
Ubiquitin	Mouse	Genetex	1:500	-
BiP	Rabbit	Abcam	-	1:1000
ATF	Mouse	Abcam	-	1:1500
CHOP	Mouse	Abcam	-	1:500
βActin	Mouse	Abcam	-	1:5000
GAPDH	Mouse	Abcam	-	1:1000

Table 2.1 Primary antibodies used

Table details the primary antibodies, and their corresponding concentrations, used in immunocytochemistry or western blots.

25µl reagent A and S). Plates were incubated at room temperature for 15 minutes and absorbance measured at 750nm on a spectrophotometer.

Two chambers for Western Blotting were assembled for according to manufacturer's instructions (Bio-Rad™). Resolving gel was prepared with acrylamide concentration between 5% and 15% according to the molecular weight of protein being investigated (Protogel 4X resolving buffer, distilled water, 40% acrylamide, 10% ammonium persulphate, tetramethylethylenediamine (TEMED)). Resolving gel was poured into chambers and covered with a thin layer of water-saturated butanol before being left at room temperature for one hour to polymerise. Stacking gel was prepared as manufacturer's instructions (Protogel stacking buffer, 40% acrylamide, 10% ammonium persulphate, TEMED) and poured over the polymerised resolving gel. Combs were inserted with care to ensure absence of no air bubbles and the stacking gel left to polymerise for 30 minutes at room temperature. Protein samples were combined in 1:1 ratio with sample buffer, ensuring uniform protein content across all samples, then boiled and loaded into the wells created by combs. One well in each gel was loaded with a protein marker (5 µl, Bio-Rad) to allow subsequent determination of molecular weight. Gels were transferred into a frame according to manufacturer's instructions and placed within a tank filled with electrode buffer (TRIS base, glycine, SDS in distilled water). Gels were run at 160V for approximately 1 hour to achieve adequate separation of protein bands. Gels were then removed from their frames and placed on a nitrocellose membrane (Amersham™) within a frame, bracketed by filter paper and sponges within transfer frames, immersed in transfer buffer (Tris-Glycine transfer buffer, National Diagnostics™) at 2°C. 13. Transfer of proteins to the membrane was achieved by running at 100V for 60 minutes and confirmed with a Ponceau stain. Blots were blocked for 1 hour in PBS+0.1% Tween 20+5% milk fat protein before incubation with primary antibody at 4°C overnight. Following three washes in PBS-Tween, blots were incubated in an HRP conjugated secondary antibody (Dako, 1:1000) for 2 hours, while shaking. Blots were visualised with Amersham ECL reagent (GE Lifesciences™) or Supersignal (Thermoscientific™) according to manufacturer's instructions and then developed on Kodak film or

visualised under a fluorescent camera with FluorChem. Band densitometry was performed by ImageJ (open software). For this, rectangular regions of interest of equal size were superimposed over each band and the background signal subtracted before the density was determined. The density corresponding to each band of interest was then expressed relative to that corresponding to the control protein (e.g. GAPDH). This was then compared across a minimum of three blots per condition under experimentation. This mean optical density then calculated relative to that of same protein by the relevant control population.

2.3.3 MTT assay

The MTT 3-(4,5-Dimethylthiazol-2-yl)-2,5-diphenyltetrazolium bromide assay was employed as a standard measure of cell viability. Broadly, the MTT assay provides an estimate of mitochondrial activity, which is linearly proportional to the number of viable cells. It is a colorimetric assay which depends on the reduction of yellow tetrazolium dye to water-insoluble purple formazan crystals by mitochondrial dehydrogenase enzymes. This colour change can be quantified spectrophotometrically. As discussed above (see Chapter 1, Section 1.3.2.3), mitochondrial impairment is an important characteristic of IBM tissue. Therefore, in comparison to other viability assays, for example the LDH based assay, the MTT appears more directly relevant in this context. Finally, it is widely used in early stage evaluation of drugs, lending itself to the desired high-throughput of a pre-clinical evaluation system that is the underlying purpose of these experiments (Kaspers et al. 2005).

An MTT working solution was prepared from 12mM Thiazolyl blue solution-PBS (Sigma™) diluted 1:10 with incubating medium. 50µl of this working solution substituted existing cell culture medium in each well for 4 hours at 37°C. The resulting precipitate was dissolved in 100µl of 0.4M HCl and the absorbance measured at 570nm by spectrophotometry. Each sample, representing an individual well, was run in triplicate and the mean then calculated.

2.3.4 Live cell Calcium imaging

The refinement of the technique used for determination of cytosolic calcium is described in Chapter 4 Results. The basis of the method is described below.

2.3.4.1 Selection of Ca^{2+} fluorescent dye

A variety of Ca^{2+} indicators are available, each of which has its own advantages and disadvantages. Broadly, indicators can be described as either ratiometric or non-ratiometric. The former employ methods based on a ratio between two fluorescence intensities. These indicators, such as Fura-2 demonstrate a shift in emission or excitation spectra upon calcium binding; therefore two excitation lasers or two detection ranges are required. An intensity ratio is calculated at the wavelength at which there is maximal difference between fluorescence in the bound and free indicator. The advantage of this technique relates to correction of artefact consequent to dye bleaching or changes in laser intensity. However, they frequently require ultraviolet activation, which is associated with direct phototoxic effects on the cell being tested and also overlaps with the excitation and emission peaks of other intracellular chemicals such as NADH, thereby confounding the overall fluorescent signal through 'autofluorescence' (Takahashi et al. 1999). Non-ratiometric or 'single wave' dyes such as Fluo4, typically have a low basal fluorescence intensity which itself shifts upon binding to Ca^{2+}. This means that increase in intensity directly reflects a change in $[Ca^{2+}]$ and calculation of $[Ca^{2+}]$ is more straightforward. Further considerations include the approximate concentration of Ca^{2+} being measured, whether organelle loading is desired (which it is typically not) and propensity for technical issues related to most dyes, such as uneven loading, bleaching and quenching. The dye Fluo-4 AM (Fig 2.1) is the most widely applied dye for cell calcium imaging, likely because of its dissociation constant (Kd) approximating cytosolic $[Ca^{2+}]$, which corresponds to the range in which fluorescent dyes are most accurate (Takahashi et al. 1999). It is an analogue of Fluo-3, originally described by Tsien and colleagues (Minta et al. 1989) but is preferred due to increased fluorescence excitation at 488nm. Fluo-4 is synthesised as an acetoxymethyl (AM) ester derivative that is membrane permeant. Within the cell, the ester group is cleaved by esterases, leaving the now impermeant Ca^{2+}

sensitive dye trapped inside it. It is most suitable for the experimental protocol detailed here, which relies on depletion of ER calcium, as it has low tendency to organelle loading.

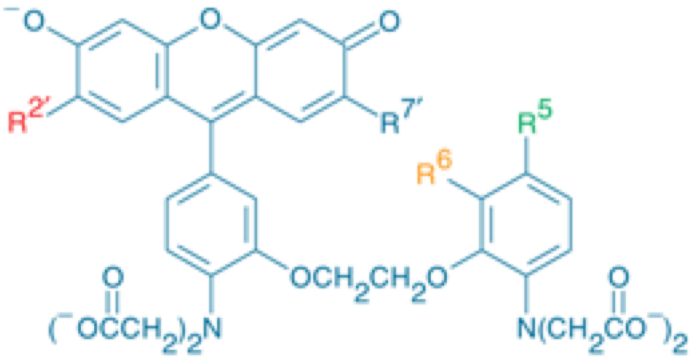

Indicator	$K_d(Ca^{2+})$	$R^{2'}$	$R^{7'}$	R^5	R^6
Fluo-3	0.39 µM	Cl	Cl	CH_3	H
Fluo-4	0.35 µM	F	F	CH_3	H
Fluo-5F	2.3 µM	F	F	F	H
Fluo-5N	90 µM	F	F	NO_2	H
Fluo-4FF	9.7 µM	F	F	F	F

Figure 2.1 Chemical structure of Fluo dyes

From Lifetechnologies The Molecular Probes® Handbook

2.3.4.2 ER calcium depletion with Thapsigargin

Thapsigargin (TG) non-competitively and specifically inhibits the sarco/endoplasmic reticulum ATPase (SERCA) pump, located on the ER membrane, without directly affecting plasma membrane Ca^{2+} ATPases (Treiman et al. 1998). This rapidly depletes ER Ca^{2+} since uptake of cytosolic calcium is precluded, whilst calcium release via ER ryanodine and IP3 receptors persists. The Ca^{2+} release from the ER leads to elevation of the cytosolic [Ca^{2+}], which is reflected in increased fluorescence intensity of the calcium dye (in this case Fluo 4-AM). Therefore, the magnitude of this change indicates the initial ER [Ca^{2+}]. Previous work suggests the ER is unlikely to be entirely depleted of Ca^{2+}, rather

by approximately 85% (Verma et al. 1990). However, to determine absolute ER [Ca^{2+}] accurately requires direct measurement, which is experimentally challenging (it is relatively precluded through the use of chemical fluorescent dyes due to the high [Ca^{2+}] significantly exceeding their Kd) and not the purpose of these experiments. Here, the purpose is to examine is the effect of IBM-like conditions on cytosolic and ER [Ca^{2+}], which is achieved through comparison with control cultures.

2.3.4.3 Determination of cytosolic and ER Ca^{2+}

Confocal images were obtained on a Leica SPE inverted confocal laser scanning microscope. Cells were kept at 37°C and 5% CO2 within a specialised imaging incubator. Coverslips were loaded with 500 ml of 5 mM Fluo 4-AM (Invitrogen™) and 0.005% pluronic acid (a dispersing agent that facilitates cell loading) diluted in confocal recording medium. Coverslips were incubated in the dark for approximately 30 minutes at 37°C. Fluo 4-AM was excited at 488 nm and the emission fluorescence was measured at 518 nm. A z stack of images was taken approximately every one second within a field of interest that was maintained for the duration of the protocol. Thapsigargin was applied and, after diminishment of the subsequent elevation of fluorescence, the ionophore ionomycin was applied, which releases calcium from all intracellular organelles, providing a maximum calibration point (Figure 2.2).

Images were collected until the peak response to ionomycin had been reached. Myotubes were randomly selected for or specifically excluded from analysis as described in Chapter 4. Background fluorescence was subtracted. Fluorescence values were then converted to a [Ca^{2+}] concentration in nM using the formula below.

$$[Ca2+] = \frac{Kd(F/Fmax - 1/Rf)}{1 - F/Fmax}$$

For Fluo 4-AM: Kd = 350nM, Fmax = maximum fluorescence which is determined by application of Ionomycin, Rf = 100 (Maravall et al. 2000).

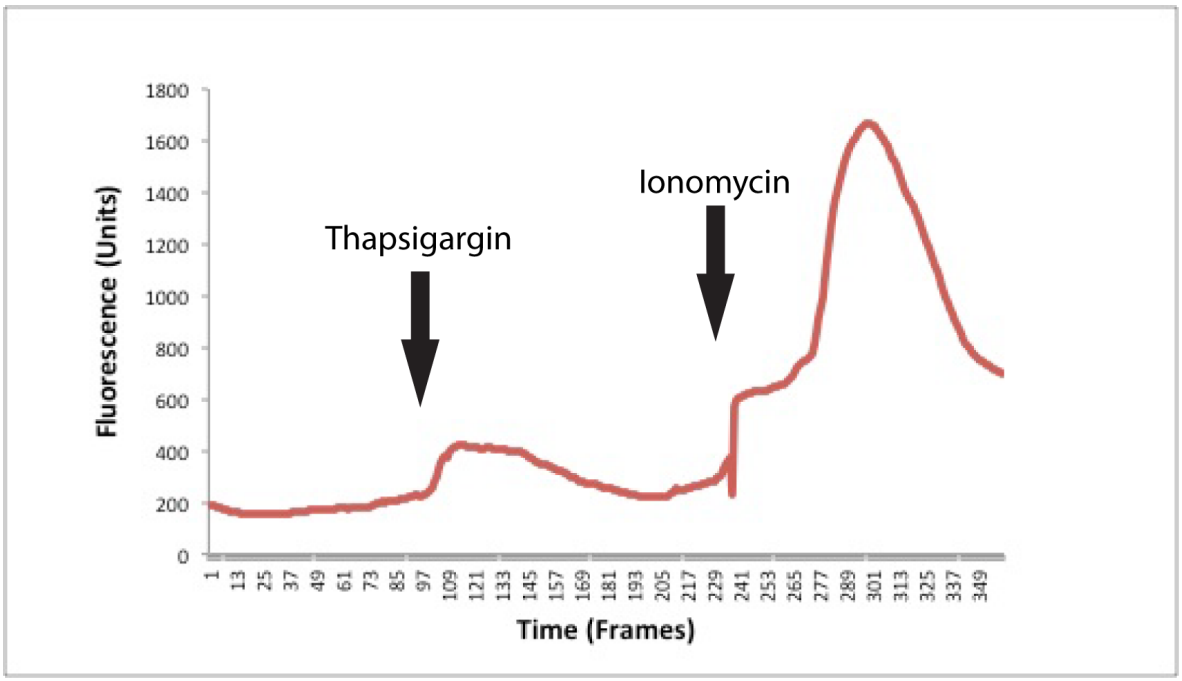

Figure 2.2 Live cell Ca^{2+} imaging protocol

Example trace of Ca^{2+} fluorescence from one cell during the protocol used to determine cytosolic and ER [Ca^{2+}]

2.4 Statistical analysis

Analysis of normally distributed results was performed using a t-test or, for comparison of greater than two groups, a one-way ANOVA. For non-Gaussian distributed results, the non-parametric Mann–Whitney U-test was used. As standard, $p<0.05$ was considered to reject the null hypothesis and indicate statistical significance in this thesis unless otherwise stated.

Chapter 3: Development of an *in vitro* model of IBM pathology

This Chapter describes experiments related to the first specific aim of this thesis, the development of a preclinical model of IBM pathology. First, the relative merits of various types of disease model were considered. After selecting an *in vitro* technique, a variety of cultures conditions were evaluated using primary myogenic satellite cell cultures, before IBM-like conditions were induced.

3.1 Introduction: justification for an IBM model

The lack of treatment for IBM reflects the absence of a coordinated programme of translational research. Historically, investigation into potential treatments for IBM has taken the form of small clinical trials (Schmidt et al. 2013) and no meaningful preclinical drug studies have been undertaken. This demonstrates the lack of widely accepted pre-clinical disease models. The method of repeated empirical clinical trials is expensive, complicated, lengthy and limited by its restriction to agents that are already licensed for other indications. There are additional concerns about the previous human treatment trials in IBM stemming from the lack of standardised diagnostic criteria, limited understanding of the disease's natural history and absence of validated biomarkers (Hilton-Jones et al. 2010). The relative rarity of the condition significantly limits the feasibility and size of early phase trials.

A more sustainable pathway to the development of IBM treatment must include preclinical screening of larger panels of drugs, allowing more promising agents to be advanced towards clinical testing. This also affords the advantage of selecting particular disease components for investigation. In turn, this advances understanding of IBM pathogenesis and allows targeting of treatments to those mechanisms deemed most active in propagating the disease.

IBM is a sporadic disease, which presents inherent challenges in creating pre-clinical disease models. Whereas monogenetic disorders have a clear primary

cause that can be correspondingly expressed in a cellular or animal system, a sporadic disorder represents a particular combination of genetic susceptibility and environment. Therefore, a model of sporadic disease must be tailored according to the specific requirement that model seeks to explore. For example, to investigate the role of immunological mechanisms in IBM would require a wholly different approach to determining its genetic risk factors. The lack of consensus on which of IBM's numerous pathological processes lies furthest upstream complicates matters further. Here, the decision process on how to approach the problem of disease modeling was approached with these arguments in mind, relating to the primary aim of this work; to develop a system in which the initial efficacy of potential treatments could be tested in a disease relevant way. Additionally, the fact this would represent an early stage in the translational research pathway meant that the ability to gain preliminary results quickly, allowing adjustment or redesign, was a further priority.

The following criteria were required of the disease model:

i. To reflect elements of IBM pathology which are relevant, preferably unique

ii. To incorporate the potentially different primary pathologies present in IBM

iii. To allow the determination of quantifiable outcome measures

iv. To allow high throughput of compounds for testing

v. To be reproducible within efficient time and financial constraints

The traditional pathway of preclinical drug assessment begins *in vitro* and promising agents are advanced to *in vivo* animal studies. There are advantages of either, most basically summarized as there being a greater propensity for detecting treatment effects *in vitro* but a greater likelihood of effects detected *in vivo* translating to clinical effect. Therefore, both options were considered.

3.1.1 Animal versus cellular models

There are general comparisons to be made between animal and cellular models of disease, and further comparisons specific to IBM.

Characteristic	Animal Model	Cellular Model
Time for development and characterisation	Longer	**Shorter**
Time for evaluation of drugs	Longer	**Shorter**
Number of testable drugs in given time	Fewer	**More**
Ease of changes during course of experimental programme	Harder	**Easier**
Likelihood of detecting a treatment effect (whether genuine or false positive)	Lower	Higher
Likely accuracy of representation of the corresponding human disease	**Higher**	Lower
Likelihood of translation to clinically meaningful results	**Higher**	Lower
Cost	Higher	**Lower**

Table 3.1: Relative merits of animal and cellular models of disease

Advantages are highlighted in bold

The weighting of the general comparators listed above is not equal, and depends on the priority of the particular experiment or programme concerned. The greater likelihood of animal models to represent the relevant disease is particularly dependent upon the contemporaneous status of overall understanding on that disease and the animal being well characterised. There are additional constraints of finance, labour and time. This limits their use to a few candidate drugs.

3.1.2 Lack of an established animal model of IBM

Since the pathogenesis of IBM in human patients remains unexplained, it follows that an animal model that recapitulates all features of the disease has not been established. There are, however, several animal models that do share

several important characteristics with human IBM and these have some capacity as preclinical models for investigation of potential therapeutic agents. Moreover, the descriptions of these animals offer a degree of insight into potential mechanisms of sporadic IBM, particularly those that link inflammatory and degenerative processes.

3.1.2.1 Mice over-expressing MHCI

The upregulation of Major Histocompatibility Complex Class I (MHCI) is a characteristic histopathological feature of muscle tissue affected by IBM. It has been proposed as a central feature in driving both downstream inflammatory processes and degenerative mechanisms such as ER stress (Dalakas 2006). Nagaraju and colleagues described a transgenic mouse that over-expresses MHCI specifically in skeletal muscle, resulting in severe and self-sustaining myositis, associated with myositis-specific antibodies (Nagaraju et al. 2000). Despite significant inflammation, and development of non-specific features of muscle damage such as centralised nuclei and variation in fibre size, there was conspicuous absence of degenerative features such as rimmed vacuoles, intracellular inclusions or mitochondrial abnormalities. Indeed, the inflammation *per se* was predominantly by mononuclear cells, with only occasional T-cells, which were $CD3^+$ rather than the $CD8^+$ form that characterise IBM. This implies that aspects of both the inflammatory and degenerative components of IBM require additional triggers beyond the upregulation of MHCI, thereby limiting the scope of these mice to model this disease.

3.1.2.2 Mice over-expressing β-Amyloid in skeletal muscle

La Ferla and colleagues described two transgenic mouse lines in which βAPP was selectively overexpressed in skeletal muscle by means of a muscle creatine kinase promoter (Kitazawa 2006). In one double transgenic line, the Aβ42 oligomer was selectively augmented by crossing the original βAPP-over-expressing mice with others harbouring a presenelin-1 mutation. The Aβ42 form is considered more pathogenic than its Aβ40 relative and is more

amyloidogenic (Ferreira 2007). These mice displayed IBM-like muscle pathology, including infiltration by $CD8^+$ T-lymphocytes, intracellular accumulation of Aβ42 and elevation of phosphorylated tau. This pathology was associated with a decline in motor performance. Further characterisation of βAPP transgenic mice has revealed impairment of muscle force, SR calcium release and calcium uptake via the SERCA, implying a direct pathological effect of amyloid species on muscle function (Shtifman 2008). It is unclear whether the resulting inflammation stems from a direct pro-inflammatory effect of βAPP or is a secondary response to the expression of a human protein within the mouse. Importantly, in practical terms, it was 24 months before the mice demonstrated the full plethora of phenotypic and histological effects compared to controls.

3.1.2.3 VCP transgenic mice

Inclusion Body Myopathy, Frontotemporal dementia and Paget's disease of bone are combined in the rare autosomal dominantly inherited condition IBMPFD. This is caused by mutant valosin-containing protein (VCP), the normal protein being a type 2 AAA^+ protein (*A*TPase *A*ssociated with diverse cellular *A*ctivities) associated with a wide range of functions. Interestingly, it appears that VCP is involved in the extraction and degradation of abnormally folded proteins from the ER. Pestronk and colleagues describe a transgenic mouse line expressing mutant VCP, which is associated with motor impairment preceded by ubiquinated intracellular inclusions and formation of autophagosomes (Weihl 2007). This model, whilst it shares some aspects of IBMPFD, is unsuitable as a model of sporadic IBM. There are fundamental clinical and pathological differences between the clinical myopathy displayed by each condition (Kimonis et al. 2000; Kovach et al. 2001). Further, and notably, this model does not demonstrate endomysial inflammation, a defining characteristic of sporadic IBM.

Taylor and colleagues more recently characterised a further transgenic mouse model of IBMPFD, harbouring either expressing the R155H or A232E mutant forms of VCP, which are associated with the human form of the disease (Custer

2010). These mice demonstrate numerous characteristics of IBMPFD, both phenotypically and in tissue from muscle, bone and brain. Muscle pathology includes rimmed vacuolation, activation of the NFκB cascade and cytoplasmic dispersion of TDP-43 where ubiquinated inclusions are formed. These changes account for progressive muscle weakness and reduced body mass. These mice, therefore, appear to represent a robust model of IBMPFD and, due to several myopathological similarities, may offer insight into some pathogenic aspects of sporadic IBM. Again, however, the notable clinical disparity between this distinct genetic disease and sporadic IBM represents a significant limitation.

3.1.3 Previous cellular models of IBM and consideration of IBM-relevant stimuli in vitro

In reflection of the contrasting wider views on the fundamental cause of IBM, previous efforts to study IBM *in vitro* have typically explored either a primary degenerative or inflammatory stimulus.

3.1.3.1 Overexpression of βAPP

Having detected βAPP immunoreactivity within intracellular aggregates of IBM tissue, the work of Askanas and colleagues has established that the over-expression of βAPP in cultured human myocytes reproduces several of the fundamental pathological features demonstrated in IBM muscle. These include the formation of intracellular proteinaceous aggregates (Askanas et al. 1997), the inhibition of proteasomal function (Fratta et al. 2005), increased production of myostatin precursor protein (Wojcik et al. 2007) and impairment of mitochondrial function (Askanas et al. 1997). This supports other cellular work describing amyloid toxicity in myoblasts (Jayaraman 2008) as well as the *in vivo* studies of APP over-expression described above (see Section 3.1.2.2).

3.1.3.2 Exposure to inflammatory cytokines

Schmidt and colleagues established that the exposure of cultured human myocytes to a variety of inflammatory cytokines, including IL1β, IFNγ and TNFα, appeared to elevate the intracellular concentration of βAPP, broadly suggesting that the inflammatory mechanisms in IBM could, via βAPP, drive the degenerative process (Schmidt et al. 2008). It is also known that such mediators upregulate MHC Class I in cultured myotubes (Michaelis et al. 1993).

Cytokines are low molecular weight proteins that function as chemical messengers between tissues and the innate and adaptive immune systems, and are therefore important drivers of a tissue specific inflammatory response such as that seen in IBM. The interleukin (IL), interferon (IFN) and tumour necrosis factor (TNF) subgroups are those most associated with myositis. Indeed, expression of mRNA of IL1β, IFNγ and TNFα are all elevated in IBM versus normal controls. Moreover, IFNγ mRNA is significantly higher in IBM that PM or DM, and TNFα mRNA significantly higher than in DM (Schmidt et al. 2008). IFNs have broad immune functions, including maturation of B-calls, activation of dendritic cells and lymphocytes and antiviral immunity, all of which are either demonstrated by or have been postulated in IBM (Greenberg et al. 2007; De Paepe et al. 2009). Interleukin-1 cytokines augment the expression of adhesion molecules by endothelium, permitting leukocyte transmigration and also promote antibody production. IL1β has been demonstrated to colocalise with MHC I in myofibres affected by IBM. This distinguishes IBM from Polymyositis and Dermatomyositis, where IL1β is only detected at sites of marked inflammation or in leukocytes (De Paepe et al. 2009). All these cytokine families are linked by their potentially central pathogenic contribution to IBM, and indeed to the established primary myositides, through the upregulation of MHC I, which is reproduced by myotubes *in vitro* (Bao et al. 1990).

Chemokines are a subset of cytokines that influence the migration of lymphocytes through a concentration gradient in a process termed chemotaxis. These small molecules are further categorized by amino acid positions that influence the position of their first two cysteine residues, with the majority falling into α/'CXCL' or β/'CCL' classes. The Mig (CXCL9) and IP-10 (CXCL10)

mRNA chemokines, which are induced by IFNγ, have been found in increased quantity in IBM muscle *in vivo* (Raju et al. 2003), implying that IFNγ contributes to recruitment of the T-cells which represent the predominant inflammatory cell demonstrated in the condition. MCP-1 (CCL3), upregulated by TNFα, is also known to be expressed at sites of inflammation in IBM *in vivo,* as is CCL4 (De Bleecker et al. 2002). Cultured human myotubes also upregulate a similar chemokine profile in response to cytokine exposure *in vitro* (Schmidt et al. 2008). In addition, they also increase expression of intercellular adhesion molecules such as CD54 under such stimuli (Michaelis et al. 1993).

3.1.3.3 Satellite cells of patients with IBM

Satellite cells harvested from IBM patients appear to differ from those of normal subjects. They demonstrated impaired proliferation rates, telomeric shortening and a propensity to accumulate amyloid (Morosetti et al. 2010). However, since IBM is not proposed to be a primary disease of satellite cell dysfunction, these findings suggest the unsuitability of patient satellite cells for disease modeling.

3.1.4 Overall comparison between in vitro and in vivo models of IBM

Basic comparison between the relative merits of animal and cellular studies highlights the several practical advantages of *in vitro* systems. For a disease with an established and reproducible primary cause, along with a theoretically sound treatment target, *in vivo* studies appear appropriate. In the context of IBM, the doubt that surrounds the pathogenesis obliges investigation of potentially downstream or secondary disease markers. The evaluation of drug action on animal models of limited accuracy is a potentially costly and inefficient process. Any results would be open to criticism regards their advancement toward human studies. The relative malleability of cellular studies in response to new developments in the field is a significant advantage in this context. Therefore, in combination with the existing data to support their use, a cell based system was preferred for the experiments undertaken in this thesis.

3.1.5 Muscle cell culture: history and development

3.1.5.1 Selection of primary cultures

The first step in the development of a cellular model was to decide whether to use primary cells or an immortalised cell line. The existing literature supported the possibility that primary muscle cell cultures could be manipulated to show certain characteristics of IBM (Askanas et al. 1997; Schmidt et al. 2008). Given that primary cells are generally felt to represent the activities of cells *in vivo* more closely, and the inherent conflict presented by investigating a disease of aged tissue in an immortalised line, primary cells were preferred. Furthermore, the study of muscle lends itself to primary cell culture given that all muscles contain a population of precursor cells that can be readily extracted and cultured, thereby preventing the need for multiple passages of subclones. Therefore, a review of this technique was performed.

3.1.5.2 Satellite cells

As post-mitotic tissue, skeletal muscle can only replace lost constituent cells rather than reproduce them through cell division as occurs in skin. Initially described in 1961, satellite cells are responsible for much of adult skeletal muscle's considerable properties of recovery and regeneration after insult or injury (Mauro 1961). Under basal conditions, these precursor cells are located between the sarcolemma and basal lamina where they reside in a quiescent and non-proliferative state (Muir et al. 1965). Indeed, there is no apparent turnover in normal adult skeletal muscle (Decary et al. 1997). Satellite cells appear to represent a heterogeneous population comprising true stem cells and committed progenitors (Kuang et al. 2007). Their origins are in embryonic somites as Pax3/Pax7-expressing cells, the dorsal embryonic aorta and also adult stem cells during regeneration (Polesskaya et al. 2003; Ben-Yair et al. 2005).

Activation triggers a cascade of pro-myogenic differentiation that is reminiscent of skeletal muscle development. Satellite cells evolve to myoblasts, primitive myogenic cells, which readily fuse to form elongated and multinucleated myotubes, the terminally differentiated basic building block of the myofibre.

Stimulation of the satellite cell, therefore, restores mature muscle either by replacement with new fibres or by the incorporation of myocytes into existing fibres (Moss et al. 1971). This process is accompanied by generation of progeny that restore the original quiescent satellite cell pool (Fig 3.1).

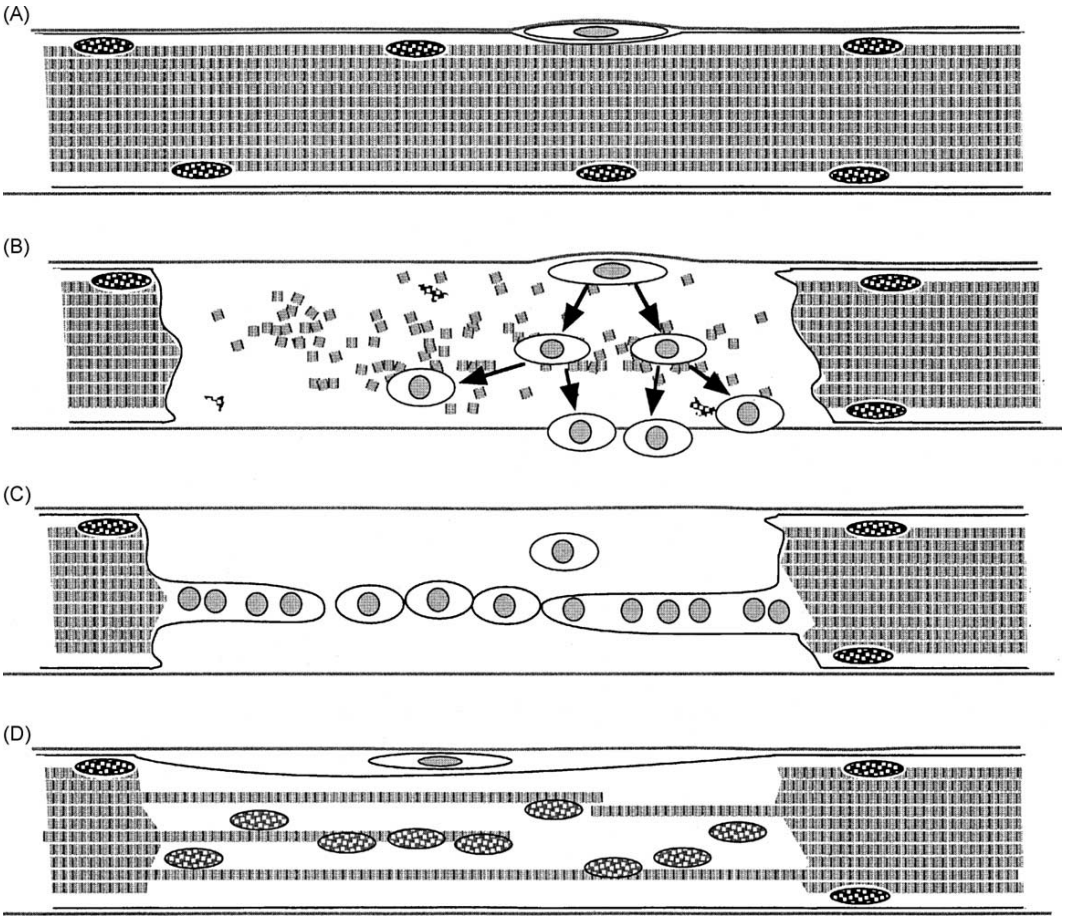

Figure 3.1 Regenerating muscle fibre

Regenerating muscle fibre. (A) Normal muscle fibre with myonuclei and a satellite cell. (B) Damaged muscle fibre. The satellite cell has become activated and proliferated in response to the damaged fibre. (C) Muscle precursor cells derived from the satellite cell have fused together to repair the damaged muscle fibre. (D) Regenerated muscle fibre, with a new satellite cell and centrally-placed, newly-regenerated myonuclei. Reproduced from (Morgan et al. 2003).

The genetic expression status of satellite cells alters markedly during this process of differentiation (Fig 3.2). Whereas the quiescent status is marked by Pax7 (Seale et al. 2000), M-cadherin (Cornelison et al. 1997), NCAM and VCAM (Covault et al. 1986), activated cells express desmin and MyoD (Cornelison et al. 1997). Indeed, the expression of MyoD appears fundamental and can cells other than satellite cells, such as fibroblasts and chondroblasts into myogenic cells (Choi et al. 1990).

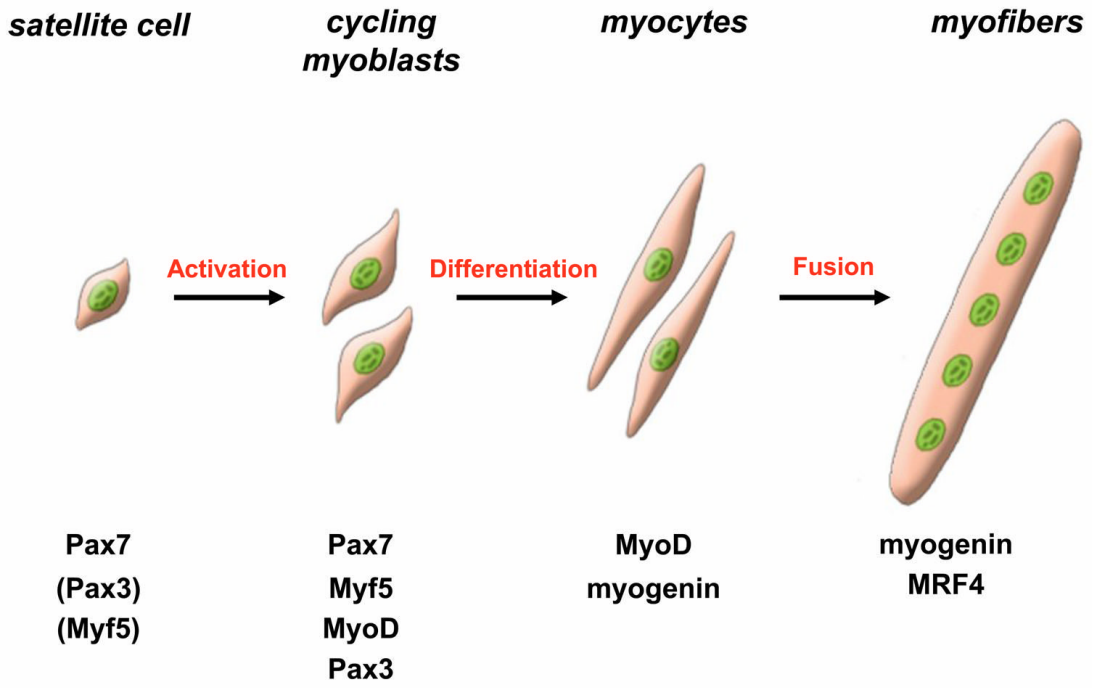

Figure 3.2 Schematic representation of adult myogenesis

Quiescent skeletal muscle satellite cell can are activated by stimuli from their associated fibre or microenvironment. Their progeny, skeletal myoblasts, express the paired-box transcriptions factors Pax7 and Pax3, as well as the myogenic regulatory factors Myf5 and MyoD. Once committed to differentiation, myoblasts stop proliferating and reduce expression of Pax7, Pax3 and Myf5. Differentiating myogenin positive myocytes then align and fuse to form multinucleated myofibres. MRF4 is required for hypertrophy of these new fibers. Reproduced from (Le Grand et al. 2007).

3.1.5.3 Satellite cell culture

It has been established for some time that muscle can be dissociated to release intact satellite cells and these can, in turn, be cultured *in vitro* (Cossu et al. 1980), (Hantai, Tassin et al. 1985). Here they replicate at a decelerating rate, initially doubling in number over approximately twenty-four hours before differentiating and fusing to form multinucleated myotubes (Le Moigne et al. 1990). This technique has been widely exploited to investigate normal mechanisms of muscle development and regeneration and the pathogenic processes of muscle disease.

3.1.6 Limitations and considerations of cell culture

In the knowledge that elements of IBM-relevant pathology had previously been induced in cultured muscle *in vitro* (Askanas et al. 1997; Schmidt et al. 2008), a number of initial considerations were made to evaluate the suitability of this technique in the context of the specific aims of this work.

3.1.6.1 Purity

Myogenic progenitor cells that can be harvested from skeletal muscle appear to represent two groups, satellite cells and a 'side population' (Hawke et al. 2001) that do not express those cellular markers typical of a satellite cell, such as Pax7. Whilst the cells constituting the side population do not typically enter myogenic differentiation, when cultured in isolation, subjected intramuscular transplantation, co-cultured with myoblasts or induced to express MyoD, they do form myocytes (Asakura et al. 2002). Interestingly, satellite cells also appear to be pluripotent and can differentiate to osteocytes or adipocytes following exposure to bone morphogenic proteins or adipogenic factor, even where MyoD, Pax7 and desmin have been expressed previously (Asakura et al. 2001). Therefore, primary muscle culture has the potential to include mixed cell populations. Whilst maintenance of heterogeneity in culture is required for the release of supportive growth factors (Husmann et al. 1996), and may more accurately reflect the *in vivo* environment, it is important to optimise the culture

environment to achieve the desired proportions of cell types in a reproducible fashion. In the context of these experiments, the characteristic morphology of the multinucleated myotube was identified as advantageous, particularly since this would allow imaging experiments, such as functional confocal microscopy, specific to myogenic cells without the need for potentially confounding additional fluorescent labeling. Since myotubes are post-mitotic and possess active contractile machinery, these are clearly the most closely representative of muscle *in vivo*. Previous studies suggested that demonstrable myogenicity of greater than 80% was achievable in non-passaged primary satellite cell cultures (Park et al. 2006).

3.1.6.2 Culture Techniques

Mechanical and enzymatic dissociation with collagenase or trypsin releases myogenic precursor cells from samples of fresh skeletal muscle. These cells can be identified by light microscopy and plated at the desired density, where they adhere within a few hours to an appropriate culture surface. During the first few days, the doubling time has been estimated as daily and this continues until approximately day four when alignment and fusion into myotubes occurs. Myotubes develop functional contractile machinery and appear striated on electron microscopy (Askanas et al. 1975).

Myotubes themselves are not mitotic but may incorporate additional adjacent satellite cells. Therefore the doubling time drastically reduces to approximately six further days (Le Moigne et al. 1990). This is a potentially useful feature in the context of studies on IBM since the propensity of IBM tissue to display disordered homeostasis may well reflect the postmitotic nature of skeletal muscle and its consequent inability to reduce misfolded protein load by mitotic dilution. Therefore, the induction of IBM-relevant conditions after the formation of myotubes appeared desirable. It is widely accepted that a step reduction in the concentration of serum in the growth medium is a stimulus of fusion into myotubes (Mau et al. 2008). Therefore, most primary muscle culture protocols employ two growth media, the initial comprising by fetal serum that facilitates proliferation and a subsequent differentiation medium (Fig 3.3).

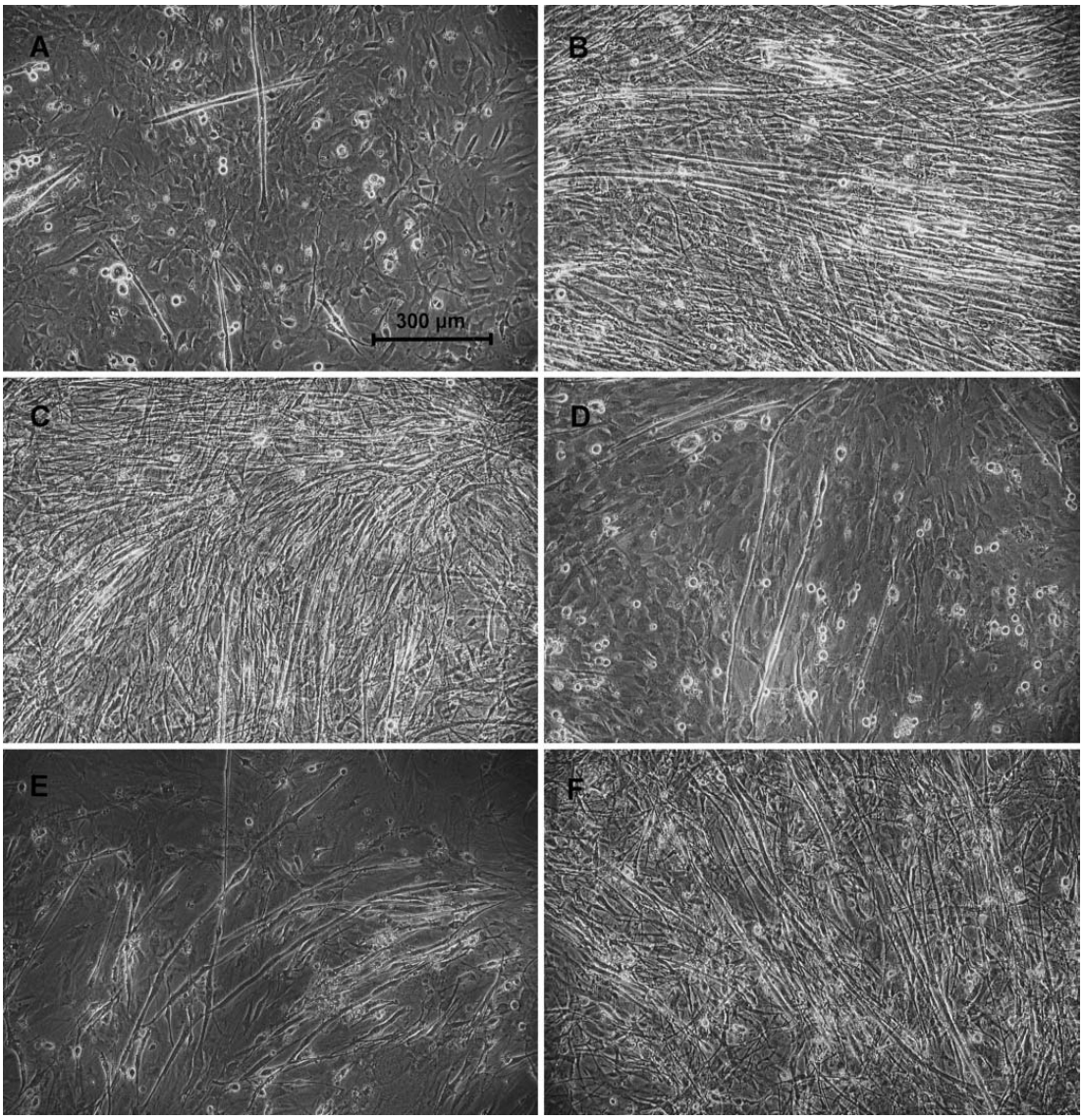

Figure 3.3 Light microscopy of satellite cell cultures forming distinctive myotubes.

Satellite cell cultures from various lines of laboratory mice at different days of cultivation in growth medium (A–D) or after a change from growth to maintenance medium at day 6 (E, F). Reproduced from (Rehfeldt et al. 2002)

3.1.7 Choice of species

Consideration was given to whether to use muscle derived from humans or rodents as the source of satellite cells. The principal advantages offered by human tissue are the presumed closer representation of human pathology and that the majority of relevant previous cellular work in IBM has occurred on cell

cultures harvested from human muscle biopsies from subjects who were subsequently found to be free of muscle disease (Askanas 1996, Schmidt 2008). However, numerous disadvantages of using human tissue were also identified. There are considerable practical hurdles to overcome if a sustainable source of human myoblasts is to be maintained. These exceed the additional legal, ethical and regulatory requirements posed by study of human tissue.

Based on the inevitability that any programme of study employing primary cell culture will require the use of multiple pieces of tissue from multiple donors, it is important to consider that human myoblast biobanks reflect an extremely heterogeneous population. They include patients of widely differing ages and genetic backgrounds, making cross-muscle culture comparison difficult to validate. Alternatively, multiple passages of individual harvests are required, which represents selection of a subclone of cells that may not represent the majority. Furthermore, it is difficult to be certain that all individuals are absolutely free of any genetic or acquired muscle condition or predisposition. Even supposing this is the case, there are substantial differences in both the absolute numbers and inherent properties of myoblasts sourced from donors of different ages. Indeed, it is proposed that such differences contribute to the sarcopenia of 'normal' ageing, which is a potentially crucial underlying susceptibility in the pathogenesis of IBM. Therefore, it was necessary to review these differences in consideration of whether to pursue a human source of satellite cells.

Whereas approximately 30% of sublaminar nuclei in neonatal rodent muscle represents satellite cells (Hawke et al. 2001), the proportion of satellite cells in adult human muscle has been estimated at only 1.3% (Mackey et al. 2009). Satellite cell number does not appear to be influenced by type or size of fibre with which those satellite cells are associated (Kadi et al. 2006). Despite the larger size of human biopsy samples than rodent muscles, any small advantage this presents is superseded by the greater availability of rodents for investigative use. Therefore, use of human tissue would provide a significantly reduced stock of satellite cells, a potential disadvantage to the development of a high throughput screening tool. The use of repeated passages to address this

issue is also undesirable; changes in satellite cell function such as the propensity to accumulate amyloid species were observed when satellite cells derived from IBM patients were studied in this way (Morosetti et al. 2010). The same study also demonstrated telomeric shortening, reduced proliferative ability and reduced differentiation in IBM patient satellite cells, which, is evidence against employing them in this work. Moreover, it was not a hypothesis of this work that IBM is a satellite cell mediated disease.

It was foreseen that comparison between cultures would form a considerable part of this work. Therefore, it was important to minimise any inherent variability in the culture system itself that might mask or exaggerate experimental effect. Differences in satellite cell function between subjects of different ages and from different muscle groups were considered. Brack and colleagues demonstrated increased Wnt signaling during ageing of satellite cells, which were also associated with increased fibrogenicity (Brack et al. 2007). This impaired myogenicity was not restored by exposure of aged satellite cells to a more youthful environment, which has important connotations for the sourcing of satellite cells in this work. It is clear that to study IBM using cultured muscle, whilst accepting the premise that underlying ageing of skeletal muscle contributes in some way to the disease, the age of the primary cell donor must be standardised as far as possible.

For these reasons, the disadvantages associated with use of human myoblast cultures promoted the use of rodent cultures to the preferred initial choice. Such disadvantages presented by the use of human cultures may be largely superseded in the context of genetic conditions, where the direct representation of the disease by cells harvested from an affected donor confers a significant benefit. Although, as described above, genetic forms of 'IBM' exist, these are substantially phenotypically and distinct to the sporadic condition. They are also extremely rare, precluding realistic use in this context.

Upon deciding to pursue rodent derived cultures, it was apparent that neonatal pups would probably represent the most efficient source of satellite cells. Even accounting for the increasing size of muscle with age, the absolute number of

satellite cells reduces with advancing age, reportedly from $3.1x10^5$ in EDL aged one month versus $1.3x10^5$ at 24 months (Gibson et al. 1983).

3.1.8 Specific aims of this Chapter

1. To optimise a protocol for primary myogenic cell culture, with high myogenicity and myotube formation.

2. To determine whether IBM-relevant pathology can be induced consistently in these cells.

3.2 Results

The first step in the development of an *in vitro* model of IBM pathology was to optimise the technique of culturing satellite cells to differentiate into myocytes and myotubes that could then be maintained sufficiently for further experimentation. This process began with evaluation of mouse and rat primary satellite cell cultures before examination of various plating densities and media constituents. Subsequently, several myogenic cell purification techniques were compared, including pre-plating, density centrifugation and fluorescently activated cell sorting (FACS).

3.2.1 Neonatal mouse satellite cell cultures

Using the standard culture protocol (see Chapter 2: Methods), satellite cells harvested from the hindlimb muscles of wild-type C57-B6/SJLF1 neonatal mice at postnatal day 0-4 were plated at 50 to 100,000 / cm^2. A variety of culture conditions were evaluated. First medium change, which removes debris remaining from the harvest process or detached cells, was evaluated at either 24 or 48 hours. Further examination was made on the effect of different media constituents (between 20 and 30% fetal calf serum (FCS), between 5 and 15% horse serum (HS), and with or without chick embryo extract). Demonstrable myogenicity of up to 44% (±12%, n=5 cultures per condition, minimum of 6 wells per culture) was achieved, with a myotube fusion index of 23% (±8%, n=5) (Figure 3.4) Based on cell morphology, the non-myogenic fraction predominantly comprised fibroblasts, although imunocytochemical staining for fibroblast specific markers was inconsistent and some cells that assumed a fibroblastic morphology demonstrated myocytic features on immunocytochemistry, as has been described previously (Molnar et al. 1996). Absolute variability in myogenicity between individual wells derived from the same harvest was up to 27%. Comparison between harvests demonstrated an absolute variability in myogenicity of 18%. Mouse satellite cell cultures were typically limited to approximately 7 days *in vitro*, primarily due to detachment from the coverslip.

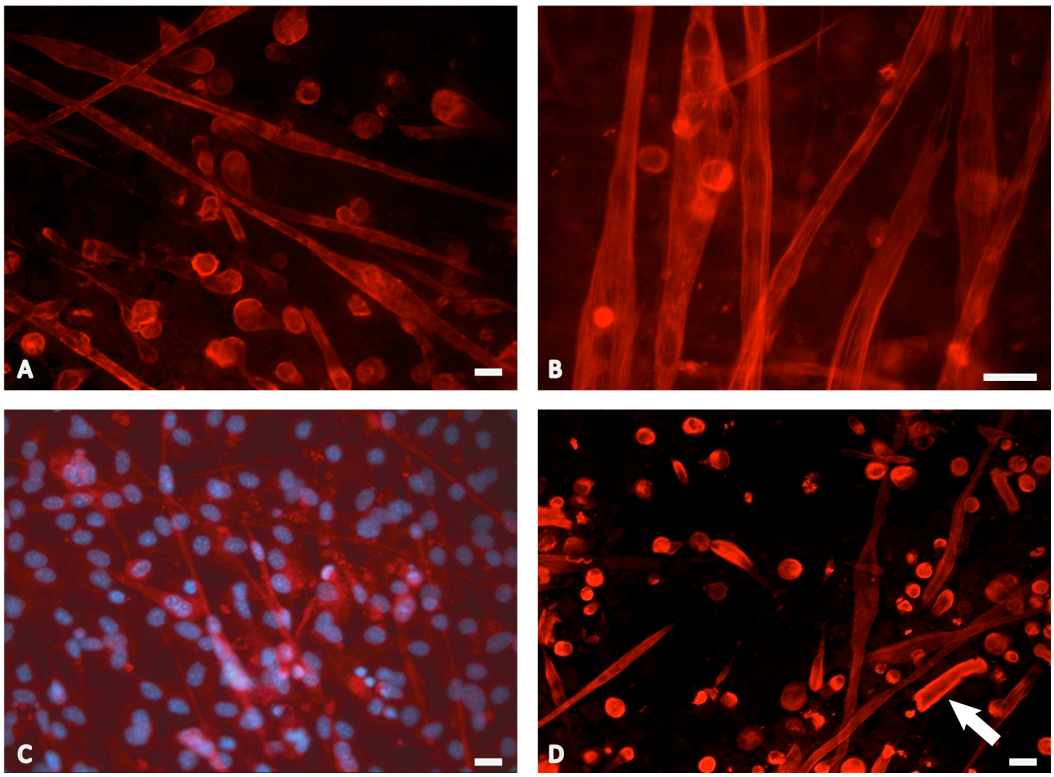

Figure 3.4 Immunocytochemisty of mouse satellite cell cultures

Myogenic cells were manifest as elongated, multinucleated myotubes, or as myocytes. The latter were more common in most experiments. Co-stained DAPI images suggested a high proportion of cells were not demonstrably myogenic (C). By 7 days *in vitro*, there was evidence of detached or fragmented myotubes (arrow in D). Anti-myosin heavy chain (red). Nuclei labeled with DAPI (blue). Scale Bars = 20μm

3.2.2 Neonatal rat cultures

In light of the considerable variation in myogenicity demonstrated by mouse satellite cell cultures, the standard culture protocol was then applied to satellite cells harvested from neonatal wild-type Sprague Dawley rats at postnatal day 0-3. Approximately $6x10^6$/ml cells for subsequent culture were yielded per animal. An isolated preliminary experiment demonstrated myogenicity of 54%, superior to that demonstrated in neonatal mouse culture. Additionally, the fusion index of 67% was greater, with the majority of cells forming distinctive, frequently aligned multinucleated myotubes. Fragmentation and detachment were less apparent than in mouse cultures. Indeed, cultures were maintained for 14 days *in vitro* (DIV) prior to detachment, which was approximately 7 days superior to neonatal mouse cultures. Continued culture beyond the point of detachment demonstrated that remaining plated cells were then apparently induced to differentiate to myotubes (Figure 3.5). It was noted that the lack of hair on neonatal rat pups, unlike their mouse counterparts, might reduce the risk of subsequent culture infection. Therefore more detailed evaluation of different culture conditions was performed to optimise the protocol using rat satellite cells.

3.2.3 Culture Medium

Cultures were performed using a variety of different of medium constituents, in order to optimise the conditions for differentiation to myogenic lineage. Subtle differences in the constitution of growth medium and timing of medium changes had significant effects on both overall myogenicity and the differentiation of myogenic cells into mature myotubes (Table 3.2). The highest myogenicity as assessed by desmin immunostaining (mean 78%, ±7%, n=3) followed the initial use of 25% Fetal Calf Serum, as proliferation medium, then 10% Horse Serum, as differentiation medium, at 48 hours onwards, with inclusion of Chick Embryo Extract. This was significantly greater than in cultures using the same medium that were left for 48 hours prior to the first medium change (mean 61%, ±6%, $p<0.05$). Non-significant differences were observed between this medium and those employing subtly different concentrations of FCS or HS.

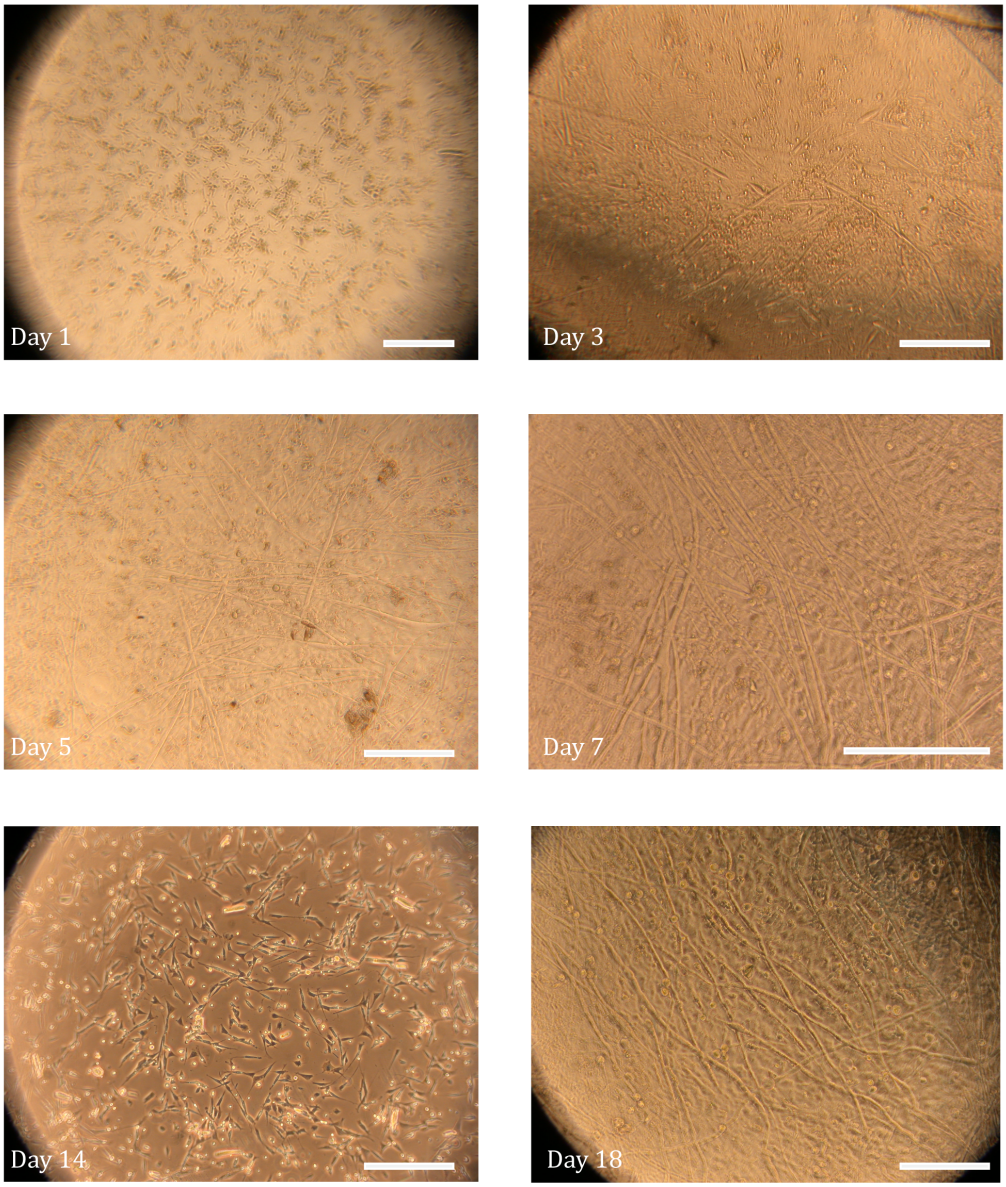

Figure 3.5 Maturation of rat satellite cell cultures

Light microscopy of satellite cells over time demonstrates differentiation into elongated myotubes. After detachment of the myotubes, typically at day 14, continued culture of the remaining adherent cells leads to further myogenesis and differentiation to myotubes. Scale Bars=2mm

Time of First Medium Change (hrs after plating)	Spacing of Subsequent Medium Changes (hrs)	Fetal Calf Serum (%)	Horse Serum (%)	Chick Embryo Extract (+/-)	**Myogenicity (%, SEM)**	**Fusion index (%, SEM)**
24	48	20	15	-	**72 ±6**	**72 ±3**
24	48	20	10	-	**70 ±5**	**81 ±3**
24	48	20	10	+	**74 ±4**	**80 ±5**
24	48	25	10	+	**78 ±7**	**86 ±4**
24	48	30	10	+	**69 ±5**	**77 ±4**
24	48	25	5	+	**63 ±4**	**81 ±7**
24	72	25	10	+	**71 ±5**	**72 ±7**
48	48	20	10	+	**64 ±7**	**83 ±5**
48	48	25	10	+	**61 ±6**	**77 ±3**

Table 3.2 Effect of culture medium constitution on culture myogenicity and differentiation

All cultures subject to pre-plating. Mean percentages for myogenicity and fusion index at 7 days are shown to 2 significant figures. (n=3)

Nevertheless, this medium constitution was selected for application to all subsequent cultures. These media all conferred a high fusion index, the highest being 86% (±4%, n=3) as demonstrated with light microscopy and immunocytochemistry by formation of characteristic elongated, multinucleated myotubes (Figure 3.6). Regardless of medium, cultures could be maintained for up to 14 days, at which time spontaneous contraction of myotubes, viewable on light microscopy, precipitated detachment of cells from the culture well.

3.2.4 Plating density

Plating density was also observed to increase the rapidity and extent of fusion to myotubes, proportionally up to 100,000 cells/cm^2. Beyond this, confluence was demonstrated at approximately 7 days and detachment occurred by 10 days, thereby reducing the lifespan of the culture. Therefore, the 100,000 cells/cm^2 standard was subsequently applied routinely.

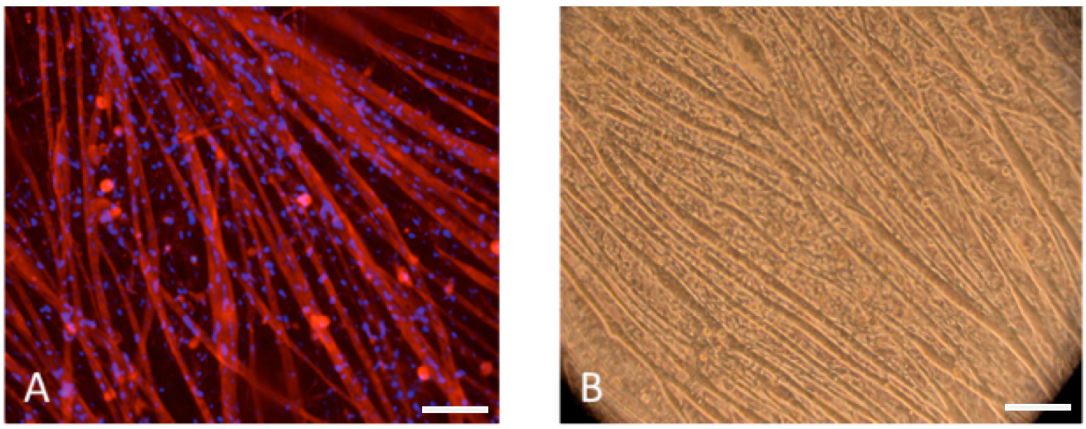

Figure 3.6 Comparison of different culture media on satellite cell cultures

A: By 7 days *in vitro*, myocytes fuse to form multinucleated myotubes, visible with fluorescently labelled desmin immunostaining (red). Nuclei are labelled with DAPI (blue). (Scale Bar = 100μm)

B: Light microscopy at 20x magnification of satellite cell culture at 7 days *in vitro* demonstrating characteristic elongated structure and alignment of orientation. (Scale Bar = 100μm)

3.2.5 Culture purification techniques

After optimising culture medium and seeding densities, a high proportion of myogenic cells was achieved. However, for the purposes of future high sensitivity biochemical analysis, several established techniques for further purification of myogenic cultures were examined.

3.2.5.1 Preplating

Pre-plating the cell suspension after completing the preparation of cells for culture within a plastic container, prior to transfer of the suspension to growth plates, is reported to increase the myogenic fraction by exploiting the greater propensity of fibroblasts to adhere to plastic surfaces. The impact of this technique was examined and preplating for 15-20 minutes prior to final plating improved myogenicity.

Preplating was associated with a change from 69%, (±6%, n=3) myogenic purity to 78% (±7%, n=3) (Figure 3.7). This difference was not statistically significant, reflecting the fairly broad variance in purity between cultures under equivalent conditions. Nevertheless, since pre-plating was a straightforward process to incorporate in the protocol, and was not associated with a decline in overall cellular yield, it was included in subsequent cultures.

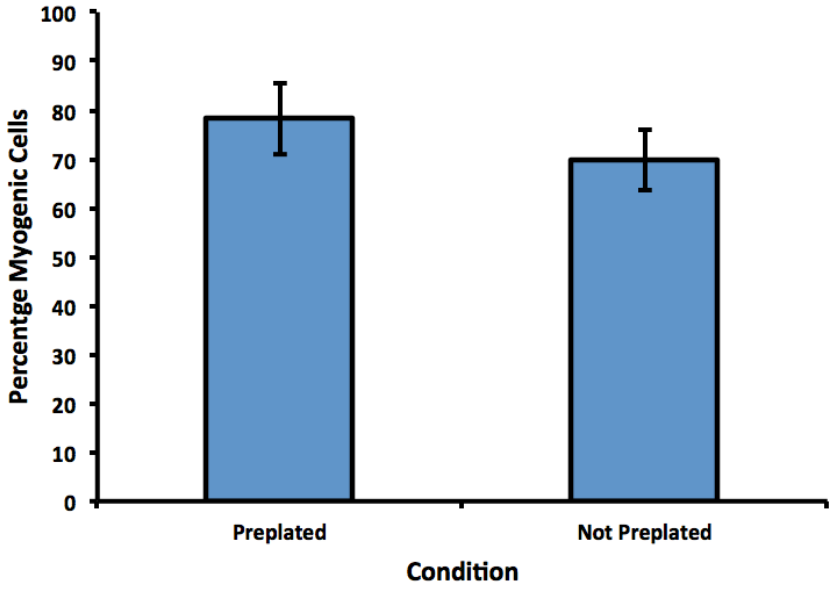

Figure 3.7 Effect of Preplating on Myogenicity

The bar chart compares preplated and non-preplated cultures. This technique did not significantly affect the proportion of myogenic cells.
(Error bars = SEM, n=3)

3.2.5.2 Differential centrifugation

Various differential centrifugation gradients and centrifugation forces were tested on muscle cell suspensions to isolate fractions of high myogenicity (Fig 3.8). Those which resulted in most consistent separation of cell subtypes were 90%/40%/25% layers and 70%/50%/35% layers, spun at 1250g. Three bands of cellular material were collected and cultured separately to determine myogenicity. Band 2 (as indicated in Fig 3.8) was that which consistently displayed the highest myogenicity on subsequent culture and was also the

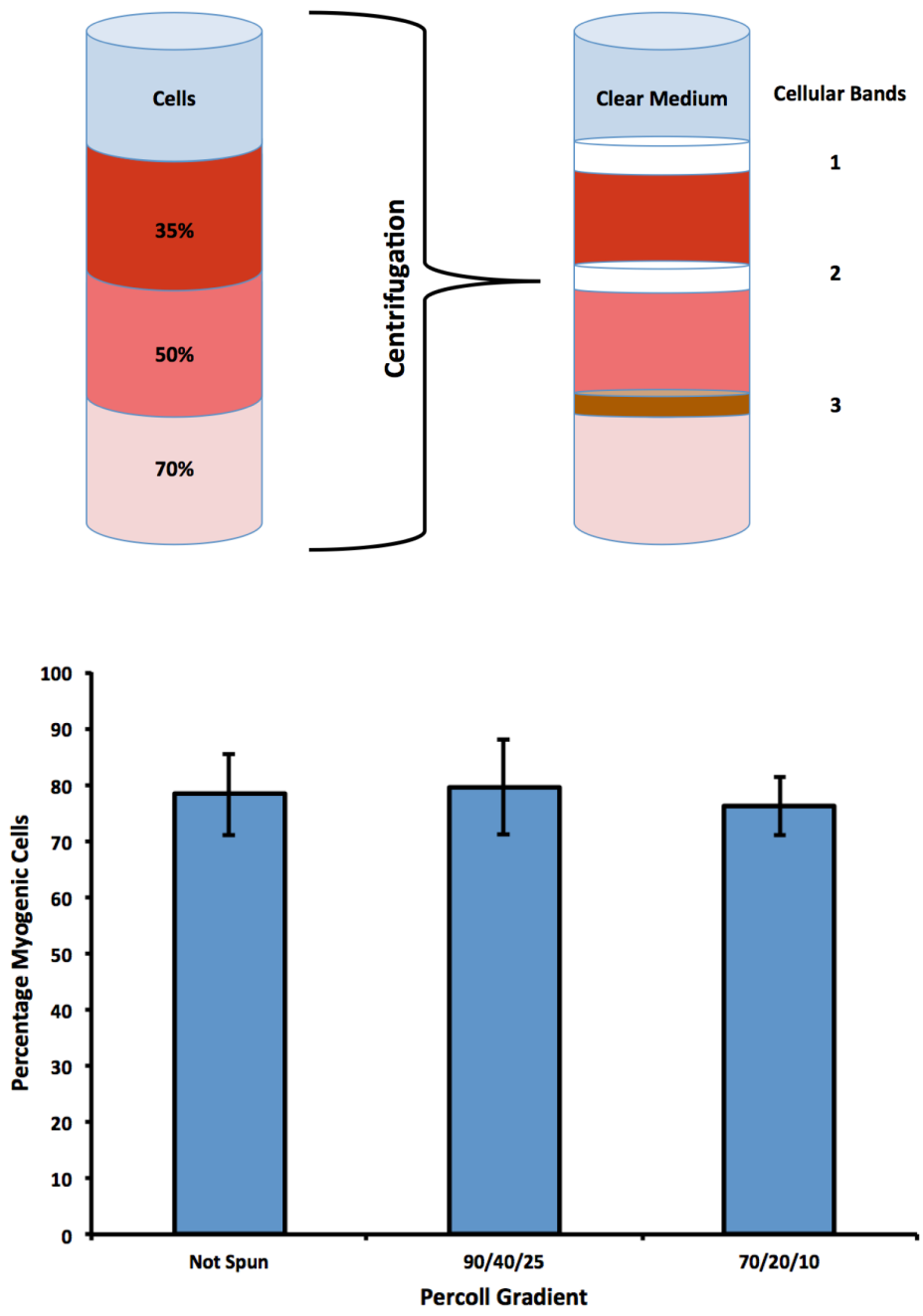

Figure 3.8 Effect of differential centrifugation on myogenicity

Top: schematic representation of the layered density technique with cell fraction separation.

Bottom: Bar chart demonstrates the effect of differential centrifugation on myogenicity of cultures. All represent cultures from cellular band 2 of the respective experiment.

(Error Bars = SEM, n=3,).

consistently largest band. Band 1 also demonstrated predominant myogenicity, at approximately 11% absolute reduction compared with band 2. Band 3 was typically smaller and displayed a reddish colour, in contrast to the white colour of the other two bands. It did not yield sufficient cell numbers to allow cultures of comparable plating densities. When cultures from band 2 were compared with those prepared without the use of Percoll®, no significant difference in myogenicity was detected (Fig 3.8, bar graph). Furthermore, the use of differential centrifugation reduced the final cellular yield substantially, from approximately 6 million/ml per animal to 2.5 million/ml per animal, necessitating the use of more animals to achieve an equivalent number of culture wells. Therefore, this technique was not incorporated into the final culture protocol.

3.2.5.3 Fluorescence Activated Cell Sorting (FACS)

FACS allows highly specific identification or selection of a desired cell type through simultaneous detection of multiple surface antigens using antibody labelling. FACS has previously been applied to satellite cell populations, often in work examining subtypes of differentiating cells (Ieronimakis et al. 2010). Briefly, cells in suspension are passed through a high flow stream in which an electrical charge is applied to the liquid droplet containing each cell according to it's physical or fluorescent properties as it passes through the device, thereby allowing sorting on this basis. FACS was tested here to determine whether a subpopulation of myogenic specific cells could be isolated from overall cell population after initial harvesting. This would allow the selective culture of pure myogenic cells at a similar stage of maturation at the time of plating.

3.2.5.4 Unlabelled Cells

Before FACS analysis, an initial examination of the cell population based upon size and morphology was performed on cell suspensions in order to identify any distinct subpopulations (Figure 3.9). Examination of Side Scattering (SSC) of light and Forward Scattering (FSC) in unlabelled suspensions (i.e. not exposed

to any antibody) suggested there might be two cell populations, distinguished by size and shape. Propidium Iodide (PI) staining identified a small minority (2.8% ±0.2%) of non-viable cells within the original suspension.

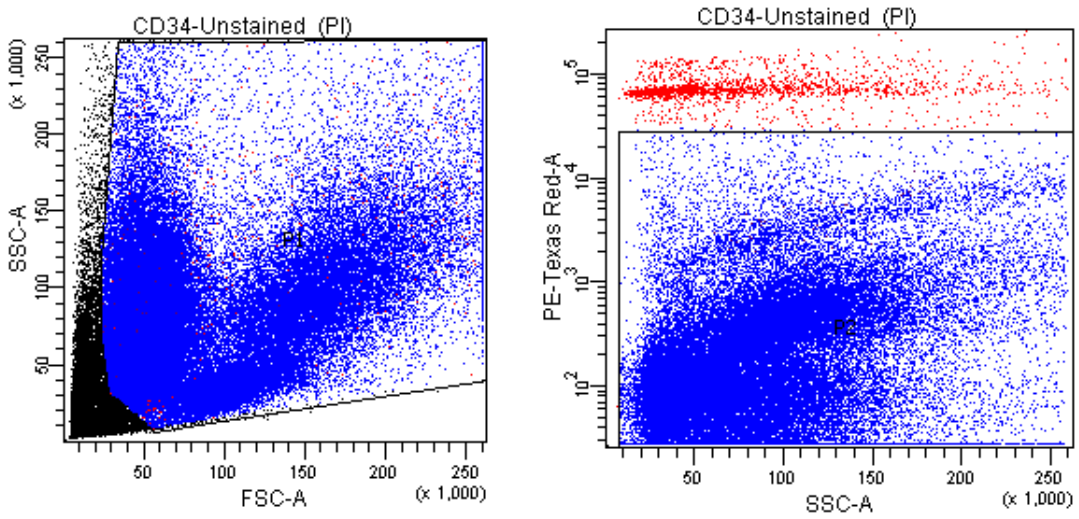

Figure 3.9 FACS analysis of unlabelled satellite cells in suspension

Blue and red dots represent individual cells. SSC=side scatter (arbitrary units). FSC=forward scatter (arbitrary units). PI=Propidium Iodide. Scatter plots of the physical characteristics of cells (left) suggests two types constitute the overall cell population. PE-Texas Red filtering (y-axis, right) identifies PI staining of non-viable cells (red dots), which represents approximately 3% of all cells.

3.2.5.5 Antibody Labelling

Some satellite cells are distinguished from other cell types by their expression of the sialomucin surface receptor CD34 (Alfaro et al. 2011). Therefore, to determine whether this sub-group could be identified and isolated from the whole cell population, FACS analysis was conducted after exposure to anti-CD34 antibody. A very small proportion, approximately 0.2%, of all suspended cells demonstrated positive CD34 labelling (Fig 3.10). There was no impact from increased incubation time up to 1 hour. Two possible reasons for the low yield of CD34 positive cells were tested. First, whether expression of CD34 required differentiation beyond the stage at which the cells were harvested from the animal and, secondly, whether the use of enzymatic digestion in the culture protocol might alter the expression of cell surface markers. The latter hypothesis has been described in other cell populations *in vitro* (Abuzakouk et al. 1996). Therefore, cells were plated for 24 hours prior to FACS analysis.

However, the process of extracting these cells from culture plates resulted in an intolerably high degree of cell death. Thereafter, the culture protocol was adjusted to replace the use of collagenase with trypsin and, subsequently, with purely mechanical dissociation of muscle using scissors and pipette trituration. Although mechanical dissociation was associated with an increased CD34 positive fraction, the cells that were subsequently sorted and cultured on this basis failed to differentiate after seven days *in vitro*. Different established markers of myogenic lineage were tested using the same technique, including NCAM (Fig 3.11) but very few cells demonstrated positive binding with the antibody. Therefore, FACS was not used as a method to increase cell purity in subsequent cultures.

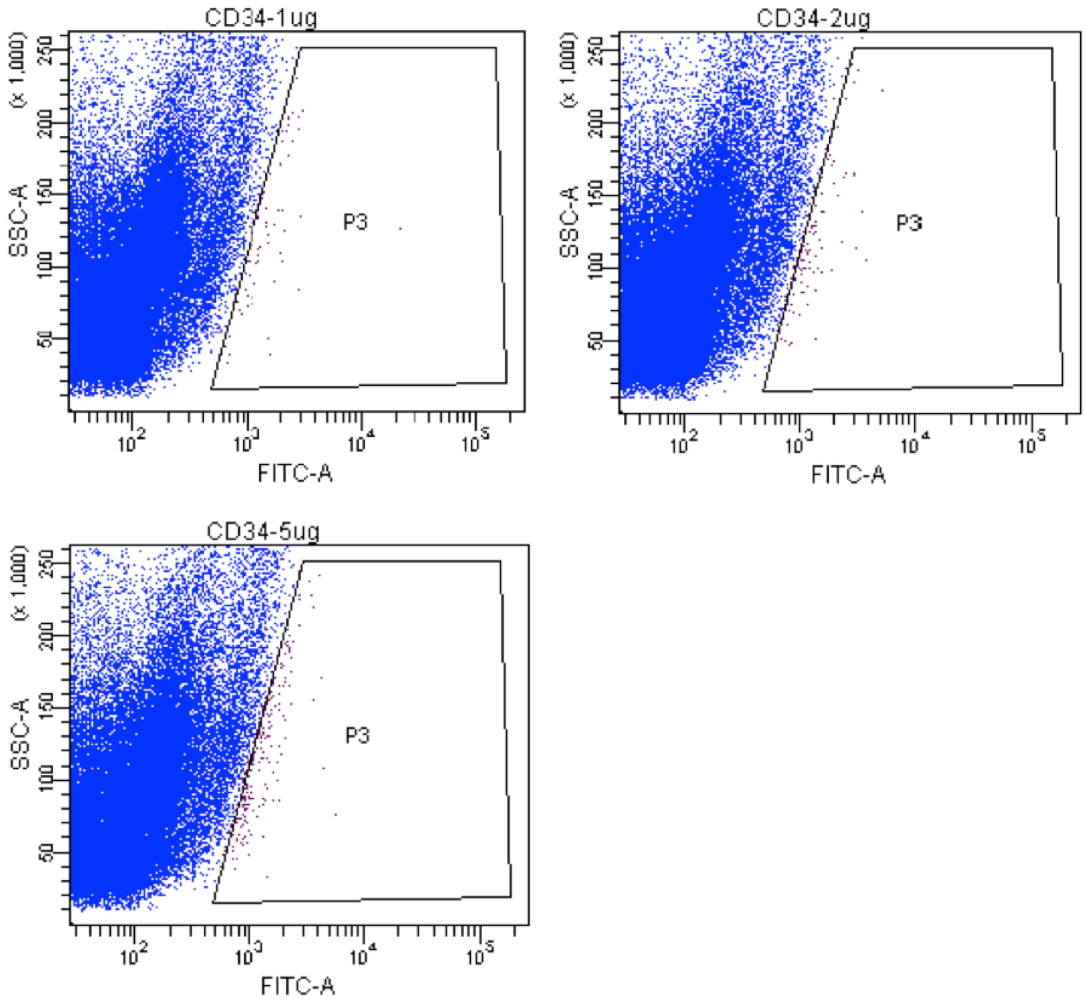

Figure 3.10 FACS analysis of CD34 binding in a satellite cell suspension

Standard thresholds were applied to detect the proportion of cells in suspension (represented by individual dots) bound by anti-CD34 antibody (identified by dots within black bordered rhomboids labeled P3). This represented only 0.2% of the cell population. Concentrations of antibody exposure at 1µg, 2µg and 5µg/ml are shown (clockwise from top left).

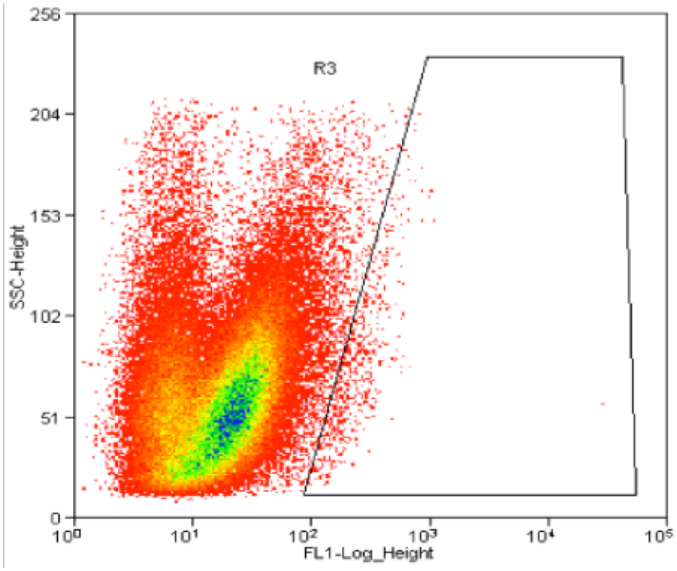

Figure 3.11 FACS analysis of NCAM binding in a satellite cell suspension

Dots represent individual cells. Those representing the small number of cells successfully labelled with anti-NCAM antibody are contained in the black rhomboid.

3.2.6 Induction of IBM-like Pathology in Myogenic Cells

Optimisation of medium constituents and the incorporation of pre-plating allowed cultures of consistently highly myogenicity to be maintained. The next step was to determine how to recapitulate salient aspects of IBM pathology. The following histopathological features of IBM were considered particularly important characteristics:

1. Upregulation of MHC Class I
2. Cytoplasmic Translocation of TDP43
3. The formation of proteinaceous intracellular inclusions
4. Activation of NFκB

The upregulation of MHC Class I was considered essential, on the grounds that absence of this feature on muscle biopsy *in vivo* is legitimately used as evidence to query the diagnosis of IBM and its potentially central pathogenic role.

Previous studies on human satellite cells suggested two stimuli with which to trigger the development of IBM features *in vitro*. Over-expression of βAPP had

been shown to result in cytoplasmic inclusion formation, mitochondrial impairment and proteasomal inhibition (Askanas et al. 1996; Askanas et al. 1997). In turn, exposure to inflammatory cytokines IL1β, TNFα or IFNγ had been demonstrated to upregulate endogenous expression of βAPP (Schmidt et al. 2008). Furthermore, IFNγ was a potent inducer of MHCI, including in cultured myocytes (Bao et al. 1990). Therefore, both of these methods were evaluated further using primary rat satellite cell cultures.

3.2.7 Overexpression of βAPP

First, a variety of βAPP transfection conditions were examined to optimise the overexpression of βAPP and/or β-amyloid oligomers with Lipofectamine™. Given the theoretical potential for selective cytotoxicity from the transfection process, the impact on myogenicity of each condition was also examined. The effect of βAPP-containing vector transfection was compared against that of an empty vector as control. All conditions were also compared to a further control of non-transfected cultures.

3.2.7.1 The effect of βAPP transfection protocol on culture myogenicity

Compared to untransfected cultures, transfection with βAPP reduced the percentage of myogenic cells at all DNA to Lipofectamine™ ratios, but only to a significant extent at ratios of 1:1, 2:1 and 5:1 ($p<0.05$, n=3) (Fig 3.12). The greatest reductions were observed at ratios of 1:1 and 2:1, where the myogenic proportion was 23% ±7.2% and 31% ±5.4% respectively (n=3). Only at these ratios was a significantly lower myogenicity observed compared to empty vector ($p<0.05$, n=3). The myogenicity associated with empty vector transfection itself (58% ±7.6%, n=3) was not significantly different to that of untransfected cultures, implying the βAPP-independent aspects of the technique are not selectively cytotoxic to myogenic cells. The apparent reduction of myogenicity was attenuated at all ratios by transfecting at the later time point of 96 hours post-plating rather than at 48 hours (Fig 3.12). However, only at the 2:1 ratio was the comparison of these time points significant 31%

±2.3% to 49% ± 3.5% (n=3, p<0.05). Overall, the DNA:Lipofectamine ratios of 3:1 and 4:1 demonstrated greatest myogenic purity at both the 48 and 96 hour transfection time points.

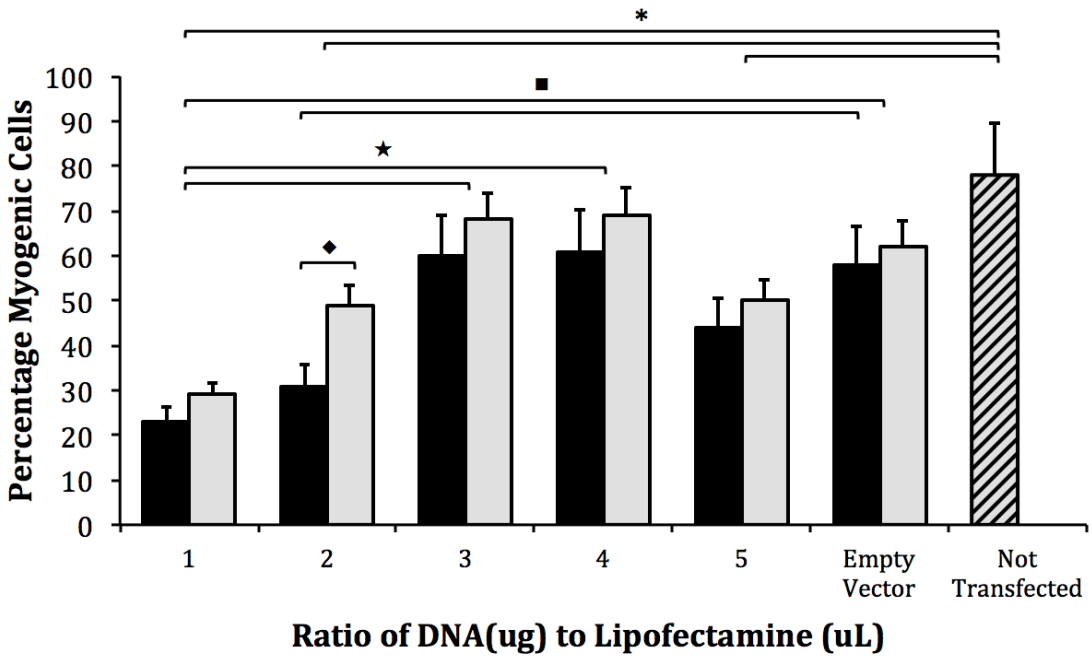

Figure 3.12 Effect of βAPP transfection conditions on culture myogenicity

When applied to βAPP transfection, the DNA:Lipofectamine ratios of 1:1 and 2:1, significantly reduced the subsequent proportion of myogenic cells compared to empty vector transfection and untransfected cultures. This was not observed at higher ratios between 3:1 and 5:1. Transfection at 96 hours *in vitro* (grey bars), compared to at 48 hours (black bars) was generally associated with higher myogenicity, but this was only significant at the 2:1 transfection ratio.

(Error Bars=SEM, n=3, Asterisk=p<0.05 vs. untransfected cultures, Square=p<0.05 vs. empty vector transfection, Star=p<0.05 between transfection ratios, Diamond=p<0.05 between time points)

The distinctive morphology of the multinucleated myotube was considered potentially advantageous for subsequent experiments in which myogenic cells would need to be distinguished from non-myogenic cells. Therefore, it was preferable to maintain a high fusion index (the proportion of myogenic cells

represented by myotubes). Across all the conditions tested, transfection at 48 hours with empty vector or βAPP significantly reduced the fusion index ($p<0.05$, $n=3$ per condition). This effect was most marked at the 1:1 DNA to Lipofectamine™ transfection ratio, where 17% (±6%) of myogenic cells were myotubes, compared to 86% (±4%, $p<0.05$, $n=3$) in untransfected controls. This implies the transfection technique either delayed maturation of myocytes or their fusion directly, or affected these indirectly through cytotoxicity and reduced cell density. At the transfection ratios between 3:1 and 5:1, no significant difference in fusion index was observed between βAPP transfected and empty vector transfected cultures, suggesting no effect was conferred by βAPP *per se* (Fig 3.13).

The reduction in myotube formation associated with transfection was attenuated by transfecting cultures at 96 hours after plating rather than 48 hours (Fig 3.14). At the 96-hour time point, maturation to myotubes approached that of standard culture conditions and, for empty vector and DNA:Lipofectamine ratios between 3:1 and 5:1, there was no significant difference to untransfected controls. Therefore, the 96-hour time point conferred some advantage over the 48-hour time point; myocyte differentiation was not significantly altered versus standard culture conditions, and demonstrated the high fusion index desired for further experimentation.

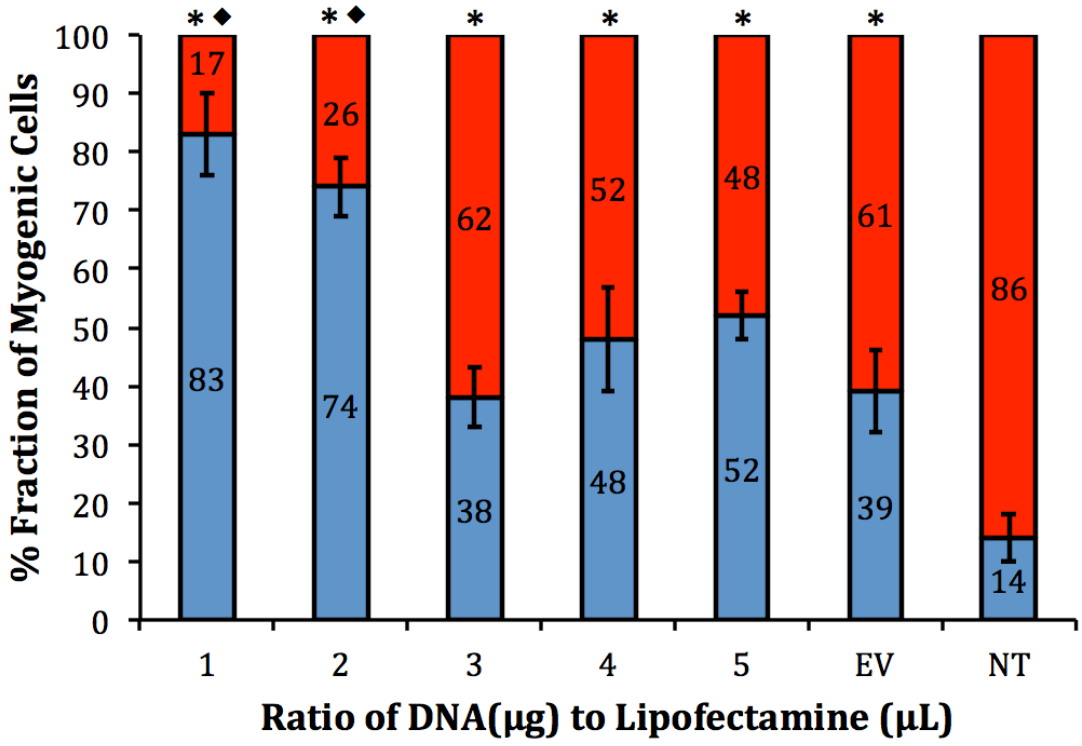

Figure 3.13 Effect of transfection at 48 hours *in vitro* on myogenic cell types

Transfection reduced the fusion of myocytes to form myotubes compared to untransfected cultures. No significant difference was observed between empty vector and DNA:Lipofectamine ratios 3:1, 4:1 and 5:1. Blue bars=myocytes, Red bars=myotubes, EV=empty vector transfection, NT=not transfected.

(Error Bars=SEM, n=3, Asterisk=$p<0.05$ vs. NT, Diamond=$p<0.05$ vs. EV)

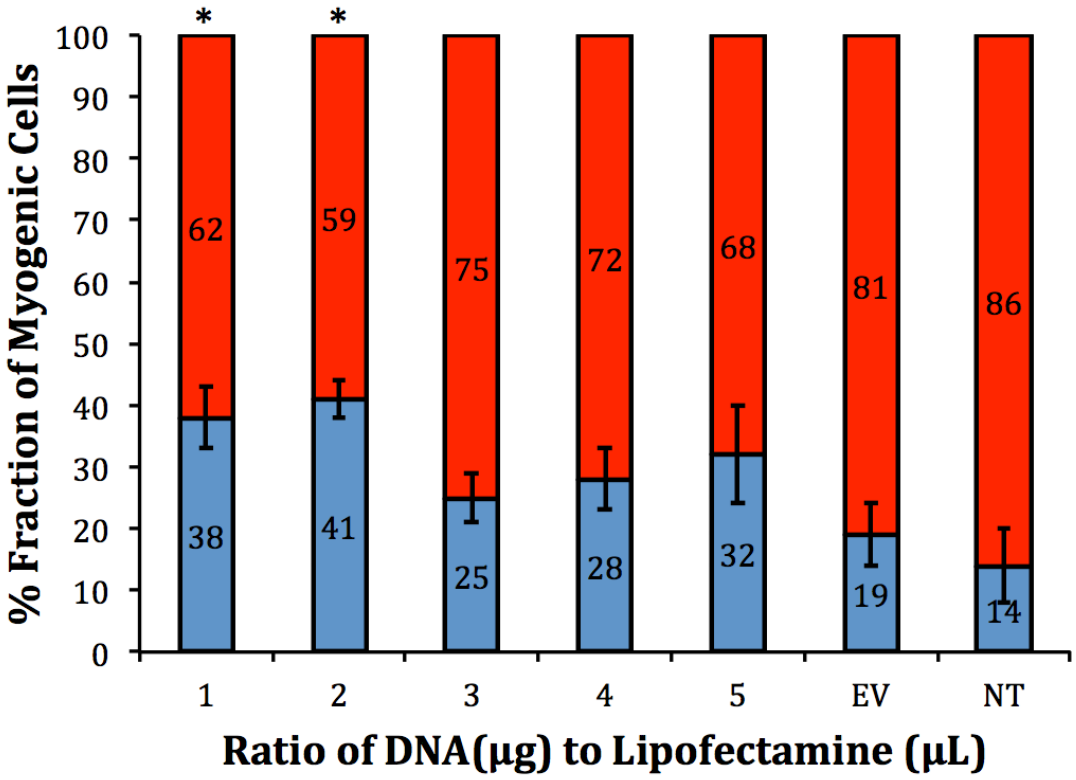

Figure 3.14 Effect of transfection at 96 hours *in vitro* on myogenic cell types

In contrast to transfection after 48 hours, transfection at 96 hours was not associated with significant alteration of the myogenic cell sub-types compared to untransfected controls. Blue bars=myocytes, Red bars=myotubes, EV=empty vector transfection, NT=not transfected.

(Error Bars=SEM, n=3, Asterisk=$p<0.05$ vs. NT)

3.2.7.2 The effect of βAPP transfection on expression of β-Amyloid oligomers

For western blot analysis, the optical density of bands corresponding to βAPP, Aβ42 and Aβ40 was determined relative to contemporaneous protein control, α-tubulin (Fig 3.15). Transfection with the βAPP plasmid significantly upregulated the expression of each of these proteins, compared to either non-transfected cultures or empty vector (EV) control. Versus EV, after βAPP transfection the relative expression of βAPP increased 2.51 fold ($p<0.01$), Aβ42 increased 2.59 fold ($p<0.01$) and Aβ40 increased 5.00 fold ($p<0.01$).

The increase in expression of amyloid species demonstrated by western blots was supported by quantification of the proportion of myogenic cells that were

immunoreactive for βAPP, Aβ42 and Aβ40. This was compared at the 48 and 96-hour transfection time points.

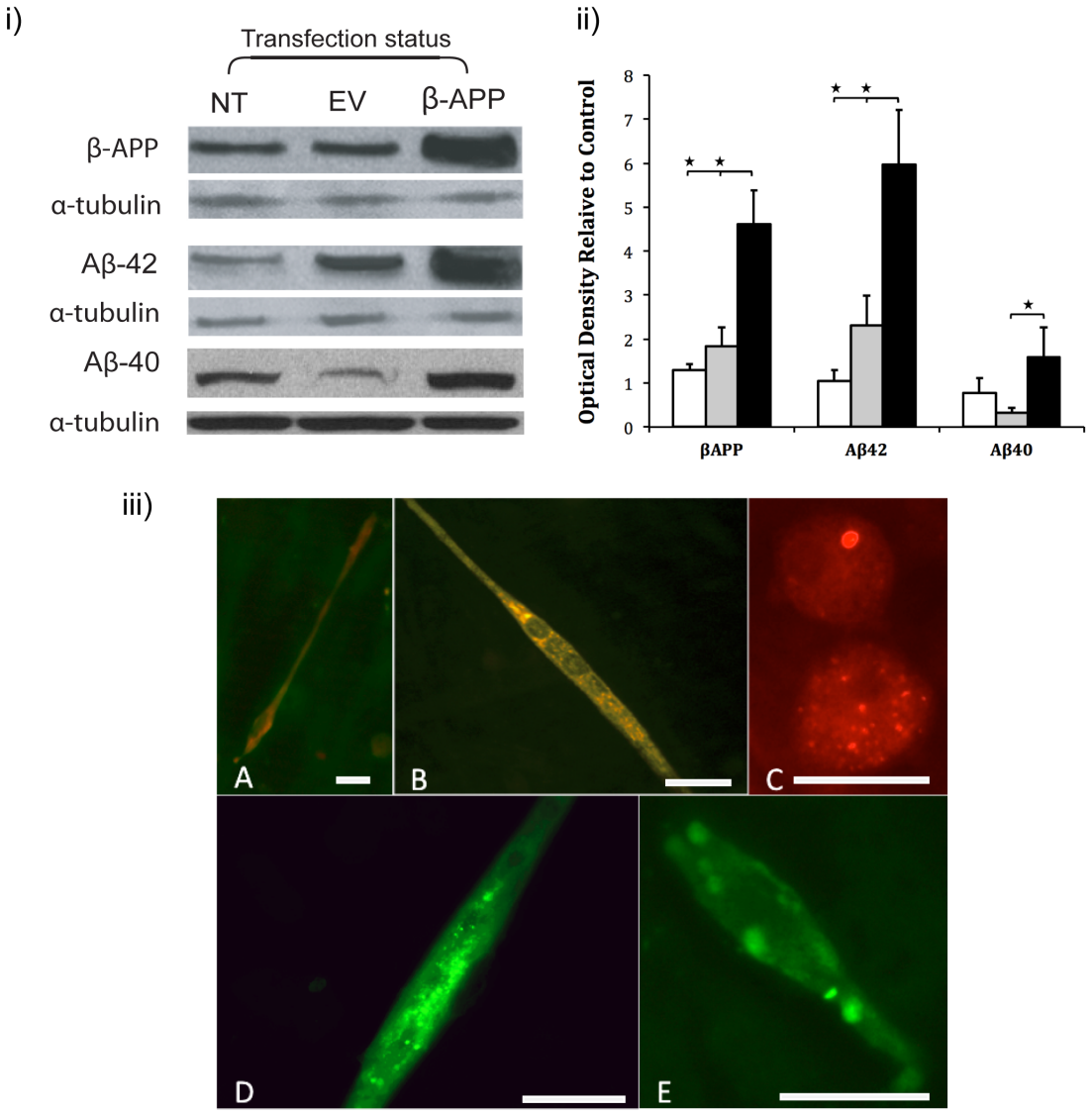

Figure 3.15 Effect of βAPP transfection on amyloid expression

i) Representative western blot comparing expression levels of βAPP and amyloid oligomers under non-transfected (NT), empty vector transfected (EV) and βAPP transfected culture conditions.

ii) Optical density of western blots for amyloid species. White bars=non-transfected, Grey bars=Empty Vector, Black Bars=βAPP transfected (n=3, Error Bars=SEM, Stars=$p<0.05$)

iii) Immunocytochemisty of myocytes and myotubes transfected with βAPP demonstrated intracellular protein aggregates. A: Positive desmin (green) and

Aβ42 staining (red) within a myotubes B: Colocalisation of ubiquitin and Aβ42 (yellow inclusions) was observed in the cytoplasm. C/D/E: Frequently, Aβ42 was demonstrated as discrete intracellular inclusions, of varying patterns such as large cytoplasmic bodies in C and E, or scattered cytoplasmic and perinuclear bodies in D. (Scale bar=50μM)

Next, the proportion of myogenic cells demonstrating positive immunostaining for amyloid oligomers was quantified. Aβ40, the oligomer considered to be less cytotoxic than Aβ42, showed that there was a higher constitutive expression of this protein than Aβ42 by untransfected cells (36% ±2.6%, n=3). After transfection at 48 hours, Aβ40 expression was elevated fairly uniformly across the tested transfection conditions, with significant increases versus empty vector control demonstrated, in a broadly proportional manner, at all transfected ratios above 1:1 (Fig 3.16). At 3:1, the most effective ratio regards Aβ42 expression, the proportion of cells demonstrating Aβ40 positivity was elevated to 57% (±3.7%, n=3, $p<0.05$). This increase was significant regardless of whether all myogenic cells or purely myocytes, rather than elongated multinucleated myotubes, were studied.

Following transfection at 96 hours after plating, there was also significant elevation in Aβ40 positivity across all transfection ratios (Fig 3.17). However, compared with the 48 hour time point, the typical proportion of myogenic cells positive was slightly reduced, for example 57% ±3.7% versus 43 ±4.1% at the 3:1 transfection ratio. At the majority of transfection ratios, this difference was less marked when only myocytes rather than the overall myogenic population were considered. This implies that multinucleated myotubes, which represent an increasing proportion of the myogenic culture population between the time points studied, are either less likely to be transfected than myocytes or more quickly undergo cell death if they are transfected, perhaps indicative of increased vulnerability to protein overexpression in the terminally differentiated, post-mitotic state.

Aβ42 immunostaining revealed that transfection with the βAPP plasmid at 48 hours, using transfection ratios of 1:1, 3:1, 4:1 or 5:1 significantly increased the expression of Aβ42 in myogenic cells versus empty vector transfection (Fig 3.18). Compared with 12% ±2.4% in non-transfected cultures, a βAPP

transfection ratio of 3:1 DNA (μL) to Lipofectamine (μL) resulted in 63% ±8% of myogenic cells demonstrating positive Aβ42 staining ($p<0.01$, $n=3$). Empty vector had no significant impact on Aβ42 expression, indicating that the upregulation of Aβ42 was not a byproduct of the transfection process *per se*. At the 96-hour transfection time point, there was also significant elevation of Aβ42 positivity, at ratios between 1:1 and 4:1 (Fig 3.19). As was the case at the 48 hour time point, the most significant increase was observed using the 3:1 ratio at approximately 8-fold that of empty vector ($p<0.01$, $n=3$).

A consistent feature of cultures was the greater proportion of myocytes than mature multinucleated myotubes which appeared to express either or both amyloid oligomer. This was reflected across transfection conditions, notably at 3:1, where over 60% of myocytes demonstrated Aβ42 positivity, whereas 42% of the overall myogenic population were positive ($p<0.05$). The differential expression by myocytes and myotubes was less pronounced for Aβ40 than for Aβ42 staining but remained apparent (mean 69% of myocytes at 3:1).

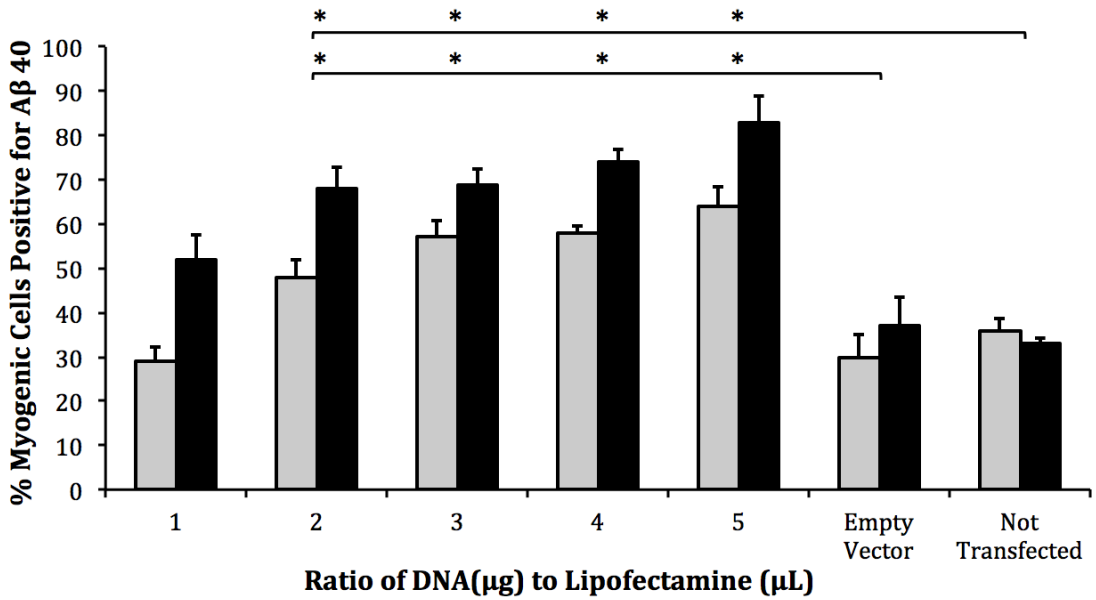

Figure 3.16 Effect of βAPP transfection at 48 hours *in vitro* on expression of Aβ40 in myogenic cells

At transfection ratios between 2:1 and 5:1, βAPP transfection was associated with a significantly elevated proportion of myogenic cells that were Aβ40 immunopositive compared to empty vector transfection and untransfected controls. Grey bars = all myogenic cells, Black bars = myocytes only

(Error Bars=SEM, n=3, Asterisk=$p<0.05$)

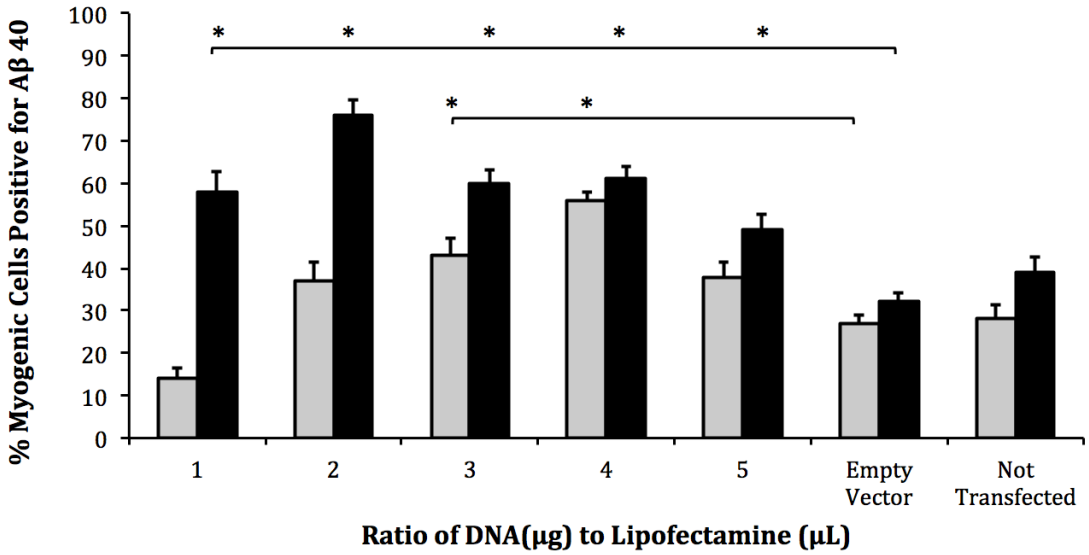

Figure 3.17 Effect of transfection at 96 hours *in vitro* on expression of Aβ40 in myogenic cells

At all transfection ratios tested, βAPP transfection was associated with a significantly elevated proportion of myocytes that were Aβ40 immunopositive compared to empty vector transfection. At transfection ratios 3:1 and 4:1, this effect was maintained when all myogenic cells were compared. Grey bars = all myogenic cells, Black bars = myocytes only

(Error Bars=SEM, n=3, Asterisk=$p<0.05$)

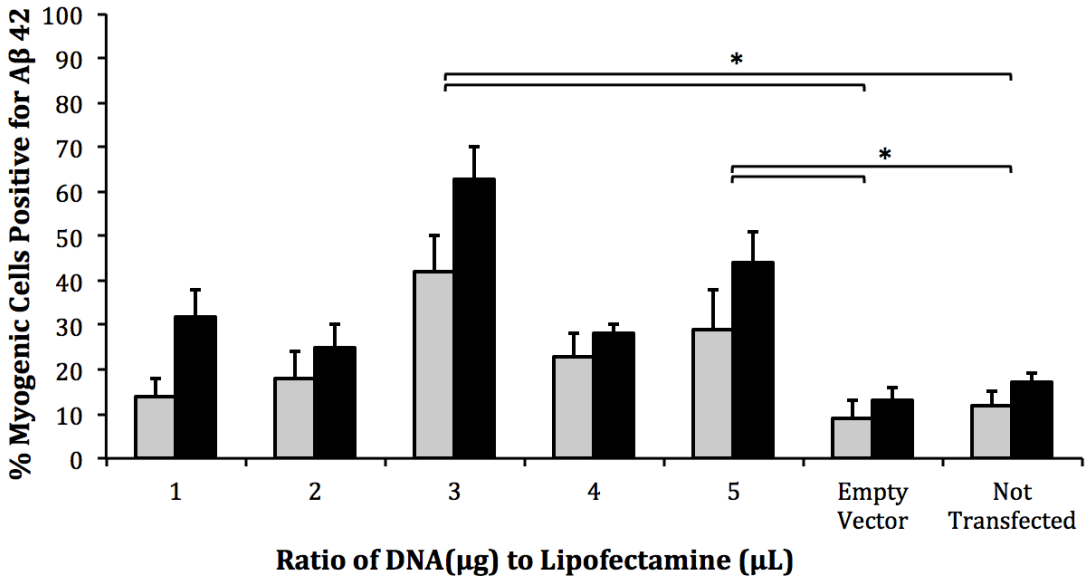

Figure 3.18 Effect of transfection at 48 hours *in vitro* on expression of Aβ42 in myogenic cells

At transfection ratios between 3:1 and 5:1, βAPP transfection was associated with a significantly elevated proportion of myogenic cells that were Aβ42 immunopositive compared to empty vector transfection and untransfected controls. Grey bars = all myogenic cells, Black bars = myocytes only

(Error Bars=SEM, n=3, Asterisk=$p<0.05$)

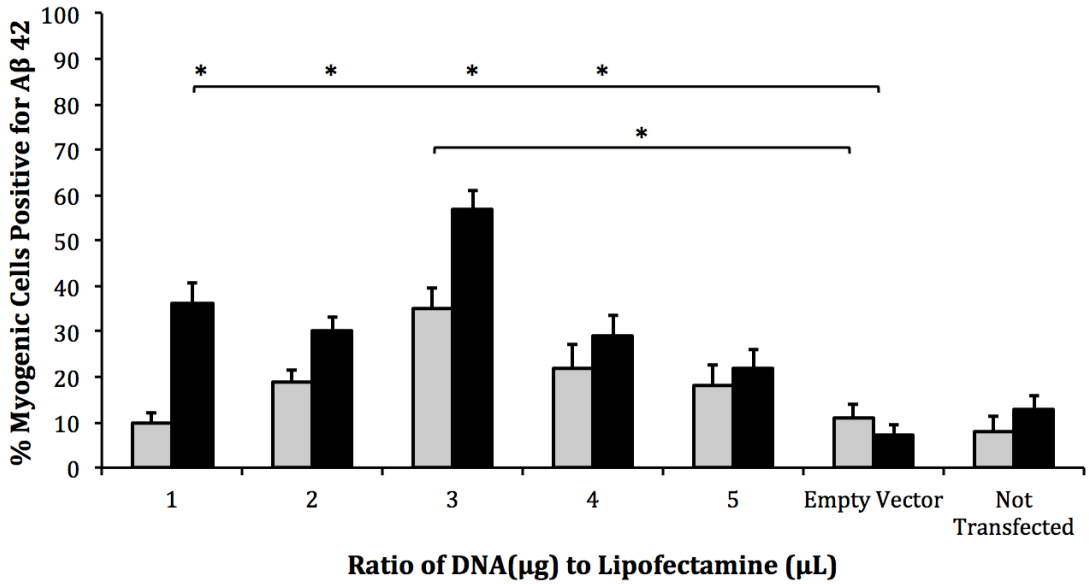

Figure 3.19 Effect of transfection at 96 hours *in vitro* on expression of Aβ42 in myogenic cells

At all transfection ratios between 1:1 and 4:1, βAPP transfection was associated with a significantly elevated proportion of myocytes that were Aβ42 immunopositive compared to empty vector transfection. At transfection ratio 3:1, this effect was maintained when all myogenic cells were compared. Grey bars = all myogenic cells, Black bars = myocytes only

(Error Bars=SEM, n=3, Asterisk=$p<0.05$)

3.2.7.3 Overall analysis of transfection optimisation

The effect of transfection DNA:Lipofectamine ratios and transfection time points on myogenic cell purity, differentiation and production of amyloid oligomers suggested that a DNA to Lipofectamine ratio of 3:1 at 96 hours after plating achieved the results most suited to subsequent investigation. High myogenicity was maintained, with no significant change in the apparent maturation of the cells, as evidence by a fusion index comparable with non-transfected cultures. Significant elevation of βAPP, Aβ40 and Aβ42 was consistently demonstrated and was maximal at the 3:1 ratio, indicating successful transfection. In the context of modeling IBM, the production of the Aβ42 oligomer was prioritised since due to the greater proposed significance of Aβ42 in induction of

downstream pathology such as proteasomal inhibition and ER dysfunction, reflected by its increased likelihood to aggregate. The 3:1 DNA to Lipofectamine ratio was, therefore, used in all subsequent experiments involving transfections.

3.2.8 The effect of inflammatory cytokines on amyloid expression

The inflammatory cytokines IL1β and IFNγ have previously been demonstrated to augment the expression of βAPP in human satellite cell cultures but not in rat. (Schmidt et al. 2008) Together with TNFα, these inflammatory mediators were evaluated as potential inducers of IBM-like pathology in myogenic cell cultures. Therefore, their impact on β-amyloid expression was also examined. Western blot analysis demonstrates that, at various concentrations, exposure to IL1β, TNFα or IFNγ significantly elevated the expression of βAPP and Aβ42 ($p<0.05$) (Figure 3.20). The magnitude of this effect was less marked than that following βAPP transfection, at least throughout the range of concentrations tested.

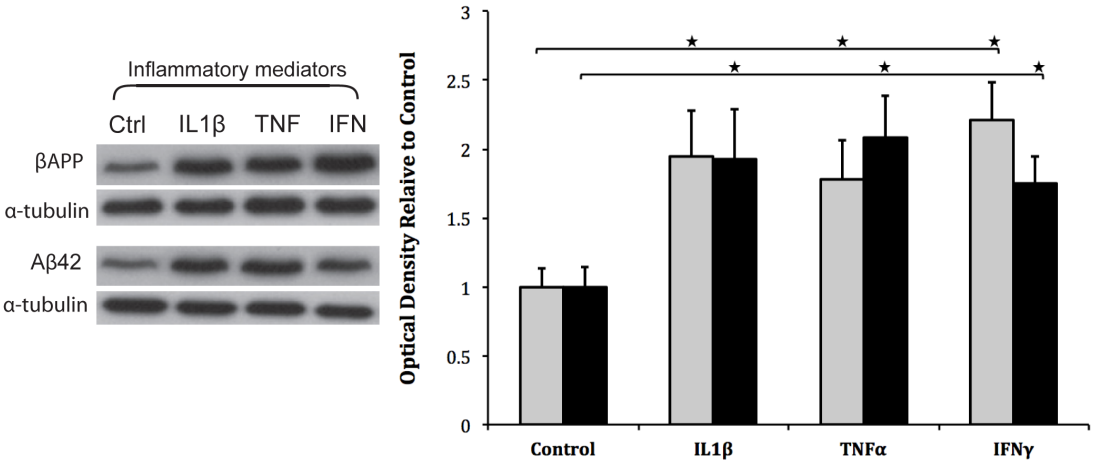

Figure 3.20 Effect of cytokines on β-amyloid proteins

Representative western blot and corresponding optical densitometry for β-amyloid proteins following exposure to inflammatory cytokines. Significant elevation of βAPP and Aβ42 was observed. Control=unexposed cultures, expressed as a comparative value of 1. Grey bars=βAPP, Black Bars=Aβ42
(Error Bars=SEM, n=3, Star=$p<0.05$)

A range of concentrations of each inflammatory cytokine was tested to determine which cytokines, and at which concentration, should be taken forward to further experiments.

Western blot densitometry showed that exposure of myogenic cultures to IL1β between 5 and 20ng/ml, elevated βAPP and Aβ42 significantly ($p<0.05$). There was a strong logarithmic relationship between cytokine concentrations of 1 to 20ng/ml and β-amyloid protein expression (βAPP $R^2 = 0.96$ and Aβ42 $R^2 = 0.98$. Fig 3.21, A). At 40ng/ml, IL1β was associated with a paradoxically minimal effect on β-amyloid, concentrations, perhaps indicating this was a cytotoxic dose (Fig 3.21, B).

Exposure of cultures to TNFα at 2.5, 10 and 20ng/ml was also associated with significant elevation of βAPP and Aβ42 expression ($p<0.05$). There was a strong relationship between cytokine concentration and effect on β-amyloid proteins (βAPP $R^2 = 0.65$ and Aβ42 $R^2 = 0.72$. Fig 3.21, C).

IFNγ was only associated with significant elevation either β-amyloid protein at a concentration of 1000 U/ml, with a suggestion of a proportional dose response relationship on βAPP (βAPP $R^2 = 0.54$ and Aβ42 $R^2 = 0.38$. Fig 3.21, D).

Comparison of βAPP and Aβ42 mean levels at all concentrations of cytokines (Figure 3.22) demonstrated a strong correlation between the two proteins ($R^2 = 0.745$), consistent with the βAPP being the predominant source of Aβ42 here.

Together, these data demonstrate that the cytokines IL1β and TNFα induce a concentration dependent, significant elevation of βAPP and Aβ42 in myogenic cell cultures. IFNγ at higher concentration also elevated the expression of these proteins. The tight correlation between βAPP and Aβ42 (Fig 3.22) is consistent with the logic that Aβ42, as a breakdown produce of βAPP, is elevated as a consequence of the upregulation or reduced breakdown of βAPP that succeeds cytokine exposure. It is possible that other IBM-relevant effects of IL1β and TNFα on myogenic cultures might be distinguished from those of IFNγ, at least at the lower concentrations tested, through mechanisms that respectively involve or are independent of β-amyloid.

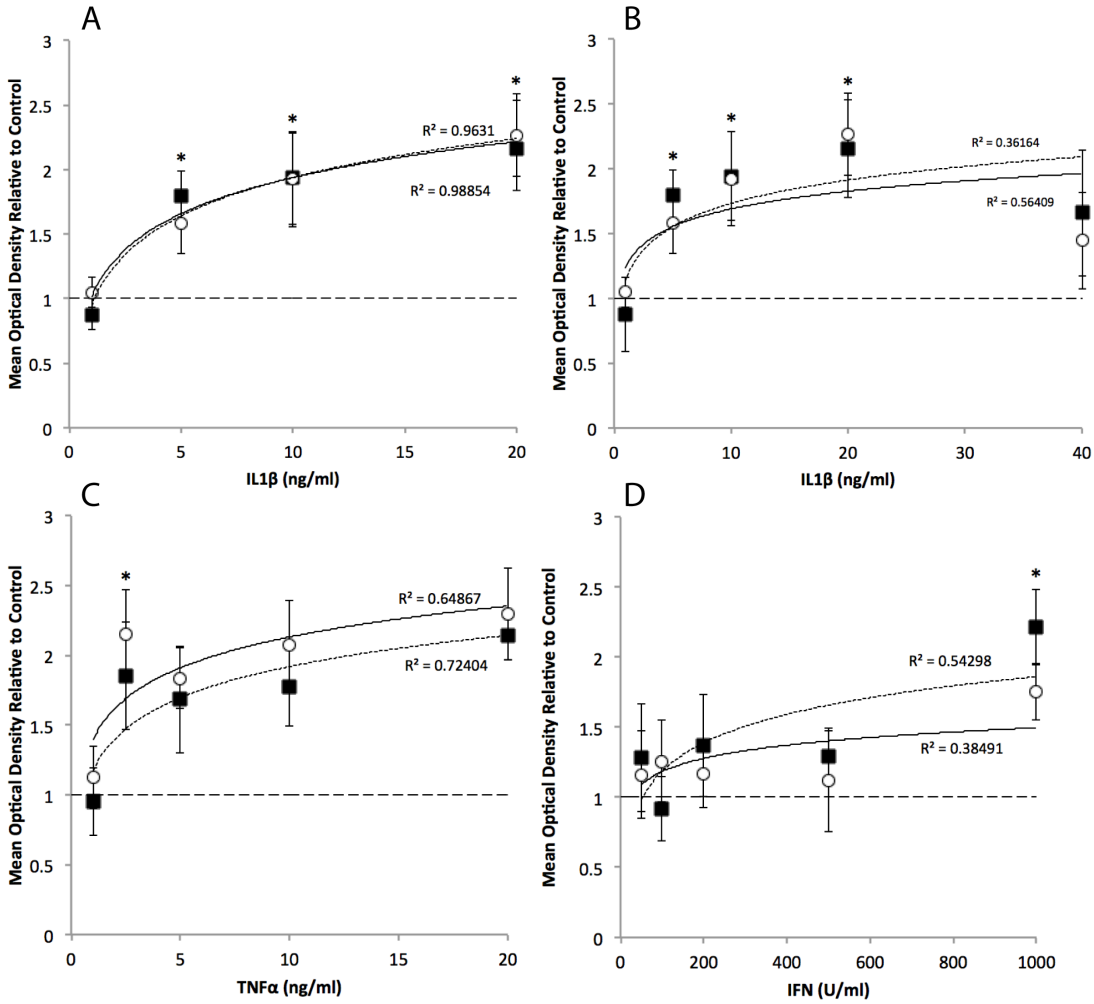

Figure 3.21 Effect of cytokine concentration on β-amyloid protein expression

After cultures were exposed to a range of cytokine concentrations, optical densitometry of western blots determined βAPP and Aβ42 levels relative to untreated control cultures. A: Between 0 and 20ng/ml, IL1β was associated with a closely proportional response of both β-amyloid proteins, demonstrated by correlation coefficients (R^2) that approach a value of 1. B: 40ng/ml IL1β was associated with a paradoxical reduction of β-amyloid protein levels, perhaps due to cytotoxicity. C: Between 0 and 20ng/ml, TNFα was associated with a proportional change in β-amyloid protein levels. D: The change of β-amyloid protein levels after exposure to IFNγ was less strongly correlated. Black squares and dashed best-fit lines=βAPP, Open circles and solid best-fit lines=Aβ42 (Error Bars=SEM, n=3, Asterisk=$p<0.05$)

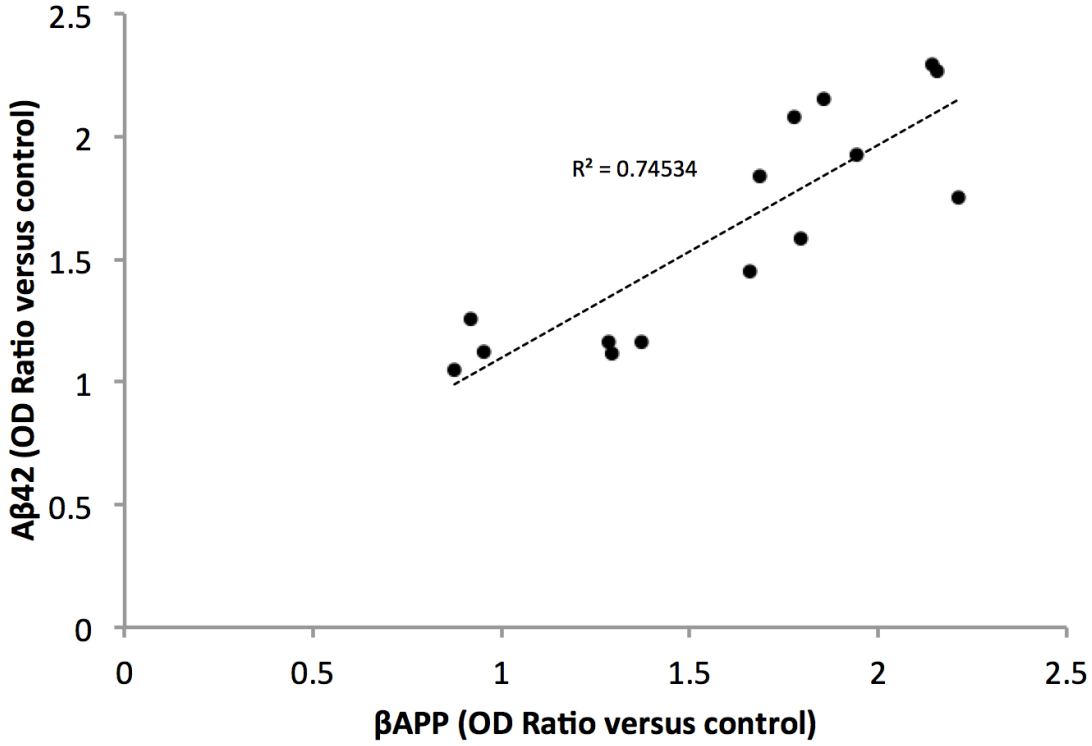

Figure 3.22 Relationship between βAPP and Aβ42 levels following exposure to inflammatory cytokines

Individual markers represent the βAPP and Aβ42 levels, measured by western blot optical densitometry, after exposure to a given cytokine concentration, as charted in Figure 3.22. This suggests that, regardless of the underlying cytokine stimulus, the elevation of Aβ42 is strongly proportional to that of βAPP (R^2=0.745). (n=3 per cytokine concentration tested)

3.2.9 MHC Class I expression following βAPP transfection and exposure to inflammatory cytokines

Since upregulation of Major Histocompatibility Class I protein (MHCI) is fundamental element of IBM histopathology, and a proposed central mechanism in IBM pathogenesis, it was important to determine what effects any proposed technique to induce IBM-like pathology had on MHCI expression. Unlike mature skeletal muscle fibres, which do not constitutively express MHCI, myocytes in culture express this protein constitutively, albeit at low levels. (Michaelis et al. 1993), Whilst inflammatory cytokines, particularly IL1β, are known inducers of MHCI expression in a variety of tissues, less was known about the impact of amyloid oligomers on MHCI expression.

As expected, MHCI immunostaining of standard cultures revealed constitutive expression. Positive immunostaining also followed βAPP transfection or exposure to IL1β or TNFα (Figure 3.23). Therefore, western blots were employed to quantify the differences in MHCI levels. As anticipated, exposure to inflammatory cytokines IL1β or TNFα induced significant upregulation of MHCI, where increases over control of 5.48 fold (±1.7, n=3) and 5.14 fold (±1.4, n=3) were demonstrated respectively ($p<0.05$). Interestingly, this effect was also observed following treatment with βAPP, where an increase of 4.51 fold (±0.98, n=3) was demonstrated in comparison to untreated cultures. However, empty vector transfection also induced a significant increase in MHCI of 2.40 fold (±0.33, n=3). Therefore, the true impact of βAPP transfection was likely subtler, with a 1.74 fold increase in MHCI compared to empty vector transfection. Nevertheless this difference remained significant ($p<0.05$).

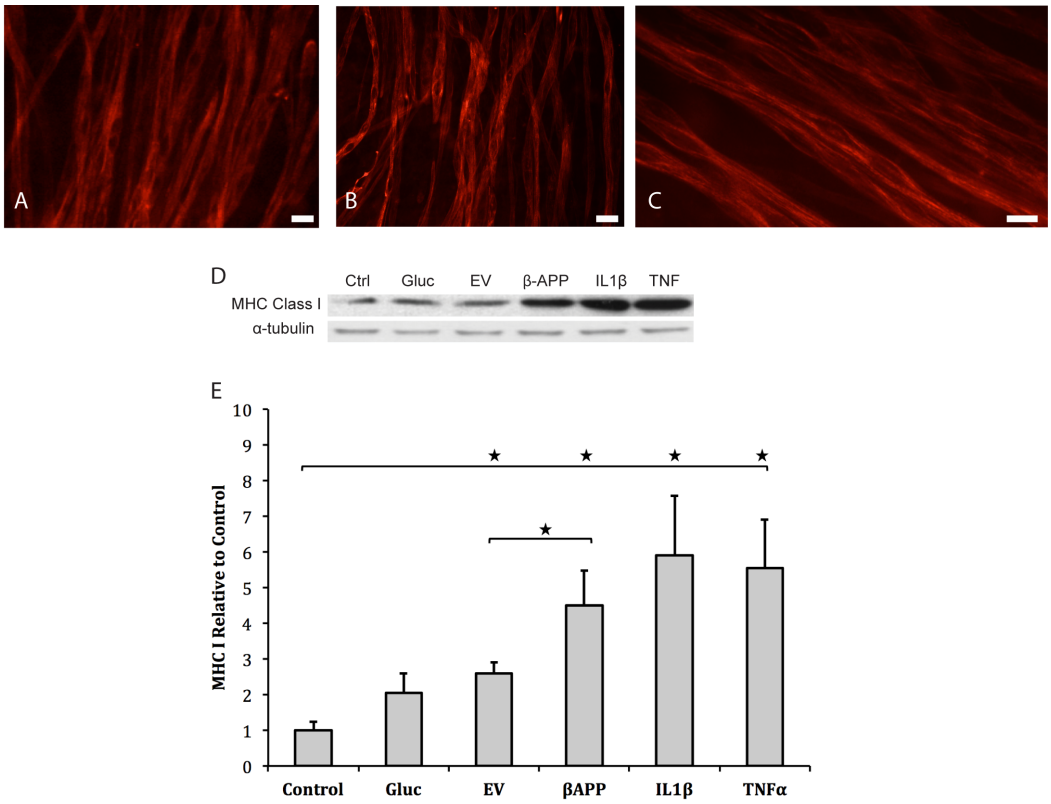

Figure 3.23 Effect of β-APP transfection and inflammatory cytokines on MHCI

Cultures were immunostained for MHC Class I (Red) following exposure to:

A) 5ng/ml TNFα, B) 10ng/ml IL1B, C) βAPP Transfection (Scale Bar=40μm)

D: Western Blots for MHCI at 50kDa. Ctrl = untreated cultures. Gluc = Cultures subject to 2 hours glucose deprivation. EV = empty vector

E: MHC I levels by optical densitometry of western blots relative to standard culture control, expressed as nominal value of 1

(Error Bars=SEM, n=3, Star=$p<0.05$)

3.2.10 Formation of proteinaceous aggregates

A characteristic feature of human muscle affected by IBM is the appearance of inclusion bodies that represent a number of aggregated proteins in addition to β-amyloid products. In order to establish whether these pathological characteristics of IBM were modeled by these myogenic cultures, a number of these were examined *in vitro*. After over-expression of βAPP, immunostaining demonstrated inclusions containing phosphorylated tau, p62 and TDP-43. Tau and TDP-43 inclusions were frequently ubiquinated.

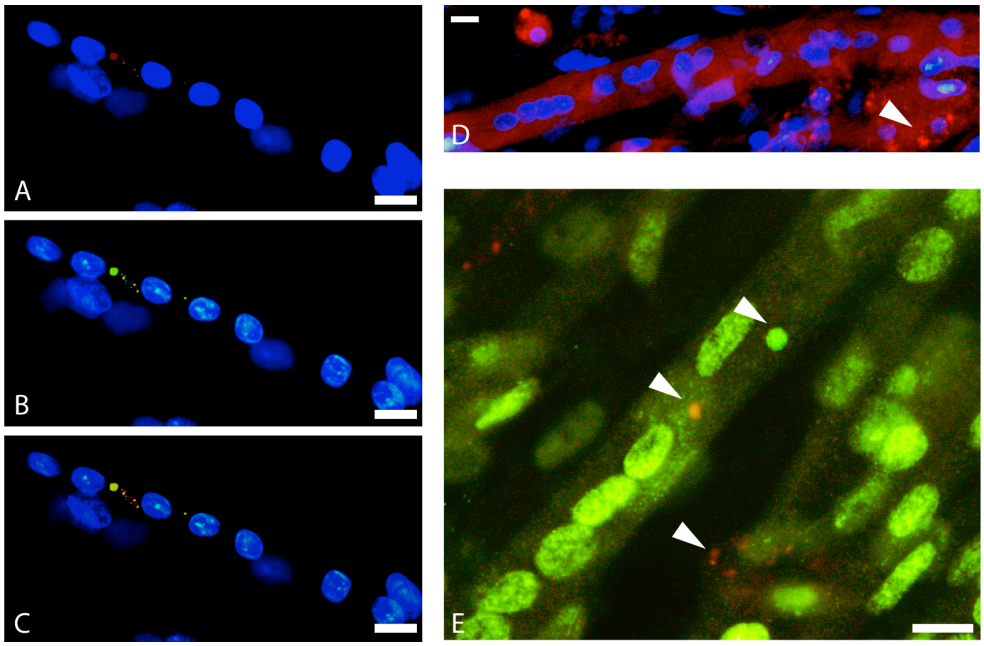

Figure 3.24 Inclusion and aggregate formation in cultured myotubes

Following βAPP transfection, cytoplasmic proteinaceous aggregates, frequently ubiquinated, were demonstrated with immunocytochemistry.

A: Phosphorylated tau (red), B: ubiquitin (green) and C: merged images demonstrate colocalisation (yellow). D: p62 (red), E: TDP-43 (green) and ubiquitin (red) positive inclusions were observed within individual cells.

Nuclear staining with DAPI (A-D), arrows indicate inclusions

(Scale Bars=20μm)

3.2.11 Summary of results

1. Primary satellite cell cultures from mice demonstrated limited myogenicity, considerable variability between cultures and a restricted lifespan *in vitro* before detachment from the coverslip. These features precluded their use in further experiments

2. Primary satellite cell cultures from rats displayed superior myogenicity, consistency and lifespan, particularly when the growth conditions were optimised. This involved refinement of the culture medium constituents, plating density and pre-plating. Other purification techniques, density centrifugation and FACS, were not associated with significantly improved culture quality so were not incorporated into the final method used in subsequent experiments.

3. IBM-like pathology was induced with two types of stimuli, related to the proposed degenerative and inflammatory components of IBM pathogenesis. Overexpression of βAPP was successfully achieved using Lipofectamine™ transfection and was optimal at a DNA (μg):Lipofectamine™ (μL) ratio of 3:1, where no significant impact was demonstrated on culture myogenicity or differentiation to myotubes. The overexpression of βAPP was associated with proportionately increased levels of Aβ40 and Aβ42 species.

4. In turn, βAPP overexpression reproduced ubiquinated and non-ubiquinated intracellular proteinaceous inclusions that contained several of the degenerative markers that characterise muscle affected by IBM, including amyloid proteins, TDP-43, tau and p62.

5. The exposure of myogenic cultures to inflammatory cytokines IL1β and TNFα was associated with a significant and strongly correlated increase in βAPP and Aβ42 levels.

6. Both βAPP overexpression and exposure to inflammatory cytokines were associated with significant upregulation of MHCI.

3.3 Discussion

The aim of the experiments described in this chapter was to determine whether certain markers of IBM pathology could be reliably reproduced *in vitro*, in order to provide a preclinical disease model on which quantifiable, disease-relevant pathological outcome measures could then be developed and, in turn, used to measure the impact of potential treatments.

3.3.1 Optimisation of an in vitro model of IBM

A number of cell culture conditions were first compared using primary satellite cells harvested from neonatal mouse and rat hindlimb muscles. Mouse satellite cell cultures lacked a number of properties required of a reliable model. First, myogenicity was limited, with only 44% of cells displaying muscle specific immunocytochemical staining for desmin, reflecting that approximately half of the cultured cells were not demonstrably myogenic. Only around 25% of these cells proceeded fuse to form multinucleated myotubes, the cell type of most interest for further experiments. Furthermore, the variability in myogenicity was large, up to 27% between culture wells derived from the same satellite cell harvest. Finally, the longevity of these cultures was limited to approximately 7 days, which would preclude sufficient maturation for subsequent manipulation through transfection of βAPP or exposure to other compounds. Therefore, the superior myogenic yields provided by neonatal rat cultures supported further work using these animals.

As there is no consensus on experimental protocol in the field of primary satellite cell culture, a number of purification techniques were then compared in order to achieve the highest reliable demonstrable myogenicity, without compromising the maturation or longevity of the cultures. Just as in mature skeletal muscle, a number of supportive cell types exist in addition to the myogenic majority and these are important both *in vivo* and *in vitro*. Furthermore, a significant proportion of myogenic cells exist as a 'side population' (Hawke et al. 2001) and do not express standard myogenic cell markers. Therefore, it was neither desirable nor realistic to attain absolute purity. More important was to attain consistency and high rate of fusion to

myotubes, since these are the post-mitotic cell type *in vitro* which most closely represent functional skeletal muscle and are also readily identifiable through their characteristic morphology.

Modification of the growth medium had the greatest impact on these cultures, where the time of first medium change, spacing of subsequent medium changes, and proportions of constituents were all associated with changes to myogenicity or fusion index. The incorporation of a 15-minute pre-plating step was supported by improved myogenic purity, using the optimal medium, from 69% to 78% and was, therefore, incorporated into the protocol used for subsequent experiments in this thesis. This is in keeping with previously described benefits of a pre-plating step on myogenic purity (Park et al. 2006).

Differential centrifugation is a cell selection technique based on the principle of isopycnic separation, which exploits differences in density between given cell types. The application of high gravitational force facilitates density dependent separation and, when performed within a solution of graded densities, a given mass or cell type reaches a point of equilibrium beyond which it will not sediment further regardless of whether further centrifugation is applied. This has previously been effective in isolating satellite cell cultures (Bischoff 1997; Mau et al. 2008). Here, however, two different gradient compositions were not associated with a significant change in overall myogenicity. Furthermore, the incorporation of this step reduced the final satellite cell yield by almost 50%. Therefore, this step was not incorporated in further experiments. Three distinct cellular bands were consistently isolated; that of greatest density appeared through a distinctive red colouration to include a significant number red blood cells. The largest two cellular bands, however, were both predominantly myogenic, implying that two broad groups of satellite cells, of different densities, exist in neonatal rat hindlimb muscles. This might reflect different coordinated stages of differentiation, as the satellite cell population is highly active during the muscle maturation of early life. Indeed, such distinct colonies of satellite cells, of differing sizes, have previously been described (Molnar et al. 1996).

Finally, fluorescence activated cell sorting was also evaluated. This allows highly specific identification or selection of a desired cell type through simultaneous

detection of multiple surface antigens using antibody labelling. However, the physical or fluorescent characteristics on which sorting is based are continuous rather than nominal. Therefore, arbitrary selection margins must be manually applied to select a given cellular subpopulation from the overall suspension. FACS has previously been applied to satellite cell populations, often in work examining subtypes of differentiating cells (Ieronimakis et al. 2010). It was investigated here in case near pure cultures were required for future experiments. Examination of satellite cells based on side and forward light scattering properties suggests the presence of two cell populations of approximately equal numbers, distinguished by shape and size. This corroborates the equivalent finding after density centrifugation. Fluorescent labeling with the satellite cell marker CD34 was unsuccessful when applied immediately to the satellite cell suspension, implying either lack of expression of the protein due to relative cell immaturity or reduced expression resulting from the harvesting protocol. Indeed, removal of collagenase from the protocol was associated with increased CD34 positivity but the resulting cells could not be cultured successfully. Additional satellite cell markers, including NCAM were associated with similar results.

FACS sorting is limited by the need to apply a combination of cell surface markers in order to achieve the specificity intended, which is achieved at the price of subselecting a subpopulation of cells which may not fully represent the characteristics of all. Additionally, the effects of antibody binding or passage through the FACS machine on subsequent cell function are not fully appreciated.

In summary, refinement of previously published protocols for satellite cell cultures achieve the desired outcome of consistent, highly myogenic populations, which could be maintained for sufficient time in culture to allow further experimentation.

3.3.2 Induction of IBM-like pathology in myogenic cultures

In using βAPP transfection and exposure to cytokines, two distinct potential stimuli of IBM-like changes were explored. The role of β-amyloid proteins in IBM *in vivo* is debated and it is unclear whether primary over-expression of

βAPP is a significant upstream event in pathogenesis. (Greenberg 2009; Schmidt et al. 2013) However, it was evaluated here on the basis of previous data that suggest that it can induce certain downstream pathological changes, such as aggregate formation, mitochondrial dysfunction and proteasome inhibition *in vitro* (Askanas et al. 2003). Such an 'overload' of cellular protein degradation mechanisms may be analogous to the limitation protein degradative capacity of aged muscle which is evidenced by the cytoplasmic accumulation of numerous proteins in IBM. This technique was therefore thought preferable to, and more relevant than, the application of a generic cell 'stressor' such as application of direct cytotoxins or glucose deprivation. Similarly, the exposure to inflammatory cytokines has previously been shown to lead to upregulation of both β-amyloid proteins (Schmidt et al. 2008) and MHC Class I (Michaelis et al. 1993) in cultured myotubes. Since a sustained, predominantly T-cell mediated inflammatory response is a fundamental pathological component of IBM, it was logical to evaluate this further.

3.3.2.1 Overexpression of βAPP can be achieved without reduction of culture myogenicity

The purpose of these experiments was to achieve a balance between a sufficient overall overexpression of βAPP in myogenic cells to allow both demonstration that the technique had worked and to produce downstream effects, but to avoid excessive cytotoxicity, particularly if predominant among myogenic cells. First, therefore, it was important to determine a protocol for transfection of the βAPP-containing plasmid that was still associated with an acceptable degree of myogenicity in these cultures. It was anticipated that the postmitotic state of multinucleated myotubes might render them particularly susceptible to the toxicity of the technique *per se*, in addition to any toxic consequences of βAPP.

Examination of βAPP transfection at different time points (48 and 96 hours after plating) with different DNA to Lipofectamine™ ratios (between 1:1 and 5:1) revealed a significant effect in certain combinations on overall myogenicity and myotube formation. This could either represent direct selective toxicity on myogenic cells or delay in their maturation toward expression of myocyte

specific proteins. Nevertheless, two transfection ratios, 3:1 and 4:1 were not associated with a significant reduction in overall myogenicity, demonstrating that the overall toxicity of the technique is acceptable in this context.

The time point at which cells were transfected was of significance in myogenic maturation of the cultures. Following transfection at 48-hours, the proportion of myogenic cells represented by multinucleated myotubes was significantly attenuated across all transfection ratios with βAPP and empty vector. This effect was overcome by delaying transfection to 96 hours after plating, when no significant difference in myotube proportion was detected at three of the tested transfection ratios, including those (3:1 and 4:1) which also did not detract from overall myogenicity.

As the time period between 48 and 96 hours is that in which the majority of myotube formation is observed, these results are likely to represent an inhibitory effect of the transfection process on the differentiation of satellite cells, particularly their fusion into myotubes, rather than a direct cytotoxic effect.

3.3.2.2 Overexpression of βAPP in myogenic cells is associated with increased formation of Aβ40/42 oligomers

Having determined the transfection conditions that appeared suitable for further experiments, the effects of βAPP transfection on the concentrations and handling of β-amyloid proteins were next examined. Western blot analysis confirmed successful overexpression through significantly elevated concentration of βAPP compared to untransfected cultures. Furthermore, the significant increase compared to empty vector transfection implies that this effect did reflect increased expression of βAPP specific to the plasmid concerned, rather than being a generic response to the transfection technique itself. Untransfected cultures displayed relatively similar proportions of βAPP, Aβ42 and Aβ40 compared to control housekeeping proteins. However, this balance altered substantially following βAPP transfection, where far greater elevation of Aβ42 was demonstrated than Aβ40. Although both proteins are implicated in human disease, the Aβ42 oligomer is the more fibrillogenic and, therefore,

cytotoxic, notably in Alzheimer's Disease (AD) (Chen et al. 2006). Therefore, the propensity of skeletal muscle to accumulate Aβ42 in response to overexpression of βAPP might hint at a similar susceptibility to that displayed by cortical neurons in AD (Walsh et al. 2007). The tissues are analogous in their postmitotic, highly metabolically active state. Extrapolating to IBM *in vivo*, the relatively acidotic environment represented by Type 2 fast-twitch fibres of the forearm flexor compartment and quadriceps might alter βAPP processing, as has been demonstrated in neurons (Brewer 1997). Correspondingly, proteomic analysis of IBM muscle through mass spectrometry demonstrated substantial loss of Type 2 fibre proteins, particularly ACTN3 and MYBPC2, and glycolytic pathway proteins, in excess to that seen in comparable diseases and to other downregulated proteins in IBM tissue (Parker et al. 2009). Altered βAPP processing in IBM muscle *in vivo* is suggested by accumulation of BACE1 and BACE2 proteins (beta-site amyloid precursor protein cleaving enzymes), which release amyloidogenic proteins from cleavage of βAPP, in cytoplasmic inclusions and in increased concentration on western blot (Vattemi et al. 2003). Furthermore, BACE1 mRNA is significantly increased in IBM tissue (Nogalska et al. 2010).

Interestingly, approximately one third of myogenic cells grown under standard conditions were immunoreactive for the Aβ40 oligomer. This compared to fewer than 20% of cells positive for Aβ42. The normal constitutive characteristics of β-amyloid proteins in skeletal muscle and myotubes *in vitro* are not well described. Nevertheless, formation of proteinaceous inclusions in individual myotubes grown under standard cultures conditions was extremely rare. Therefore, the expression level of β-amyloid proteins *per se* may not be the only factor that leads to protein aggregation. Altered βAPP processing, and the underlying cellular milieu may dictate the degree of susceptibility to the further burdens of inflammation and other pathologies that coexist in IBM.

3.3.2.3 Overexpression of βAPP in myogenic cells leads to formation of proteinaceous aggregates

βAPP transfection was associated with formation of cytoplasmic proteinaceous aggregates, mirroring the histological changes observed in IBM tissue and those seen in cultured human myocytes following the same stimulus (Askanas et al. 2003). These changes were observed in both mononuclear myocytes and multinuclear myotubes, implying that the postmitotic state is not the sole susceptibility factor in aggregate formation. The formation of proteinaceous inclusions is a consistent feature of numerous neurodegenerative diseases including AD, Frontotemporal dementia, Lewy Body Dementia, Parkinson's Disease, Huntington's Disease and Motor Neuron Disease, in addition to systemic diseases including type 2 diabetes, inherited cataracts, some forms of atherosclerosis and amyloidosis (Reynaud 2010). Briefly, they represent the consequence of inappropriate exposure of hydrophobic surfaces that are usually concealed internally or at the interface with other protein subunits. This is particularly relevant to membrane proteins, which often contain large hydrophobic domains that are normally contained in the lipid bilayer. Exposure of these hydrophobic regions leads to abnormal confirmations of protein that subsequently interact to form aggregates which are often resistant to degradation or refolding (Johnston et al. 1998). The stimulus for this process is provided when a cell's capacity to degrade or refold misfolded proteins is exceeded. This represents overwhelming of the numerous protective 'chaperone' responses, primarily involving the ubiquitin-proteasome or autophagic pathways that have evolved to minimise the likelihood of such a scenario. It is conceptually difficult, therefore, to determine whether the formation of proteinaceous inclusions represent another stage of cellular defence or are directly cytotoxic, and this question remains unanswered. Rather, their presence are best inferred as an imbalance between the production of abnormal proteins and the capacity to process them.

The cytoplasmic proteinaceous inclusions identified in these experiments took a variety of appearances and sizes, as is well described in the literature (Narhi et al. 2012). Immunocytochemical staining of the inclusions revealed a number of

proteins that are also detected in IBM tissue, including phosphorylated tau, TDP-43 and p62 (Nogalska et al. 2009; Salajegheh et al. 2009). Their frequent ubiquination implies identification for intended proteasomal degradation. The larger, well-defined perinuclear inclusions might represent aggresomes, which are thought to have greater structural organisation than other forms of inclusion (Johnston et al. 1998). Nevertheless, the presence of each type served to demonstrate here that the degree of βAPP over-expression achieved with this transfection process did exceed the degradative capacities of myotubes *in vitro*, thereby reproducing one downstream element of IBM pathology. The accumulation of other typically 'degenerative' proteins within the inclusions further suggests impairment of protein degradation by βAPP, Aβ40 and Aβ42 or the activation of pathogenic cascades that affect the production or breakdown of those proteins specifically. The induction of ER stress therefore appeared an attractive mechanism for further investigation.

3.3.2.4 Inflammatory cytokines induce β-amyloid expression in satellite cell cultures

In keeping with previous work on human myocytes (Schmidt et al. 2008), exposure to inflammatory cytokines IL1β, IFNγ and TNFα was associated with increased concentrations of βAPP and Aβ42. The advantage of this technique over direct βAPP overexpression is the homogenous level of exposure to the stimulus, compared with typically heterogeneous success of transfection. Furthermore, following exposure to IL1β or TNFα, a dose dependent increase in βAPP and Aβ42 was observed. This allows adjustment of the magnitude of induced expression of β-amyloid proteins that is not possible with transfection. The observation of dose dependence strengthens the conclusion that increased expression β-amyloid proteins are a consequence of the cytokines. Strong correlation between βAPP and Aβ42 levels across the experimental conditions implies that the increase in Aβ42 in these conditions is, indeed, the direct consequence of increased βAPP expression.

The magnitude of increases in βAPP and Aβ42 concentration following cytokine exposure was up to 2.5 times that of control, which is less than that observed

following transfection where increases of βAPP and Aβ42 were approximately 4 and 6 fold respectively. This might account for the relative lack of proteinaceous inclusion formation displayed by myotubes exposed to cytokines, in contrast to those transfected with βAPP. This would depend on a critical threshold of βAPP expression above which inclusion formation occurs. This may relate to absolute concentration of β-amyloid, simultaneous upregulation of other proteins, or direct effects on protein degradation of either experimental technique used here. Alternatively, the rate of increase in βAPP or Aβ42 expression might be important, and a more rapid induction associated with transfection might thereby account for the greater association with inclusion formation.

3.3.2.5 MHC Class I upregulation can be driven by β-amyloid proteins in addition to inflammatory cytokines

The expression of MHC Class I (MHCI) by skeletal muscle, which is one of the few tissues that does not constitutively express the protein, is a hallmark of IBM pathology. In addition to representing the chronic, self-perpetuating inflammatory response of the disease, it is implicated in driving ER stress and activation of the NFκB cascade, which themselves are potentially central mechanisms in IBM pathogenesis.(Dalakas 2006). Unsurprisingly, satellite cell cultures demonstrated significantly increased MHCI expression following exposure to IL1β and TNFα. This effect was not reproduced through glucose deprivation, implying that increased MHCI expression is not a generic 'stress response' of myogenic cells in culture. Interestingly, even when accounting for the effect of empty vector transfection, βAPP transfection was also associated with significant elevation of MHCI expression. This implies a previously undescribed pathway of potential relevance to IBM, in which β-amyloid proteins appear to contribute to a fundamentally pro-inflammatory stimulus. The potential mechanisms of this are explored in Chapter 4. The interpretation of MHCI results must, however, be cautious given the disparity between immature satellite cells in culture, which do constitutively express MHCI unlike the mature tissue. The protein may have additional roles in satellite cell maturation (Honda et al. 1989). However, this effect is likely to be small since MHCI expression falls

quickly upon formation of multinucleated myotubes, which represent the predominant cell type in the cultures described here.

3.3.3 Overall Summary

The experiments presented in this Chapter demonstrate that highly myogenic cell cultures, with high rates of multinucleated myotube formation, can be established consistently following harvest and plating of satellite cells from neonatal rats. The transfection of βAPP with Lipofectamine™ successfully increases the cellular concentration of βAPP, Aβ42 and Aβ40 in myogenic cells, which, in turn, is associated with the formation of cytoplasmic proteinaceous inclusions containing degenerative proteins found in IBM tissue in vivo. It is also associated with upregulation of MHC Class I, indicating a further potential link between 'inflammatory' and 'degenerative' mechanisms. MHCI upregulation is reproduced by exposure to IL1β and TNFα, and these inflammatory cytokines are further associated with increased concentration of β-amyloid proteins, albeit to a lesser degree than direct transfection and without consistent inclusion deposition.

This work laid the required foundation to explore the pathological mechanisms associated with these two stimuli of IBM-like pathology, and to investigate which might be used to test new therapeutic strategies.

Chapter 4: Characterisation of pathological outcome measures of IBM *in vitro* to investigate a novel therapeutic approach

4.1 Introduction

Having established a reproducible cellular model in which salient degenerative and inflammatory features of IBM pathology were represented, the next set of experiments sought to characterise further IBM-relevant markers and thereby develop a panel of pathological outcome measures on which potential therapies can be evaluated. Subsequently, a pre-clinical *in vitro* evaluation of a novel therapeutic approach was undertaken using these measures; pharmacological augmentation of the cytoprotective Heat Shock Response with the co-inducer Arimoclomol.

First, consideration was given to those processes that, from reviewing the literature, are key distinguishing features or potentially central pathogenic mechanisms of IBM, particularly those that lie at the junction between inflammation and degeneration. These are:

1. TDP-43, which appears to be the most specific and sensitive histological marker of IBM (Salajegheh et al. 2009).
2. NFκB activation, which is activated by both ER stress and pro-inflammatory stimuli, and appears well placed to perpetuate the inflammatory response in IBM, in addition to promoting muscular atrophy (Dalakas 2006).
3. Endoplasmic reticulum (ER) stress, which is a common feature of neurodegenerative diseases, intimately related to the cellular milieu of protein misfolding and aggregation, which distinguish IBM from the primary myositides (Roussel et al. 2013; Schmidt et al. 2013).

4.1.1 TDP-43

Tar DNA Binding Protein 43 (TDP-43) is a 414 amino acid protein, the extent of whose normal cellular functions remain under investigation. It was initially investigated in a pathological context as the major constituent of proteinaceous intraneuronal aggregates characterised by ALS and FTD, now intriguingly connected at two ends of a TDP-43-opathic disease spectrum through common C9orf72 mutations, which have not been detected thus far in IBM (Wood 2011). Nevertheless, TDP-43's normal functions appear to relate primarily to RNA regulation, mediated chiefly via its RRM1 domain (Figure 4.1) (Lee et al. 2012).

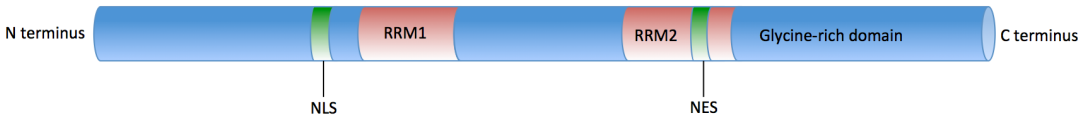

Figure 4.1 Illustration of the structure of TAR DNA-binding protein 43 (TDP-43)

Key elements include two RNA-recognition motifs; RNA-recognition motif 1 (RRM1) and RRM2), a carboxy-terminal glycine-rich domain, nuclear localization signal (NLS) and a nuclear export signal (NES). Mutations linked to sporadic and familial forms of amyotrophic lateral sclerosis and frontotemporal lobar degeneration are almost exclusively located in or adjacent to the glycine-rich domain.

The RNA types to which TDP-43 possesses binding capability represent approximately one third of the transcriptome (Tollervey et al. 2011). There is a preponderance of introns and non-coding RNAs. Subsequent postulated nuclear functions include pre-mRNA splicing, as a heterogeneous nuclear ribonucleoprotein (hnRNP) (Buratti et al. 2005), and transcriptional repression via single stranded DNA promoter silencing. TDP-43's characteristic nuclear-cytoplasmic shuttling may assist mRNA trafficking (Wang et al. 2008), with further cytoplasmic roles in mRNA stability and protection, through stress granule sequestration (McDonald et al. 2011).

TDP-43 pathology is characterised by two features: translocation from the nucleus to the cytoplasm with consequent clearance of TDP-43 from the nucleus, and the formation of cytoplasmic proteinaceous aggregates as non-ubiquinated 'pre-inclusions' or ubiquinated 'inclusions'. Nuclear aggregates are less frequently demonstrated. TDP-43 appears to be inherently prone to aggregation, characteristic feature of an important neurodegenerative protein (Johnson et al. 2009). However, the nuclear clearance phenomenon appears to be a distinguishing factor from other typical neurodegenerative proteins, such as Huntingtin or β-amyloid (DiFiglia et al. 1997).

The lack of clarity on TDP-43's normal functions adds complexity to the puzzle of how it contributes to degenerative pathology. It follows that the majority of previous work has focussed on gain of toxic function rather than the loss of as yet undetermined physiological roles. Much of this, in turn, depends on the interpretation of whether TDP-43 cytoplasmic aggregates are pathogenic or cytoprotective. Certainly, it is rational to hypothesise that the loss of normal RNA binding in the nucleus disturbs a number of the processes with which TDP-43 has been linked through genomic studies (Lee et al. 2012). If its RNA binding property is maintained upon translocation to the cytoplasm, this may lead to subsequent abnormalities of RNA processing. Nuclear clearance appears to occur early in 'TDP-43-opathies' ALS and FTD (Giordana et al. 2010). Furthermore, TDP-43 aggregates do not appear necessary for TDP-43 related neurodegeneration to occur. Further investigation of a 'loss of function' hypothesis has been hindered by the fact that TDP-43 knockout is lethal in mice (Chiang et al. 2010).

4.1.1.1 Relevance of TDP-43 to IBM

Although TDP-43 has been studied primarily in the context of FTD and ALS, it appears that IBM tissue displays several similar features of TDP-43 degenerative pathology. Indeed, these features strongly distinguish IBM from PM and DM. Histopathological studies have demonstrated mislocalised TDP-43, with characteristic loss of nuclear staining and formation of cytoplasmic TDP-43 aggregates (Figure 4.2).

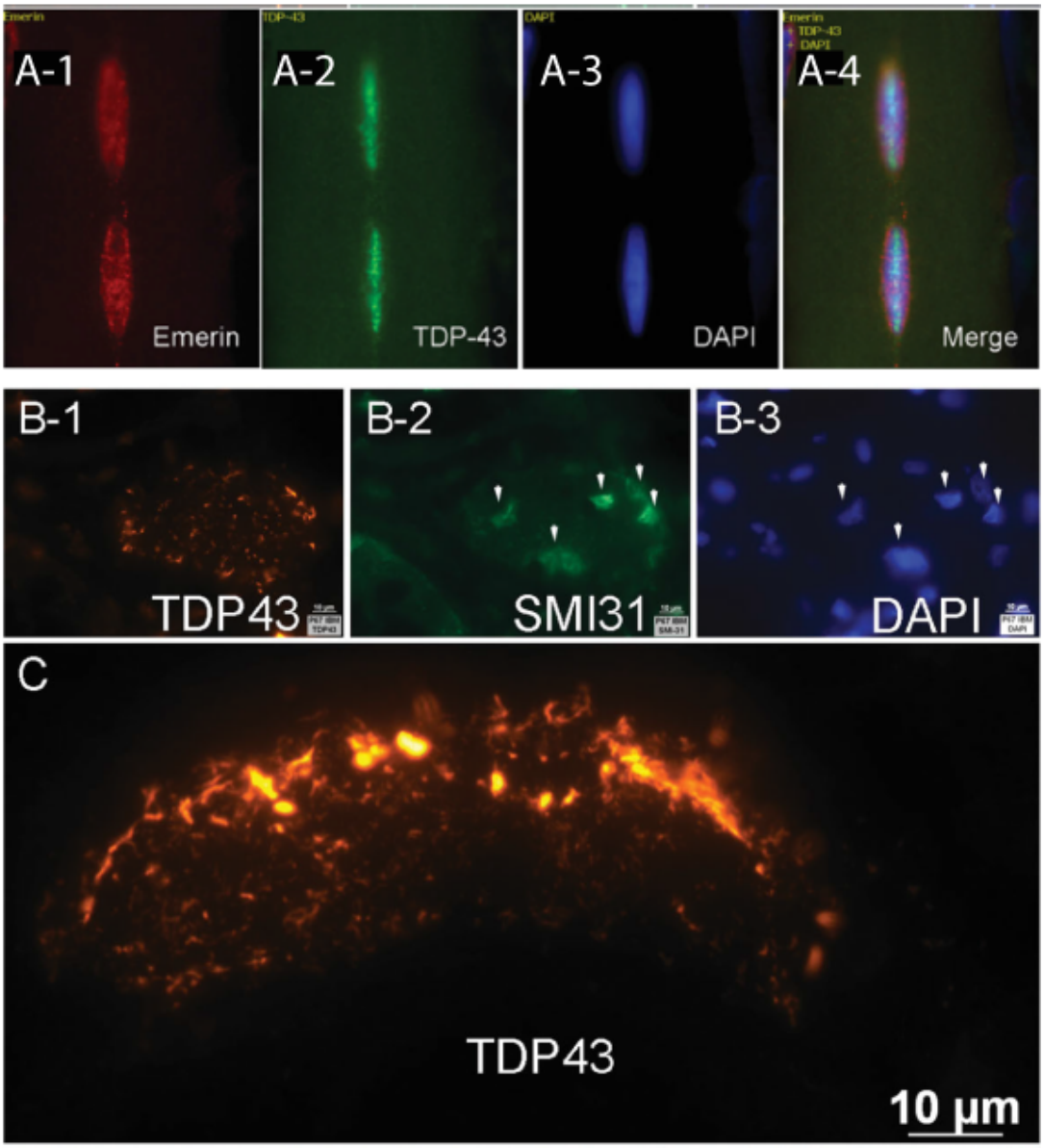

Figure 4.2 Illustration of TDP-43 pathology in IBM tissue

From (Salajegheh et al. 2009) A1-4: Fluorescent images of myonuclei in normal skeletal muscle demonstrate nuclear TDP-43 staining, evidenced by colocalisation with DAPI. B-1 and C: Skeletal muscle from IBM patients demonstrates redistribution of TDP-43, with loss of nuclear staining and cytoplasmic translocation.

Notably, such features were demonstrated in one study by up to a quarter of muscle fibres in IBM tissue, making this clearly the most common histopathological hallmark of IBM. By comparison, rimmed vacuoles were observed in fewer than 3% of fibres in the same study. TDP-43 expression was also increased in IBM cases versus disease controls. Consistent with its relative absence in PM tissue, this TDP-43 pathology is far more characteristic of degenerative than inflammatory disease. Indeed, fibres of hereditary IBM and myofibrillar myopathies demonstrated similar features (Salajegheh et al. 2009).

IBM is linked to FTD, a characteristic TDP-43-opathy, through the VCP mutant condition IBM-FTD-PD (Watts et al. 2007). This is among other factors that suggest IBM could be considered as the peripheral end of a disease spectrum that whose central nervous system phenotype is FTD, bridged by ALS (Chapter 1, Section 1.6.2). However, there are marked phenotypic and pathological differences between 'IBM' in VCP mutations and the sporadic disease, and none of the genetic mutations, most notably C9Orf72, have yet been demonstrated in cases of apparently sporadic IBM.

4.1.2 Endoplasmic reticulum pathophysiology

The intracellular organelle endoplasmic reticulum (ER) has two broad related functions. First, it processes and modifies newly translated membrane and secretory proteins, serving a 'quality control' purpose in determining what is passed on to the Golgi apparatus. Secondly, it is the principle intracellular calcium store, the regulation of which is fundamental to all cell functions through calcium signaling. Indeed, the regulation of intracellular calcium is demonstrated by all living cells. Close functional connectivity with cell membrane and mitochondria further convey the ER's wide influence. The specialised ER in muscle, sarcoplasmic reticulum (SR), has a further key function in excitation-contraction coupling. It follows that the ER's own function is highly Ca^{2+}-dependent and its disturbance results in a cascade of highly conserved pathways that are collectively referred to as 'ER stress'. Disturbance of the ER is associated with a wide variety of stimuli, is a common characteristic

of all neurodegenerative diseases in which it has been studied, and is a potentially central component of IBM pathology.

4.1.2.1 ER/SR Calcium

Luminal ER/SR Ca^{2+} is dynamic but tightly regulated at concentrations several thousand times that of the cytosol through homeostatic mechanisms that regulate the magnitude and velocity of ER Ca^{2+} uptake and release according to both ER and cytosolic [Ca^{2+}] (Burdakov et al. 2005). Uptake is mediated by the Sarco/Endoplasmic Reticulum ATPase (SERCA) pump, which actively transports Ca^{2+} against this concentration gradient, into the ER lumen. Ca^{2+} release is dictated by the inositol 1,4,5-triphosphate (IP_3) and ryanodine receptors. The rapid kinetics of ER Ca^{2+} release rely on the low resting resistance of the ER membrane, which precludes the significant shift of membrane potential during Ca^{2+} movement that slows or ceases the process in most other transmembrane ionic shifts. Broadly, the ryanodine receptor pathway represents the principle pathway of Ca^{2+} induced Ca^{2+} release (CICR), which underlies excitation contraction coupling and is demonstrated by excitable cells. IP_3 pathways, however, relate to 'capacitative' or 'store operated' calcium entry mechanisms via the plasma membrane that are signaled by the ER in response to depletion of its Ca^{2+} through a variety of proteins such as transient receptor proteins (TRPs). This was initially thought to relate primarily to non-excitable cells but it increasingly appears common to excitable tissues also. One putative mechanism depends upon the stromal interacting molecule 1 (STIM1), which may detect depleted ER Ca^{2+}, including in skeletal muscle and myotubes (Stiber et al. 2008). Upon stimulation, STIM1 translocates to the membrane and facilitates the formation of functional Ca^{2+} channels by TRPs or Orai1, through which cytosolic rises and ER Ca^{2+} consequently repletes (Perez et al. 2003; Prakriya et al. 2006).

Elevated cytosolic [Ca^{2+}] is characteristic of cytotoxic conditions, in which the ER appears to serve as a protective buffer. Ca^{2+} is sequestered from the cytosol, assisted by induced expression of SERCA2b (Wu et al. 2001). However, implying

dysfunction or insufficiency in this mechanism, the cellular milieu of most pathology appears to combine depleted ER Ca^{2+} with elevated cytosolic [Ca^{2+}].

4.1.2.2 Consequences of disturbed intraluminal ER Calcium

In keeping with its protein trafficking role, a large number of chaperone proteins are resident in the ER. The majority of these display multiple Ca^{2+} binding sites, which regulate their activity and expression (Michalak et al. 2002). Therefore, the cytoprotective responses to accumulation of unfolded proteins in the ER, such as is typical of neurodegenerative diseases, are highly dependent on ER Ca^{2+}. Indeed, the lectin group of ER chaperones, including calreticulin and calnexin, has ER Ca^{2+} buffering properties. Consequently, it is unsurprising that depletion of ER Ca^{2+} inhibits protein folding (Wetmore et al. 1996). Sufficiently low concentrations of ER Ca^{2+} appear to switch off ER chaperone responses completely (Corbett et al. 2000). It, therefore, appears that disturbed ER Ca^{2+} can both trigger ER dysfunction and also hinder the ER chaperone response, depending on the magnitude of the insult. Conversely, the initiation of ER stress also contributes to further ER Ca^{2+} disturbance through induction of truncated SERCA1 isoforms, which contribute to further ER Ca^{2+} leak (Hammadi et al. 2013). The resulting ER dysfunction, or 'ER Stress' includes the unfolded-protein response (UPR), ER overload response (EOR) and ER-associated degradation (ERAD), the particular combination of which appears to depend on the nature of the underlying stimulus.

4.1.2.3 The Unfolded Protein Response (UPR)

The UPR (Figure 4.3) is mediated by three ER membrane receptor proteins: pancreatic ER kinase (PERK), activating transcription factor 6 (ATF6) and inositol-requiring enzyme 1 (IRE1). These are maintained in a quiescent state by the glucose-regulated protein 78, otherwise referred to as binding immunoglobulin protein (BiP), to which they are bound. The accumulation of unfolded protein in the ER leads to dissociation of BiP from these three receptors, and thereby the UPR activates, leading to processes that reduce the protein

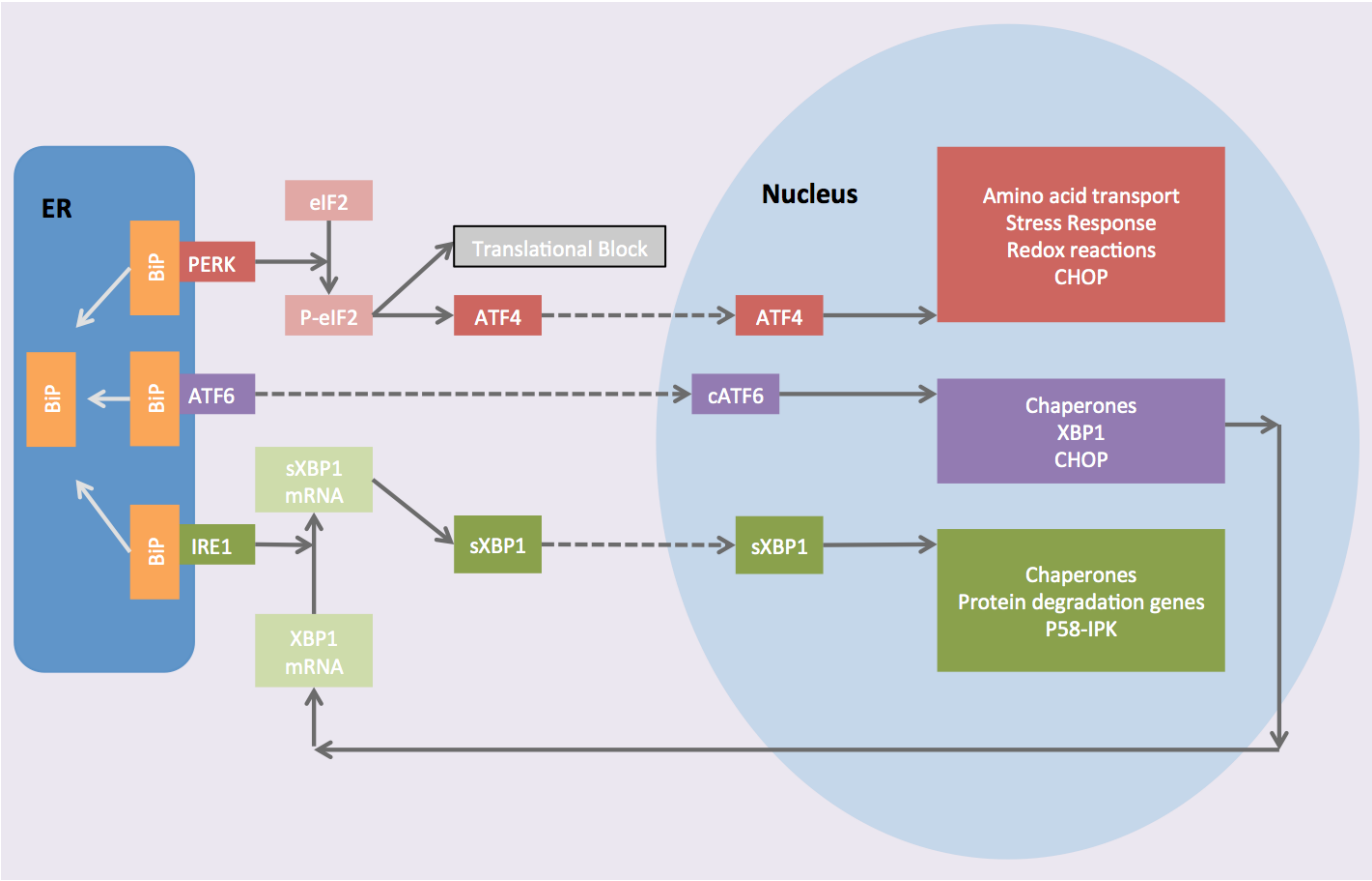

Figure 4.3 The three main pathways of the Unfolded Protein Response

The UPR is initiated by the dissociation of BiP from three ER membrane proteins, which are maintained in a quiescent state when bound. BiP subsequently interacts, as a chaperone, with unfolded proteins in the ER lumen. Continued onto next page.

Red pathway – dissociation of BiP from PERK leads to phosphorylation of eIF2 and generalised inhibition of protein translation. ATF4 is exempt from eIF2 translational block, and indeed is translated more efficiently under such conditions, and translocates to the nucleus where it triggers expression on predominantly pro-survival genes but is also a strong inducer of pro-apoptotic CHOP pathways.

Purple pathway – after dissociation of BiP, ATF6 is cleaved and then translocates to the nucleus where it induces expression of chaperone proteins. It also further upregulates BiP expression and, like ATF4, also CHOP. However, unlike that related to ATF4, this does not appear to trigger apoptotic signals.

Green pathway – inositol-requiring enzyme (IRE1) also dissociates from BiP and splices X box binding protein (XBP1), leading to its nuclear translocation and upregulation of ER chaperones. It also triggers delayed expression of P58-IPK, an HSP40 protein, which has been postulated as representing the UPR-ending signal, the absence of which leads to a shift towards pro-apoptotic rather than cytoprotective signaling.
Adapted from (Szegezdi et al. 2006)

accumulation responsible. Prolonged activation, however, triggers an apoptotic signal.

Notably, the PERK and ATF6 pathways both culminate in upregulation of CHOP (also known as GADD53). This is typically considered pro-apoptotic and, indeed, CHOP knockout animals are resistant to ER stress induced cell death (Marciniak et al. 2004). However, it appears that CHOP's target genes are not actually directly apoptotic but, rather, relate to protein secretion. It may be that CHOP serves as an amplifier of the UPR such that, at milder levels of ER stress, it does not trigger cell death. Nevertheless, under prolonged or sufficient stimulation, CHOP is the primary connection between the UPR and apoptosis.

4.1.2.4 Other ER Stress pathways

ERAD refers to the elimination of misfolded or unassembled proteins from the ER, culminating in their degradation by the ubiquitin-proteasome system (UPS). This is a critical pathway, particularly in post-mitotic tissue, and loss of function mutations are associated with disease, such as in Parkin related familial Parkinson's disease (Meusser et al. 2005). Interestingly, the AAA-ATPase VCP, mutations of which cause IBMPFD, appears to have an important role in dislocation, the element of ERAD in which the substrate is transported to the cytoplasm to undergo degradation.

The EOR is less well characterised than the other ER stress responses but represents one of the distinguishing features of the mammalian response versus that observed in more primitive organisms such as yeast. Of note, it appears to induce pro-inflammatory signaling, predominantly via activation of the NFκB cascade, and is frequently coactivated with the UPR, of which ATF6 appears to further stimulate NFκB (Kaufman 1999; Yamazaki et al. 2009).

4.1.2.5 ER Stress in neurological disease and IBM

ER dysfunction is widely implicated in neurodegenerative diseases, notably Huntington's disease, ALS, Alzheimer's disease, prion diseases and Parkinson's disease. It is also considered important in the pathogenesis of several otherwise disparate, typically inherited, conditions including CMT1A/1B, tuberous sclerosis, Gaucher's disease, Wolfram syndrome and Torsion dystonia 1 (Roussel et al. 2013). Furthermore, there is evidence for ER stress playing a significant role in the common disease groups of autoimmunity, cancer, stroke and diabetes (Kim et al. 2008). In the context of most diseases, it is still generally assumed that the initial participation of the ER, particularly the UPR, is appropriate and cytoprotective before the sustained activation ultimately contributes to apoptosis, having been unable to address the insult of misfolded protein.

Interestingly, Familial encephalopathy with neuroserpin inclusion bodies (FENIB), which is characterised by intraneuronal inclusions, appears to result in selective induction of the EOR, with consequent NFκB activation, without coactivation of the UPR, before degradation of protein occurs via the ERAD and autophagic pathways (Roussel, Kruppa et al. 2013). This phenomenon is postulated to arise from the accumulation of well folded protein in the ER, which draws parallels with the hypothesis in which upregulation of MHCI in IBM might lead to such a form of ER stress, perpetuating a self-propagating cycle of pro-inflammatory stimuli and ER overload that eventually overwhelms degradative mechanisms, leading to activation of the UPR and, eventually, cell death.

Immunoelectron microscopy studies of IBM muscle have demonstrated increased expression of UPR markers, including chaperones BiP and GRP94, disulfide isomerase ERp72, and the lectins/calcium-buffering proteins calnexin and calreticulin. Additional apparent colocalisation with degenerative proteins that subsequently form cytoplasmic aggregates, including βamyloid, implies insufficiency of this response (Vattemi et al. 2004). In cultured myotubes, ER stress appears to induce the expression negative muscle growth regulator myostatin, which might also be a consequence of the NFκB activation that

follows (Nogalska et al. 2007). The primary trigger of ER stress in IBM remains unclear. This leaves open the possibility that ER stress is, itself, a triggering pathogenic event. Indeed, the 'ER handicap' that is evidenced by aged tissue is an interesting concept. As approximately 30% of cell synthesized proteins fail to acquire their fully folded conformation, post-mitotic tissues are heavily reliant upon the ER protein processing functions of their constituent cells (Romisch 2004). Aged tissue demonstrates reduced UPR responsiveness and a shift towards pro-apoptotic signaling, with impaired enzymatic activity of key ER chaperones BiP, calnexin and GRP94, possibly due to progressive oxidation (Nuss et al. 2008). Furthermore, expression of BiP and PERK falls with age (Paz Gavilan et al. 2006; Naidoo et al. 2008). ATF4-mediated translational block is suppressed by increased expression of GADD34 in aged mice, which reduces the efficiency of the UPR. This allows continuation of the protein stimulus which is likely to have triggered ER stress, and promotes CHOP-mediated apoptosis (Hussain et al. 2007).

4.1.3 Nuclear Factor κB (NFκB)

NFκB refers to a heterogeneous collection of five inducible dimeric transcription factors that comprises p65 (or 'RelA'), Rel B, c-Rel, NFκB1 (p50) and NFκB2 (p52). Its activation cascade is ubiquitous and highly evolutionarily conserved with functions including pro-inflammatory signalling and apoptotic modulation, particularly under conditions of immune and inflammatory stress (Fig 4.4). The proinflammatory transcription functions of NFκB are of particular interest in IBM. Its products include the inflammatory cytokines IL1β and TNFα, inflammatory enzymes COX-2 and inducible nitric oxide synthase, chemotactic chemokines, adhesion molecules, and the T-cell receptor (Barnes et al. 1997). It is notable that IL1β and TNFα are both stimuli and products of the cascade and represent a positive feedback loop that is postulated to perpetuate local inflammatory responses. This represents one mechanism through which viral infection, which often exploits NFκB in its own replication, may trigger a prolonged inflammatory process of autoimmunity. Indeed, a viral trigger is one of several proposed stimuli in the pathogenesis of IBM (Dalakas 2006).

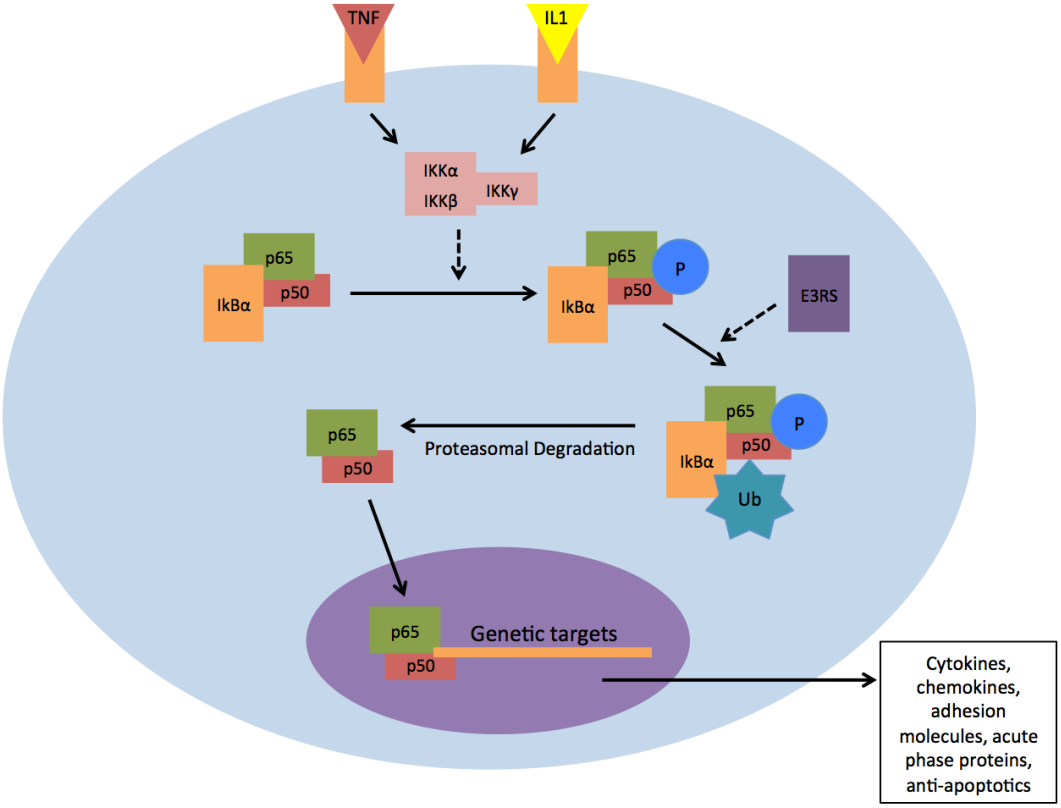

Figure 4.4 Illustration of canonical NFκB activation

In its inactive form, NFκB (represented as its dominant p50/p65 subunit) is mainly cytoplasmic, where it is maintained under inhibition of IκB proteins that mask its nuclear localisation signal. Successful stimuli, notably IL1β and TNFα, activate IκB kinase (IKK), which phosphorylates the complex. In turn, this leads to recognition by E3RS which ubiquinates IκB, leading to its rapid degradation by the 26S proteasome. This exposes the p50/p65 nuclear localisation signal, resulting in translocation to the nucleus where it adjusts transcription of target genes.

Such is the influence that NFκB over the inflammatory and immune systems that it is implicated in most, if not all, chronic inflammatory conditions. Further, the effectiveness of glucocorticoids in such conditions is likely to reflect their inhibitory effect on NFκB.

NFκB plays a significant role in myositis, not only that which represents primary autoimmunity, and this is an important consideration in the hypothesis that the inflammation observed in IBM may too be secondary. For example, dystrophinopathies, notably Duchenne muscular dystrophy (DMD), are classically associated with a considerable inflammatory response, in which the chronic NFκB activation displayed by the majority of myofibres has been strongly implicated (Messina et al. 2011). Indeed, mdx transgenic mice haploinsufficient for the NFκB p65 subunit demonstrate reduced inflammatory infiltrate and muscle necrosis (Messina et al. 2006).

NFκB activation does appear to occur in IBM muscle and is proposed to result from ER stress in addition to inflammatory stimuli (Nogalska et al. 2007). This is similarly observed in transgenic mice overexpressing MHCI, via the ER overload response (Nagaraju et al. 2005). NFκB also appears to be a unifying pathological mechanism through which VCP mutations cause the constellation of IBM, Frontotemporal Dementia and Paget's disease of bone (Custer et al. 2010). It may, therefore, represent an important point of interaction between degenerative and inflammatory processes in IBM.

Finally, skeletal muscle atrophy, a defining component of IBM, may be driven by NFκB, via inhibition of Myo-D and upregulation of Myostatin Precursor Protein (Wojcik et al. 2008). Similarly, in cultured myotubes, the protein loss associated with exposure to TNFα appears to be mediated by NFκB. Muscle-specific activation of NFκB causes profound muscle wasting in mice and inhibition of the cascade appears to reverse the atrophic phenotype. Conversely, muscle-specific inhibition of NFκB is not associated with an altered phenotype (Jackman et al. 2004).

4.1.4 A novel therapeutic hypothesis in IBM

The failure of all clinically tested drugs in IBM, all of which are primarily immune modulating treatments, supports consideration of alternative therapeutic avenues in this disabling condition. The combination of degenerative features, such as protein misfolding and ER stress, with inflammatory elements raised the hypothesis that cellular chaperone systems

represented an attractive target. In particular, augmentation of the heat shock response (HSR) has translated to pathological and functional improvement in preclinical models of other conditions characterised by similar pathology, such as ALS (Kieran et al. 2004).

4.1.4.1 The potential role of Heat Shock Proteins (HSPs) in IBM pathogenesis

HSPs are a family of highly conserved, ubiquitously expressed stress response proteins that function as molecular chaperones, facilitating protein folding, preventing protein aggregation, or targeting improperly folded proteins to specific degradative pathways. The heat shock response (HSR) derives its name from the original description of this cytoprotective reaction to elevated temperature, although the spectrum of stimuli *in vivo* is far wider, encompassing ischaemia, infection, inflammation and degenerative disease (Fulda et al. 2010). Common to the majority of these processes is the formation of misfolded proteins, which can culminate in the formation of nuclear and cytoplasmic aggregates or ubiquinated inclusions that are the hallmark of neurodegenerative conditions and, indeed, a distinguishing characteristic of IBM.

HSPs are grouped according to their molecular weight and arbitrarily referred to as 'small HSPs' when below 30kDa. Common larger HSPs include HSP40/60/70 and 90 (Lindquist et al. 1988). After induction and considerable upregulation in response to cellular stress, they act on a number of processes that are chiefly anti-apoptotic, notably those that result from diminishment of cytoplasmic protein aggregation. Indeed, HSPs are known to reduce cytotoxic intracellular accumulation of protein, as observed in IBM (Muchowski et al. 2005). Further, they prevent inappropriate interactions within and between non-native polypeptides, can enhance the efficiency of *de novo* protein folding, and promote refolding and repair of misfolded proteins (Sherman et al. 2001). In addition to their protein repair activity, HSPs can mediate targeting of misfolded proteins to the proteasome, dysfunctional in IBM, or to lysosomes, resulting in selective degradation of the misfolded protein through ERAD or autophagy respectively. Of particular interest here, HSP70 and 90 have been

shown to inhibit early stages of Aβ42 aggregation *in vitro* (Evans et al. 2006). HSP70 also promotes degradation and inhibits intracellular aggregation of amyloidogenic light chains (Dul et al. 2001). One study determined that selective reduction of Aβ42 delays progression of tau pathology, suggesting a close connection between βamyloid and tau pathology. βamyloid accumulation is known to decrease levels of the HSP70 co-chaperone CHIP, so it is notable that the Aβ42-induced effects on tau can be rescued by restoration of CHIP levels (Oddo et al. 2008).

Further actions of HSPs are directly related to the inflammatory and degenerative mechanisms of IBM. Activation of the proinflammatory transcription factor NFκB is dependent upon activation of IkB kinase, which is inhibited by HSP70, possibly via interaction with IKK. This translates to reduced induction of iNOS, a chief contributor to oxidative stress (Feinstein et al. 1996; Feinstein et al. 1997; Ran et al. 2004). Indeed, HSP-induced down-regulation of inflammatory gene transcription has been demonstrated through reduced metalloproteinase-9 mRNA (Lee et al. 2004). Conversely, HSP induction or over-expression reduces levels of inflammatory mediators (Hayashi et al. 2002; Weiss et al. 2002). In models of endotoxin-induced cellular inflammation, this is reflected in reduced levels of cytokines TNFα, IL1β, IL-10 and IL-12 (Ding et al. 2001). Finally, IKB induced NFκB activation can be inhibited by HSP27 with consequent reduction of skeletal muscle atrophy (Dodd et al. 2009).

4.1.4.2 Pharmacological induction of Heat Shock Proteins

A wide variety of cellular stresses can activate the HSR resulting in upregulation in HSP expression. However, under certain pathological conditions, such as prolonged exposure during chronic disease, genetic predisposition or otherwise, the HSR is insufficient to prevent accumulation of misfolded proteins, as observed in IBM. Notably, the endogenous inducibility of the HSR is thought to decline in normal ageing (Sherman et al. 2001). Therefore, augmentation of the HSR appears an attractive approach for the treatment of many diseases. This has been investigated particularly extensively in the context of ALS, whose pathological and clinical similarities with IBM are considerable.

Genetic upregulation of HSPs has been studied using a number of transgenic mice, in which HSP70 concentrations approaching ten times that of normal controls have been demonstrated, and through direct injection of recombinant HSP70 in the $SOD1^{G93A}$ mouse model of ALS. These approaches have had limited success, having failed to improve lifespan or motor neuron survival respectively (Liu et al. 2005; Gifondorwa et al. 2007). Furthermore, primary genetic manipulation is not currently clinically practical. Pharmacological HSR manipulation is more pragmatic and, indeed, has been more successful in preclinical models. Relevant compounds that upregulate the HSR, include 17-AAG (17-N-Allylamino-17-demethoxygeldanamycin), Celastrol and Arimoclomol (Kalmar et al. 2014). Limited data exist on 17-AAG, which acts via activation of HSF1 and ameliorates aggregation of polyglutamine proteins and α-synuclein *in vitro* and in a mouse model of spinobulbar muscular atrophy through induction of autophagy (Waza et al. 2006; Riedel et al. 2010). It also appears to protect against TDP-43 mediated neurotoxicity (Gregory et al. 2012). Celastrol, at high concentration, induces HSP70 and has been associated with cytoprotective actions and functional improvement in animal models of ALS, Parkinson's disease and Huntington's disease, along with the demonstration of anti-inflammatory effects through NFκB inhibition. However, its application appears to be limited by cytotoxicity at low concentration in *in vitro* toxicity studies, proteasomal inhibiting actions and its indiscriminate activation of the HSR, which is likely to be an undesirable effect in the treatment of human disease (Kalmar et al. 2014).

The most extensive pre-clinical efficacy data and early clinical safety data exist for the hydroxylamine derivatives Bimoclomol and its analogue Arimoclomol (/+/−(2R),(Z)-N-[2-hydroxy-3-(piperidin-1-yl)propoxy]-pyridine-1-oxide-3-carbox-imidoyl chloride citrate (1:1)) (Figure 4.5).

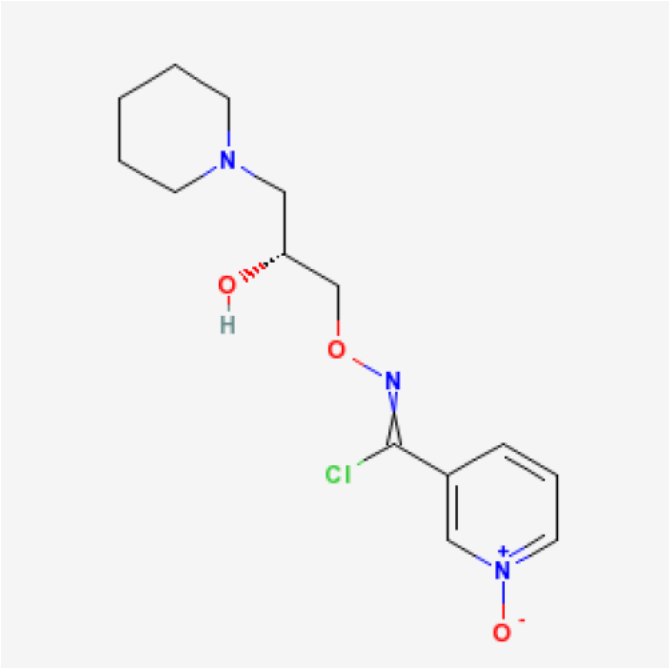

Figure 4.5 The chemical structure of Arimoclomol

These compounds stabilise the activated phosphorylated trimer of HSF1, which prolongs its binding to DNA binding regions, termed Heat Shock Elements, leading to increased translation of several HSPs under the conditions of cellular stress. The upregulated products include HSPs 60/70/90 and GRP94, but HSP70 and HSP90 are preferentially expressed. The critical element of this mechanism is the dependency on the pre-activated form of HSF1 since this targets the HSR augmentation function of Arimoclomol to those cells and tissues already subject to HSR stimulation (i.e. those under stress). This hypothesis has been confirmed by *in vitro* work that found Arimoclomol does not induce HSP expression in motor neurons in culture without contemporaneous pro-apoptotic stimulation and *in vivo* studies which demonstrate a similar lack of effect of Arimoclomol in control animal tissue (Kalmar et al. 2009). No comprehensive studies of HSP expression in IBM have been undertaken but HSP70 is upregulated in IBM compared to normal controls (Parker et al. 2009), indicating a suitable environment for Arimoclomol's action.

Several *in vitro* and *in vivo* studies have supported HSR manipulation with Arimoclomol in neurodegenerative disease. These include prolonged survival in $SOD1^{G93A}$ mice treated with Arimoclomol, with concurrent delay of disease

onset, neuronal viability, hind limb muscular strength and reduction of proteinaceous aggregates. Importantly, these effects manifested when treatment was delayed after phenotypic manifestation (Kieran et al. 2004). Similarly, Arimoclomol was effective in a mouse model of the trinucleotide expansion disorder spinobulbar muscular atrophy (Kennedy's disease), with augmented HSP expression associated with delayed clinical onset, improved muscle function and improved neuronal survival (Malik et al. 2013).

Looking further forward, Arimoclomol had the additional advantage of being supported by early-phase clinical safety and toxicity studies, facilitating the translation of laboratory work to examination in patients. This is discussed further in Chapter 5.

4.1.5 Summary and Specific Aims

Several aspects of IBM pathogenesis warranted further characterisation in this cellular model, such that quantifiable disease-relevant pathological outcome measures can be developed. The lack of such a system has contributed towards restriction of attempted drug treatments to the inflammatory component of IBM, which have been ineffective. A key element in the development of these measures is their feasibility of determining a pharmacological effect. There is considerable evidence to suggest that manipulation of the HSR, as it has done in models of comparable conditions, may counteract some pathogenic elements of both inflammation and degeneration that are active in IBM. Arimoclomol, as a co-inducer of large HSPs, particularly HSP70, represents an attractive new therapeutic avenue.

In order to determine whether this approach would be feasible, the following specific aims were addressed in the experiments described in this Chapter:

1. Characterisation of the HSR in an *in vitro* model of IBM; since Arimoclomol functions as a co-inducer of the HSR, it would only be maximally effective if the HSR were already be active in cultured cells.

2. Determination of Baseline Cytotoxicity; although considerable data support Arimoclomol's toxicity profile *in vitro*, no previous studies examined its effects on primary muscle satellite cell cultures. Furthermore, this step would represent an early component of an IBM screening system, since the significance of subtler effects on individual pathological elements would be reduced without demonstration of improved overall cellular viability.
3. Characterisation and quantification of TDP-43 pathology, ER function and NFκB activity, to further understand the nature of these processes in IBM, to determine their feasibility as drug screening tools, and to examine the effect of Arimoclomol thereon.

4.2 Results

4.2.1 The Heat Shock Response in myogenic cultures under IBM-relevant stimuli and treatment with Arimoclomol

Immunocytochemistry and western blotting demonstrated that control cultures express a constitutive level of HSP70 expression. This was not significantly altered by empty vector transfection. Exposure to IL1β (10ng/ml) was associated with significantly elevated HSP70 concentration, to 2.3 fold of control ($n=3$, $p<0.05$). However, although a 1.8 fold increase in HSP70 was observed following TNFα (10ng/ml) exposure, this was not significant. βAPP overexpression was the most potent stimulus of HSP70 expression, where an increase of 3.7 fold was observed ($n=3$, $p<0.05$).

Arimoclomol treatment (10μM, 24 hours after onset of IBM-relevant stimulus) significantly augmented the expression of HSP70. The magnitude of this effect was similar across all conditions tested; by 2.4 fold after βAPP transfection, 2.1 fold after IL1β exposure and 2.5 fold after TNFα exposure ($p<0.05$, $n=3$ per condition) (Figures 4.6 and 4.7).

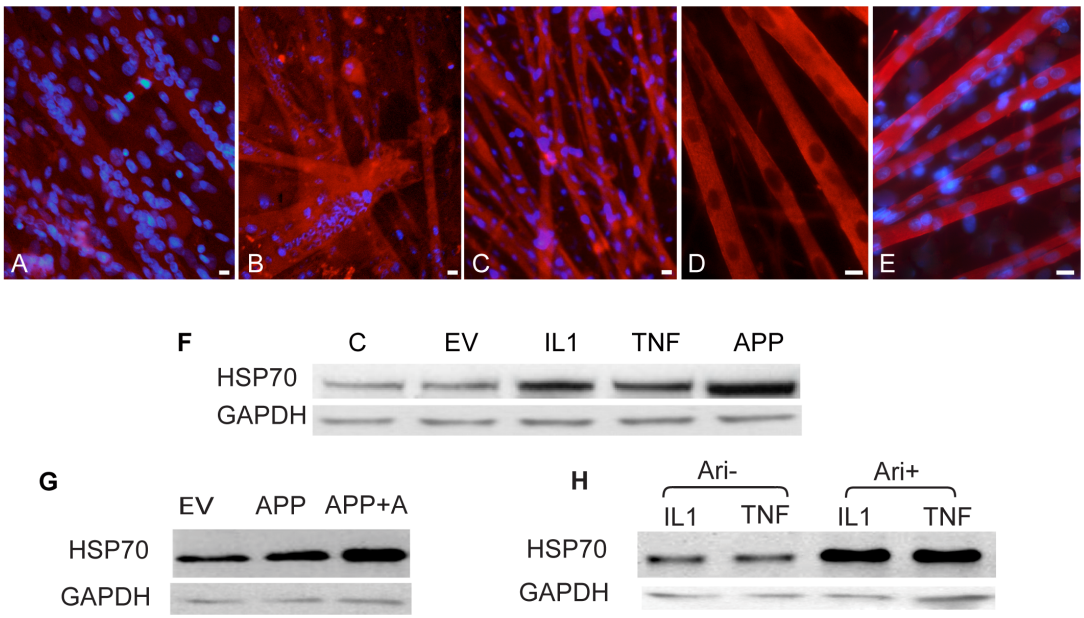

Figure 4.6 Augmentation of HSP70 expression in myogenic cells with Arimoclomol, following transfection with βAPP or exposure to inflammatory cytokines

A-E: HSP70 immunocytochemistry (red) was positive in cultures grown under control conditions (A), and more pronounced following exposure to IL1β (B) or transfection with βAPP (C), and when these conditions were succeeded by Arimoclomol treatment (following βAPP transfection in D and IL1β in E). Nuclear co-staining with DAPI (blue).

F-H: HSP70 representative western blots. C=control, EV=empty vector transfection, APP=βAPP transfection, +A or Ari+ indicates Arimoclomol treated cultures.

(Scale Bars=10μm)

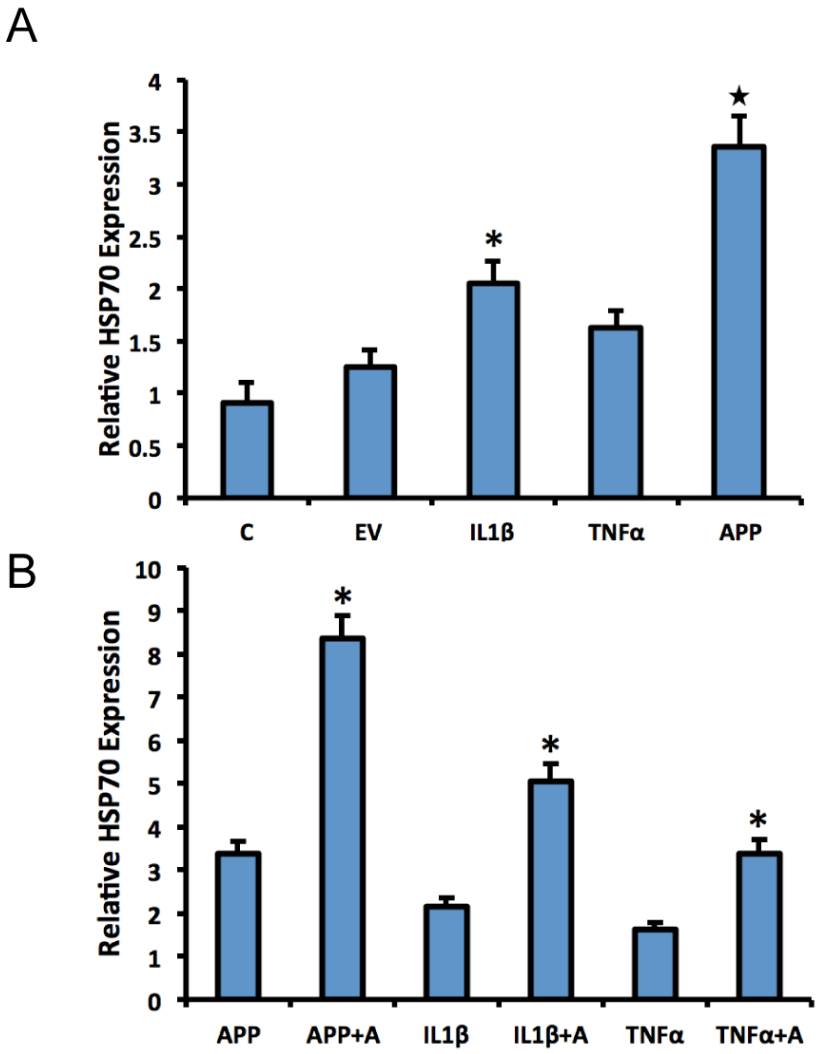

Figure 4.7 Quantification of HSP70 upregulation in myogenic cells following transfection of βAPP or exposure to inflammatory mediators and treatment with Arimoclomol

A: HSP70 expression relative to control protein (GAPDH) was determined by optical densitometry of western blots. This indicated significant upregulation of HSP70 levels after exposure to IL1β and, compared to empty vector transfection, βAPP overexpression.

B: Arimoclomol treatment (indicated by suffix +A) was associated with significant additional increase in HSP70 levels, following each pathological stimulus.

(Error Bars=SEM, n=3, Asterisk=$p<0.05$ vs. untreated control, Star=$p<0.05$ vs. empty vector transfection)

4.2.2 MTT cell viability assays

First, to determine whether cell viability could be examined in primary myogenic cultures by MTT assay, reduced glucose concentration in growth media for 2 hours, as a known inducer of cellular stress *in vitro*, was examined as a positive control. At 50% glucose concentration, MTT reduction was significantly reduced to 23.1% ±8.6% of standard cultures ($n=5$, $p<0.01$) thereby supporting the further use of the MTT assay to then determine the impact of IBM-like conditions on the viability of myogenic cell cultures.

MTT assays were then performed on βAPP over-expressing cultures. The cultures were examined at two time points: 48 or 96 hours after transfection. These correspond to the midpoint and endpoint in the typical overexpression period associated with Lipofectamine™ mediated transfection. At 48 hours, βAPP overexpression induced significant cytotoxicity compared with EV, reflected by impaired MTT reduction, measured at 53% ±4.3% versus 68% ±5.2% of control cultures ($n=5$, $p<0.05$). By 96 hours, this effect was exacerbated, where absorbance fell to 47% ±4.9% of control, compared to 74% ±7.2% of control with empty vector ($n=5$, $p<0.05$). EV transfection was associated with significantly lower MTT reduction compared to standard cultures ($p<0.05$) but there was no significant difference between the magnitude of this effect at 48 and 96 hours (Fig 4.8).

Exposure to the cytokines IL1β, TNFα also each resulted in significant attenuation of MTT reduction, reflecting cytotoxicity. A variety of concentrations were employed to establish a suitable panel for subsequent testing and to determine whether the cytotoxic effect was proportional. For either mediator, the effect indeed occurred in a dose-dependent fashion. Between 5ng/ml and 20ng/ml, IL1β was associated with absorbance between 69% ±4.4% and 48% ±5.1% of control ($n=5$, $p<0.01$). Between 5 ng/ml and 15 ng/ml, TNFα attenuated MTT reduction significantly, to between 87% ±6.8% ($p<0.05$) and 65% ±5.9% of control ($n=5$, $p<0.01$) (Fig 4.8).

Next, the effect of Arimoclomol treatment on cell viability following βAPP or exposure to cytokines was examined. At concentrations between 0.1 and 100μM, Arimoclomol had no significant effect on the MTT reduction in untreated standard control cultures (n=5). Arimoclomol (10μM) was applied to experimental cultures 24 hours after induction of the respective condition of cellular stress. In βAPP overexpressing cultures, no significant difference in MTT reduction was detected after a further 24 hours (i.e. 48 hours post-transfection). However, by 96 hours post-transfection, Arimoclomol treated cultures demonstrated significantly greater MTT reduction than untreated βAPP overexpressing cultures, at 76% ±6.1% versus 47% ±4.9% of control respectively ($n=5$, $p<0.01$). Therefore, subsequent analyses of cultures were undertaken at the 96-hour time point.

Following IL1β exposure, Arimoclomol was associated with a mean improvement in absorbance across concentrations of 13.25%, with significant differences demonstrated at 5, 15 and 20ng/ml concentrations. The largest increase, from 48% ±5.1% to 69% ±5.9% of control absorbance, was demonstrated at 20ng/ml ($n=5$, $p<0.01$).

The impact of Arimoclomol on TNFα-induced cytotoxicity was more modest, with a mean improvement of 6.75% across the tested concentrations. However, the lowest concentration of TNFα did not induce significant change in MTT reduction compared to control. Some of this apparent lack of treatment effect may reflect the limited action of Arimoclomol, as a co-inducer, on 'unstressed' cells. Nevertheless, a significant treatment effect was demonstrated at 10ng/ml TNFα, where absorbance increased from 69% ±4.9% to 82% 3.8% of control ($n=5$, $p<0.05$) (Fig 4.8).

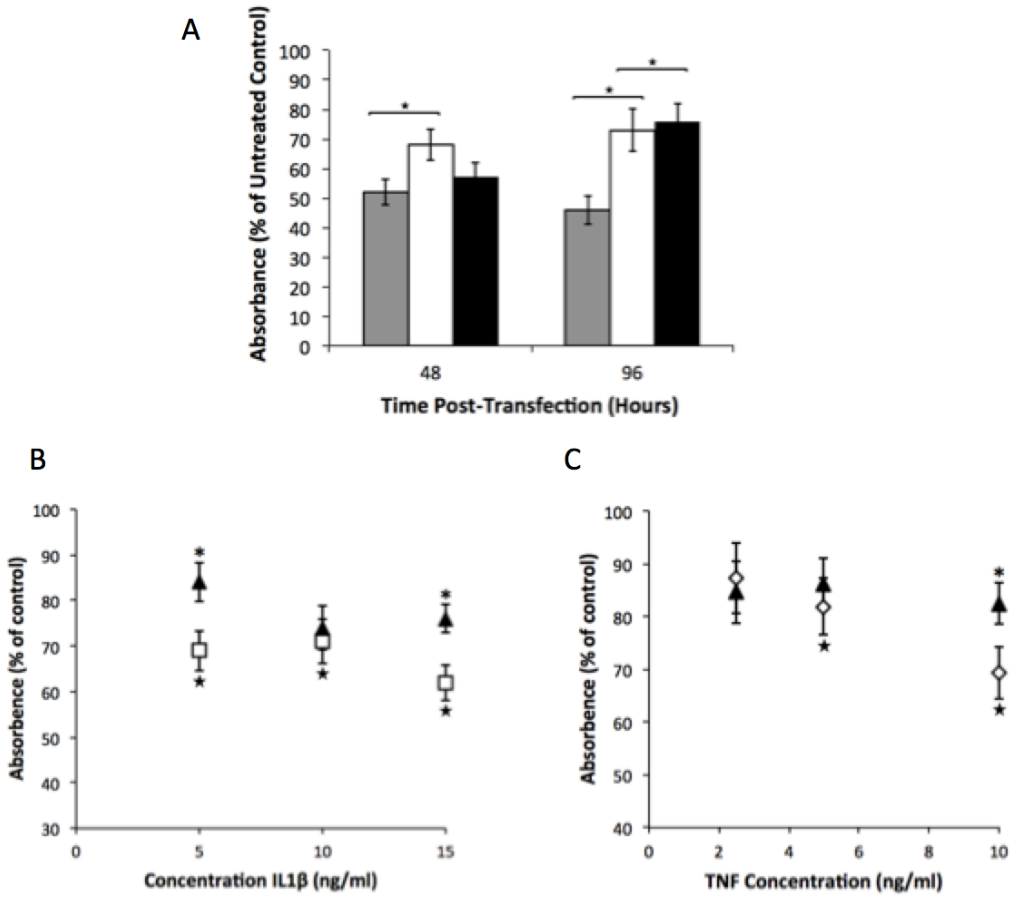

Figure 4.8 Cell viability following βAPP transfection or exposure to inflammatory cytokines and the effect Arimoclomol treatment

As determined by MTT assays, the reduction of cell viability associated with βAPP transfection and cytokine exposure was significantly attenuated by Arimoclomol treatment. White markers=control cultures without Arimoclomol, Grey=Empty Vector control, Black markers=with Arimoclomol

(Error Bars=SEM, n=5, Star=$p<0.05$)

4.2.3 TDP-43

The evidence that TDP-43 mislocalisation distinguishes IBM from its differential diagnoses is stronger than that for other proteins that constitute the cytoplasmic inclusions observed in affected muscle. Additionally, IBM tissue demonstrates increased TDP-43 concentration, which has not been established with for other proteins. Therefore, these experiments prioritised the development of an assay of TDP-43 pathology over other inclusion-forming proteins. Furthermore, it was noted in preliminary experiments that TDP-43 C-terminus staining exhibited a fairly predictable spectrum of change, which was conducive to quantification. Normal nuclear staining evolved, under pathological conditions, to cytoplasmic inclusion formation with retained nuclear staining, to loss of nuclear staining with or without cytoplasmic inclusions. This cytoplasmic translocation mirrors the pattern of TDP-43 pathology described in other tissues (Janssens et al. 2013).

4.2.3.1 TDP-43 immunostaining in untreated primary myogenic cultures

Under normal culture conditions, TDP-43 immunostaining in myotubes was predominantly nuclear, which was readily identifiable, with some largely homogenous cytoplasmic staining at lower intensity. Comparison with nuclear staining using DAPI demonstrated that only exceptionally rarely were myotubular nuclei TDP-43 immunonegative (Figure 4.9). Therefore, additional DAPI staining was not employed in the further determination of TDP-43 nuclear immunoreactivity.

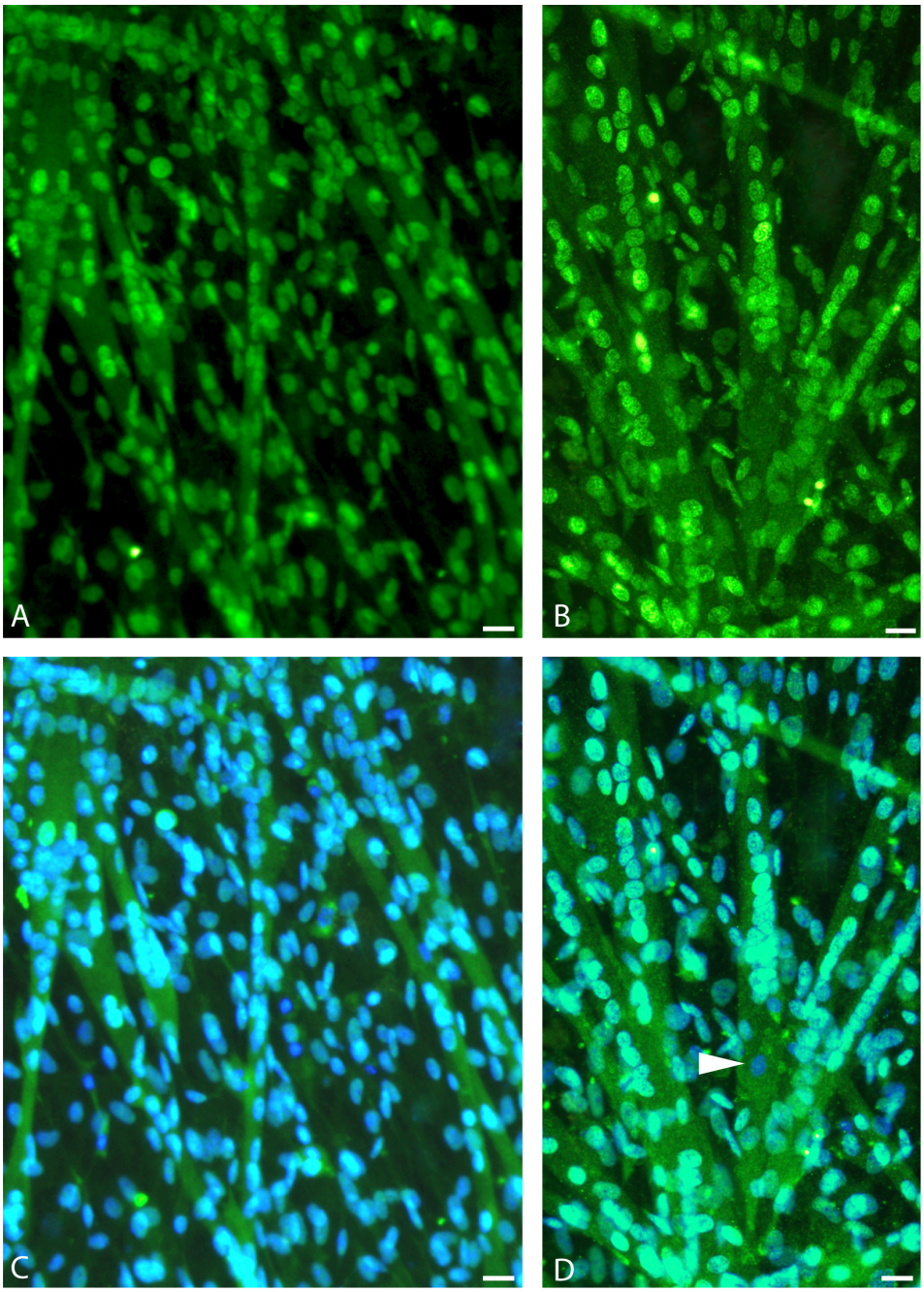

Figure 4.9 TDP-43 under normal culture conditions

Under normal conditions, TDP-43 (green) immunostaining is predominantly nuclear, with cytoplasmic staining of lower intensity. Comparison with matched images including additional DAPI staining (overlayed blue in C, D) reveals almost 100% concordance of nuclear identification. On rare occasions, myotubular nuclei identified by DAPI staining lacked TDP-43 staining (such as nucleus arrowed in D).

(Scale Bars=20μm)

4.2.3.2 Quantification of TDP-43 immunostaining

The overexpression of βAPP or exposure to inflammatory cytokines induced a range of pathological features in cultured myotubes. The loss of nuclear TDP-43 staining was examined as the primary measure in quantifying the TDP-43 response to IBM-relevant conditions. Counting the absolute number of TDP-43 cytoplasmic inclusions was impractical due to their small size, high number and frequent clustering. Furthermore, since it remains unclear whether such structures represent a cytoprotective or cytotoxic response, it is difficult to use this parameter as an indicator of the beneficial effect of potential therapeutic compounds. Rather, the presence or absence of cytoplasmic inclusions was noted after determination of the nuclear staining pattern.

4.7.3.3 Cytoplasmic translocation and nuclear depletion of TDP-43

Under normal culture conditions, fewer that 10% of myotubes demonstrated absence of normal nuclear TDP-43 immunoreactivity. However, over-expression of βAPP or exposure to cytokines produced a significant increase in translocation of TDP-43 from the nucleus to the cytoplasm (Fig 4.10).

Compared to EV transfection, βAPP overexpression was associated with an increase in non-nuclear TDP-43 staining from 7.31% ±0.78% to 75.28% ±6.9% ($n=5$, $p<0.001$), an absolute increase of 67.97% and relative increase of 10.3 fold.

IL1β exposure, between 5 ng/ml and 20 ng/ml increased non-nuclear TDP-43 staining in a dose-dependent manner, from 4.53% ±0.67% to a maximum of 47.56% ±2.76% ($n=5$, $p<0.01$) at 20 ng/ml. The maximal effect represented an absolute increase of 43.03% and relative increase of 10.5 fold.

TNFα exposure was also associated with a significant reduction of TDP-43 nuclear immunoreactivity between 5 ng/ml and 20 ng/ml. The maximal effect was observed at 20 ng/ml, where non-nuclear TDP-43 staining increased from 2.32% ±0.31% to 62.18% ±3.31% ($n=5$, $p<0.001$), an absolute increase of 59.86% and relative increase of 26.8 fold.

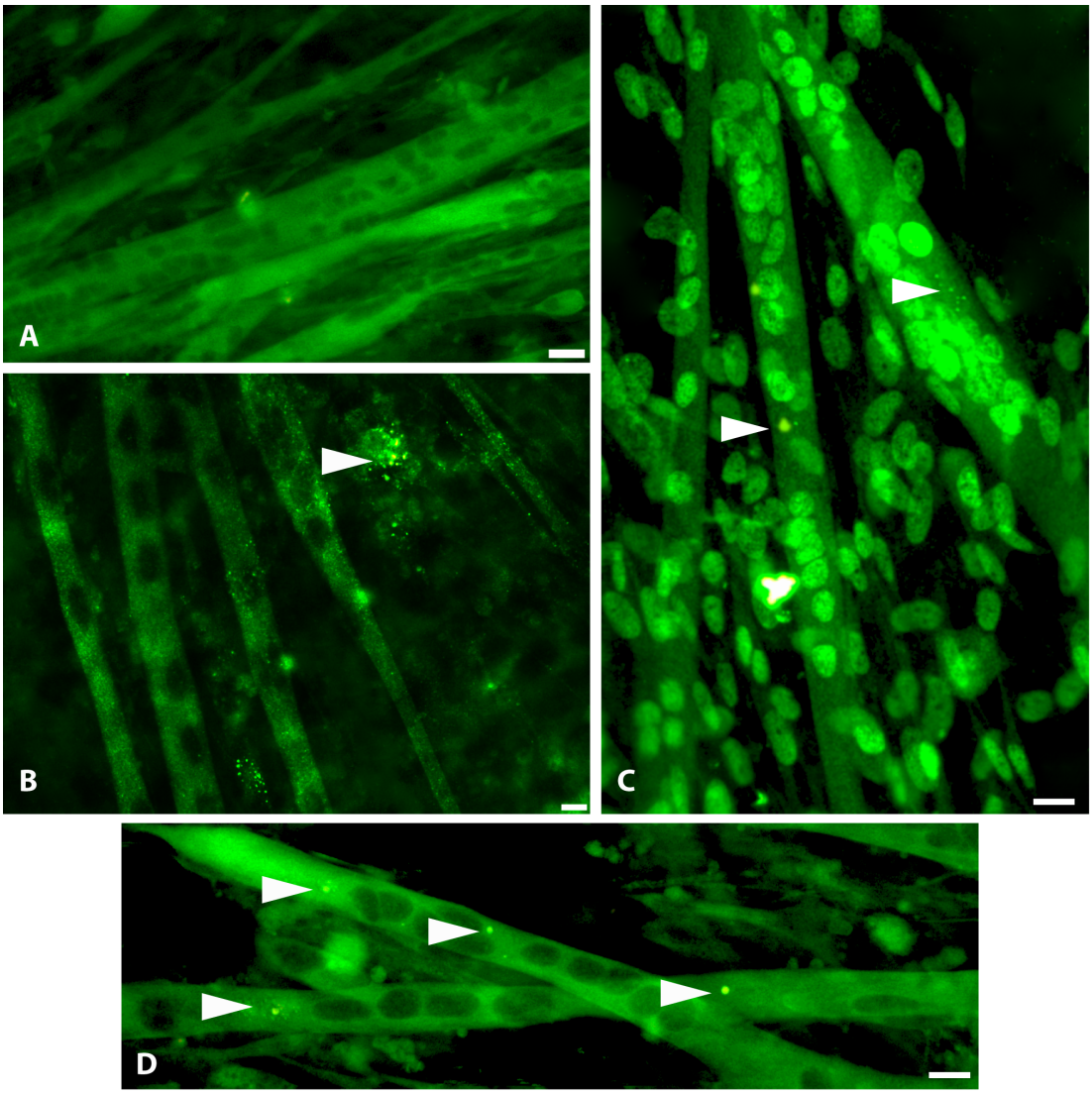

Figure 4.10 Spectrum of TDP-43 pathology after overexpression of βAPP or exposure to inflammatory cytokines

Immunostaining of TDP-43 (green) following exposure to TNFα (A), IL1β (B) or βAPP overexpression (C and D) demonstrated that loss of nuclear staining was the most characteristic finding under all conditions. This was observed with and without the appearance of cytoplasmic TDP-43 aggregates (arrows in B, C and D). More rarely, nuclear staining was retained in the presence of cytoplasmic aggregates (C), perhaps indicating an earlier stage of the pathological spectrum (Scale Bars=20μm)

The absence of significant TDP-43 pathology following the non-specific 'stressor' of empty vector transfection implies a degree of specificity to the IBM-relevant stimuli examined in the other experiments. To examine this hypothesis further, the generic stimulus of glucose deprivation, which had previously been demonstrated to produce a quantifiable proportional reduction of overall cell viability in myogenic cultures, was examined. At concentrations between 20% and 80% of control medium glucose concentration, no significant impact on TDP-43 staining was observed (n=3).

4.7.3.4 The effect of Arimoclomol on TDP-43 localisation

Arimoclomol treatment attenuated the effect of βAPP and cytokines on the localisation of TDP-43 immunoreactivity (Figs 4.11 and 4.12).

Following βAPP over-expression, treatment with Arimoclomol was associated with a reduction in the proportion of myotubes demonstrating non-nuclear TDP-43 from 75.28% ±6.9% to 57.67% ±6.1% (n=5, $p<0.05$), an absolute reduction of 17.61% and relative reduction of 23.3%.

Arimoclomol significantly attenuated the effect of IL1β exposure, at 5 ng/ml and 20 ng/ml, on TDP-43 localisation. Across all IL1β concentrations tested, the mean absolute reduction in the number of myotubes demonstrating non-nuclear TDP-43 was 11%. The maximum effect was observed at 20 ng/ml, with an absolute reduction of 23.27% and relative reduction of 48.9%.

Arimoclomol also reduced the impact of TNFα on TDP-43 localisation, at a mean absolute reduction of 16% across all TNFα concentrations (n=5). The maximum significant effect was demonstrated at 10 ng/ml, with an absolute reduction of 29.34% and relative reduction of 51.1%.

Notably, Arimoclomol had no effect on the localisation of TDP-43 in control cultures. This implies the low frequency of TDP-43 changes seen in those cells either reflect normal variation or are dependent on another pathway that Arimoclomol does not affect.

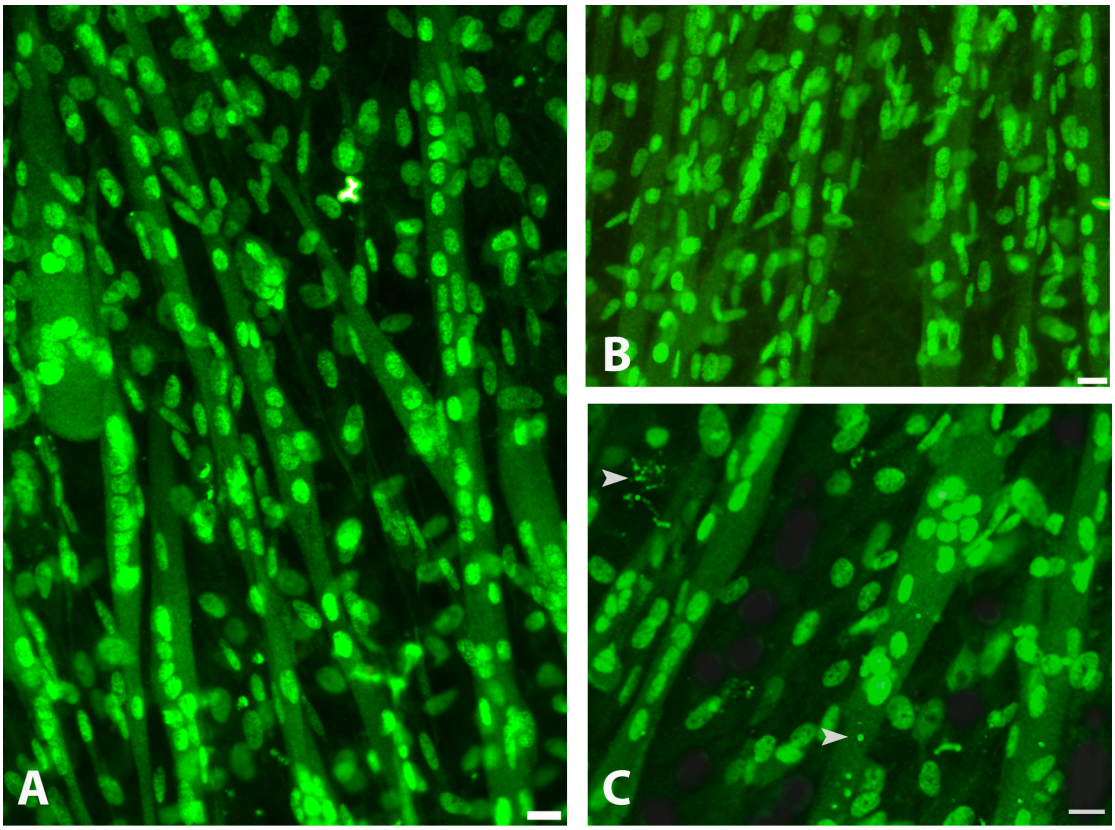

Figure 4.11 Effect of Arimoclomol treatment on the pattern of TDP-43 immunoreactivity in myogenic cultures

Following Arimoclomol treatment of cultures under conditions of IL1β exposure (A), TNFα (B) or βAPP overexpression (C), TDP-43 immunostaining demonstrated a significant increase of cells with the predominantly nuclear staining characteristic of normal control cultures, and reduction of cells with loss of nuclear staining. Some myotubes that retained nuclear staining also displayed elements of mislocalisation such as cytoplasmic aggregates (arrowed in C).

(Scale Bars=20μm)

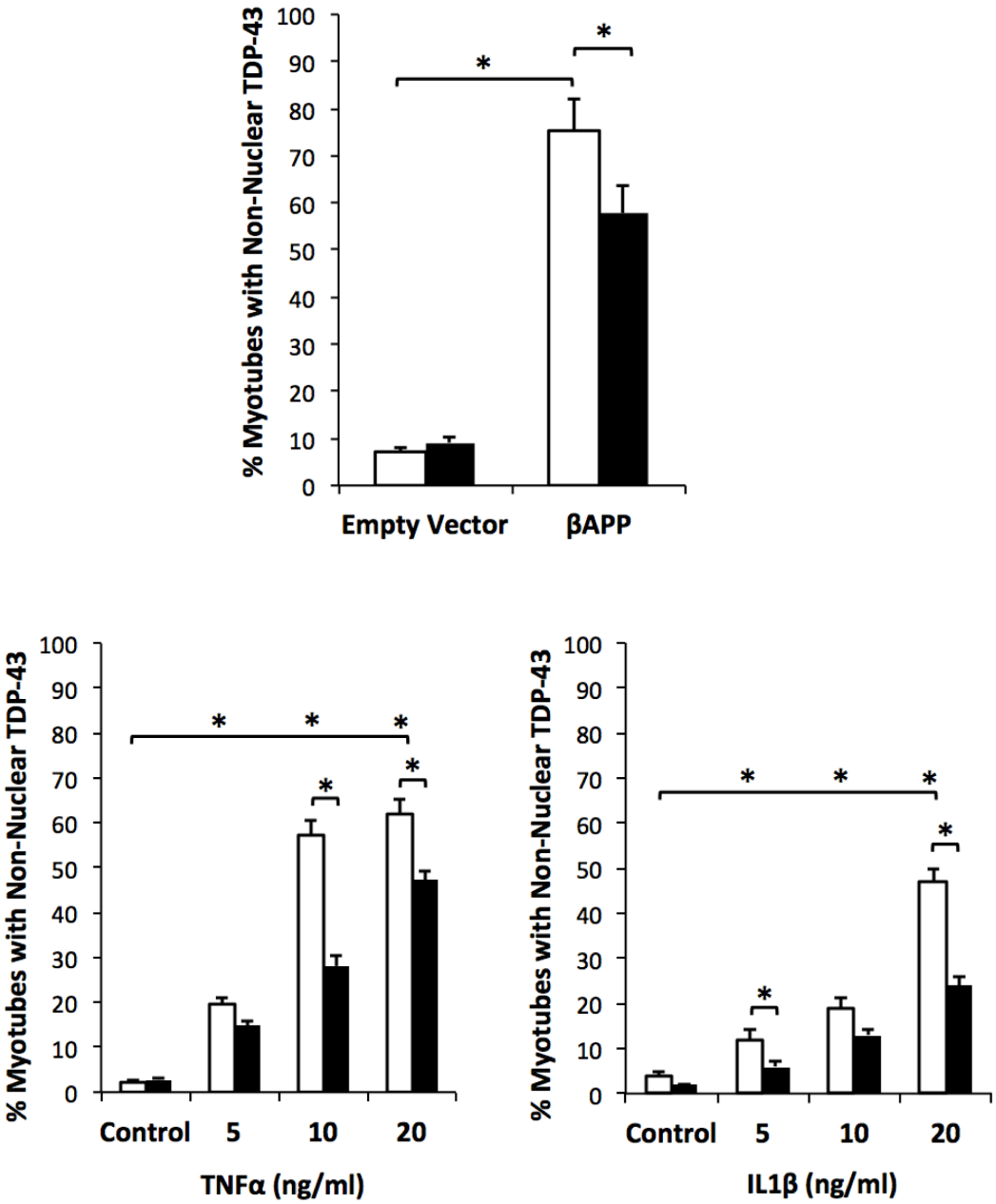

Figure 4.12 Quantification of TDP-43 mislocalisation in myogenic cultures following overexpression of βAPP, exposure to inflammatory cytokines and treatment with Arimoclomol

The proportion of myotubes that displayed mislocalised (non-nuclear) TDP-43 was significantly increased by overexpression of βAPP versus empty vector control and by exposure to cytokines versus unexposed control cultures (white bars). Treatment with Arimoclomol (black bars) significantly attenuated the mislocalisation of TDP-43 associated with these conditions.

(Error Bars=SEM, n=5 per condition, Asterisk=$p<0.05$)

Next, it was determined whether the magnitude of the effect of Arimoclomol to attenuate TDP-43 mislocalisation simply reflected the comparative magnitude of that mislocalisation in the corresponding untreated control culture. Plotting the relative change associated with Arimoclomol treatment against the absolute values of TDP-43 suggests there is not a proportional relationship between these two factors (Figure 4.13). In turn, this strengthens the likelihood that the effect of Arimoclomol is not a generic action but, in combination, depends on the other major variable in these experiments, the means through which TDP-43 pathology was induced.

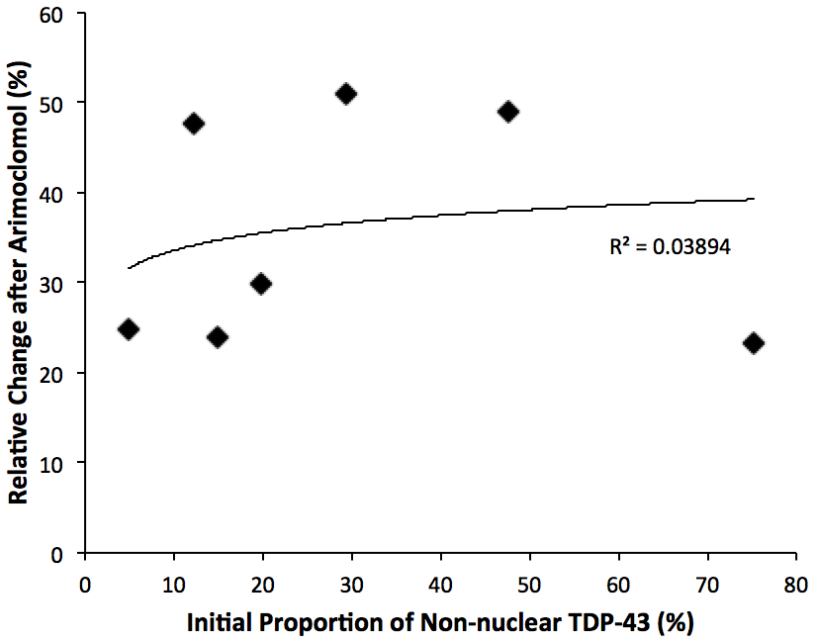

Figure 4.13 Examination of the specificity of Arimoclomol's effect

The mean change in TDP-43 mislocalisation after Arimoclomol treatment is plotted against the mean proportion of TDP-43 mislocalisation under all experimental conditions without Arimoclomol (the data in Fig 4.13). The lack of proportional relationship (R^2=0.04) implies the effect of Arimoclomol does not simply reflect the pre-treatment state of TDP-43 localisation in a given culture.

4.2.3.5 The effect of βAPP overexpression, exposure to inflammatory cytokines and Arimoclomol treatment on TDP-43 expression

Next, the impact of βAPP over-expression and exposure to inflammatory cytokines on TDP-43 concentration was examined using western blotting. Compared to control cultures, empty vector transfection did not significantly affect the level of TDP-43 expression. However, βAPP transfection was associated with a significant increase in TDP-43 expression, at 2.53 fold over that of control ($n=3$, $p<0.01$). Glucose deprivation also produced a small, but significant, effect of a 1.36 fold increase over control ($n=3$, $p<0.05$) (Fig 4.14).

Exposure to the cytokines TNFα and IFNγ significantly increased TDP-43 concentration, at 2.01 and 1.77 fold greater than control respectively ($n=3$, $p<0.05$). However, IL1β was not associated with a significant increase in TDP-43 expression (Fig 4.15).

Treatment of βAPP transfected or cytokine exposed myogenic cultures with Arimoclomol was associated with a significant reduction in the level of TDP-43 expression. Typically this reflected attenuation of the increase in TDP-43 associated with the given IBM-relevant stimulus, rather than a reduction versus unexposed control cultures. After βAPP over-expression, Arimoclomol treated cultures demonstrated TDP-43 expression at 59.9% of the untreated population. This level of expression was not significantly different to that of untransfected control cultures ($n=3$, $p=0.051$) (Fig 4.14).

Although the impact of inflammatory cytokines was generally less marked than that of βAPP, the effect of Arimoclomol appeared proportionately greater under these conditions. Indeed, after Arimoclomol treatment of cultures exposed to each cytokine, TDP-43 concentration was lower than that of unexposed control. Relative to the untreated comparator, the TDP-43 expression levels after Arimoclomol treatment of IL1β, TNFα and IFNγ exposed cultures were 51.2%, 35.8% and 24.3% respectively ($n=3$, $p<0.05$) (Fig 4.15).

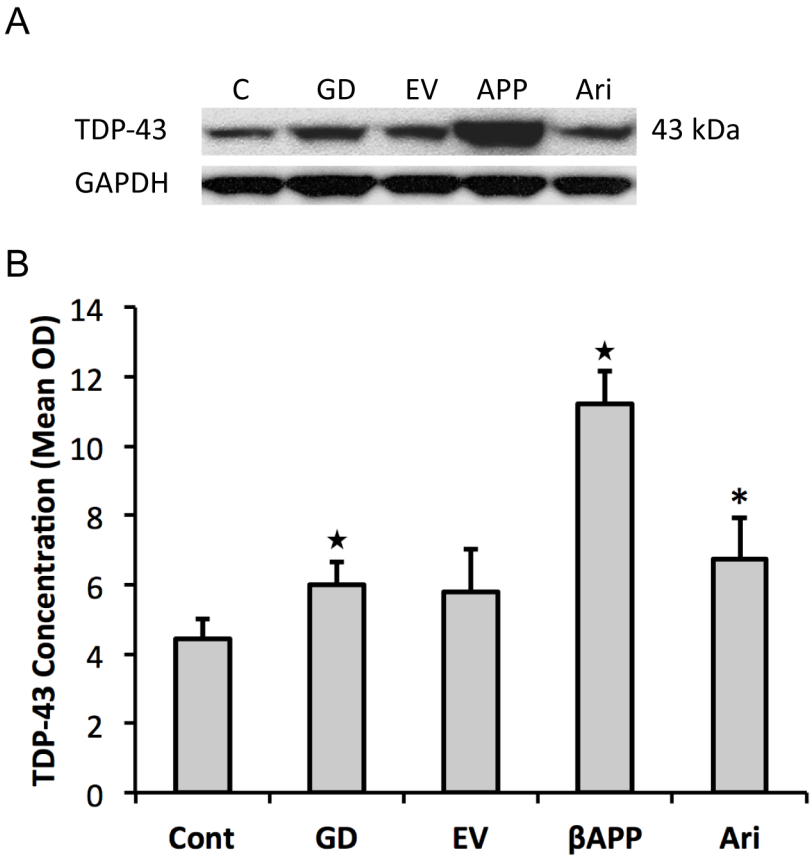

Figure 4.14 TDP-43 expression in myogenic cultures following βAPP over-expression and Arimoclomol treatment

A: Representative western blot for TDP-43 in myogenic cultures under control conditions (C), 2 hours of Glucose Deprivation (GD), Empty Vector transfection (EV), βAPP overexpression (APP) and βAPP overexpression with Arimoclomol treatment (Ari).

B: Mean optical densitometry of western blots demonstrates that βAPP overexpression significantly elevates TDP-43 concentration compared to empty vector control. Arimoclomol treatment prevents this effect and, here, TDP-43 concentration is not significantly different to control.

(Error Bars=SEM, n=3, Star=$p<0.05$ vs. corresponding control culture, Asterisk=$p<0.05$ vs. βAPP overexpression)

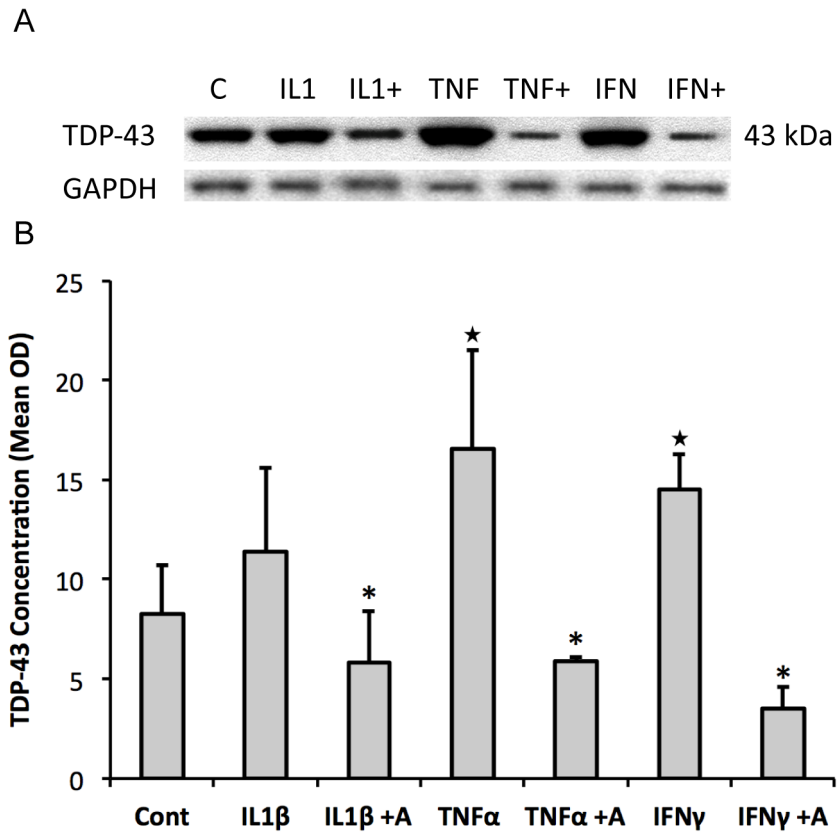

Figure 4.15 TDP-43 expression in myogenic cultures following exposure to inflammatory cytokines and treatment with Arimoclomol

A: Representative western blot for TDP-43 in myogenic cultures under control conditions (C) or exposure to IL1β (IL1), TNFα (TNF) or IFNγ (IFN). The addition of Arimoclomol treatment to these conditions is indicated with plus sign.

B: Mean optical densitometry of western blots demonstrates that TNFα and IFNγ were associated with significant increases in TDP-43 expression. IL1β, however, was not. Arimoclomol treatment (indicated by +A) was associated with a significant reduction of TDP-43 expression compared to the relevant untreated control condition.

(Error Bars=SEM, n=3, Star=$p<0.05$ versus control culture not exposed to cytokines, Asterisk=$p<0.05$ vs. same condition minus Arimoclomol treatment)

4.2.4 Endoplasmic reticulum function and calcium homeostasis

As described above (Chapter 4, Section 4.3), ER stress and its close association with disturbed intracellular calcium (Ca^{2+}) signalling are proposed as a central and early indicators of IBM pathology. Therefore, these represent attractive therapeutic targets. The next set of experiments sought to determine whether ER stress or Ca^{2+} dyshomeostasis were evident in myogenic cultures exposed to IBM-relevant stimuli and to what degree these pathological processes could be quantified. This was examined using live confocal imaging of intracellular Ca^{2+}, with the fluorescent dye Fluo4-AM, and the determination of the expression of ER stress markers using western blots.

4.2.4.1 Live cell Ca^{2+} Imaging: baseline fluorescence

It was first necessary to determine whether the proposed experimental protocol could be completed within a period during which a stable fluorescent signal corresponding to Ca^{2+}-bound Fluo-4AM could be obtained, independently of any pharmacological manipulation. Therefore, myotubes were observed for approximately twice the maximum anticipated time required to complete the proposed protocol. Myotubes did not demonstrate a significant persistent deviation from baseline during this period (Figure 4.16) (n=27 cells, corresponding to 3 cells from 3 random coverslips from 3 cultures).

4.2.4.2 Determination of cell types used for analysis of intracellular Ca^{2+}

Elongated myotubes were readily identifiable and distinguishable from the circular conformation of contracted myotubes or myocytes, meaning experimental data could be restricted purely to this cell type of interest. Only myotubes that obeyed predetermined characteristics were included in the analysis of Ca^{2+} response (Figure 4.17).

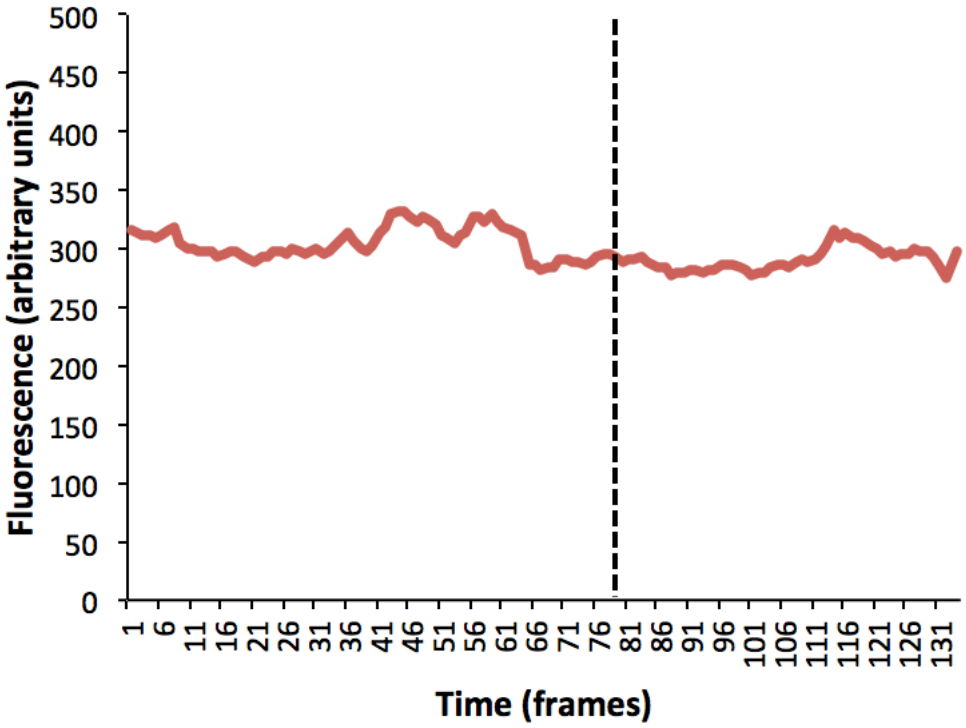

Figure 4.16 Baseline Ca^{2+} fluorescence with Fluo-4AM in a myotube from a control culture

Representative Fluo4-AM fluorescence trace (red line) of an individual myotube, grown under standard culture conditions, observed for approximately twice the anticipated length of the experimental protocol intended to examine ER Ca^{2+} in myogenic cultures. Dotted black line indicates the anticipated time limit of this protocol.

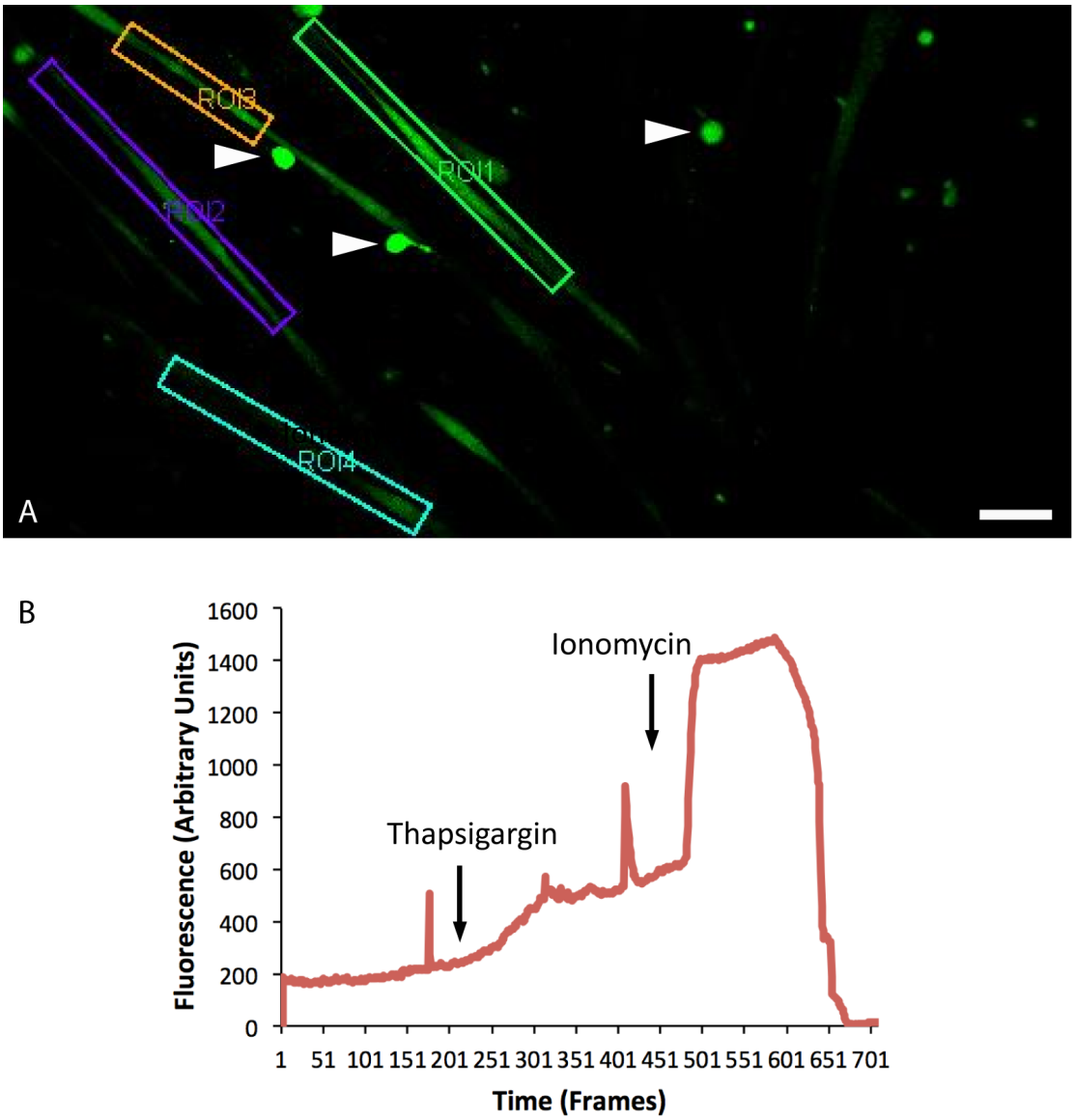

Figure 4.17 Identification of myotubes for Ca^{2+} analysis

A: Four myotubes labelled with region of interest (ROI) rectangles. Myocytes are indicated by white arrows. ROI 13 (orange rectangle) demonstrates myotubes with two closely adjacent myocytes, which would preclude this cell from analysis.

B: Representative example trace of myotube throughout experimental protocol, with administration of thapsigargin and ionomycin as indicated. This myotube demonstrates spontaneous spikes in fluorescence prior to administration of experimental compounds. This would exclude this cell from analysis.

To minimise other potentially confounding variables, parameters were set with which myotubes were selected for inclusion in the analysis. The following characteristics excluded a cell from use in analysis:

1. Overlapping with another other cell or with other cells in close proximity meaning the region of interest box could include more than one cell (Fig 4.18, A)
2. Morphology other than that of the distinctive, elongated, multinuclear myotube
3. Any cell which appeared disproportionately bright to initial inspection compared to other cells within the field (i.e. that might represent bleaching of dye)
4. Any cell with spontaneous changes in fluorescence, either on microscopy or subsequent plotted data analysis (Fig 4.17, B).

It was noted, in keeping with the expected maturation of calcium dependent excitation contraction coupling machinery, that spontaneous changes in fluorescence became markedly more common after 10 days in culture. Therefore all calcium fluorescence imaging experiments were conducted before this time point. Figure 4.18 illustrates the typical Ca^{2+} response of a group of myotubes using the optimised experimental protocol.

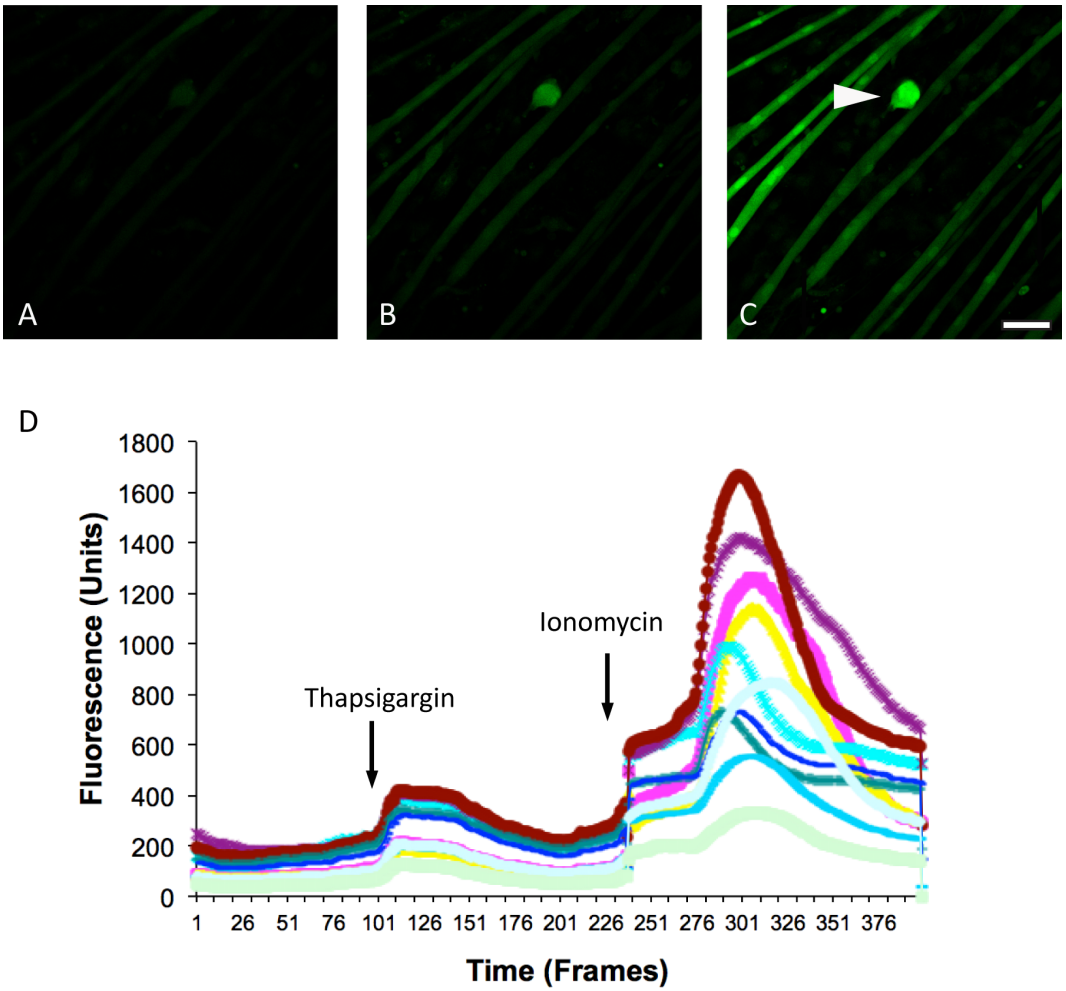

Figure 4.18 Experimental protocol for determination of cytosolic and ER calcium

A-C: representative images of one viewing region of myotubes during different stages of the protocol. A=at baseline, B=after administration of Thapsigargin, C=after administration of Ionomycin. Contracted myotubes such as that indicated (arrow in C) were not included in the analysis. (Scale Bar=100μm)

D: corresponding representative trace of fluorescence within individual myotubes from one experiment (each myotube represented by one coloured trace). Each myotube demonstrated increased fluorescence (reflecting increased cytosolic [Ca^{2+}]) after the administration of Thapsigargin, a non-competitive inhibitor of the SERCA. This approximates the discharge of ER Ca^{2+} into the cytosol. After this response completed, the calibration point for maximal fluorescence (required to calculate [Ca^{2+}] from fluorescence readings) was acquired through the administration of ionomycin.

4.2.4.3 Baseline cytosolic Calcium

Fluorescence prior to the administration of thapsigargin was used to determine the baseline mean cytosolic calcium concentration, $[Ca^{2+}]_{Cyto}$, of myotubes across experimental conditions (Figure 4.19).

Under standard culture conditions, $[Ca^{2+}]_{Cyto}$ was 262.42 nM ±28.5nM. After βAPP over-expression, this increased significantly to 373.49 nM ±21.2nM (n=5, $p<0.05$). Empty vector was not associated with a significant change in $[Ca^{2+}]_{Cyto}$.

At each concentration tested between, 5 and 20 ng/ml, IL1β exposure was associated with a significant increase in $[Ca^{2+}]_{Cyto}$. This did not appear to be a concentration dependent effect. Mean $[Ca^{2+}]_{Cyto}$ across concentrations was 354.45 nM (n=5, $p<0.01$).

At 5 and 10 ng/ml, TNFα exposure also significantly increased $[Ca^{2+}]_{Cyto}$ but, at 20 ng/ml, was not associated with a significant change. Mean $[Ca^{2+}]_{Cyto}$ across concentrations was 316.89 nM (n=5, $p<0.01$).

Treatment with Arimoclomol was not associated with a significant difference in $[Ca^{2+}]_{Cyto}$ after application to control cultures or to the single experimental condition (TNFα 20 ng/ml) that was not associated with a significant change to $[Ca^{2+}]_{Cyto}$. However, Arimoclomol attenuated the elevation of $[Ca^{2+}]_{Cyto}$ associated with IBM-relevant stimuli. Following βAPP over-expression, $[Ca^{2+}]_{Cyto}$ was reduced from 373.49 nM ±21.2 nM to 282.5 nM ± 17.5 nM (n=5, $p<0.01$), which is a concentration not significantly different to that of control. Further significant effects of Arimoclomol were demonstrated in association with IL1β, at each concentration tested between 5 and 20 ng/ml. Mean $[Ca^{2+}]_{Cyto}$ fell from 354.35 nM to 253.5 nM (n=5, $p<0.01$), a relative reduction of 28.5%. Following TNFα exposure, other than at 20 ng/ml which had not been associated with a change in the underlying $[Ca^{2+}]_{Cyto}$, Arimoclomol produced a significant reduction of $[Ca^{2+}]_{Cyto}$. Across the concentrations tested, mean $[Ca^{2+}]_{Cyto}$ fell from 316.89 nM to 268.92 nM (n=5, $p<0.01$), a relative reduction of 14.8%. As observed after βAPP over-expression, the effect of Arimoclomol following cytokine exposure restored $[Ca^{2+}]_{Cyto}$ to a level not significantly different to control cultures.

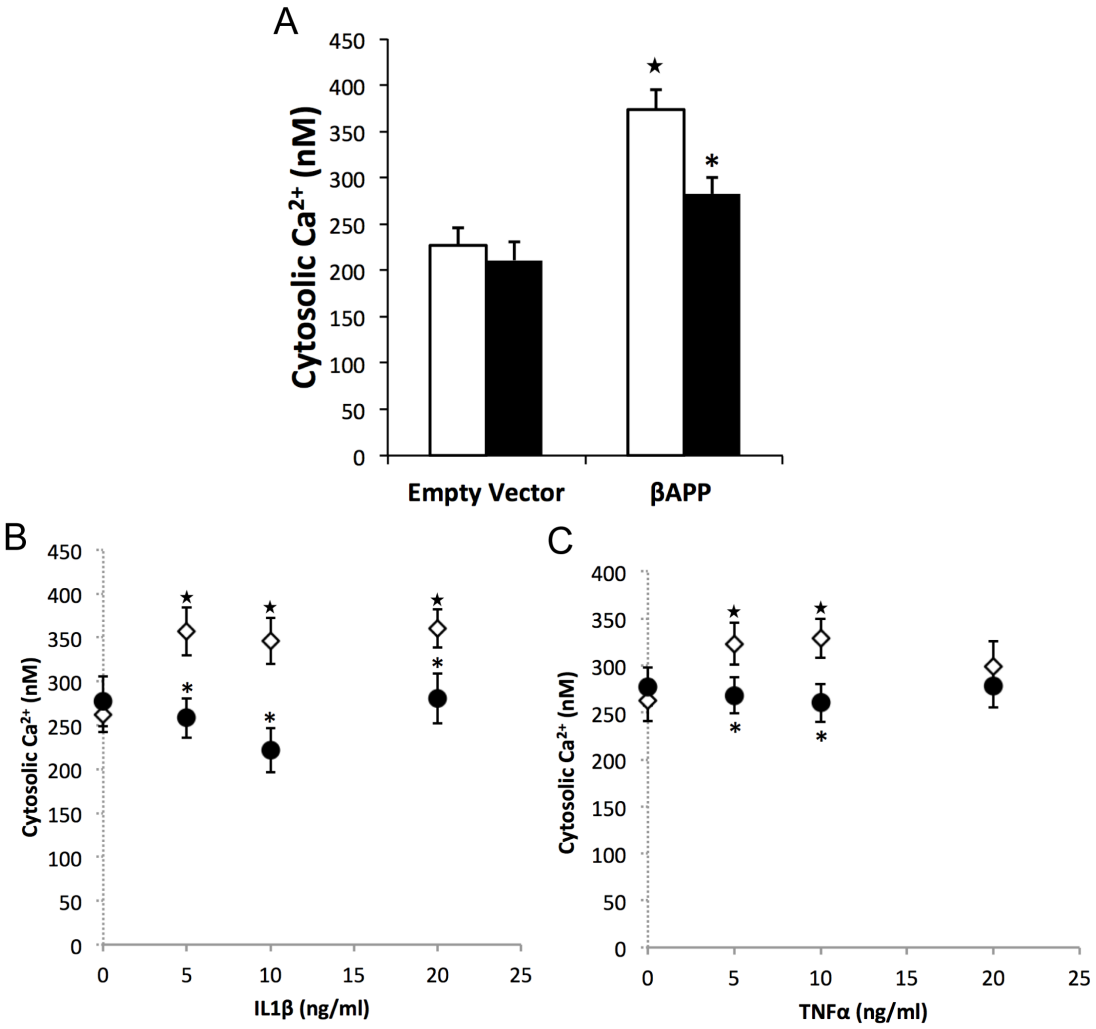

Figure 4.19 Effect of Arimoclomol on baseline cytosolic Calcium following βAPP overexpression or exposure to inflammatory cytokines

A: Overexpression of βAPP significantly elevated $[Ca^{2+}]_{Cyto}$ versus empty vector transfected controls (white bars). Arimoclomol treatment after βAPP overexpression inhibited this effect and was associated with a $[Ca^{2+}]_{Cyto}$ not significantly different to empty vector control (black bars). Arimoclomol treatment had no significant effect on empty vector control.

B/C: Arimoclomol treatment (black symbols) significantly attenuated the elevation of $[Ca^{2+}]_{Cyto}$ that followed exposure to cytokines IL1β or TNFα (white symbols). $[Ca^{2+}]_{Cyto}$ was restored to levels insignificantly different to control cultures.

(Error Bars=SEM, n=5 per condition, Star=$p<0.05$ vs. empty vector or unexposed cultures, Asterisk=$p<0.05$ vs. control not treated with Arimoclomol)

4.2.4.4 Inferred ER Calcium under IBM-like conditions

ER calcium concentration $[Ca^{2+}]_{ER}$, inferred from the change in cytosolic fluorescence after SERCA inhibition by thapsigargin, was significantly altered by IBM-like conditions (Figure 4.20).

Compared to contemporaneous control cultures, where mean $[Ca^{2+}]_{ER}$ was 350.89 nM ±22.3 nM, empty vector transfection (EV) was associated with a consistently lower $[Ca^{2+}]_{ER}$ but this was not significant 280.4 nM ±20.8 nM (n=5, p=0.09). βAPP overexpression, however, was associated with a significantly lower $[Ca^{2+}]_{ER}$ compared to EV, at 190.58 nM ±22.8 nM (n=5, $p<0.05$). This equated to a relative reduction of 32%.

IL1β exposure was associated with a dose dependent reduction in $[Ca^{2+}]_{ER}$ (R^2=0.89), which was significant at each concentration tested when compared to contemporaneous control cultures. At the lowest concentration, IL1β 5ng/ml, $[Ca^{2+}]_{ER}$ fell to 226.4 nM ±18.5 nM (n=5, $p<0.01$), which represented a relative reduction of 37.2%. At the highest concentration, IL1β 20 ng/ml, $[Ca^{2+}]_{ER}$ fell to 122.4 nM ±18.9 nM (n=5, $p<0.01$), a greater relative reduction of 66%.

The effect of TNFα exposure was also broadly dose dependent, but less tightly so than with IL1β (R^2=0.645). Significant reductions of $[Ca^{2+}]_{ER}$ were observed at 2.5, 5 and 20 ng/ml concentrations. At the lowest concentration, TNFα 2.5 ng/ml, $[Ca^{2+}]_{ER}$ fell to 260.56 nM ±25.2 nM (n=5, $p<0.05$), a relative reduction of 26.7%. At the highest concentration, TNFα 20 ng/ml, $[Ca^{2+}]_{ER}$ fell to 190.54 nM ±19.3 nM (n=5, $p<0.01$), a greater relative reduction of 46%.

4.2.4.5 The effect of Arimoclomol on inferred ER Calcium

Arimoclomol attenuated the impact of IBM-like conditions on $[Ca^{2+}]_{ER}$. Arimoclomol did not affect $[Ca^{2+}]_{ER}$ the control cultures significantly (339.5 nM, ±20.7nM, p=0.72). Similarly, EV cultures were not affected significantly (320.9 nM, ±21.4nM, p=0.25). However, following βAPP overexpression, Arimoclomol significantly attenuated the reduction of $[Ca^{2+}]_{ER}$ to 290.2 nM ±26.1nM (n=5, $p<0.05$).

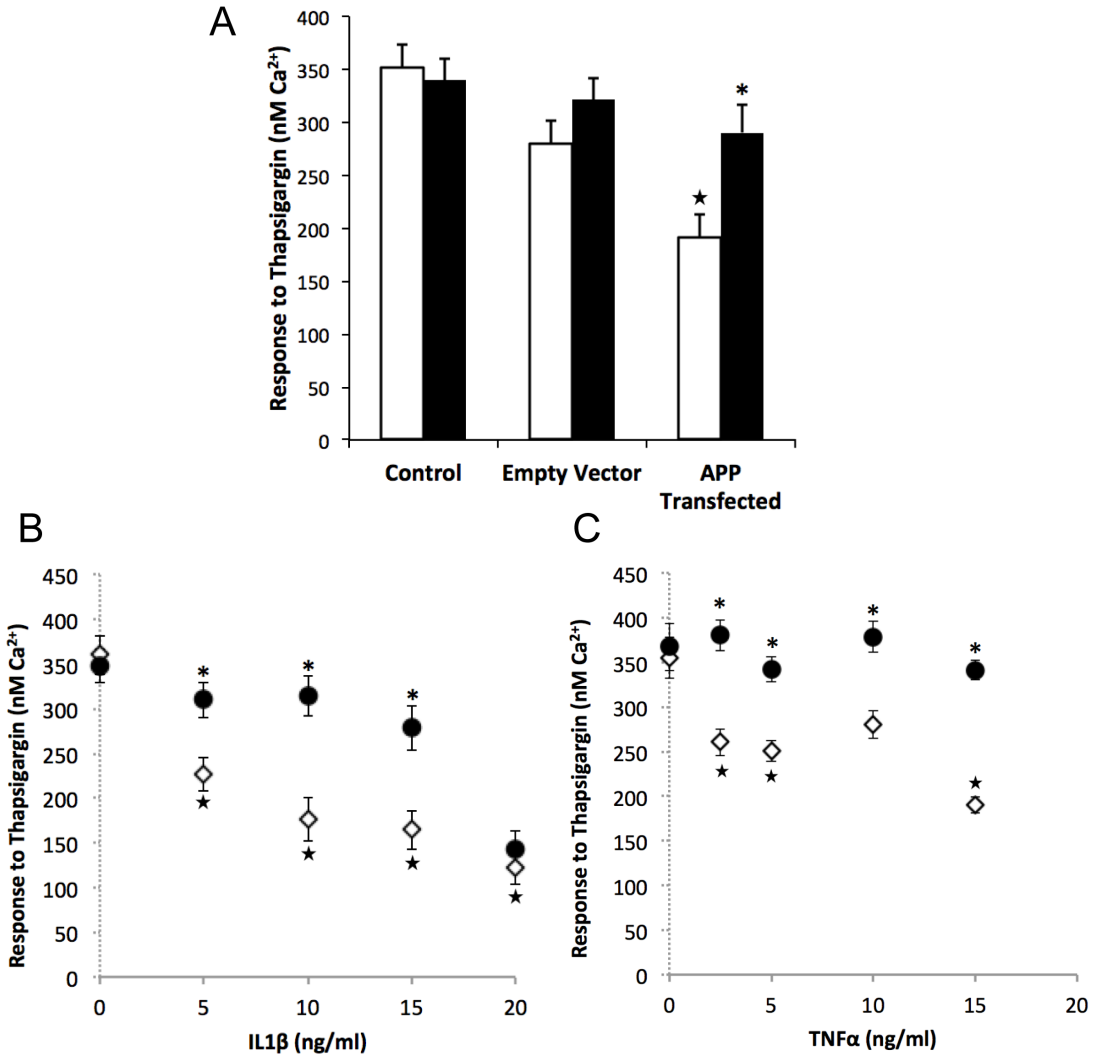

Figure 4.20 Effect of Arimoclomol on $[Ca^{2+}]_{ER}$ following βAPP overexpression or exposure to inflammatory cytokines

A: $[Ca^{2+}]_{ER}$ was estimated by measuring the increase in cytosolic $[Ca^{2+}]$ following administration of thapsigargin. Transfection with empty vector did not significantly affect $[Ca^{2+}]_{ER}$ relative to untransfected control. However, overexpression of βAPP significantly reduced $[Ca^{2+}]_{ER}$ in myotubes relative to empty vector transfected cultures (white bars). Treatment with Arimoclomol (black bars) had no significant effect on untransfected or empty vector transfected cultures but significantly attenuated the effect of βAPP transfection on $[Ca^{2+}]_{ER}$.

B/C: The reduction of $[Ca^{2+}]_{ER}$ associated with exposure to IL1β or TNFα (white bars) was significantly attenuated by treatment with Arimoclomol (black bars).

(Error Bars=SEM, n=5 per condition, Star=$p<0.05$ vs. empty vector or unexposed cultures, Asterisk=$p<0.05$ vs. control not treated with Arimoclomol)

Furthermore, this effect was sufficiently marked that $[Ca^{2+}]_{ER}$ in the Arimoclomol treated group did not differ significantly from standard control cultures (p=0.15).

Arimoclomol also attenuated the effect of IL1β on $[Ca^{2+}]_{ER}$. The magnitude of this effect was not linearly dependent upon the degree to which $[Ca^{2+}]_{ER}$ was depressed by the respective experimental condition. Rather, between IL1β at 5 and 15 ng/ml, there was a restoration of $[Ca^{2+}]_{ER}$ to concentration not significantly different to those of control cultures (5 ng/ml, p=0.16; 10 ng/ml, p=0.21; 15 ng/ml, p=0.0699). At each of these concentrations, the difference between Arimoclomol treated cultures and the corresponding untreated comparator was significant (5 ng/ml, p=0.03; 10 ng/ml, p=0.01; 15 ng/ml, p=0.027). The greatest effect was observed at 10ng/ml IL1β, where Arimoclomol treatment increased $[Ca^{2+}]_{ER}$ to 314.4 nM ±12.4 nM compared to 176.7 nM ± 14.5 nM (n=5, p<0.01). At 20 ng/ml, the highest concentration tested, Arimoclomol was not associated with a significant impact on $[Ca^{2+}]_{ER}$. However, $[Ca^{2+}]_{ER}$ after IL1β 20ng/ml was not significantly different to that after IL1β 15ng/ml, on which Arimoclomol did have a significant impact.

After TNFα exposure, Arimoclomol had a similar effect to that observed after IL1β. At concentrations between 2.5 ng/ml and 20 ng/ml, there was a significant elevation of $[Ca^{2+}]_{ER}$ (2.5 ng/ml, p=0.03, 5 ng/ml, p=0.046; 10 ng/ml, p=0.034; 20 ng/ml, p=0.006). At each concentration, $[Ca^{2+}]_{ER}$ was increased to a concentration not significantly different to control cultures (2.5 ng/ml, p=0.523, 5 ng/ml, p=0.718; 10 ng/ml, p=0.466; 20 ng/ml, p=0.678). The largest effect was observed at TNFα 15 ng/ml, where Arimoclomol treatment was associated with an increased $[Ca^{2+}]_{ER}$ of 341.5 nM ±11.1 nM versus 190.5 nM ±9.3 nM in the untreated control (n=5, p<0.01).

4.2.4.6 Protein markers of ER Stress (UPR)

To investigate further the nature of ER stress under experimental IBM-like conditions in myogenic cultures, and the influence of Arimoclomol, a panel of proteins with important functions in the unfolded protein response (UPR) element of ER stress was examined.

First, it was determined that there was no significant difference in concentration of ER stress markers across the control groups: cultures grown in standard conditions with or without Arimoclomol and empty vector transfection (Fig 4.21). Therefore, myogenic cultures unexposed to either cytokines or transfection were used as controls for the subsequent experiments comparing expression of UPR proteins.

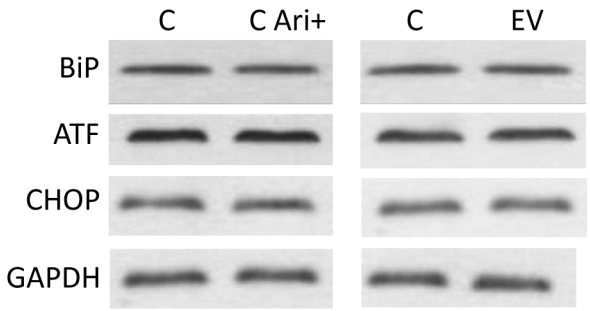

Figure 4.21 Determination of a suitable control for ER stress experiments using empty vector transfection and Arimoclomol treatment

Representative western blot demonstrates that treatment of myogenic cultures (C) with Arimoclomol (C Ari+) or transfection with empty vector (EV) had no significant effect on the expression of ER stress proteins BiP, ATF or CHOP.

βAPP overexpression was associated with significant elevation of the expression of BiP, where the increase was 2.58 ±0.68 fold over control (n=3, $p<0.05$) and CHOP, at 2.56 ±0.58 fold over control (n=3, $p<0.05$). Although ATF expression was consistently higher following βAPP, the magnitude of this increase was not significant.

Exposure of myogenic cultures to IL1β had a similar effect to βAPP; there was significant elevation of BiP of 3.33 ±0.93 fold of control (n=3, $p<0.05$) and of CHOP of 2.47 ±0.62 fold (n=3, $p<0.05$). TNFα exposure was associated with a significant elevation of CHOP of 2.32 ±0.54 fold (n=3, $p<0.05$).

Treatment with Arimoclomol appeared comparatively to reduce the expression of ER stress markers induced by βAPP overexpression or cytokine exposure. A

consistently lower band densitometry was observed across each western blots performed (n=3). However, this apparent reduction only reached statistical significance for CHOP following βAPP overexpression, where expression was reduced to 49.6% ±4.3% of control (n=3, $p<0.05$) and following exposure to IL1β, where CHOP expression was reduced to 62.7% ±6.4% of control (n=3, $p<0.05$) (Fig 4.22).

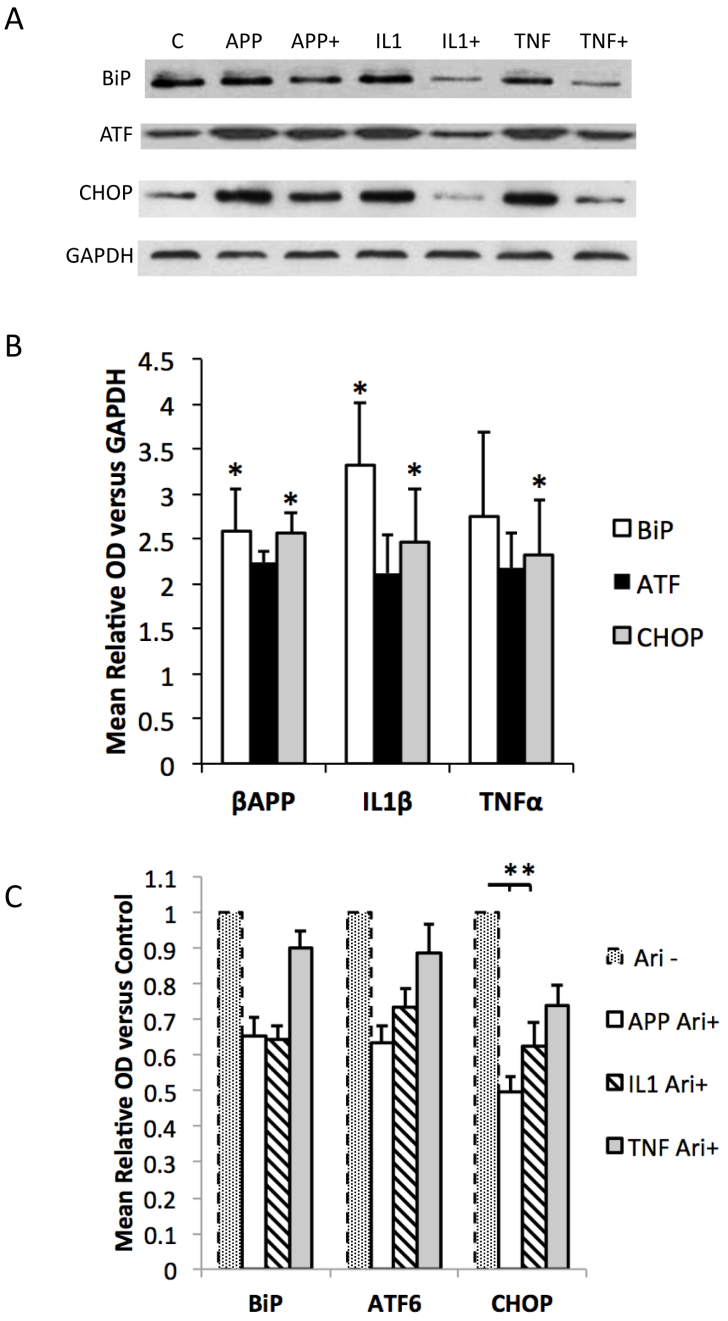

Figure 4.22 Effect of Arimoclomol of UPR Markers under IBM conditions

A: Representative western blots examining Bip, ATF and CHOP expression in myogenic cultures under control conditions (C), overexpression of βAPP or exposure to IL1β/TNFα. Arimoclomol treatment is indicated by plus sign.

B: Overexpression of βAPP or exposure to IL1β/TNFα were each associated with significant elevation of UPR markers.

C: Arimoclomol treatment significantly reduced the expression of CHOP following overexpression of βAPP and exposure to IL1β.

(Error Bars=SEM, n=3, Asterisk=$p<0.05$)

4.2.5 NFκB activation in myogenic cultures under IBM-like conditions

The status of NFκB activation in myogenic cultures was examined by determining the extent of nuclear staining for the p65 subunit. Positive NFκB activation was defined as a multinucleated cell in which greater than 50% of the nuclei were immunoreactive for NFκB. As a positive control, lipopolysaccharide exposure at concentrations between 20 and 100 ng/ml resulted in mean NFκB activation at close to 100% of cells (between 92.6% and 95.9% respectively). Under standard culture conditions, between 4% and 9% of myotubes demonstrated NFκB activation. Although this apparent difference between the control populations of different experiments was not significant, each cytokine and the effect of APP overexpression were compared against their own contemporaneous control population cultured in different wells of the same plate, thereby minimizing the impact of inter-culture variability on the apparent effect of each condition. The generic stressor of glucose deprivation for 2 hours was not associated with a significant change in the extent of NFκB activation (n=3).

Exposure of cultures to cytokines was associated with a significant increase in the proportion of cells that demonstrated NFκB activation. Following IL1β exposure, between 5ng/ml and 20ng/ml, the significant increase in the proportion of cells demonstrating NFκB activation occurred in a concentration dependent manner. Compared to 4.4% ±1.3% of cells in the control population, NFκB activation was detected in 49.3% ±2.9% cells following exposure at 5 ng/ml (n=5, $p<0.01$) and 88.1% ±6.3% cells following exposure at 20ng/ml (n=5, $p<0.01$). TNFα exposure also induced NFκB activation. Against 9.2% ±1.3%, of cells grown in standard conditions, this proportion increased to between 46.6% ±3.7% at 5 ng/ml (n=5, $p<0.01$) and 67.2% ±4.6% at 20 ng/ml (n=5, $p<0.01$).

Interestingly, βAPP overexpression was also associated with NFκB activation. Compared with empty vector transfection, the proportion of cells in which most nuclei stained for the p65 subunit increased from 8.8% ±1.2% to 43.1% ±6.2% (n=5, $p<0.01$) (Figs 4.23 and 4.24).

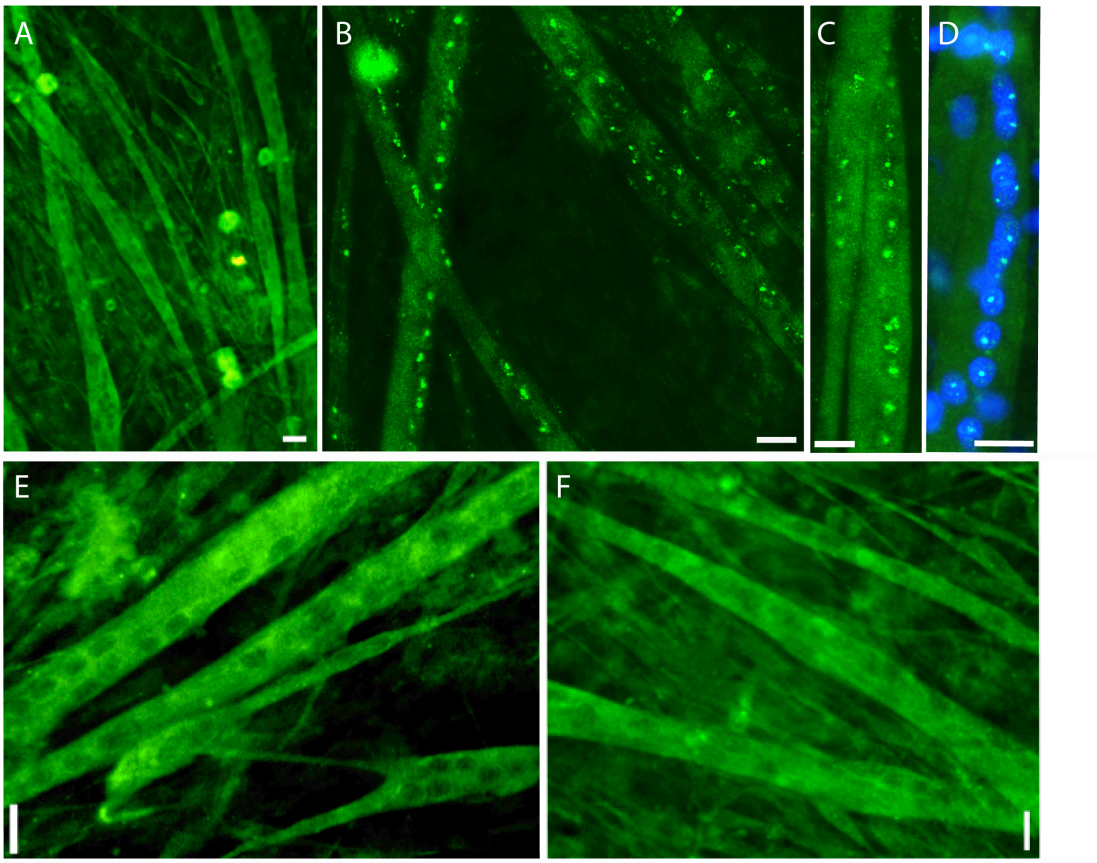

Figure 4.23 Effect of βAPP or exposure to inflammatory cytokines on NFκB activation in myogenic cultures

Myogenic cultures grown under standard conditions (A) demonstrate diffuse homogenous cytoplasmic NFκB p65 staining, in contrast to a lack of associated nuclear immunopositivity. Exposure to IL1β (B) or TNFα (C), or βAPP over-expression (D) induced nuclear translocation, confirmed by colocalisation with DAPI (D). In each condition, Arimoclomol treatment was associated with a reduction of nuclear translocation (following βAPP overexpression in E or exposure to IL1β in F).

(Scale Bars=20μm)

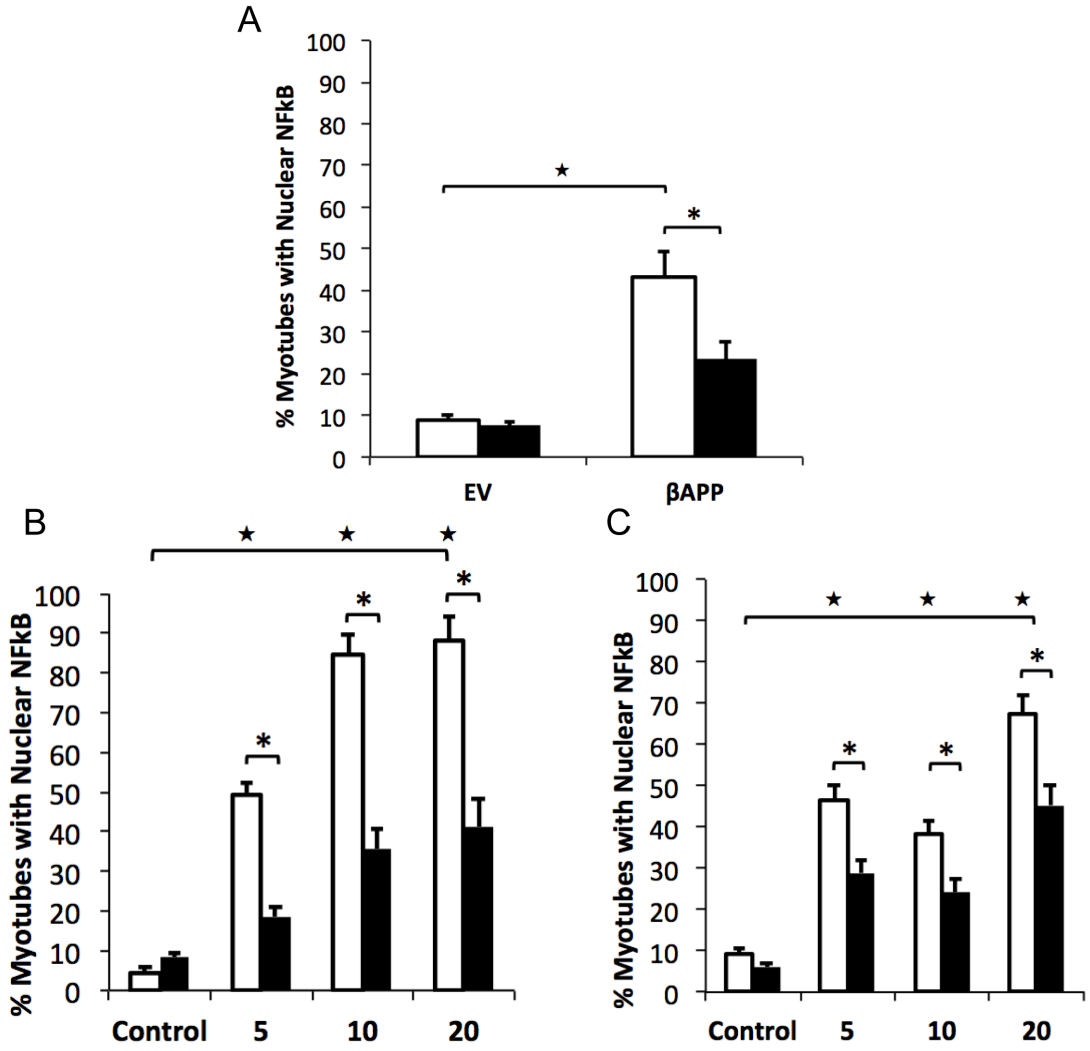

Figure 4.24 Effect of Arimoclomol on NFκB activation in myogenic cultures following overexpression of βAPP or exposure to inflammatory cytokines

Overexpression of βAPP (A) or exposure to IL1β (B) or TNFα (C) significantly increased NFκB activation compared to cultures transfected with empty vector or unexposed to cytokines respectively (white bars). In each condition, this effect was significantly inhibited by Arimoclomol treatment (black bars).

(Error Bars=SEM, n=5, Star=$p<0.05$ vs. untransfected or unexposed control cultures, Asterisk=$p<0.05$ vs. corresponding condition minus Arimoclomol treatment)

4.2.5.1 The effect of Arimoclomol on NFκB activation in myogenic cultures under IBM-like conditions

Treatment of myogenic cells cultured under standard conditions with Arimoclomol was not associated with a significant change in the extent of NFκB activation. This might reflect a small percentage of non-specific immunocytochemical positivity that is not amenable to pharmacological manipulation, or that the mechanism of Arimoclomol's effect depends on an NFκB activation pathway that is only active under the IBM-like conditions tested. This is consistent with Arimoclomol's known property as a coinducer of the HSR, which relies upon existing HSR activation at the time of treatment. In contrast, following βAPP overexpression or exposure to inflammatory cytokines, Arimoclomol treatment was associated with significant reduction of the proportion of myogenic cells with positive p65 nuclear staining.

Following IL1β exposure, the maximal effect of Arimoclomol treatment was observed at 10ng/ml IL1β, where nuclear p65 staining was reduced to 35.7% ±5.2% compared to 84.9% ±4.6% in the untreated comparator ($n=5$, $p<0.01$). Across all IL1β concentrations, the mean absolute reduction following Arimoclomol treatment was 42.2% and mean relative reduction was 57.8%.

Following TNFα exposure, the maximal effect of Arimoclomol treatment was observed at 20ng/ml TNFα. Here, nuclear p65 staining was reduced from 67.2% ±4.6% to 45.3% ±4.8% ($n=5$, $p<0.05$). Across the concentrations tested, the mean absolute reduction following Arimoclomol treatment was 17.9% and mean relative reduction was 35.9%.

Following βAPP over-expression, Arimoclomol also significantly reduced apparent NFκB activation. Compared to 43.1% ±6.2%, nuclear p65 staining was reduced to 23.6% ±4.2% of cells ($n=5$, $p<0.05$). This equates to an absolute reduction of 19.5% and relative reduction 45.2%.

4.2.6 The effect of Arimoclomol on βAPP or MHCI expression in myogenic cultures

Two of the notable effects of both βAPP transfection and exposure to inflammatory cytokines were the consequent upregulation of βAPP and MHCI. In these experiments, the upregulation of βAPP was an evidently upstream effect through direct overexpression. In IBM *in vivo*, the upregulation of MHCI is postulated to be an upstream and central pathogenic feature. Therefore, it was hypothesised that Arimoclomol's mechanism could depend on either of these two features. However, western blots demonstrated that Arimoclomol did not significantly affect the concentration of either βAPP or MHCI, when either was upregulated following βAPP overexpression or exposure to IL1β or TNFα (Figure 4.25).

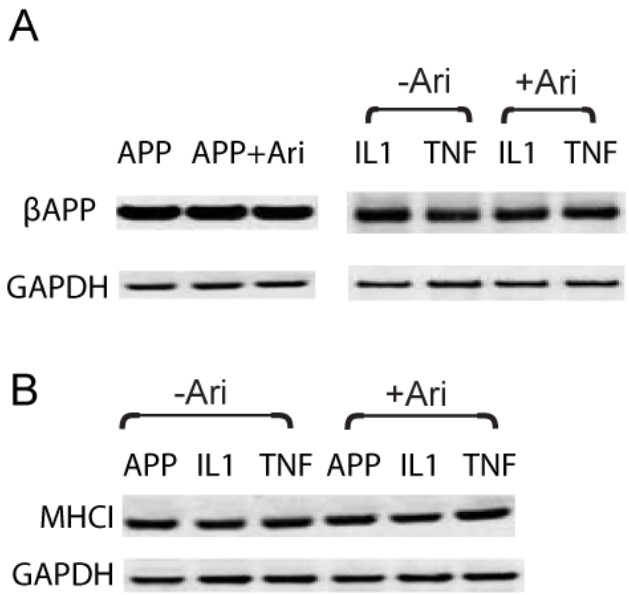

Figure 4.25 Effect of Arimoclomol on βAPP and MHC Class I expression

Representative western blots demonstrate that Arimoclomol treatment (+Ari) has no significant effect on the expression of βAPP (A) or MHCI (B) in myogenic cultures after transfection of βAPP or exposure to inflammatory cytokines.

4.*2.7 Summary of Results*

1. The Heat Shock Response (HSR), determined by expression of key Heat Shock Protein, HSP70, is activated in primary myogenic cell cultures by overexpression of βAPP or exposure to cytokines IL1β and TNFα. This effect can be significantly augmented through treatment with the HSR co-inducer Arimoclomol.
2. Overexpression of βAPP or exposure to cytokines IL1β and TNFα are cytotoxic to myogenic cells, determined by the MTT cell viability assay. Arimoclomol treatment significantly improves cell viability under these conditions.
3. TDP-43 translocation from the nucleus to the cytoplasm can be induced through overexpression of βAPP or exposure to cytokines IL1β and TNFα. This is quantifiable through the phenomenon of loss of normal nuclear immunostaining. Arimoclomol treatment significantly attenuates this TDP-43 mislocalisation.
4. TDP-43 expression is increased by the same IBM-relevant stimuli and can be restored to levels of control cultures by Arimoclomol treatment.
5. Calcium dyshomeostasis is evidenced in myogenic cultures following βAPP or exposure to cytokines IL1β and TNFα through elevated basal cytosolic calcium concentration and reduced ER calcium concentration. Arimoclomol treatment confers significant protection against these effects.
6. ER stress is further evidenced in these conditions through elevated expression of key markers of the UPR. Arimoclomol treatment reduces this evidence of ER stress in myogenic cultures.
7. NFκB activation is demonstrated by myogenic cultures following βAPP or exposure to cytokines IL1β and TNFα. This is inhibited by Arimoclomol treatment.
8. The effects of Arimoclomol to reduce these features of IBM pathology, recapitulated in primary myogenic cultures, are not dependent on alteration of βAPP or MHCI expression.

4.3 Discussion

4.3.1 Augmentation of the Heat Shock Response by Arimoclomol

The baseline HSP70 expression demonstrated by control cultures could reflect a number of scenarios. It is unlikely that this reflects non-specific antibody staining since there is consistency between immunocytochemical and immunoblotting techniques. There may be a constitutive level of HSP70 expression in myotubes and, as is the case in MHC Class I expression, this may reflect normal upregulation during maturation rather than in response to a cytotoxic stimulus. The normal concentration of HSP70 in skeletal muscle *in vivo* has not been examined so estimation of a comparable baseline here is difficult. Nevertheless, it is reasonable to consider even 'control' *in vitro* conditions as representing an element of cellular stress, which would be expected to trigger a cytoprotective heat shock response.

Transfection of primary myogenic cultures with βAPP or exposure to cytokines results in a number of pathological features that indicate cellular stress, therefore it is unsurprising that these conditions are associated with increased expression of HSP70. This is consistent with the upregulation of HSP70 observed in IBM tissue *in vivo* (Parker et al. 2009).

Treatment with Arimoclomol augmented the upregulation of HSP70 after βAPP over-expression or exposure to cytokines, in keeping with its known pharmacological action. Interestingly, this effect was not uniform. Whilst a comparable magnitude of upregulation, of 4 to 5 fold of control, was observed following exposure to cytokines, the effect was more pronounced in association with βAPP over-expression, to approximately 8 fold. Clearly, as the 'strength' of the stimulus cannot be standardised between these two quite different stresses, inferences about the significance of this differential response depended on further information regards the magnitude of other pathological outcomes, as examined in subsequent experiments. However, this does suggest that the effect of Arimoclomol might depend on other factors beyond only the extent to which the HSR is activated at the time of treatment.

In the *in vitro* environment, it would be useful to determine the impact of HSR inhibition or HSP70 down-regulation on the susceptibility to the various

pathological features described in Chapter 3 and below. This may help to clarify whether physiological activation of the HSR confers cytoprotective benefit, which is particularly relevant in considering the role of ageing in IBM. This could be further studied through examination of the inducibility of the HSR in IBM tissue compared to age-matched and non-age matched controls.

4.3.2 Exposure to IBM-relevant stress induces cell death in primary myogenic cultures

A high throughput viability assay represents an important component of a cell model based technique for analysing the effect of drugs. The MTT assay, through its broad dependence of mitochondrial reduction enzyme activity represented an IBM-relevant selection from the standard panel of assays. This could form the primary 'screening' tool for selection of promising compounds from a given selection, before more disease specific tools are employed to provide greater detail on mechanism of action (van Meerloo et al. 2011).

Control experiments using the generic stimulus of glucose deprivation demonstrated that the technique was both reproducible and sufficiently sensitive to detect the impact of a pathological insult of graded magnitude. Furthermore, the correlation between the outcome of the MTT assay and the magnitude of the insult (i.e. degree of glucose deprivation) appeared strong, implying that the MTT assay could be used to estimate the magnitude of both the subsequent IBM-relevant insults and effect of drug treatment. However, the relatively large inter-experimental variance in absolute MTT reduction was noted as a potential limitation of the technique.

Although the dependence of the MTT assay on mitochondrial enzyme activity implies mitochondrial dysfunction as a mechanism of the cytotoxicity demonstrated by the tested conditions, this may simply represent a final common pathway phenomenon and does not prove that mitochondrial dysfunction is either a central or upstream component of the corresponding pathological mechanism.

4.3.2.1 βAPP over-expression in myogenic cells is cytotoxic

Since Lipofectamine™ transfection achieves transient overexpression of the corresponding gene, the effect of βAPP overexpression was examined at both 48 and 96 hours after transfection. By 48 hours, βAPP overexpression was associated with significantly reduced cell viability and this effect was greater by 96 hours, implying accumulation of cytotoxic processes. It is likely this represents either an increase in concentration of βAPP which, if directly cytotoxic, would reduce cell viability or that the initial trigger of βAPP overexpression triggers a pathological cascade that advances for at least 96 hours after initial transfection. Although EV transfection was also cytotoxic in comparison to non-transfected controls, this was not a progressive effect. It is known that plasmid transfection can be associated with inherent cytotoxicity, in addition to any effects of the transfected product. However, the effects of βAPP were significantly greater than EV, suggesting a specific cytotoxic impact through βAPP itself.

4.3.2.2 Exposure of myogenic cells to inflammatory mediators is cytotoxic

Inflammatory mediators were characterised by a dose dependent and significant reduction in cell viability, indicated by the MTT assay. However, the character of this effect differed between mediators, such as the flatter response observed with LPS and steeper response observed with TNFα. Nevertheless, the proportional nature of each relationship suggests that LPS, IL1β and TNFα elicit a direct and specific cytotoxic effect on myotubes *in vitro*. Furthermore, these experiments demonstrate that the concentrations of cytokines used are appropriate in this context, where a significant pathological stimulus is required, but not to the extent that its effects are uniformly cytotoxic. Interestingly, a comparable magnitude of cytotoxicity was associated with βAPP transfection and exposure to cytokines at these concentrations. This permits some comparison to be made in subsequent investigation of pathological mechanisms, which may otherwise have simply reflected different magnitudes of stimuli.

4.3.2.3 Treatment with Arimoclomol improves cell viability in myogenic cells exposed to IBM-relevant stress

Treatment of control cultures with Arimoclomol had no significant effect on cell viability, as would be expected of a co-inducer of the HSR whose function is restricted to environments of existing HSR activation through cellular stress (Kalmar et al. 2014). Furthermore, the absence of effect on control cultures demonstrates that Arimoclomol's effects under IBM-like stresses are not simply the consequence of non-specific elevation in MTT activity by Arimoclomol. Rather, Arimoclomol appeared to attenuate the cytotoxic impact of IBM-relevant stimuli.

Following βAPP overexpression, the effect of Arimoclomol was dependent on the time at which the cells were analysed. By 48 hours, a significant cytotoxic effect was evident but this was not significantly attenuated by Arimoclomol. By 96 hours, the magnitude of the cytotoxic effect was more pronounced and the impact of Arimoclomol considerably greater, restoring cell viability to that of EV control. The discrepancy in this effect of Arimoclomol at various time points after transfection could reflect one or more of three factors. First, the effect of Arimoclomol might depend on the degree of underlying cell stress. Secondly, the cytotoxic effects of the stimulus or cytoprotective effects of Arimoclomol may not manifest within the shorter time frame of 48 hours. Thirdly, the additional medium change and thereby additional provision of Arimoclomol included in the 96-hour experiment may enhance cytoprotection. Regardless of the nature of the phenomenon, Arimoclomol is clearly cytoprotective under conditions of IBM-relevant cellular stress. These experiments also supported the use of the 96-hour post-transfection time-point for subsequent experiments involving Arimoclomol.

Arimoclomol also significantly attenuated the cytotoxic impact of inflammatory mediators on myogenic cells. The magnitude of this effect was not simply proportional to the degree of cytotoxicity, implying specificity of the drug action to the mechanisms of the pathological stimuli.

4.3.3 IBM-relevant stress induces TDP-43 pathology in myogenic cells

As observed in control cultures, TDP-43 was normally located in the cell nuclei. When cells were exposed to inflammatory cytokines or βAPP overexpression, TDP-43 translocated to the cytoplasm. There was subsequent loss of nuclear staining and formation of discrete TDP-43 cytoplasmic aggregates, which were both ubiquinated inclusions and non-ubiquinated. Western blots revealed that the concentration of TDP-43 rose in response to IL1β, TNFα and βAPP.

The overwhelming predominance of nuclear based TDP-43 immunostaining under control conditions, with subsequent cytoplasmic translocation following pathological stimuli, is in keeping with previous work on muscle and other tissues (Salajegheh et al. 2009; Giordana et al. 2010). The additional low intensity homogenous cytoplasmic staining under normal conditions may either reflect non-specific staining or known low-level nuclear-cytoplasmic TDP-43 shuttling (Ayala et al. 2008).

It is unclear whether the marked redistribution of TDP-43, under IBM-relevant stress represents a physiological change in shuttling or a pathogenic factor. The cytoplasmic proteinaceous aggregates of TDP-43 observed in these experiments are likely to represent a combination of the non-ubiquinated 'pre-inclusions' and more typical ubiquinated inclusions that characterise TDP-43 pathology in muscle and other tissues (Lee et al. 2012). Most notably, a comparison can be drawn with work on skeletal muscle biopsies that demonstrated a highly similar phenomenon in IBM muscle (Chapter 4 Introduction, Figure 4.2). The reproduction of this feature, which appears to be highly specific to IBM in the context of skeletal muscle disease, in myotubes *in vitro* is an important component of this model. The results here also shed further light on the pattern through which this cytoplasmic redistribution occurs, in that cytoplasmic TDP-43 aggregates typically preceded loss of nuclear staining. However, the loss of nuclear staining in some cells without contemporaneous cytoplasmic inclusions is intriguing. This might reflect sufficient UPS or autophagic processing among certain cells that prevents accumulation of TDP-43 inclusions or facilitates their breakdown. Equally, the presence of cytoplasmic TDP-43 does not necessarily appear to be fundamental to its pathogenic effects (Igaz et al. 2011). The various

morphologies observed in these experiments may simply reflect the broad spectrum of TDP-43 pathological characteristics. In models of TDP-43 pathology in neurons, loss of nuclear TDP-43 has appeared to be both a consistent feature and, through its association with the 'pre-inclusions' or ubiquitin-negative inclusions that precede other types of proteinaceous aggregate, an apparently early component of the TDP-43 pathological spectrum (Walker et al. 2013).

Further work could determine what proportion of mislocalised TDP-43 represents stress granules, pre-inclusion or mature inclusions, which would help determine the time course of morphological changes demonstrated in these experiments. It would also be interesting to determine whether the 25kDa C-terminal fragments are detectable in this model. A corresponding protein was not detected in significant quantity on western blotting, implying that this is not a predominant form here.

Despite the variety of morphological patterns detected, those cells within an individual culture were typically consistent in their appearance. This is most likely to reflect consistency of the response to a controlled stimulus. However, the notion of intercellular influence, through prion-like cell-to-cell propagation of TDP-43 pathology, is increasingly entertained as a mechanism in neurodegenerative disease *in vivo*. A prion-like domain was detected in the C-terminus of TDP-43 (Cushman et al. 2010). There is evidence to support the TDP-43 being transferred between neuronal cell types via exosomes (Nonaka et al. 2013). The phenomenon has not yet been demonstrated in skeletal muscle. However, this would be an interesting concept in the context of degenerative muscle diseases, each of whose particular anatomical distribution remains largely unexplained. This might mirror the predilection of certain degenerative diseases of the central nervous system for particular lobes of the brain, such as fronto-temporal dementia. If a mechanism such as TDP-43 pathology were to spread akin to an infectious agent, conditions specific to myofibres of individual muscles (for example subtle pH differences or fibre type distributions) could initiate a pathogenic cascade that would evolve geographically from the original focus, thereby involving an increasing proportion of each muscle. This would

ultimately explain the more pronounced clinical manifestations in those regions rather than in others.

4.3.3.1 TDP-43 concentration increases under IBM-relevant stress

Several stimuli have previously been shown to increase TDP-43 concentration, including axotomy (Moisse et al. 2009), oxidative stress (Colombrita et al. 2009), heat shock and thapsigargin treatment (McDonald et al. 2011). Therefore, it is unsurprising that what appears to be a generic 'stress' response was activated in by IBM-like conditions in these experiments, and by the generic stimulus of glucose deprivation. No direct response has previously been demonstrated to IL1β, TNFα or overexpression of βAPP although the coexistence of TDP-43 and amyloid pathology in neurodegenerative diseases such as Alzheimer's disease suggests overlap in their pathogenic mechanisms. In general, overexpression of full-length TDP-43 in other cell models has not produced cytoplasmic TDP-43 aggregation (Ash et al. 2010). If that applies here, a deficiency of cellular breakdown machinery rather than the increased concentration, demonstrated by the western blots, could account the morphological features detected. Indeed, inhibition of the UPS has been shown to increase TDP-43 aggregates *in vitro* (Winton et al. 2008). This mechanism is likely to be augmented by the proteasomal inhibition that results from intracellular accumulation of TDP-43 (Nonaka et al. 2013). Consistently, the overexpression of p62 reduces TDP-43 aggregation through autophagic and proteasomal breakdown pathways (Brady et al. 2011). Cytoplasmic redistribution of TDP-43, through sequestration and nuclear loss, has also been proposed to disturb its autoregulation by upregulating TDP-43 expression, thereby establishing a potentially pathogenic positive cycle (Lee et al. 2012). Regardless, increased concentration of full-length of TDP-43, whether contributory to the cytoplasmic aggregation load or otherwise, appears to be cytotoxic (Li et al. 2010) and, indeed, is sufficient to reproduce disease phenotypes such as FTD (Tsai et al. 2010).

4.3.3.2 Consequences of TDP-43 translocation

These data support the hypothesis that TDP-43 mislocalisation in IBM could be a consequence of upstream degenerative or inflammatory triggers, which may

not be specific to IBM. However, it is useful to consider the additional possibility that TDP-43 pathology could represent an early event in IBM *in vivo*, which cannot be tested in the cellular model used here. Further understanding of the potential consequences of TDP-43 mislocalisation and aggregation would help clarify its position in IBM pathogenesis, particularly with respect to inflammation. For example, the distinction between PM and IBM might represent a different threshold for initiation of TDP-43 pathology under inflammatory mediated 'stress', due to underlying genetic predisposition or the relatively more aged cellular milieu. Alternatively, activation of NFκB in TDP-43 disease states such as IBM-FTD-PD may contribute to a secondary inflammatory response, such as that observed in myofibrillar myopathy, in which TDP-43 pathology is also observed, or in Duchenne muscular dystrophy (Olive et al. 2009; Messina et al. 2011). Intriguingly, increased prevalence of autoimmune diseases has been observed in the semantic variants of FTD and progranulin mutation carriers (Miller et al. 2013). Progranulin appears to have several inflammatory functions, notably TNFα antagonism, meaning its deficiency through mutation might augment the TNFα immune response. Indeed, there is *in vitro* evidence that TDP-43 can induce neuroinflammation, increasing concentrations of IL-6 and TNFα (Herman et al. 2012).

4.3.3.3 Arimoclomol attenuates TDP-43 pathology following IBM-relevant stress in myogenic cells

A small proportion of cells in control populations, including those transfected with empty vector, demonstrated TDP-43 pathology. This implies either that this process of culture induces a degree of TDP-43 pathology or that myotubes *in vitro*, unlike skeletal muscle *in vivo*, display a constitutive level of TDP-43 mislocalisation. Treatment with Arimoclomol did not affect this background phenomenon. Although this might suggest that it is not the result of cellular stress, Arimoclomol attenuated, rather than fully reversed the more pronounced TDP-43 pathology observed under IBM-like conditions. Therefore multiple pathways might contribute towards TDP-43 mislocalisation, not all of which are influenced or entirely blocked by Arimoclomol or the HSR.

Notably, Arimoclomol was found to confer significant protection against TDP-43 pathology, whether induced by degenerative or inflammatory stimuli. The magnitude of this effect was not simply proportional to the degree of TDP-43 mislocalisation related to the untreated comparator population, implying some selectivity of effect. However, following TNFα and IL1β exposure, there the extent of TDP-43 pathology after Arimoclomol treatment remained dependent on the cytokine dose. This may reflect a limitation of Arimoclomol's action in this context or, again, that it does not influence all the processes that contribute to TDP-43 pathology. It was notable that cells within an individual culture well tended to display a relatively homogenous TDP-43 pattern, particularly whether nuclear staining was retained or lost. The numerical differences described between conditions thereby reflect a tendency to pathology within defined groups of cells rather than of random individual cells within the overall population. This might reflect subtle differences between conditions in given wells related to a threshold at which TDP-43 mislocalisation occurs or can be reversed.

A likely mechanism through which Arimoclomol attenuates TDP-43 mislocalisation is augmented chaperoning through increased expression of HSPs such as HSP70. HSP70, in addition to HSP40, has been shown to regulate

nuclear aggregation of TDP-43 in response to heat shock (Udan-Johns et al. 2014), which could influence its propensity to translocate and form cytoplasmic inclusions. The cytoprotective effect of Arimoclomol described in other models of proteinaceous aggregation, discussed above, indicate that Arimoclomol's anti-aggregation properties are likely to contribute to the reduced cytoplasmic TDP-43 aggregation observed in these experiments. These properties appear to depend primarily on upregulation of HSPs. The auto-feedback loop demonstrated by TDP-43 (Lee et al. 2012) might explain the associated decline in concentration. Down-regulation of TDP-43 gene expression, either by HSPs or Arimoclomol directly, is also possible and this may, in turn, minimise the amount that subsequently translocates or aggregates.

Finally, it is also possible that Arimoclomol exerts an HSR-independent mechanism on TDP-43 pathology, which could be explored through HSP knockdown or contemporaneous inhibition. Indeed, hydroxylamine derivatives such as Arimoclomol have been suggested to alter the metabolism of membrane lipid rafts, resulting in an HSF-independent mechanism of HSR activation that improves resistance to cellular stress (Kalmar et al. 2014). Equally, an inhibitory action on reactive oxygen species has been postulated, which may contribute to attenuating the stimulus for TDP-43 translocation.

4.3.4 ER stress and Calcium dyshomeostasis

4.3.4.1 IBM-relevant stress increases cytosolic Calcium in myogenic cells

The significantly elevated cytosolic calcium concentration, $[Ca^{2+}]_{Cyto}$, of myotubes following βAPP over-expression or exposure to IL1β or TNFα is consistent with the pathogenic nature of these stimuli, supported by their impact on other parameters investigated here. Interestingly, the response of $[Ca^{2+}]_{Cyto}$ to inflammatory mediators did not appear to be dose dependent, implying either an upper threshold beyond which cells died (and therefore were not detectable by the technique employed here) or that ER buffering mechanisms remained successful in limiting the magnitude of this phenomenon under the conditions tested. The mechanism of elevated $[Ca^{2+}]_{Cyto}$, which is

demonstrated by cells in various pathological conditions, is likely to be closely related to the depleted $[Ca^{2+}]_{ER}$ contemporaneously demonstrated by these myotubes, discussed below. Indeed, ER Ca^{2+} leak via ryanodine and IP3 receptors is a commonly postulated process. Interestingly, however, basal ER Ca^{2+} leak does not appear to rely on either of these channels, and alternative suggested pathways include an ATP-induced leak and BCL2 pores, or a ribosome-translocon complex (Camello et al. 2002). Additionally, other 'non-ER' purported mechanisms of raised $[Ca^{2+}]_{Cyto}$ in skeletal muscle disease include increased permeability to Ca^{2+} of the cell membrane, entry through TRPC1 channels and hyperactive store-operated uptake (Altamirano et al. 2012). In the context of skeletal muscle, the MCK-βAPP transgenic mouse displays similar calcium dyshomeostasis to that observed here, with significantly elevated $[Ca^{2+}]_{Cyto}$, thought to result from Aβ42 modulation of ryanodine receptors to increase their open probability. This translates to reduction of contraction force in fast-twitch muscles (Moussa et al. 2006; Shtifman et al. 2010).

The pathological consequences of elevated $[Ca^{2+}]_{Cyto}$ are likely to be broad and can impair numerous fundamental cellular functions, leading to necrosis and/or apoptosis. Mitochondrial disturbance is a notable outcome, thought to include Ca^{2+}-mediated opening of the mitochondrial permeability transition pore, and release of cytochrome C to the cytoplasm, which is a potent apoptotic trigger, via the calpain pathway (Brustovetsky et al. 2002; Millay et al. 2008). Of further relevance of other IBM pathogenesis is that elevated $[Ca^{2+}]_{Cyto}$ induces the NFκB cascade (Altamirano et al. 2012).

The impact of Arimoclomol was restricted to myotubes under IBM-relevant conditions, such that it only impacted upon $[Ca^{2+}]_{Cyto}$ when significantly disturbed from baseline. This implies that Arimoclomol does not have a non-specific action to reduce $[Ca^{2+}]_{Cyto}$ generally, but rather mitigates one of the mechanisms through which elevated $[Ca^{2+}]_{Cyto}$ is triggered or maintained. The magnitude of the effect was significant and, under several of the tested conditions, approached normalisation of the disturbance.

Figure 4.26 summarises potential contributors to and consequences of $[Ca^{2+}]_{Cyto}$.

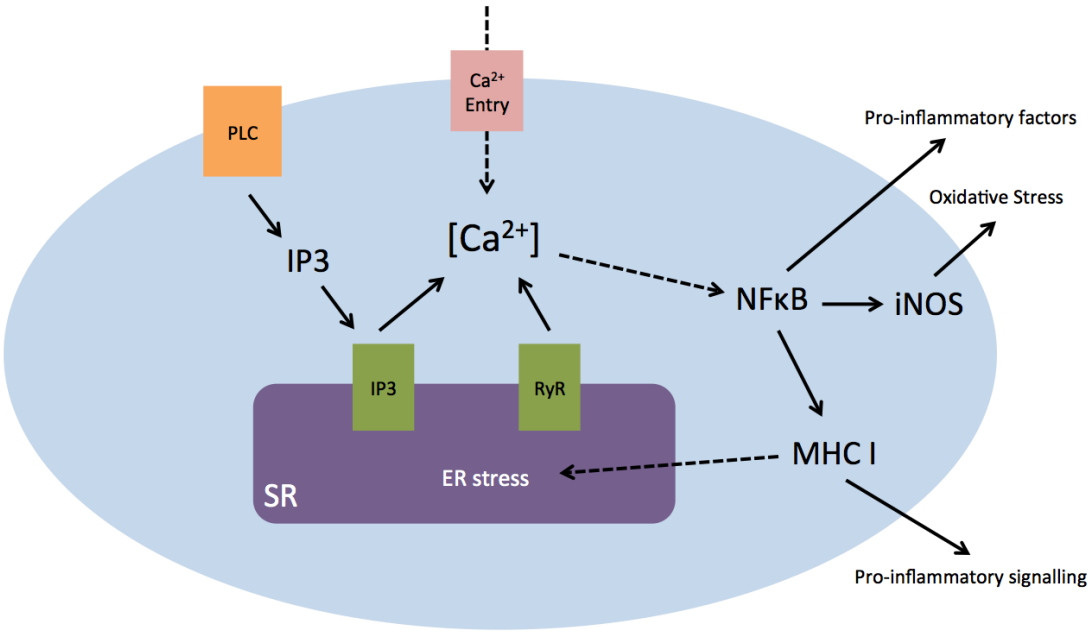

Figure 4.27 Illustration of intracellular calcium dyshomeostasis

Ca^{2+} entry via TRPC1 channels or store operated calcium entry (SOCE) combines with SR Ca^{2+} leak through IP3 and RyR channels. IP3 is replenished via hydrolysis of PIP2 by PLC on the plasma membrane. The consequent elevation of intracellular Ca^{2+} activates NFκB, leading to expression of pro-inflammatory factors and oxidative stress via inducible nitric oxide synthase (iNOS). NFκB mediated upregulation of MHCI sets up a self-perpetuating cycle via added ER overload.

4.3.4.2 IBM-like conditions induce ER stress in myogenic cells

The significant reduction of $[Ca^{2+}]_{ER}$ following βAPP over-expression or exposure to IL1β or TNFα indicates that these IBM-relevant stimuli induce ER stress. This is corroborated by the upregulation of UPR markers demonstrated by western blotting. These effects may reflect a direct influence of βAPP, IL1β or TNFα on the ER but may be secondary to other effects.

βAPP overexpression reduced inferred $[Ca^{2+}]_{ER}$ by more than one third of control and significantly upregulated the ER stress markers BiP and CHOP, to approximately 2.5 times that of control. Most studies that have examined the effects of βAPP on ER stress have been in the context Alzheimer's disease, in which several markers of UPR activity are demonstrated, including increased disulphide isomerase, PERK and XBP1 mRNA (Roussel et al. 2013). More

specifically, application of βamyloid to cortical neurons *in vitro* activates ER stress directly (Resende et al. 2008), and increases expression of PERK and eIF2, and the subsequent expression of CHOP (Ghribi et al. 2001; Lee do et al. 2010). It is likely that the effect of βAPP, and particularly Aβ42, to induce ER Ca^{2+} depletion via increased ryanodine receptor leak is relevant to the combination of low $[Ca^{2+}]_{ER}$ and high $[Ca^{2+}]_{Cyto}$ observed here.

The effect of inflammatory cytokines to induce ER stress may reflect MHCI upregulation, both *in vitro* here and also in IBM *in vivo*. Through the nature of burdening the ER with normally folded protein, this process is likely to selectively trigger the Endoplasmic Reticulum Overload Response (EOR), which is a further potent inducer of NFκB, thereby leading to a self perpetuating degenerative and inflammatory cycle. Indeed, in human primary myositic conditions, and mice over-expressing MHCI, ER stress and NFκB are strongly evident (Nagaraju et al. 2005). This serves an interesting point of comparison with IBM, which displays the additional canonical degenerative hallmarks of protein aggregation and nuclear degeneration that are conspicuously absent from the primary myositides. Such a distinction further highlights the potential contribution of the aged cell environment and molecular chaperones to determining the final pathological makeup. However, relatively little is known on the direct influence of cytokines on ER function in skeletal muscle. In pancreatic islet cells, also post-mitotic, IL1β and TNFα down-regulate expression SERCA2b, thereby reducing ER calcium, and inducing ER stress (Cardozo et al. 2005). Such a mechanism is certainly possible in the experiments described here. Additionally, through their action to increase βAPP and Aβ42, the effect of cytokines could also include the mechanisms attributed to amyloid.

None of the experimental conditions described here affected ATF6 concentration significantly. This could reflect a relatively selective effect of IBM pathology on other elements of the UPR but the transient nature of ATF upregulation means it may simply not be significantly upregulated at the point of testing and these data do not prove the absence of its involvement. Equally, its cleavage as part of the activation process may reduce detection by the antibody, thereby underestimating its concentration.

Limitations of Ca^{2+} fluorescence imaging must be considered and this technique, by the nature of detecting secondary alterations in $[Ca^{2+}]_{Cyto}$, does not examine $[Ca^{2+}]_{ER}$ directly. Therefore, dilution of the ER Ca^{2+} release in the cytosol in response to thapsigargin may underestimate the magnitude of the effect. Additionally, this method could be confounded by contemporaneous effects of altered plasma membrane Ca^{2+} handling, albeit that existing evidence suggests these are unlikely to be significant. There are also inherent limitations of all fluorescent dyes such as heterogeneous cell or organelle loading, leakage and bleaching. Direct measurement of $[Ca^{2+}]_{ER}$ is difficult and impractical in this context.

4.3.4.3 Arimoclomol treatment attenuates ER stress in myogenic cells

The treatment of primary myogenic cell cultures with Arimoclomol attenuated the ER stress induced by IBM-like conditions. The association of reduced $[Ca^{2+}]_{ER}$ with raised $[Ca^{2+}]_{Cyto}$ and the contemporaneous attenuation of both disturbances with Arimoclomol implies that the underlying disturbance caused by IBM-like conditions primarily relates to ER-cytosolic Ca^{2+} signaling rather than mechanisms dependent on plasma membrane permeability. This is consistent with existing evidence that ER Ca^{2+} leak is a fundamental component of ER stress.

The significant attenuation of $[Ca^{2+}]_{ER}$ disturbance under IBM-like conditions following treatment with Arimoclomol implies it offers protection against ER stress. This is further supported by the significant reduction in CHOP expression when associated with βAPP over-expression or IL1β exposure. In comparison, the lack of significant effect on CHOP following TNFα exposure further suggests that the mechanism by with Arimoclomol attenuates ER stress is not dependent on alteration of MHCI processing since this was similarly upregulated by IL1β and TNFα. The lack of significant impact by Arimoclomol on BiP and ATF6 concentrations suggests its action may lie downstream of these components in the UPR pathway. Indeed, it is not surprising that Arimoclomol had no significant effect on BiP and ATF6 concentration. As a chaperone protein, BiP could even be expected to have increased in concentration under HSR

augmentation. Indeed, there is some evidence to suggest this is the case in a transgenic mouse model of retinitis pigmentosa (Parfitt et al. 2014). However, the response of the ER to Arimoclomol or heat shock proteins in the context of contemporaneous ER *dysfunction* may be different. Models in which HSR augmentation has apparently enhanced UPR have not been shown to have coexistent alteration of $[Ca^{2+}]_{ER}$, as is the case here.

Modulation of BiP chaperone function remains is a tempting hypothesis, since this has been shown to dictate the conformation of the ER translocon protein complex, through which ER Ca^{2+} leak is postulated to occur in this context. Indeed, BiP-mediated reduction of this leak appears to be anti-apoptotic and associated with maintained protein folding (Hammadi et al. 2013). Nevertheless, the effect of Arimoclomol to reduce expression of CHOP, and attenuate $[Ca^{2+}]_{ER}$ disturbance could also reflect an indirect consequence of downstream actions of HSPs to reduce ER load. This could occur, for example, through cytoplasmic refolding of misfolded proteins or augmentation of ERAD (Liu et al. 2008).

A direct effect of Arimoclomol on the ER/SR calcium channels is also possible. Bimoclomol, from which Arimoclomol is derived, has been shown to act on cardiac ryanodine receptors, thereby affecting ER/SR calcium handling. However, the skeletal muscle ryanodine receptor represents a different isoform, on which no such effect is described (Nanasi et al. 2001).

Finally, upregulation of HSP70 by Arimoclomol may ameliorate ER stress by direct HSP70 binding to and stabilisation of the SERCA, thereby maintaining calcium homeostasis (Tupling et al. 2004).

4.3.5 Exposure to IBM-like stress induces NFκB activation in myogenic cells

The pro-inflammatory and pro-atrophic NFκB cascade is a potentially central component of IBM pathology. Existing evidence suggested this process could be inhibited by HSPs, supporting the rationale for testing Arimoclomol in this context.

Although normal muscle maturation includes NFκB activation, this phenomenon appeared to be minimal among multinucleated myotubes, fewer

than 10% of which demonstrated it. It is not clear whether the nuclear staining for NFκB demonstrated by some cells in control cultures reflects a basal level of NFκB activation, residual activation from activation during myocytic maturation or non-specific staining. It could, therefore, be argued that this background level of could be subtracted from the absolute values demonstrated by the IBM-representative populations. This measure would increase the strength of statistical significance in the difference demonstrated after Arimoclomol treatment.

It is not surprising that exposure to inflammatory cytokines IL1β and TNFα activated NFκB. A concentration dependent response could be demonstrated here, which represents an advantage of the nuclear translocation immunostaining assay over the other commonly used electrophoretic shift assay that provides a binary result. A further advantage of this technique is its specificity to myotubes, removing the potentially confounding influence of non-specific NFκB activation by immature myogenic cells, or of non-myogenic cell types. Further, the demonstration of a concentration dependent activation of NFκB by IL1β and TNFα strengthens the arguments that this represents a specific effect. Taken together, the results indicate that NFκB activation in myotubes can be stimulated and quantified *in vitro* using inflammatory cytokines.

The mechanism of NFκB activation by these cytokines is likely to reflect a well-established direct effect (Feldmann et al. 2002). However, additional pathways of activation, notably via MHC Class I upregulation and ER stress must also be considered in the context of IBM. Indeed, the relative contributions of these direct and indirect pathways are of interest in determining the role of NFκB in IBM. In these experiments, βAPP overexpression also led to significant NFκB activation, which confirms the potential significance of such an indirect pathway, in which not only classically immune stimuli are responsible for maintenance of an immune response.

Treatment with Arimoclomol inhibited the activation of NFκB following cytokine exposure or βAPP overexpression. A comparison of the effect between TNFα (5ng/ml) and βAPP overexpression, which demonstrated similar degrees

of NFκB activation, shows that Arimoclomol had a similar impact in each condition. A similar pattern is demonstrated by comparable experiments with IL1β and TNFα. This implies that the effect of Arimoclomol, at least under the conditions tested here, is not reliant on the nature of NFκB activation. The mechanism of activation is likely to be largely direct in the case of cytokines but more likely to be indirect following βAPP, where is likely relies on MHC Class I upregulation or ER stress. Therefore, these results imply a direct inhibitory effect of Arimoclomol on the NFκB pathway *per se* rather than this being the result of other upstream actions. Such an effect would be in keeping with previous work that has demonstrated the inhibitory properties of HSP70 on NFκB activation (Feinstein et al. 1996). Nevertheless, the extent of NFκB activation following Arimoclomol treatment remains significantly greater than in control populations so the effect is an attenuation rather than full restoration. Further work could determine whether more aggressive upregulation of the HSR is able to suppress the NFκB cascade to a greater extent.

Notably, Arimoclomol had no significant effect on control cultures, in which fewer than 10% of cells demonstrated nuclear NFκB staining. If such staining does, indeed, represent NFκB activation in those cells, this implies that Arimoclomol's inhibitory effect is restricted to stress induced NFκB activation.

4.3.6 Potential mechanisms of Arimoclomol action

In these experiments, the use of βAPP as an inducer of IBM-relevant conditions and the proposed central role of MHCI in disease pathogenesis warrant specific consideration of how each of these is affected by Arimoclomol.

4.3.6.1 Effect of Arimoclomol on βAPP

As Arimoclomol was applied after the induction of βAPP over-expression through transfection, any impact on transfection efficiency would be unlikely to manifest in these experiments. However, if Arimoclomol were found to down-regulate βAPP, this would imply that it functions at a potentially upstream location, thereby attenuating the numerous consequences of βAPP over-

expression described here. However, Arimoclomol did not demonstrate a significant effect on βAPP concentration, either when induced through transfection or when as a consequence of cytokine exposure. Concentration *per se* may not indicate the conformational state of the protein and, therefore, not be proportionate to its degree of pathological stimulus. However, this could equally mean that Arimoclomol's effects on ER stress, TDP-43 and NFκB are more direct.

The lack of reliance on a directly βAPP-dependent mechanism perhaps adds further support to the significance of Arimoclomol's cytoprotective effects. First, if βAPP does transpire to be an early pathogenic trigger in IBM, it is difficult to envisage that patients could receive treatment in the earliest stage of the disease as they would likely be either presymptomatic or without a formal diagnosis. Secondly, if βAPP is not pathogenic in IBM *in vivo*, but rather can simply be used to induce IBM-relevant pathological features *in vitro*, it is more likely that Arimoclomol's *in vitro* effects in this context would translate *in vivo*.

The lack of impact by Arimoclomol on βAPP upregulation following cytokine exposure, despite contemporaneous attenuation of ER stress, NFκB activation and TDP-43 mislocalisation implies that βAPP upregulation in this context is independent of these three mechanisms. Indeed, the nature through which cytokines seem to affect βAPP metabolism remains unclear. It remains possible that this is mediated through altered APP processing by BACE-1 or macroautophagy (Vattemi et al. 2001; Lunemann et al. 2007). Again, the (mis)folding and aggregation of βamyloid oligomers is likely to be of greater importance in this context that the overall concentration of the proteins.

4.3.6.2 Effect of Arimoclomol on MHC Class I

The anticipated upregulation of MHCI in response to IL1β or TNFα was confirmed and was not affected by Arimoclomol. As this process represents a direct effect of cytokines, this lack of effect was unsurprising. However, in the context of Arimoclomol-induced inhibition of NFκB, ER stress and calcium dyshomeostasis, it does suggest that MHCI upregulation observed here does not depend significantly on any of these three processes. It would be useful to

determine whether the specific augmentation or inhibition of the ER overload response affects MHCI expression since this is likely to be the most relevant ER stress pathway on the assumption that MHCI is overexpressed but correctly folded. Conversely, that inhibition of NFκB and amelioration of ER stress are maintained despite ongoing MHCI upregulation suggest Arimoclomol acts downstream of the primary inflammatory intracellular insult, in keeping with its known functions. The situation *in vivo* may be different, given the additional factor of a systemic immune response to MHCI and NFκB. Equally, given that MHCI upregulation is widespread in IBM and does not respond to any of the immunotherapies exhibited thus far, any dependence of Arimoclomol's other effects on this factor would diminish the likelihood of translation to a meaningful effect *in vivo*. Furthermore, if Arimoclomol were to restrict IBM pathology towards a more polymyositic milieu, restricted to MHCI upregulation and inflammation, current clinical distinctions imply this may represent highly effective treatment.

The upregulation of MHCI following βAPP over-expression (see Chapter 3) differs from that related to cytokines since this is both a novel finding and is less likely to represent a direct response. It is, therefore, more difficult to make inferences from the impact of Arimoclomol. Nevertheless, in this context, the lack of impact of Arimoclomol implies that NFκB activation consequent to ER stress is unlikely to be the predominant stimulus of MHCI expression. Interestingly, ER stress in other scenarios appears to reduce MHCI surface expression, although it is not clear whether this reflects an underlying change in overall concentration, through reduction of synthesis, which could represent ATF4 translation block, or increased ERAD breakdown (Ulianich et al. 2011). Furthermore, the unusual characteristic of muscle in its lack of constitutive MHCI expression means its regulation may differ markedly to that in other tissues. Finally, its expression in maturing myotubes *in vitro* may represent an additional non-inflammatory role that is outside the influence of Arimoclomol.

4.4 Summary

The experiments described in this chapter show:

i) The HSR can be induced in primary myotube cultures through over-expression of βAPP or exposure to cytokines IL1β and TNFα.

ii) These stimuli induce IBM-like pathology including TDP-43 mislocalisation, ER stress, calcium dyshomeostasis and NFκB activation, each of which represents an important or distinguishing element of IBM pathology. The magnitude of these disturbances can be quantified using a variety of techniques, thereby allowing pre-clinical determination of therapeutic efficacy.

iii) Cell viability assays reveal that these pathological changes are associated with increased cytotoxicity.

iv) Treatment with the hydroxylamine derivative Arimoclomol significantly attenuates of these interlinking processes through augmentation of the HSR chaperone response and this translates to improved cell viability.

These findings represent the first dedicated pre-clinical evaluation of a hypothesis-driven therapeutic strategy in IBM and the first in pre-clinical or clinical studies not to focus on immunomodulation. The contemporaneous induction of the IBM-like pathological elements in these experiments adds further weight to the argument that they are intimately related. Their recapitulation *in vitro* highlights that many of them can be generated at a cellular level, absent from the influence of a systemic immune system. The nature of Arimoclomol's effect in successfully ameliorating these elements is, therefore, justification for a therapeutic approach that considers the non-inflammatory elements of IBM pathology. If the likely pathways of interaction are considered, those that Arimoclomol affects may well lie at the heart of the disease (Fig 4.28).

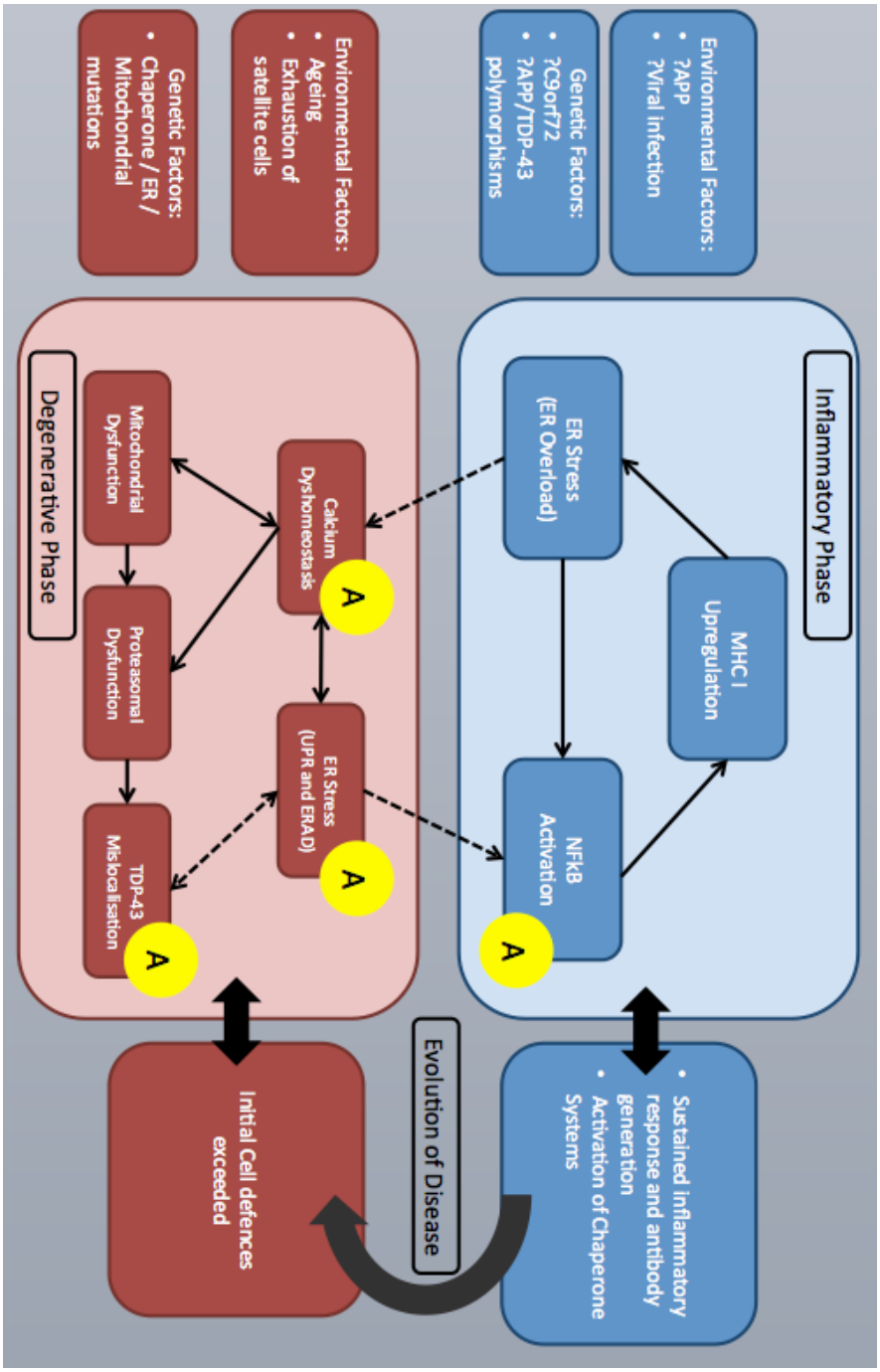

Figure 4.28 Illustration of how Arimoclomol relates to central pathogenic mechanisms in IBM.

A predominantly inflammatory phase (blue elements), interlinks with a predominantly degenerative one (red elements). Sites of Arimoclomol action are represented by yellow circles.

Chapter 5: Translating the Effects of Arimoclomol to IBM Patients; Establishing a Phase IIa Clinical Trial

5.1 Introduction

5.1.1 Translational research pathway

The translational research pathway depends on the advancement of pre-clinical scientific discoveries to early then late phase clinical trials (Fig 5.1). Each condition presents individual challenges to this process. In the context of IBM, the limitations at pre-clinical level relate to the lack of either a clearly established primary cause for the disease or the identification of a significant genetic influence, either of which would significantly reduce the inherent difficulty in developing pre-clinical models of IBM. This, in turn, slows pre-clinical development and, in particular, the lack of a suitable animal model means reliance on *in vitro*, computational or human studies. At the clinical level, in addition to generic ethical and financial considerations, the relative rarity and heterogeneity of IBM, combined with its relatively slow pace of clinical change and lack of validated outcome measures or biomarkers to quantify that change, make large efficacy trials very difficult. Previous, unsuccessful, studies of pharmacological agents for IBM have employed immune therapies already licensed for other conditions, typically in small and usually underpowered clinical trials (Section 5.1.2). The lack of detectable effect in these trials, therefore, cannot be taken as definitive evidence of the absence of an effect. Equally, these trials were initiated without significant pre-clinical evidence to support their use and were largely based on the hypothesis that attenuation of inflammation might be of benefit.

As described in Chapters 3 and 4, the development of an *in vitro* model with quantifiable IBM-relevant pathological outcome measures allowed the testing of Arimoclomol, which proved to be effective in attenuating several disease markers.

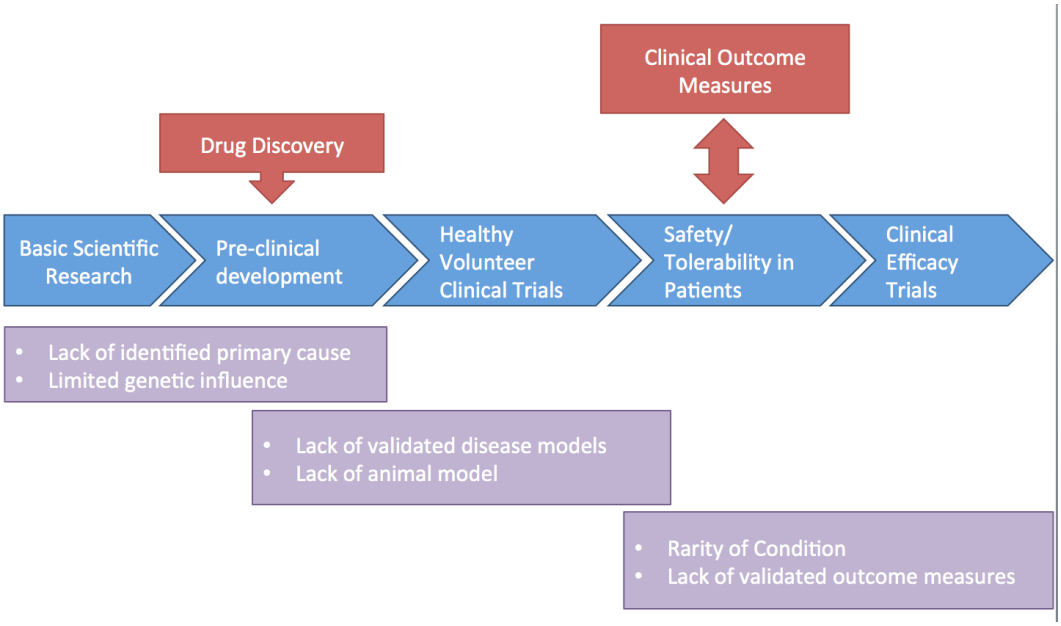

Figure 5.1 Translational research pathway of drug development

The process of advancement from laboratory research in a given condition, through to clinical studies of drug efficacy culminating in licensed treatments (Blue). Contemporaneous drug development contributes to pre-clinical development and clinical outcome measures both rely upon and contribute towards early phase clinical studies (Red). IBM represents specific challenges at each stage of the process (Purple).

5.1.2 Previous clinical trials of IBM

To determine how to advance Arimoclomol in the translational pathway, consideration was given to the potential next steps. The lack of a suitable animal model is discussed above in this thesis (see Chapter 3 Introduction, Section 3.1.2). Therefore, the feasibility of a human study was assessed by undertaking a review of previous clinical trials in IBM and the existing evidence supporting Arimoclomol's suitability in this context. Nine randomised pharmacological trials of efficacy have been undertaken in IBM, of which seven were blinded and placebo controlled (Table 5.1). Several smaller observational studies have also been performed (Table 5.2). None of these lasted more than one year, with the typical duration being far shorter and usually fewer than six months. It is unsurprising, therefore, that very few statistically or clinically significant

Trial Name	Treatment	Design	Patient No.	Primary Outcome	Secondary Outcomes	Results
Oxandrolone in IBM (Rutkove et al. 2002)	12 weeks	R, DB, PC, CO	13	MVICT	MVICT, MMT	**1. Increased MVICT of upper-extremity** 2. No significant difference in MRC scores
High Dose IvIg (Walter et al. 2000)	6 months (monthly)	R, DB, PC, CO	20	MRC Sum score	Neuromuscular Symptom Score, Arm outstretched time, EMG, CK	1. Small improvement in MRC score over 12 months (in both groups) **2. Improvement or stabilisation in 90% patients** **3. Improved Neuromuscular Symptom score in IvIg over placebo**
IvIg combined with Prednisone (Dalakas et al. 2001)	IvIg+Pred or Placebo+Pred (monthly for 3 months)	R, DB, PC	36	MRC/ QMT scores	Patient Self Assessment, Muscle Biopsy	1. No significant difference in MRC/QMT **2. Reduced number of necrotic fibres, CD3+ cells, foci of inflammation in IvIg/Pred group**
Treatment with IvIg (Dalakas et al. 1997)	3 months (monthly)	R, DB, PC, CO	19	MRC/ MVICT	Duration of Swallowing Function	1. Non-significant gain in function **2. Improved swallowing function in IvIg group**
High Dose βINF1a (MuscleStudyGroup 2004)	24 weeks	R, DB, PC	30	S+T	MVICT, MMT, DEXA,	1. No significant difference in AEs 2. No significant difference in efficacy
Pilot Trial of βINF1a (MuscleStudyGroup 2001)	24 weeks	R, DB, PC	30	S+T	MVICT, MMT, MRC, DEXA, Neopterin levels	1. AE profile similar to that of βIFN in MS 2. No significant change in efficacy measures 3. Insignificant change in Neopterin levels (marker of βIFN activity)

Anti-T-lymphocyte globulin (Lindberg et al. 2003)	Methotrexate or ATG 12 months	R	11	MVICT	Muscle Biopsy	**1. Mean strength increased 1.4% in ATG group compared with 11.1% decrease in MTX group**
Comparison of Methotrexate and Placebo (Badrising et al. 2002)	48 weeks	R, DB, PC	44	QMT sum score	MMT, activity scales, patient report, CK	1. 8/21 patients dropped out of MTX arm due to AEs 2. **Greater CK drop in MTX group**
Alemtuzumab in IBM (Dalakas et al. 2009)	4 doses	Open	13	QMT sum score	Muscle biopsy	**1. QMT Strength declined 14.9% in 12 months prior to treatment, then by 1.9% in 6 months after treatment** 2. Reduction of lymphocytic infiltrate on biopsy 3. No drug related SAEs
Etanercept in IBM (Barohn et al. 2006)	Average 17 months	Open, Retrospective controls	9	MVIC	Grip strength	1. No difference between etanercept and control

Table 5.1 Previous drug trials in IBM

Statistically significant findings are highlighted in bold. *Treatments*: IvIg= Intravenous immunoglobulin, Pred=prednisolone, AZA=azathioprine, MTX=methotrexate, TAC=tacrolimus, Ciclo=ciclosporin, ATG=Anti-T-lymphocyte globulin, IFN=interferon. *Study Designs*: R=randomised, DB=double Blind, PC=placebo controlled, CO=crossover, RA=retrospective analysis, CR=case reports. *Outcome Measures*: MMT=manual muscle testing, MRC=Medical Research Council power grade, MVICT=maximal voluntary isometric contraction testing, QMT=Quantitative muscle testing, S+T=safety and tolerability, (S)AE=(serious) adverse event, EMG=electromyography, DEXA=dual energy x-ray absorptiometry, CK=creatine kinase, ND=not defined

Trial Name	Treatment	Design	Patient No.	Primary Outcome	Secondary Outcomes	Results
Explanation of poor response to immunosuppressive therapy (Barohn et al. 1995)	Pred	No control	8	ND	CK, Muscle strength	1. Reduce serum creatine kinase 2. Muscle strength reduced after prednisone treatment
Retrospective view and randomised, prospective trial of immunosuppressive therapy. (Leff et al. 1993)	Pred, AZA, MTX (Non-standardised regimen) 3-6 months	Combined RA and R, Open	25	ND	ND	1. Prednisone 'of modest benefit' in 40% patients 2. Other therapy (AZA/MTX) 'halted progression' in 23%
Drug Therapy of the Idiopathic Inflammatory Myopathies: (Joffe et al. 1993)	Pred, AZA, MTX (Non-standardised regimen)	RA	14	ND	ND	1. IBM patients less likely to respond to all treatments than PM/DM 2. Approximately 40% IBM patients had no response to prednisone
Treatment with Ciclosporin-A or Tacrolimus (Quartuccio et al. 2007)	TAC or Ciclo in combination with Pred	Observational	3	ND	ND	1. Unquantified clinical improvement reported
IvIg for Dysphagia (Cherin et al. 2002)	IvIg or IvIg and Steroids	CR	4	ND	ND	1. Insignificant change in severe dysphagia

Table 5.2 Small clinical studies of pharmacological treatments of IBM

Statistically significant findings are highlighted in bold. *Treatments*: IvIg= Intravenous immunoglobulin, Pred=prednisolone, AZA=azathioprine, MTX=methotrexate, TAC=tacrolimus, Ciclo=ciclosporin. *Study Designs*: R=randomised, DB=double Blind, PC=placebo controlled, RA=retrospective analysis, CR=case reports. *Outcome Measures*: MMT=manual muscle testing, MRC=Medical Research Council power grade, MVICT=maximal voluntary isometric contraction testing, S+T=safety and tolerability, CK=creatine kinase, ND=not defined.

outcomes have been described. With the possible exception of apparent improvement of dysphagia with IvIg (Walter et al. 2000), it could be argued that no meaningful treatment response has been observed in any IBM trial. Whilst this does fit with the anecdotal evidence that IBM does not respond to immunotherapies, which are the only group of compounds to have been explored, it is unlikely that any of these studies were adequately powered to detect clinical changes of a realistic magnitude. This challenge reflects the lack of agreed clinical outcome measures and biomarkers in IBM. Nevertheless, the absence of evidence generated by these studies has appeared to motivate the examination of alternative drugs, implying negative outcomes of underpowered trials might be unfairly inferred as proving a lack of effect. This could lead to potentially effective treatments being overlooked. A further criticism of the vast majority of previous trial in IBM is the absence of any attempt to clarify a potential mechanism of action; very few studies have included muscle biopsy analysis, although it is notable that even in studies where inflammation has apparently reduced histologically, a clinical correlation was not necessarily detected (Barohn et al. 1995).

Therefore, a review of previous trials in IBM suggests that future studies could be improved by following a more step-wise approach to advance through the standard phases of drug development. In the absence of a pre-clinical animal model, this should include analysis of drug action in trial subjects and also establish safety, tolerability and, ideally, tendency to placebo effect (which may be particularly strong with drugs intravenously administered such as immunoglobulin). This would minimise the likelihood of advancing unsuitable compounds towards premature efficacy studies.

5.1.3 A clinical study of Arimoclomol in IBM

As an unlicensed compound, the feasibility to advance Arimoclomol to a clinical study required consideration of its existing safety and toxicity profile to assess the appropriateness of a human study. In addition to satisfactory pre-clinical toxicology studies, Arimoclomol had undergone six phase I trials in healthy volunteers and two phase II trials of patients with ALS (Tables 5.3 and 5.4). In total 261 human subjects had received the drug through oral administration, with no reported serious adverse events or deaths, no clinically meaningful or statistically significant changes in laboratory parameters and low frequency of adverse events of mild or moderate severity. These early phase clinical studies also to supported the use of a 100mg three times daily regimen, which was determine by a multicenter dose-ranging pharmacokinetic study in ALS patients.

A review of the corresponding evidence by the US Federal Drug Administration and UK Medicines and Healthcare Regulatory Agency supported a trial incorporating a 4-month Arimoclomol treatment phase in IBM patients. Accordingly, a trial was designed, with four key objectives.

5.1.4 Objectives of the clinical trial

1. To assess the *safety and tolerability of Arimoclomol* in a cohort of patients with IBM. Arimoclomol had already satisfied Phase I studies in healthy volunteers as well and been deemed safe and well tolerated in a study of population of patients with Amyotrophic Lateral Sclerosis (Cudkowicz et al. 2008). To advance drug development in IBM, satisfactory safety data is essential prior to any efficacy study.

2. To determine the impact of Arimoclomol treatment on a variety of clinical measures relevant to IBM, such as muscle strength and a functional rating scale. A safety study, such as the one described in this Chapter, is not statistically powered to detect significant changes in outcome measures of treatment efficacy based on the anticipated natural history of the disease.

Phase 1 Studies of Arimoclomol			
Study Purpose/Design	**Population**	**Arimoclomol Regimen**	**Endpoints**
Single oral doses (SC, R, DB, P)	10 healthy males	50-600mg single doses or placebo 7 days	PK, AEs, Labs, Clinical, ECG
Multiple oral doses (SC, R, DB, P)	18 healthy males	50mg od to 100mg tds 10 days	PK, AEs, Labs, Clinical, ECG
Radiolabelled mass balance study of metabolism and excretion (SC)	6 healthy males	100mg doses (^{14}C-BRX-345)	^{14}C-BRX-345 PK and metabolites in serum, urine and faeces, AEs, Labs, Clinical, ECG
Bioavailability and food effect (SC, R, OL, C)	18 healthy males and females	100mg single dose	PK in plasma (fed vs. fasted), AEs, Labs, Clinical, ECG
Safety, tolerability and maximum dose range (SC, R, DB, P)	40 healthy males (18-50 years)	100mg od to 600mg tds 7 days	PK, urinary creatinine and B2-microglobulin, protein and microalbumin, AEs, Labs, Clinical, ECG
Extended Safety and tolerability plus renal evaluation (SC, R, DB, P)	16 healthy males (18-60 years)	400mg tds 28 days	PK, GFR and renal haemodynamics, urinary creatinine and B2-microglobulin, protein and microalbumin, AEs, Clinical, ECG

Table 5.3 Phase I human studies of Arimoclomol

Six studies of Arimoclomol in healthy human volunteers demonstrated satisfactory pharmacokinetic, bioavailability and safety data to allow further evaluation in patients (CytRxCorp 2009).

(SC=single centre, R=randomised, D=double-blind, P=placebo, OL=open label, od=once daily, tds=three times daily, PK=pharmacokinetics, AEs=adverse events, Labs=routine clinical laboratory tests, ECG=electrocardiogram).

Phase IIa Studies of Arimoclomol			
Study Purpose/Design	**Population**	**Arimoclomol Regimen**	**Endpoints**
Safety, tolerability, dose-ranging and CSF penetration in ALS (MC, DB, P)	84 males and females with ALS	25mg tds to 100mg tds 12 weeks	PK, AEs, Labs, Clinical, ECG, interaction with riluzole, ALSFRS-R, vital capacity, weight, BMI, survival
Extended safety and tolerability in ALS (MC, OL)	69 males and females with ALS	100mg tds 6 months	PK, AEs, Labs, Clinical, ECG, interaction with riluzole, ALSFRS-R, vital capacity, weight, BMI, survival

Table 5.4 Previous Phase IIa human studies of Arimoclomol

Two previous Phase IIa studies of Arimoclomol in patients with Amyotrophic Lateral Sclerosis demonstrated satisfactory safety and tolerability over up to 6 months. (CytRxCorp 2009)

(MC=multicentre, DB=double-blind, P=placebo controlled, ALS=Amyotrophic Lateral Sclerosis, tds=three times daily, PK=pharmacokinetics, AEs=adverse events, Labs=routine clinical laboratory tests, ECG=electrocardiogram, ALSFRS-R=ALS functional rating scale, BMI=body mass index)

Nevertheless, the opportunity to obtain such data was taken since this would evaluate the suitability of such measures for use in future studies, estimate the practicality of performing such a measurement panel on a cohort of patients, provide data to inform future power calculations could and provide a means to detect any large impact, either positive or negative, of Arimoclomol treatment on important features of IBM.

3. To determine the effect of Arimoclomol treatment on the expression of Heat Shock Protein expression in IBM muscle. Having determined that Arimoclomol augments the expression of HSP70 under IBM-relevant conditions *in vitro*, we sought to examine whether a similar effect could be detected in patients with IBM.

4. To determine the impact of Arimoclomol on histopathological features of IBM tissue. Only one previous study of IBM has included serial muscle biopsies. We sought to evaluate the histological features of the disease using an up-to-date panel of markers. This also provided opportunity to determine markers that appeared promising as potential biomarkers of disease.

5.2 Methods

5.2.1 Contributors to the clinical trial

A transatlantic clinical trial requires the input of numerous people. The US and UK sites were led respectively by Dr Richard Barohn at Kansas University Medical Centre and Professor Michael Hanna at University College London and each site employed a team of people. My specific involvement was:

i) Trial design and set-up

- I wrote the trial protocol for the UK site to meet local and EU trial directive regulations. This was required to achieve sponsorship from UCL Joint Biomedical Research Unit. This involved extensive adaptation of the methodology and trial-reporting framework from an original US draft.
- I wrote the application to the Local Research Ethics Committee and defended the application at the corresponding meeting of the Ethics Committee.

- I wrote the documents supporting approval of the trial by the Medicines and Healthcare Regulatory Agency. I was assisted in this process by Miss Emma Lee of ChoicePharma, a third-party Contract Research Organisation.
- I wrote the grant application to the Arthritis Research Campaign (now Arthritis Research UK), who kindly funded this trial.
- I was the primary point of liaison with CytRx Corporation (the manufacturing drug company), UCL JBRU and UCL Trials Pharmacy throughout the trial set-up period. This included the processes of achieving sponsorship, inspection of the IMP manufacturing site by an EU qualified person, preparation of Investigational Medicinal Product Dossier, statistical evaluation and approval, and receipt and dispending of trial medication.
- I received valuable administrative support from Ms Gisela Barreto (Clinical Trials Coordinator) during this period.

ii) Trial conduct

- For consistency, Dr Pedro Machado (Physician, clinical assessments) and Ms Lis Dewar (Physiotherapist, quantitative myometry) and Dr Fion Bremner (Ophthalmologist, slit lamp examination) performed trial visit assessments of UK subjects wherever possible. I performed clinical assessments when this was not possible.
- After completion of the surgical procedure, I processed muscle biopsy tissue taken at the UK site (i.e. retrieval, sectioning and provision to the relevant laboratories at the National Hospital for Neurology and Neurosurgery or Institute of Neurology, UCL). I was posted sections of frozen muscle biopsies from the US site through the Fedex™ clinical sample service.
- I performed the analysis and scoring of the histology of trial muscle tissue described in this thesis. Additional analysis of the same slides was undertaken by Dr Janice Holton, Neuropathologist at the National

Hospital for Neurology and Neurosurgery for purposes of the final trial reporting and local clinical governance. As an NHS clinical report was generated for all biopsies, all histology samples at the UK site were mounted and immunostained by the Department of Neuropathology, in accordance with its established standard operating procedures.

- I conducted the ELISA analysis of Heat Shock Proteins described in this thesis. Additional analysis was undertaken by Dr Bernadette Kalmar and Dr Ching-Hua Lu at the Institute of Neurology for the purposes of final trial reporting.
- I amalgamated and analysed the data described in this thesis (additional analysis was performed by investigators in both sites as part of the final trial). Data from the UK was manually transcribed from the corresponding written case report forms (maintained by Ms Gisela Baretto) into electronic format. Data from US site was amalgamated and provided to me in digital format by Ms Laura Herbelin (Trials Coordinator at Kansas University Medical Centre).
- I attended trial safety committee meetings.

5.2.2 Trial design

In the United Kingdom, the necessary sponsorship was obtained from the UCL Joint Biomedical Research Unit. Approval was then received from the local ethics committee and Medicines and Healthcare Regulatory Agency (MHRA). In the United States of America, the equivalent approvals were received from the local ethics committee and Food and Drug Administration (FDA). The trial was conducted at University College London, UK and Kansas University Medical Centre, USA. A randomised, double blind placebo-controlled structure was employed. At each site, 8 participants were allocated oral Arimoclomol 100mg three times per day and 4 participants matching placebo. This generated a total of 24 participants, 16 of whom received Arimoclomol and 8 received placebo.

After determination of eligibility and provision of informed consent, participants entered a treatment phase lasting four months and then underwent

a further eight months of clinical follow-up. The duration of total participation was one year (Fig 5.2). During the treatment phase, assessments were made fortnightly and during the follow-up phase this was extended to monthly. In total, each participant made 18 trial visits. The nature of each visit depended on the stage of the trial, but always included determination of Adverse Events (Table 5.5).

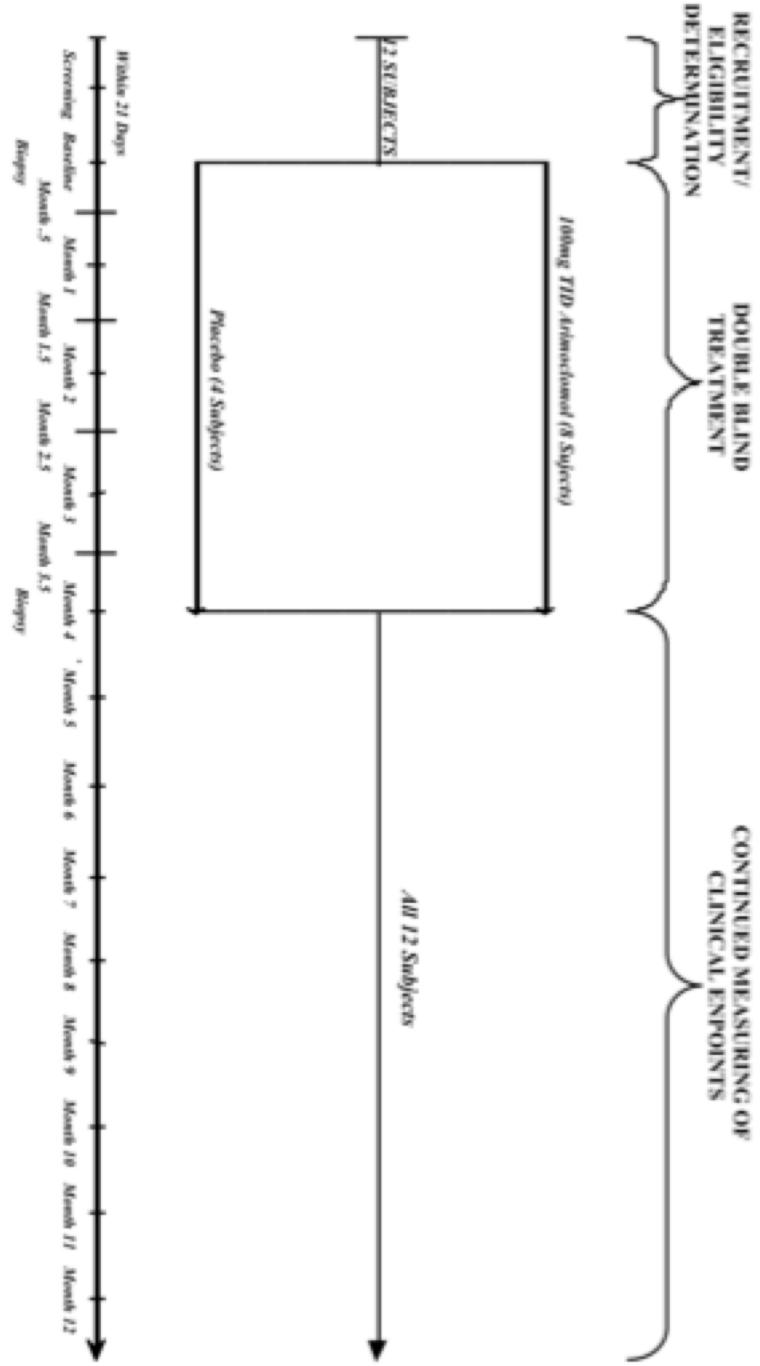

Figure 5.2 Study design for participants each of the two sites

Each site recruited 12 eligible participants who then underwent a 4-month treatment phase (8 on Arimoclomol and 4 on placebo) before completing a further 8 months of clinical evaluation.

	Placebo Controlled Drug Phase										Clinical Endpoints Phase							
Visit Number	**1**	**2**	**3**	**4**	**5**	**6**	**7**	**8**	**9**	**10**	**11**	**12**	**13**	**14**	**15**	**16**	**17**	
Month	0 (Screen)	0 (Base)	0.5	1	1.5	2	2.5	3	3.5	4	5	6	7	8	9	10	11	12
History/Exam	•	•		•		•					•	•	•	•	•	•	•	•
Neurological Examination	•									•								•
Safety Labs*	•			•		•		•		•								•
Safety Labs**			•		•		•		•									
Dispensing of Medication		•		•		•		•										
DEXA scan		•								•								X
Muscle Biopsy		•								•								
ECG	•	•		•				•										
Muscle Testing (MMT, MVICT, IBMFRS)	•	•		•		•		•		•	•	•	•	•	•	•	•	•
Ophthalmic exam	•															•		
Side Effects of medication			•	•	•	•	•	•	•	•								
Adverse Events		•	•	•	•	•	•	•	•	•	•	•	•	•	•	•	•	•

Table 5.5 Outline of trial visit schedule for each participant.

Components of each trial visit are indicated.*=Full laboratory profile, **=Partial laboratory profile

5.2.3 Patient eligibility

Participants were required to fulfill a number of inclusion and exclusion criteria, detailed below.

5.2.3.1 Inclusion criteria

Eligible study subjects had to meet all of the following criteria:

1. Meet the Griggs diagnostic criteria for definite or probable IBM (Griggs et al. 1995)
2. At least 8 of the following 16 muscle groups must have a MMT muscle grade $\geq$ 3- or greater on the modified Medical Research Council Scale: Shoulder Abductors, Elbow Flexors, Elbow Extensors, Wrist Flexors, Knee extensors, Knee flexors, Ankle dorsiflexors, Neck flexors, Neck extensors.
3. Age > 50 years.
4. Women must be post-menopausal (no menses in >12 months) or have undergone hysterectomy.

5.2.3.2 Discussion of diagnostic criteria

The most widely accepted and stringent criteria for the diagnosis of IBM remain Griggs' criteria (Table 5.6). There is likely to be a significant cohort of IBM patients who demonstrate the stereotypical clinical phenotype but lack the full range of histological features required of these criteria (Hilton-Jones et al. 2010). As these patients may logically represent those in the earlier phase of the disease, they may represent those most likely to benefit from treatment. Nevertheless, as this trial did not seek to evaluate drug efficacy but, rather, drug safety and activity, stringency of diagnosis was prioritised, at the risk of excluding that cohort of 'clinically defined' patients.

I. Diagnostic classification

A. Definite inclusion body myositis

Patients must exhibit all muscle biopsy features including invasion of nonnecrotic fibers by mononuclear cells, vacuolated muscle fibers, and intracellular (within muscle fibers) amyloid deposits or 15–18 nm tubulofilaments. None of the other clinical or laboratory features are mandatory if muscle biopsy features are diagnostic.

B. Probable inclusion body myositis

If the muscle shows inflammation (invasion of non-necrotic muscle fibers by mononuclear cells) and vacuolated fibers but without other pathological features of inclusion body myositis, then a diagnosis of probable inclusion body myositis can be given if the patient exhibits the characteristic clinical (A1,2,3) and laboratory (B1,3) features.

II. Characteristic features

A. Clinical features

1. Duration of illness > 6 months

2. Age of onset > 30 years of age

3. Muscle weakness

Must affect proximal and distal muscles of arms and leg and Patient must exhibit at least one of the following features:

a. Finger flexor weakness

b. Wrist flexor > wrist extensor weakness

c. Quadriceps muscle weakness (MRC grade 4)

B. Laboratory features

1. Serum creatine kinase < 12 times upper limit of normal

2. Muscle biopsy

a. Inflammatory myopathy characterized by mononuclear cell invasion of nonnecrotic muscle fibers

b. Vacuolated muscle fibers

c. Either

(I) Intracellular amyloid deposits (must use fluorescent method of identification before excluding the presence of amyloid) or (II) 15–18 nm tubulofilaments by electron microscopy

3. Electromyography must be consistent with features of an inflammatory myopathy (however, long-duration potentials are commonly observed and do not exclude diagnosis of sporadic inclusion body myositis).

Table 5.6 Griggs' diagnostic criteria for IBM

Minimum muscle power

Quantitative muscle testing by myometry represents a useful trial outcome measure in muscular diseases. To ensure this could be performed and, as an estimate of the level of function that would be required to complete the intensive trial visit schedule, only patients who were able to demonstrate at least Grade 3- on the MRC scale in at least eight major muscle groups were considered.

Minimum age

To minimise the chance that patients with genetic diseases, such as myofibrillar myopathy, that can mimic IBM were included in the study, a minimum age of participation of 50 years was incorporated.

Infertile female participants

Due to the unclear safety profile of Arimoclomol in pregnancy, only postmenopausal women were included in the trial.

5.2.3.3 Exclusion criteria

A variety of exclusion criteria were applied to minimise exposure of patients with coexistent medical conditions related to any previous potential side effects of Arimoclomol. These also prevented inclusion of patients unable to undergo muscle biopsy safely. Given animal data suggesting a potential interaction with Riluzole, the receipt of drug was a specified exclusion criterion (CytRx Corporation communication, unpublished toxicity data).

The presence of any of the following excluded subject participation in the study:

1. Presence of any one of the following medical conditions: diabetes mellitus or patients taking anti-diabetic medications, chronic infection, chronic renal insufficiency, cancer other than skin cancer less than 5 years previously, multiple sclerosis or prior episode of central nervous system demyelination, or other chronic serious medical illnesses.

2. Presence of any of the following on routine blood screening: WBC < $3000/cm^3$, Platelets < $100{,}000/cm^3$, haematocrit < 30%, urea > 10mmol/l, creatinine > 150µmol/l, symptomatic liver disease with serum albumin

<30g/L, prothrombin time or activated partial thromboplastin time > upper range of control values.

3. Currently taking riluzole
4. Women who are pregnant or lactating
5. History of non-compliance with other therapies
6. Coexistence of other neuromuscular disease
7. Drug or alcohol abuse within last 3 months
8. Inability to give informed consent
9. Known bleeding disorder (e.g. Haemophilia, Von Willebrand's Disease)
10. Use of potentially nephrotoxic drugs
11. Prior difficulties with local anaesthetic

5.2.4 Randomisation and blinding

An independent statistician at the Kansas University Medical Centre performed randomisation of treatment allocation using computer generated random codes. These codes were provided to the respective research pharmacies. Investigators and participants were blinded to treatment allocation. In accordance with the intention-to-treat principle, all randomised participants were included in the analysis according to the treatment group to which they were originally assigned. All randomised participants were evaluated for tolerability and safety measures.

5.2.5 Primary outcome measure

Consistent with the principle aim of the study being safety and tolerability of Arimoclomol in IBM patients, the primary outcome measure was adverse events. As the significance of one serious adverse event may exceed that of several minor adverse events, this required quantification of severity in addition to frequency. Additionally, the relationship of any adverse event to the provision of Arimoclomol was important so that likelihood of causation could be established.

5.2.5.1 Definition of adverse events

An Adverse Event (AE) was defined as any untoward medical occurrence in a subject to whom a medicinal product had been administered, including occurrences which are not necessarily caused by or related to that product.

Accordingly, an adverse event incorporated any of the following:

- intercurrent illnesses
- physical injuries
- events possibly related to concomitant medications
- significant worsening (change in nature, severity, or frequency) of the disease under study or other preexisting conditions . Therefore, progression of the disease as judged by the clinical investigators to represent the natural course of the condition was not considered an adverse event.
- drug interactions
- events occurring during diagnostic procedures
- a laboratory or diagnostic test abnormality occurring after the start of the study (once confirmed by repeat testing) that resulted in the withdrawal of the participant from the study, required medical treatment or further diagnostic work-up, or was considered by the study investigator to be clinically significant.

A Serious adverse event (SAE) was defined as any adverse event that:

- resulted in death,
- was life-threatening,
- required hospitalisation or prolongation of existing hospitalisation,
- resulted in persistent or significant disability or incapacity, or
- consisted of a congenital anomaly or birth defect;

Adverse Events were also scored according to the US National Cancer Institute Common Terminology criteria (CTC version 3.0,

http://ctep.cancer.gov/protocolDevelopment/electronic_applications/ctc.htm) that set out clinical parameters required to classify each event as Grade 1 (mild), Grade 2 (moderate), Grade 3 (severe), Grade 4 (life-threatening) or Grade 5 (death). This ensured objectivity to the scoring of Adverse Event severity.

5.2.5.2 Relationship of Adverse Events to Arimoclomol

For each adverse event, the relationship to the study drug was recorded as one of the choices on the following scale:

Definite - Causal relationship is certain

The temporal relationship between drug exposure and the adverse event onset/course is reasonable, other causes have been eliminated, and the event must be definitive pharmacologically or phenomenologically.

Probable - High degree of certainty for causal relationship

The temporal relationship between drug exposure and the adverse event onset/course is reasonable, and other causes have been eliminated or are unlikely.

Possible - Causal relationship is uncertain

The temporal relationship between drug exposure and the adverse event onset/course is reasonable or unknown, and while other potential causes may or may not exist, a causal relationship to the study drug does not appear probable.

Unlikely - Not reasonably related, although a causal relationship cannot be ruled out

While the temporal relationship between drug exposure and the adverse event onset/course does not preclude causality, there is a clear alternate cause that is more likely to have caused the adverse event than the study drug.

Not Related - No possible relationship

The temporal relationship between drug exposure and the adverse event onset/course is unreasonable or incompatible, or a causal relationship to study drug is implausible.

5.2.5.3 Classification/description of Adverse Events

The clinical description or diagnosis related to each adverse event was categorised according to trial standard World Health Organisation MedDRA nomenclature (Brown et al. 1999).

5.2.5.4 Detection of Adverse Events and relationship to safety and tolerability

Adverse events (AEs) were detected through participant reporting and at trial visits, where potential asymptomatic events were assessed through clinical examination, blood sample laboratory testing, electrocardiogram and ophthalmological review.

Participants were instructed to contact the relevant Investigators to report events that occur between study visits. At each visit, participants were questioned directly regards symptoms of potential adverse events.

Regards any 'non-serious' adverse event (NCI grade 1 or 2) the protocol dictated that the principal investigator could determine whether the study medication should be continued. This could be performed without unblinding. For Serious Adverse Events (SAEs) and AEs of Grade 3 and above, the investigator informed the independent safety monitor to make this determination. This decision would include restricted unblinding of that participant's treatment allocation to the safety monitor.

The independent safety monitor reviewed safety and tolerability data every month and any SAE immediately. The predetermined criteria for an unacceptable safety profile, in which case the safety monitor would halt the study, were as follows:

1. A rate of AEs (regardless of any severity) considered possibly or probably to trial medication that leads to discontinuation of the study in over 25% of subjects (more than 3 participants at either site).

2. Any SAE, Grade 3, 4, or 5 judged by the independent safety monitor to be secondary to the trial medication.

3. An acceleration of cataract formation in two subjects that was believed to be related to trial medication.

Pre-trial power calculations suggested that observing 0 or 1 treatment related AE among the 16 recipients of Arimoclomol would allow conclusion that the true rate of treatment related AEs is less than 23%, through a 90% one-sided confidence interval.

5.2.6 Secondary outcome measures

5.2.6.1 Manual muscle testing

Manual Muscle Testing (MMT) is a scored neurologic examination, derived from the widely employed Medical Research Council (MRC) scale. It allocates scores between 0 and 10 based on the examination of 34 muscles: neck flexors and extensors; shoulder abduction, external rotation; elbow flexion and extension; wrist extension and flexion; abductor pollicis brevis; flexor digiti minimi; hip flexors, extensors and abductors; knee extension and flexion; and ankle dorsiflexion, plantar flexion and extensor hallucis longus. Each muscle is scored from 0 to 5, with 0 representing paralysis and 5 representing normal strength. There are modifications to this scale, by adding either a minus or plus to the score. For example, a 4- represents a muscle that is slightly weaker than a score of 4, and likewise a 4+ would be a muscle that is slightly stronger than a score of 4. The +/- scores are only employed for MRC score scores 3 and above.

MRC Grade	MMT (10 Point System)
5	10
5-	9
4+	8
4	7
4-	6
3+	5
3	4
3-	3
2	2
1	1
0	0

Table 5.7 Quantification of manual muscle testing (MMT) for power

To minimise variability, MMT was, whenever possible, performed by the same investigator on a given participant. Preceding the trial, all site investigators conducted a blinded evaluation of their MMT scoring to minimise inter-

observer variability. All investigators were provided detailed information to ensure standardisation of the technique used to evaluate MMT and minimise inter-observer variability (see Chapter 7, Appendix).

5.2.6.2 Myometry

The Cybex™ myometry system was employed to provide maximum isometric voluntary contraction testing (MVICT), which has good reliability and reproducibility (FSH-DY-Group 1997). The specific protocols used are described in Chapter 7 Appendix, Section 7.1.1.2). Briefly, equipment was calibrated according to manufacturer's instructions. Twelve muscles were tested, six muscles on each side. The joint tested was placed in a specific position. 90° angles were used in joint and strap alignment for reliability purposes. Each muscle group was tested three times for at least 3 seconds while the patient was vigorously encouraged to push or pull in the desired direction. At least 10 seconds rest were allowed between contractions. The patients were tested in the supine position for the shoulder abduction, elbow flexion, and elbow extension, and sitting upright at the end of the table for the knee extension, knee flexion and hand grip.

5.2.6.3 IBM Functional Rating Scale

The IBM Functional Rating Scale (Table 5.8) is a validated scoring system used to assess functional parameters relevant to daily life in patients with IBM (Jackson et al. 2008). It was previously demonstrated to have greater sensitivity of change compared to measures of muscle power, including handgrip dynamometry and has been employed in one previous clinical trial of IBM (MuscleStudyGroup 2004). Evaluators administered the scale in accordance with written guidance reproduced in the Appendix (Chapter 7, Section 7.1.2).

1. SWALLOWING

4	Normal eating habits
3	Early eating problems – occasional choking
2	Dietary consistency changes
1	Frequent choking
0	Needs tube feeding

2. HANDWRITING (with dominant hand prior to IBM onset)

4	Normal
3	Slow or sloppy: all words legible
2	Not all words are legible
1	Able to grip pen but unable to write
0	Unable to grip pen

3. CUTTING FOOD AND HANDLING UTENSILS

4	Normal
3	Somewhat slow and clumsy, but no help needed
2	Can cut most foods, slow and clumsy; some help needed
1	Food must be cut by someone, but can still feed slowly
0	Needs to be fed

4. FINE MOTOR TASKS (opening doors, using keys. Picking up small objects)

4	Independent
3	Slow or clumsy in completing task
2	Independent but requires modified techniques or device
1	Frequently requires assistance from caregiver
0	Unable to perform

5. DRESSING

4	Normal
3	Independent but with increased effort or decreased efficiency
2	Independent but assistive device or modified technique
1	Requires assistance from caregiver for some clothing items
0	Total dependence

6. HYGIENE

4	Normal function
3	Independent but with increased effort or decreased activity
2	Independent but requires use of assistive devices
1	Requires occasional assistance
0	Completely dependent

7. TURNING IN BED AND ADJUSTING COVERS

4	Normal
3	Somewhat slow and clumsy, but no help needed
2	Can turn alone, or adjust sheets, but with great difficulty
1	Can initiate, but not turn or adjust sheets alone
0	Unable or requires total assistance

8. SIT TO STAND

4	Independent (without use of the arms)
3	Performs with substitute motions but without use of arms
2	Requires of use of arms
1	Requires assistance
0	Unable to stand

9. WALKING

4	Normal
3	Slow or mild unsteadiness
2	Intermittent use of an assistive device
1	Dependent on assistive device
0	Wheelchair dependent

10. CLIMBING STAIRS

4	Normal
3	Slow, hesitation, increased effort; uses hand rail intermittently
2	Dependent on handrail
1	Dependent on handrail and additional support (cane or person)
0	Cannot climb stair

Table 5.8 The IBM Functional Rating Scale (FRS)

5.2.6.4 Dual Energy X-Ray Absorptiometry (DEXA)

Body composition was obtained using a standard DEXA whole body scan to assess total body fat-free mass as well as total body fat mass. The scans were performed in the departments of radiology at Kansas University Medical Centre and University College London Hospital. The DEXA technique provides a reliable estimate of muscle mass because lean body mass is primarily composed of muscle. Indeed, DEXA measured lean body mass in neuromuscular patients is highly correlated with a standard method for estimation of muscle mass, urinary creatinine excretion (Tawil R 1994). DEXA has been used to measure muscle mass in previous studies of IBM (MuscleStudyGroup 2004), Duchenne dystrophy, and FSHD (Kissel et al. 1998). The technique is easily performed and safe, using a very small quantity of X-ray energy to measure body composition. The effective dose to an adult for a whole body study performed on this instrument to be 4.2 μSv, less than that of a plain chest radiograph. Thus the total effective dose for all three whole body DXA procedures in the study was 12.6 μSv.

5.2.6.5 Skeletal muscle biopsy

Informed consent for muscle biopsy was incorporated into the initial consent process for the trial. Procedure-specific consent was repeated, according to local protocols, by the operating surgeon prior to each biopsy, which was then performed under sterile conditions in an operating theatre. Open biopsy was performed in all cases, and three pieces of skeletal muscle, each of approximately 0.5cm^3, were taken via a small incision under sterile conditions. The primary biopsy site the first biopsy for all patients was biceps. If clinical examination implied this was impossible, the secondary site for the first biopsy was quadriceps. In all patients, the site of the second biopsy was the equivalent muscle of the contralateral side to that used in the first biopsy. The tissue was transferred immediately by vacuum chute to the histopathology laboratory and processed for histology or frozen in liquid nitrogen then stored at -80 °C for subsequent ELISA.

5.2.6.6 Muscle histology

Muscles biopsies were frozen and, until sectioning, were stored at −80°C. Serial tissue sections were cut in a cryostat to a thickness of 8 μm, mounted on glass slides, allowed to air dry and stored at −80°C until staining. For histochemistry, tissue sections were stained with haematoxylin and eosin (H&E), combined cytochrome oxidase (COX) succinate dehydrogenase (SDH) or Gomori Trichrome. The tissue sections for immunohistochemistry were fixed for 10 minutes and, if required, washed for 5 minutes in running water. They were then incubated in 0.5% hydrogen peroxide for 20 minutes to block endogenous peroxidase. After further washing, the sections were incubated in 5% normal goat serum (Vector Laboratories, Burlingame, California, USA) for 30 minutes. Primary antibody binding was visualised using the Dako REAL EnVision Detection System: following incubation with the particular primary antibody, tissue sections were washed in phosphate-buffered saline (PBS), incubated for 30 minutes with Horse-radish-peroxidase-labelled goat anti-rabbit/mouse secondary, washed in PBS and incubated for 3– 5 minutes in a 1:50 solution of 3,3′- diaminobenzidine (DAB). The primary antibodies used were: MHC Class I (Dako™, Clone: W6/32, dilution 1:800), p62 (BD Transduction™, Clone: 3/P62 LCK Ligand, dilution 1:200), CD3 (Leica Novocastra™, NCL-L-CD3-565, Clone: LN10, Dilution 1:180), CD4 (Leica Novocastra™, NCL-CD4-368, Clone: 4B12, Dilution 1:300), CD8 (Dako™, M7103, Clone: C8/144B, Dilution 1:60) and CD20 (Leica Novocastra™, NCL-CD20-7D1, Clone: L26, Dilution 1:100).

Slides were assessed blind to the participant identity. Five non-overlapping regions of x20 magnification (or two x20 regions in the context of COX staining or determination of inflammatory clusters) were scored in each specimen using a system adapted from a validated system for evaluation of biopsies in Dermatomyositis (Wedderburn et al. 2007). The number of fibres displaying the following degenerative features was counted: Eosinophilic hyaline inclusions, granular basophilic inclusions, rimmed vacuoles, non-rimmed vacuoles, red ragged fibres, COX deficient fibres and p62 positive inclusions. Inflammation was characterised by counting the number of endomysial and perimysial inflammatory cell clusters (defined as a constellation of 10 cells or more) for

each CD stain. A further score of 0, 1 or 2 was made for each CD stain according to the following criteria:

0 = fewer than 4 cells in a x20 field

1 = 4-20 cells in a x20 field and/or 1 cluster in five x20 fields

2 = 2 or more clusters in five x20 fields and/or diffuse infiltration (>20 cells in a x20 field)

5.2.6.7 Determination of Heat Shock Protein 70 concentration in muscle biopsies

HSP70 concentration in muscle biopsy tissue was determined by quantitative Enzyme Linked Immunosorbent Assay (ELISA) (Stressgen™, EKS-700, StressXpress® HSP70 ELISA Kit). A mouse monoclonal antibody specific for inducible Hsp70 (Stressgen™ 700-P1) was pre-coated on the wells of the provided Hsp70 Immunoassay Plate. Inducible Hsp70 was captured by the immobilized antibody and detected with a Hsp70 specific rabbit polyclonal antibody (Stressgen™, Anti-HSP Biotin Conjugate, 700-P6). The rabbit polyclonal antibody was subsequently bound by a horseradish peroxidase conjugated anti-rabbit IgG secondary antibody (Stressgen™, HRP Conjugate, 700-P8) The assay was developed with tetramethylbenzidine (TMB) substrate and a blue color develops in proportion to the amount of captured Hsp70. The color development was stopped with acid stop solution that converts the endpoint color to yellow. The intensity of the color was measured in a microplate reader at 450nm. Hsp70 concentrations from the sample were quantitated by interpolating absorbance readings from a standard curve generated with the calibrated Hsp70 protein standard provided. Samples were diluted and 100µL, in duplicate, of each of the following were added to preplated wells: prepared Hsp70 standards (0.78ng/ml to 50ng/ml), samples prepared in diluent and standard of pure sample diluent. Wells were covered with plastic wrap and incubated at room temperature for 2 hours. All wells were then washed 4 times with wash buffer and pat dried on clean paper towels. 100µL of the Hsp70 antibody were added to each well before further wrapping and incubation room temperature for 1 hour. After washing, 100µL of the

Hsp70 Conjugate were added to each well and incubated for 1 hour at room temperature. After washing, 100µL of TMB Substrate were added to each well and colour development was observed. After 30 minutes incubation at room temperature, 100µL of the Stop Solution (Hydrochloric Acid) were added to each well in the same order that the TMB Substrate was added. Absorbance was then measured at 450nm. A logarithmic curve was fitted to the HSP70 standard absorbances to allow determination of HSP70 concentration in samples.

5.3 Results

5.3.1 Fulfilment of trial protocol

24 participants were enrolled, 12 at each study site in London and Kansas. All participants successfully completed the pre-defined treatment phase of the trial other than in one case where the participant lost their final (fourth) monthly supply of treatment and the decision was taken by the Principal Investigator to curtail the treatment phase in this case to three months. The second muscle biopsy was performed at this stage, rather than incurring a period of one month without treatment prior to the biopsy. Due to long travelling distances, two patients in Kansas were unable to complete the follow-up phase (after successful completion of the treatment phase) but one returned for the final month 12 visit. There were no major deviations from the protocol.

5.3.2 Clinical baseline characteristics

Participants included 17 males and 7 females, with a mean age of 66.8 ±7.5 years and mean disease duration of 8.4 ±4.3 years. Five participants (20.8%) suffered coexistent autoimmune disease; two patients had Sjogren's disease and there was one case each of Rheumatoid Arthritis, Ulcerative Colitis and Hypothyroidism. In keeping with the stereotypical phenotype, 91.7% of patients presented with weakness of either proximal lower limb (quadriceps) or distal upper limb (forearm flexors) disease. No statistically significant differences in baseline clinical parameters were demonstrated between the Arimoclomol and Placebo groups, including the proportion of Griggs 'definite' versus 'positive' patients or IBM-FRS score (Table 5.9).

5.3.3 Safety and Adverse Events

160 AEs were recorded during the study. 108 AEs occurred in the Arimoclomol group and 52 in the placebo group. This corresponds to a mean of 6.8 AEs per patient in the Arimoclomol group (range 1-27) and 6.5 per patient in the Placebo group (range 2-10), which is not a significant difference.

	All Patients	Arimoclomol	Placebo
Male Sex, n (%)	17 (70.8)	12 (75.0)	5 (62.5)
Age (years) ± SD	66.8 ± 7.5	65.9 ± 7.9	68.8 ± 6.7
Disease duration (years) ± SD	8.4 ± 4.3	7.7 ± 4.5	9.8 ± 3.5
Griggs diagnostic category, n (%)			
Definite IBM	10 (41.7)	7 (43.8)	3 (37.5)
Probable IBM	14 (58.3)	9 (56.3)	5 (62.5)
Presenting features, n (%)			
Dysphagia	1 (4.2)	1 (6.3)	0 (0)
Prox. upper limb	1 (4.2)	1 (6.3)	0 (0)
Distal upper limb	4 (16.7)	3 (18.8)	1 (12.5)
Prox. lower limb	18 (75.0)	11 (68.8)	7 (87.5)
Distal lower limb	1 (4.2)	1 (6.3)	0 (0)
IBMFRS score ± SD	26.6 ± 6.4	27.5 ± 7.0	24.6 ± 5.1

Table 5.9 Baseline clinical characteristics of participants

A significantly higher number of AEs were reported patients at the US site (116 ±6.8, n=12) compared to the UK site (52 ±3.2, n=12, $p<0.01$).

14 AEs in the Arimoclomol group were classed as 'possibly' treatment related, compared to 8 in the Placebo group. This corresponds to a mean of 0.88 per patient and 1 per patient respectively, which is also not a significant difference. No AEs were assessed as being 'definitely' or 'probably' related to either treatment. The nature of AEs 'possibly' related Arimoclomol (bold elements in Table 5.10) was predominantly gastrointestinal, which represented 8 of the 14 AEs. No AEs clinically persisted. The two cases of hyponatraemia detected on laboratory testing were not clinically significant and normalised on repeat testing.

WHO MedDRA Class	Arimoclomol (16 patients)	Placebo (8 patients)
Blood and lymphatic system	-	-
Cardiac	Palpitations (n=1)	
Congenital, familial and genetic	-	-
Ear and labyrinth	**Dizziness/tinnitus** (n=2)	
Endocrine	-	-
Eye	Conjunctivitis (n=1), ocular pain (n=1)	Dry eyes (n=1)
Gastrointestinal	**Constipation** (n=4), **loose stools** (n=2), **nausea** (n=2), **bowel motion symptoms** (n=1), abdominal pain (n=2), pyrosis (n=1), vomiting (n=1), sore throat (n=4), glossitis (n=1),), dry mouth (n=2),	Constipation (n=4), loose stools (n=4), painful parotids (n=2)
General disorders and administration site	Weight loss (n=1), dizziness (n=1), loss of consciousness (n=1)	Fatigue (n=1)
Hepatobiliary	-	-
Immune system	-	-
Infections and infestations	Sinus infection (n=2), upper respiratory tract infection (n=7), lower respiratory tract infection (n=2), erysipelas (n=1), dental infection (n=1)	Dental infection (n=4), upper respiratory tract infection (n=3), cellulitis (n=1), leg ulcer infection (n=1)
Injury, poisoning and procedural complications	Fall (n=23), post-biopsy pain (n=3), post-biopsy fatigue (n=1)	Fall (n=9), post-biopsy pain (n=1), pruritus in biopsy scar (n=1), finger cut (n=1)
Investigations	**Hyponatraemia** (n=2), high serum thyroxine (n=1)	Spinal stenosis (n=1), herniated disk (n=1)
Metabolism and nutrition disorders	-	-
Musculoskeletal and	Musculoskeletal pain (n=10),	Musculoskeletal pain (n=2)

connective tissue	**cramps** (n=1), **rheumatoid arthritis flare** (n=1), pain in proximal lower limbs (n=1)	
Neoplasms benign, malignant and unspecified (including cysts and polyps)	-	-
Nervous system	Headache (n=7), worsening of restless leg syndrome (n=1), paraesthesia (n=1)	Headache (n=3), paraesthesia (n=1), stroke (n=1)
Pregnancy, puerperium and perinatal	-	-
Psychiatric	-	-
Renal and urinary	Haematuria (n=1)	-
Reproductive system and breast	-	Decreased libido (n=1)
Respiratory, thoracic and mediastinal	Cough (n=2)	Cough (n=1)
Skin and subcutaneous tissue	Rash (n=2), worsening of rosacea (n=1), insect bite (n=1), cold sore (n=1)	Rash (n=1)
Social circumstances	-	-
Surgical and medical procedures	Tooth extraction (n=1), sinus surgery (n=1), solar lentigines removal (n=1)	Tooth extraction (n=1)
Vascular	**Hypertension** (n=3), peripheral oedema (n=2)	Hypertension (n=3), peripheral oedema (n=3)
Mean AEs per patient	**6.8/patient**	**6.5/patient**
AEs potentially related to treatment	**14**	**8**

Table 5.10 The nature of reported Adverse Events (AEs)

One serious AE (SAE) occurred in the Arimoclomol treated group, at the UK site. After the first trial muscle biopsy and initiation of trial treatment, the patient, who had poorly controlled underlying hypertension, developed elevation of blood pressure to approximately 200 mmHg, which responded to oral antihypertensive treatment and did not recur throughout the remainder of the study. This qualified as an SAE as it met the criterion of "prolonged hospitalisation" (for one night) and Grade 3 on the NCI scale. Restricted unblinding to the safety monitor occurred in accordance with the protocol and the event was assessed as being unlikely related to trial treatment. Rather, it was attributed to the discomfort related to the muscle biopsy undertaken earlier that day. Two patients in the placebo group developed less pronounced hypertension after muscle biopsy. No SAEs occurred in the placebo group.

5.3.4 Tolerability (medication adherence)

All participants in both groups completed the treatment phase. Tolerability was inferred by measuring adherence to the prescribed regimen. The duration of one participant's treatment phase was reduced to three months following accidental loss of their medication. Adherence was measured by evaluation of participant medication diaries and counting the number of tablets remaining in their prescription box at monthly intervals during the treatment phase. The mean adherence to the regime was 99% (range 96.5% to 100%), with no difference between Arimoclomol and Placebo groups. No participant at either trial site requested early withdrawal from the treatment phase of the trial.

5.3.5 Secondary outcome measures

5.3.5.1 Manual muscle testing

At baseline, the Arimoclomol group average MMT score was 4.2 ±0.5 and Placebo group average MMT score was 3.6 ±1.4, which represented an insignificant difference. After baseline assessment, the change in MMT was determined at three 4-month intervals.

There was a strong correlation between time and the observed change of MMT in both treatment groups (Fig 5.3), (Arimoclomol group R^2=0.967, Placebo group R^2=0.999). The rate of decline appeared slower in the Arimoclomol group but no significant difference was observed between groups.

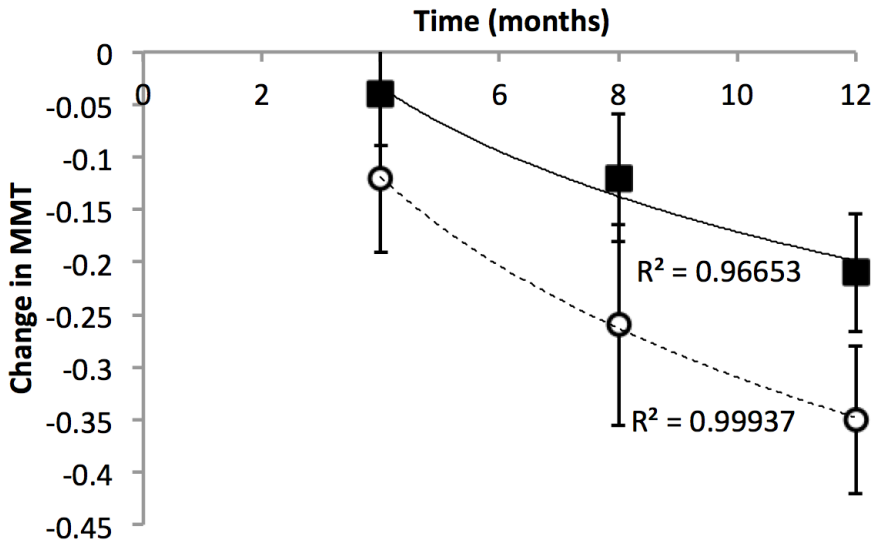

Figure 5.3 Change in manual muscle testing (MMT)

Following treatment initiation at Month 0, MMT declined steadily over 12 months in both the placebo group (white icons) and Arimoclomol group (black icons).

(Error bars = SEM, n=24)

5.3.5.2 Quantitative myometry

At baseline, the mean Maximal voluntary isometric contraction testing (MVICT) sum score was 130.4N ±70.4N in the Arimoclomol Group and 94.4N ±39.8N in the Placebo group, which is not a significant difference.

Unlike MMT, the change in MVICT was very weakly correlated with time in both treatment groups, indicating there was no appreciable trend. Furthermore, there was no significant difference between treatment groups and standard deviations were considerable; for example, these represented over 50% of the population mean value in the Arimoclomol group (Fig 5.4).

Subgroup analysis for individual IBM-relevant muscle groups, knee extension and handgrip (finger flexors) also did not demonstrate any significant differences between treatment groups. Interestingly, however, analysis of right hand grip implied a divergent trend between treatment groups (Fig 5.5). The Arimoclomol group demonstrated a fairly strong correlation of increasing grip strength with time (R^2=0.799), compared to an apparent reduction in the placebo group. However, within the time frame of this study, the greatest disparity between treatment groups, which fell at 8 months, was not significant (p=0.064).

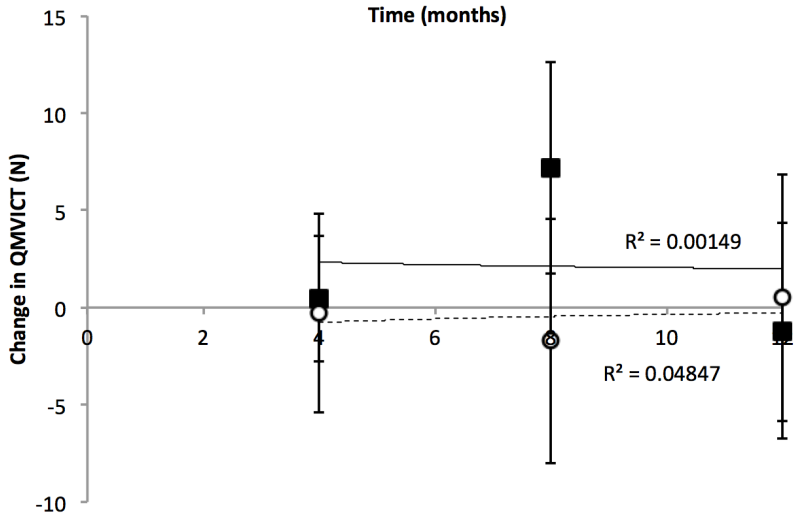

Figure 5.4 Change in QMVICT sum score

There was no significant change in myometry measurements between the Arimoclomol group (black icons) and placebo group (white icons), not was there a trend in either group over time. Standard deviations were very high relative to mean values at each data point.

(Error Bars=SEM, n=24)

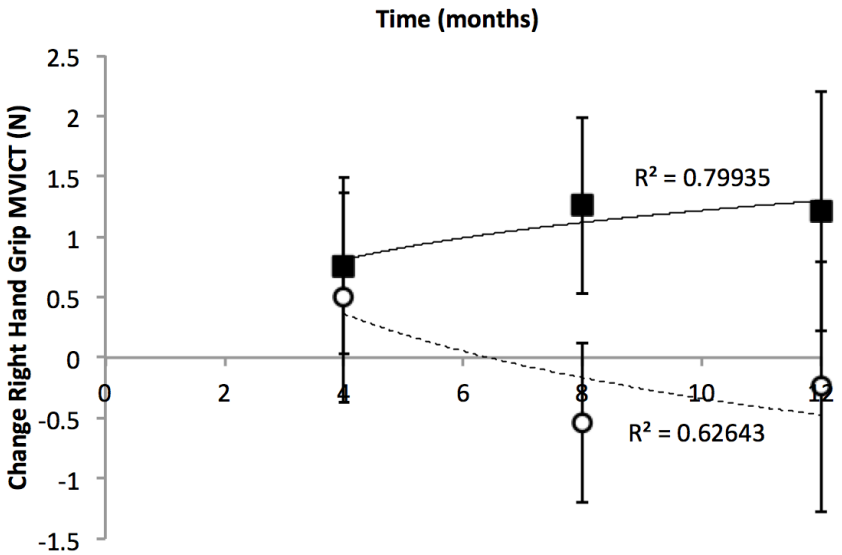

Figure 5.5 Change in right hand grip MVICT sum score (Newtons)

At 9 and 12 months, right hand grip strength increased slightly in the Arimoclomol group (black icons) but declined to slightly less than the pre-treatment baseline in the placebo group (white icons). No significant differences were detected at any of the three time points.

(Error bars = SEM, n=24)

5.3.5.3 IBM Functional Rating Scale (IBMFRS)

The change in IBMFRS observed in both groups was strongly correlated with time elapsed (Arimoclomol group R^2=0.785, Placebo group R^2=0.999). There was a trend towards a slower rate of decline in the Arimoclomol group, but no significant difference was displayed between the groups at any of the 4-monthly time points (Fig 5.6).

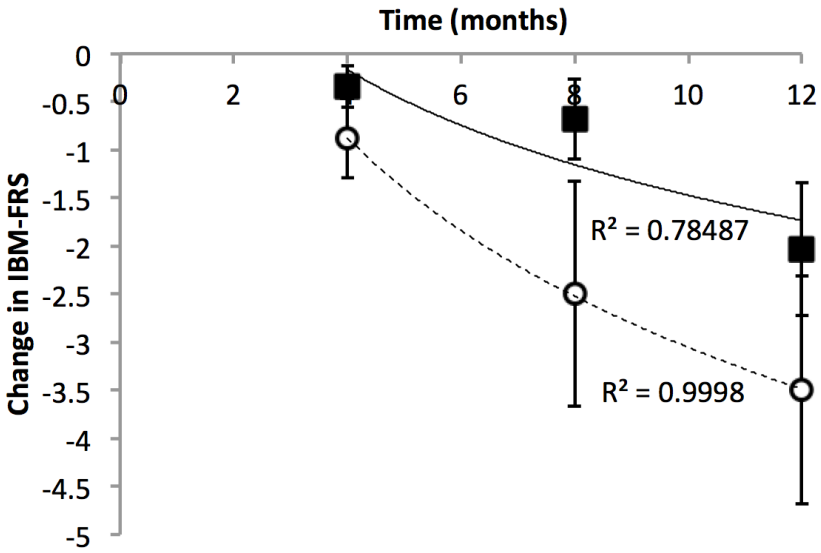

Figure 5.6 Change in IBM Functional Rating Scale

The IBMFRS declined predictably in both the Arimoclomol group (black icons), and placebo group (white icons) but no significant difference was detected between treatment groups. (Error bars = SEM, n=24)

5.3.5.4 DEXA

At baseline, the mean lean body mass (LBM), determined by DEXA, was 49.3kg (±9.7kg) in the Arimoclomol group and 42.6kg (±13.6kg) in the Placebo group, which is not significantly different. At the first subsequent measurement (4 months), LBM marginally increased in both treatment groups, before declining to below the baseline by 12 months in both groups. No significant difference was detected between treatment groups at either time point (Fig 5.7).

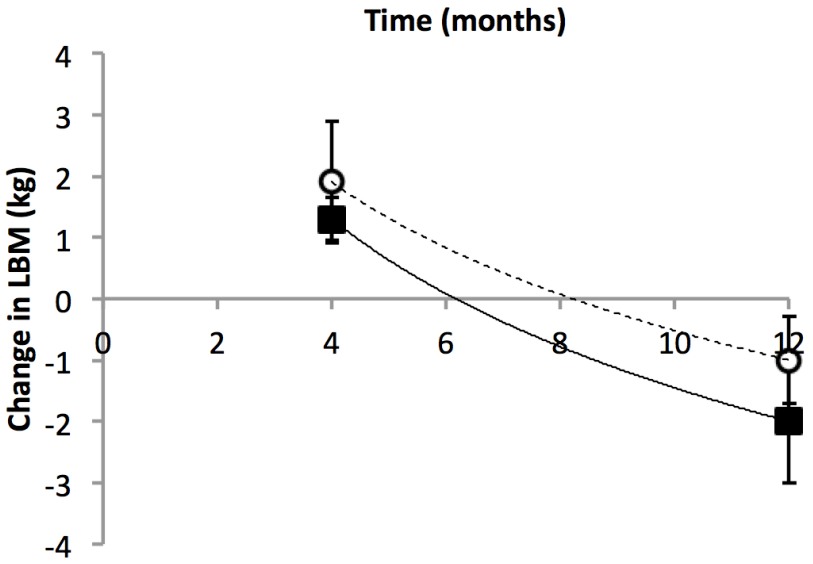

Figure 5.7 Change in Lean Body Mass

Determined by DEXA, there was no significance in LBM between Arimoclomol treated (black icons) and placebo treated (white icons) groups at either time point. (Error Bars=SEM, n=24)

5.3.5.5 Muscle histopathology

Muscle biopsies corresponding to the beginning and end of the treatment phase were successfully collected from all subjects. All samples were taken from biceps other than in one subject, in whom muscle wasting precluded this, where quadriceps was biopsied. Detailed histological analysis was performed on UK site biopsies (12 subjects), to determine degenerative (inclusions, vacuoles, p62 aggregates and red ragged fibres) and inflammatory markers (MHCI, CD3, CD4, CD8 and CD20). Only histological stains previously validated in the routine assessment of muscle biopsies at the Department of Neuropathology, NHNN, were employed. At the time of this analysis, these stains did not include TDP-43 or NFκB, meaning these characteristics of the *in vitro* experiments described in this thesis could not be examined here.

Three biopsies from the placebo group were uninterpretable as they were characterised by fatty replacement or 'end stage' tissue and only occasional identifiable myofibres. This included both biopsies from one subject and the pre-treatment biopsy from another. This made statistical comparison between

treatment groups impossible, since the placebo group comprised only two pairs of biopsies accordingly.

As subjects required existing histopathological evidence of IBM, sufficient to meet Griggs' criteria, it was unsurprising that all biopsies obtained during the trial demonstrated features stereotypical of IBM. Inflammation was characterised by endomysial and perimysial infiltration by $CD8^+$ T-cells, with a smaller proportion of $CD4^+$ T-cells. Rimmed vacuoles, cytoplasmic inclusions, red ragged fibres and COX negative fibres were all observed in keeping with the degenerative stereotype in IBM.

Nevertheless, no significant differences were demonstrated between pre and post treatment biopsies in either treatment group or between treatment groups (Figs 5.8 and 5.9). There were high degrees of variance for most histological markers, both between patients and between the biopsies of individual patients. For example, one subject's pre-treatment biopsy displayed 9 fibres containing rimmed vacuoles compared to 119 fibres in the post-treatment biopsy. This contrasts markedly with another subject, whose pre-treatment and post-treatment biopsies each displayed 2 rimmed vacuoles. Similar patterns were observed with p62 and COX staining. The inflammatory characteristics also demonstrated this high variability and no significant differences were detected whether the absolute number of inflammatory clusters or effect on the inflammation score (0-2) were examined.

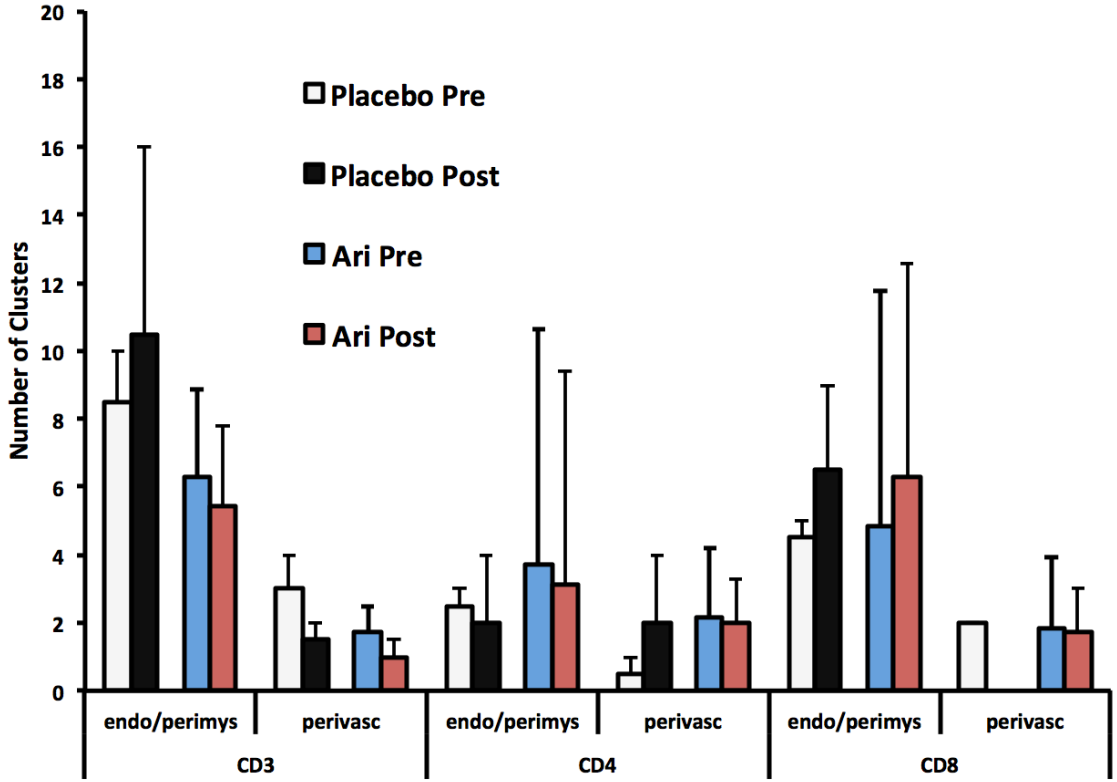

Figure 5.8 Quantification of inflammatory histopathological markers before and after treatment phase

No significant difference was observed between pre- and post-treatment biopsies from the placebo group (black or white bars) or Arimoclomol group (blue or red bars), nor was there a significant difference between the two treatment groups. This reflects high intra- and inter-subject variance in the majority of biopsy characteristics. (Endo/perimys – endomysial/perimysial inflammation, Perivasc – perivascular inflammation) (Error Bars=SEM, n=12)

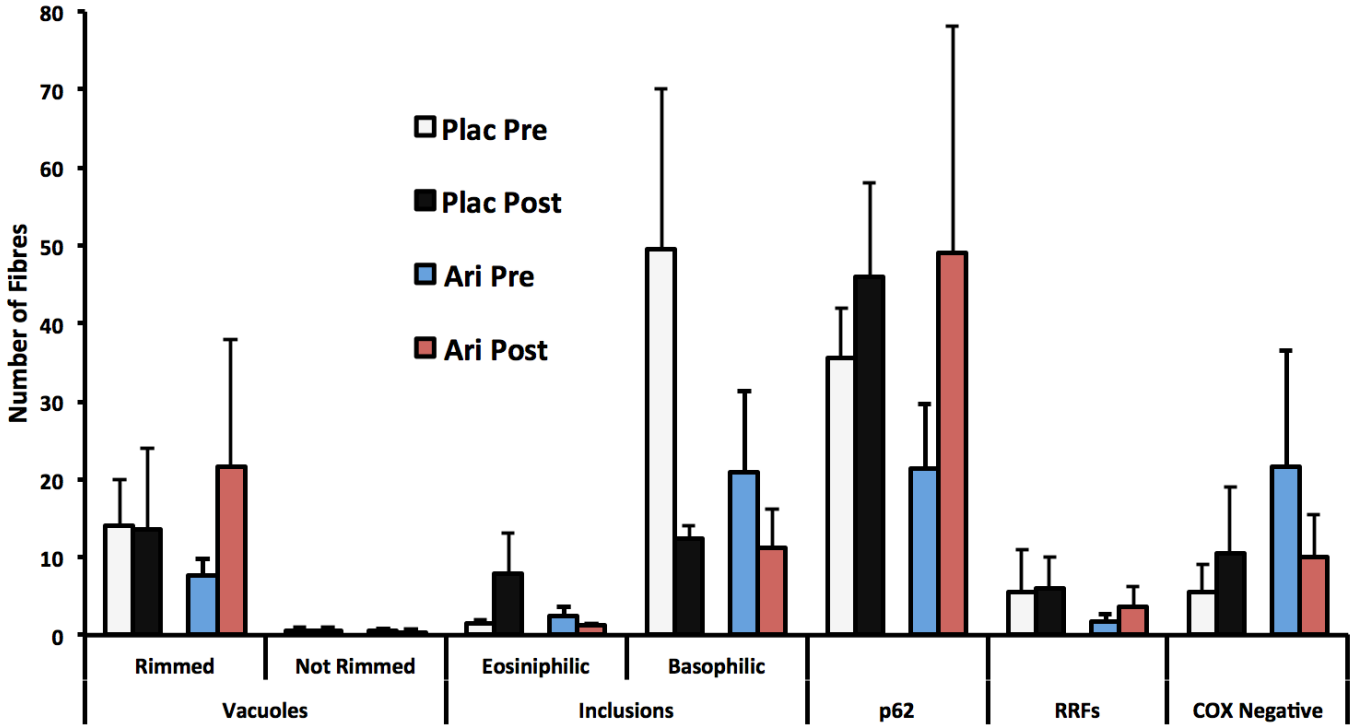

Figure 5.9 Quantification of degenerative histopathological markers before and after treatment phase

No significant difference was observed between pre- and post-treatment biopsies from the placebo group (black or white bars) or Arimoclomol group (blue or red bars), nor was there a significant difference between the two treatment groups. This reflects high intra- and inter-subject variance in the majority of biopsy characteristics. (RRFs=Red Ragged Fibres, COX Negative=Fibres lacking COX staining) (Error Bars=SEM, n=12)

5.3.5.6 HSP70 concentration in muscle biopsies

In the pretreatment muscle biopsies, mean HSP70 concentration was 7.44 μg/ml ±4.14 μg/ml in the placebo group and 9.26 μg/ml ±8.57 μg/ml in the Arimoclomol group, which is not a significant difference. Neither group demonstrated a significant change in [HSP70] in the post-treatment biopsy (Fig 5.10). There was considerable variation in [HSP70] between subjects; 5.8 μg/ml to 30.3 μg/ml in pre-treatment biopsies and 1.29 μg/ml to 23.6 μg/ml in post-treatment biopsies. Exclusive of concentration, the likelihood of observing a rise of [HSP70] in the second biopsy was no greater in the Arimoclomol group than the Placebo group.

As part of a second round of tissue evaluation in the trial, Dr Bernadette Kalmar and Dr Ching-hua Lu repeated HSP70 ELISAs with contemporaneous measurement of myosin concentration to determine whether any differential response of non-myogenic components of the biopsies contributed towards the overall result. This demonstrated a reduction of [HSP70], between first and second biopsies, of 34.7 ng/100ng ±336.3 in the Placebo group and of 100.72 ng/100ng myosin ±757 in the Arimoclomol group, which was not a significant difference. Again, there was considerable variation in baseline [HSP70] among biopsies and in the change of [HSP70] between biopsies.

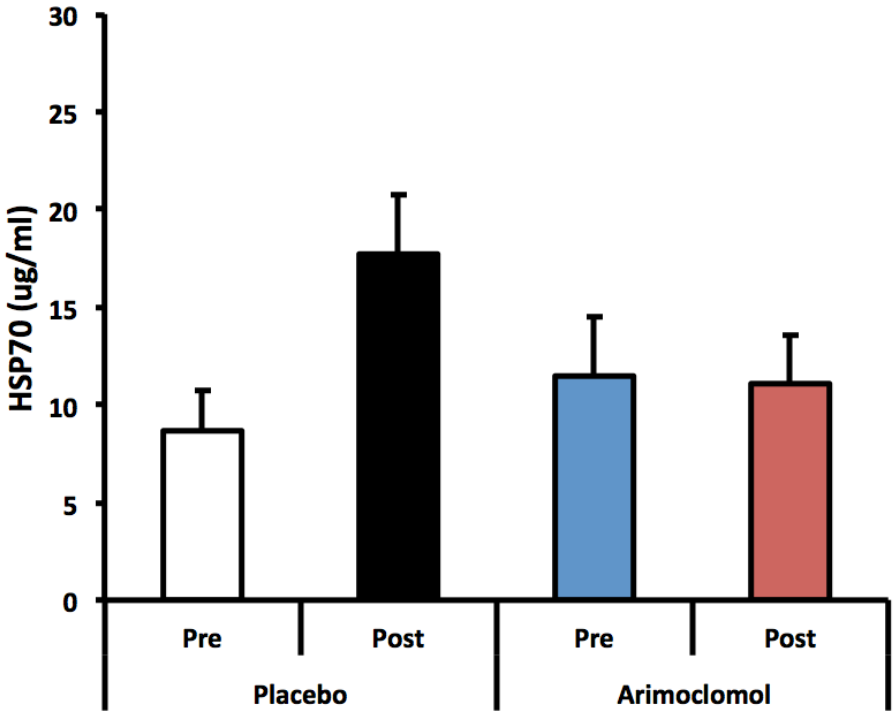

Figure 5.10 HSP70 concentration in IBM muscle

There was no significant difference in [HSP70] between Arimoclomol (blue bar) and placebo (white bar) groups before the treatment phase. After the treatment phase, there remained no significant difference between groups. There was also no significant change within either group.

(Error Bars=SEM, n=24)

5.4 Discussion

5.4.1 Arimoclomol appears safe and tolerable in IBM patients

The combination of fulfillment of the intensive trial treatment phase by all participants, in combination with adverse event data, suggests Arimoclomol (at 100mg tds) is safe in patients with IBM. The primary outcome measure, adverse events (AEs), revealed no significant difference between the Arimoclomol and placebo groups. Furthermore, the nature of AEs was predominantly gastrointestinal in both groups, implying a lack of direct causation through Arimoclomol. The fact the AE rate was significantly different between trial sites, in which the direct demands of the trial on participants were identical, but not significant between treatment groups, suggests that local clinical or cultural factors were a more relevant predictor of AE occurrence than treatment allocation. Furthermore, blood laboratory analysis, electrocardiograms and ophthalmological slit lamp examinations did not detect any clinically significant asymptomatic disturbance of haematological, renal or hepatic, cardiac or ocular function.

Clearly, the rate of AEs must be balanced with any apparent risk, however low, of a clinically serious AE related to the medication. It is, therefore, reassuring that no such event occurred. Indeed, the lack of any treatment related AEs is encouraging and is consistent with the existing early phase data from other clinical trials of Arimoclomol in healthy volunteers and patients with ALS (Cudkowicz et al. 2008). Further safety specific to the IBM population is implied by the lack of clear clinical deterioration in any of the secondary outcome measures in this study.

In addition to 100% fulfillment of the treatment phase, the near 100% adherence rate to trial medication is strong evidence to support Arimoclomol's tolerability in this patient group.

Therefore, it is reasonable to conclude that Arimoclomol was safe and well tolerated in this group of IBM patients. In combination with similar data from other early phase trials (Tables 5.2 and 5.3), it is reasonable to infer that Arimoclomol's safety and tolerability profile lies within the acceptable range for medications at this stage of development. Notwithstanding any debate about

clinical effectiveness, the safety profile is therefore appropriate for advancement of Arimoclomol to larger clinical trials.

5.4.2 Muscle strength was not affected by Arimoclomol treatment

As the trial was not specifically powered to detect changes in secondary outcome measures, firm conclusions should not be drawn from the corresponding data. Nevertheless, certain trends were of interest and warrant further investigation in suitably powered studies. The data also provide useful indicators for which measures might be preferable when designing such studies. The lack of dramatic worsening of any clinical parameters, particularly those related to the IBM phenotype, is further evidence to support a lack of harm.

It is notable that the decline manual muscle testing score (MMT) demonstrated a strong correlation with time, and to a far greater extent that MVICT. This implies that MMT could serve a useful outcome measure in future trials of efficacy in IBM. However, limitations remain. For example, the MRC scale is an ordinal scale rather than a numerical interval scale so the extrapolation of the magnitude of differences detected between time points or treatment groups to functional or symptomatic meaning is challenging. MVICT has the advantage here, through producing data distributed on an interval scale but large variance was demonstrated in the results described here, which would restrict its feasibility to detect realistic differences in future trials of drug efficacy in IBM. The issue of determining what is a clinically significant effect also remains. MMT and MVICT have demonstrated inter- and intra-observer reliability in other studies (Jain et al. 2006; Lienhard et al. 2013). The efforts to restrict MMT examinations to as few clinical examiners as possible may well have contributed to the relatively low variation demonstrated here. This should be an important consideration of future trial design if MMT is incorporated. The use of MVICT would need to be refined if it were pursued as an outcome measure and the results here would support restricting the measurement protocol to smaller number of muscles since no additional benefit was apparent through the testing of multiple muscles. Of these, handgrip is the most obvious candidate for inclusion; the relative ease of measurement due to simplicity of positioning the

limb likely contributes to its smaller variation that was the case for other muscles or the sum score. Furthermore, it is an important function in IBM, both as a commonly affected movement and a source of considerable disability through reduced manual dexterity.

It is interesting that the Arimoclomol group, versus placebo, demonstrated a reduced rate of decline over one year and a greater mean strength (by MMT) at each 4-month assessment interval. This difference was not significant, reflecting either the absence of a true treatment effect or the lack of power in this trial to detect a realistic treatment effect.

5.4.3 IBM Functional Rating Scale (IBMFRS) was not affected by Arimoclomol treatment

As the only validated disability scale in IBM, it is highly likely that IBMFRS would serve as an outcome measure in future clinical trials. It is encouraging, therefore, that the change in patients' score in this study displayed very strong correlation with time, particularly in the placebo group. The mean decline of 4 points in the placebo group over the course of one year is likely to reflect meaningful symptomatic change for patients. If restricted to one measure, it would represent decline from normality to inability or full dependency. If, as is more likely (and was the case in this study) it reflects loss of individual points across a variety of domains, this still represents a decline from normality to difficulty with a given task or from difficulty to requiring assistance. Albeit a categorical scale, meaning that quantification of change cannot easily be extrapolated back onto the individual scale, Rasch analysis of IBMFRS has been promising (Rose 2013).

No significant difference was detected between treatment groups in this study, reflecting the lack of statistical power to do so. Nevertheless, it is notable that the 8-month time point approached statistical significance ($p=0.055$) in the context of the mean IBMFRS in the Arimoclomol group exceeding that of the placebo group at all intervals. Whether this reflects the evolution of a genuine treatment effect will require a larger study.

5.4.4 Lean Body Mass (DEXA) was not affected by Arimoclomol treatment

It is unclear why the lean body mass (LBM) appeared to increase slightly in both groups between baseline assessment and the first 4 month interval, before subsequently declining to an overall reduction over one year. It is notable that the mean change over one year in the placebo group was only approximately 1kg. This has implications for the use of this technique as an outcome measure in future trials of IBM. As here, populations of mixed sex display a the wide range of LBM, reflected by the fact that the standard deviation in the placebo group approached one third of the mean baseline value. Therefore, it is unlikely that a clinical trial of pragmatic length and size could be powered to detect attenuation of an annual decline of approximately 2.5% of baseline value. It is likely that an investigational medicinal product would need to confer a rise in LBM to produce a statistically significant change, which, at least in IBM, is conceptually less likely than amelioration of the advancing underlying disease process.

5.4.5 The effect of Arimoclomol on muscle histopathology

This study demonstrated several limitations of interval muscle biopsy. The obligation to biopsy distinct sites, albeit within the same muscle group of either limb, in the context of a phenotypically asymmetrical disease, means the comparison of pre and post-treatment tissue is masked by inter-biopsy variability. Secondly, there was considerable variance in the extent to which individual patients' tissue demonstrated particular histopathological features, even within the confines of those relatively specific to IBM. This was reflected in high intra- and inter-patient variance. Third, even with experienced neurosurgeons performing the procedure, 3 of 24 biopsies transpired to contain predominantly adipose tissue and 'end stage' myofibres that rendered detailed histological interpretation and, therefore, comparison impossible.

Examining the mean values for inflammatory histological markers, it is notable that pre and post biopsies in either the placebo or Arimoclomol groups were

very similar. Therefore, the large standard error, reflective of the aforementioned high variance, does not appear to have masked a significant change. Degenerative markers, however, displayed a wider range of means so determination of any underlying pattern related to treatment is more difficult to infer. The most consistently displayed degenerative feature was p62 aggregate positivity but, again, the inter-patient variance was high and the range exceeded the value of the population mean.

These results imply that, if histological parameters are to be used to determine interval effects of a given intervention in IBM, it is likely that current immunohistochemical stains are unlikely to provide a useful outcome measure in a trial of pragmatic size. Alternative markers, perhaps related to unidentified upstream processes, may display lower inter- and intra-patient variance. More likely, tissue should be used to perform concentration based techniques such as western blotting or mass spectrometry which essentially reflect the mean concentration across the entire tissue sample taken, rather than relying on the pathological response of individual myofibres.

5.4.6 HSP70 concentration in IBM muscle is highly variable

Analysis of muscle [HSP70] demonstrated an inconsistent baseline concentration and inconsistent change over time in the Arimoclomol and placebo groups. Therefore, the lack of detected treatment effect of Arimoclomol to augment [HSP70] in this context could reflect a number of factors.

First, it is possible that a genuine treatment effect was obscured by a large underlying physiological variance. The wide range of the baseline [HSP70] among all 24 participants evidences a high inter-subject variance. Additionally, the inconsistent pattern in change of [HSP70] between the two biopsies of subjects in the placebo group suggests either a high inter-muscle variance or large physiological fluctuation of [HSP70] over time. In the overall comparison between Arimoclomol and placebo treatment groups, the standard deviations of [HSP70] approximated the value of the mean; therefore detection of a realistic treatment effect would have been masked.

Secondly, it is possible no response to Arimoclomol occurred. This could reflect a number of factors relevant to the drug or the patients. The drug dosage and bioavailability was predetermined through a number of pre-clinical and early phase clinical dosing studies so it is unlikely that an insufficient dose was used. Instead, it is more likely that any lack of action of Arimoclomol on skeletal muscle *in vivo* reflects properties of IBM tissue. The reliance of Arimoclomol on existing HSR activation in a target tissue should not preclude its action in IBM since the HSR does appear to be active in this context. Mass spectrometry has determined HSP70 is upregulated (Parker et al. 2009). Furthermore, immunohistochemical work implies upregulation of the small HSP αB-crystallin (Banwell et al. 2000). A genuine lack of response to Arimoclomol could, therefore, reflect dampening of HSR inducibility, which appears to occur in aged tissue (Sherman et al. 2001). To determine whether this is, indeed, the case, would require a study including age-matched and non-age matched disease controls. It would be particularly interesting to note whether this phenomenon occurs in all muscles among IBM patients or whether it is restricted to those muscles that display particular histopathological features. Here, the two patients in the Arimoclomol group in whom the largest relative rise in HSP70 was detected (to 155% and 181% of pre-treatment concentration respectively) displayed relatively few degenerative features, but this is not a statistically distinct sub-population.

Third, it is possible that either the concentration of HSP70, or the effect of Arimoclomol thereon, had diminished by the time of the muscle biopsy. As the harvested tissue was frozen within minutes of retrieval, this is not likely to have occurred. Nevertheless, it is possible that the action of Arimoclomol on IBM muscle is brief and transient.

Fourth, the measurement of HSP70 may have been incorrect. The high sensitivity commercial ELISA employed is strongly validated and two distinct series of analysis, with and without contemporaneous measurement of myosin concentration, failed to determine a significant change in HSP70. Therefore, this possibility appears unlikely.

Overall, it is most logical to conclude that, at least in IBM, skeletal muscle [HSP70] is likely to vary considerably between different muscles, whether from individual or multiple patients. In practical terms, this severely limits the use of muscle [HSP70] as a pathological outcome measure or biomarker.

5.4.7 Summary

The primary purpose of this study, to determine the safety and tolerability profile of Arimoclomol in IBM, was achieved and provides firm evidence that the drug does not cause significant worsening of symptoms or unanticipated side effects. The lack of biopsy related changes might reflect inherent limitations of this technique rather than an absence of effect and this means consideration would have to be given about whether the inclusion of this element to future trials can be justified, given the associated morbidity for participants. Alternative biomarker studies based on peripheral blood markers or imaging studies may be preferable outcome measures. The results of this clinical study advance Arimoclomol one step along the translational drug development pathway of IBM and support its further evaluation in humans. However, the absence of *in vivo* data on Arimoclomol's effects means the decision whether to advance it to an efficacy study must still be carefully considered. The relative rarity of IBM places its small population is at risk of trial fatigue so only studies of the most promising therapeutic agents can be justified.

Chapter 6: General Discussion

6.1 Introduction

The experiments described in this thesis sought to address the following four specific aims:

1. To establish a pre-clinical disease model of salient pathological features of IBM

2. To characterise these features in order to establish a panel of quantifiable IBM-relevant pathological outcome measures

3. To test the effectiveness of novel treatment strategies in this system, determined by consideration of the literature

4. To determine how those treatments could be advanced towards clinical effectiveness in IBM

IBM presents several particular challenges in this context, reflected by its lack of existing effective treatment. Perhaps the most fundamental of these is our limited understanding of its primary pathology. Although numerous downstream pathological features are consistently observed, the relative importance and position of these individually remain contested. The literature generally divides along the notion of whether IBM is, in essence, a primary inflammatory condition in which persistent cellular stress leads to a secondary degenerative phase or whether the inflammation observed is epiphenomenal, driven by an upstream degenerative event which leads to auto-antigen exposure and breakdown of immune tolerance, perpetuated by MHC upregulation. Both hypotheses are plausible; the former is analogous to that proposed in multiple sclerosis, whereas secondary inflammation is demonstrated by several genetic conditions of muscle, most commonly mutations of dystrophin (Stadelmann et al. 2011; De Paepe et al. 2012). Regardless of which occurs first, there are several points of interaction where either group of processes might perpetuate the other.

This debate on pathogenesis, combined with the lack of a genetic form of IBM which reproduces the clinical and pathological phenotype of the sporadic form

sufficiently accurately, means there are no consistently used preclinical cellular or animal models of IBM. In turn, efforts to treat the disease have been restricted either to anecdotal evidence or clinical trials severely limited in patient numbers and duration. The tendency of IBM to manifest clinically at a relatively advanced pathological stage presents a further considerable challenge common to neurological conditions, such as in Parkinsonism, where over half of dopaminergic neurons are be lost before clinical signs manifest (Cheng et al. 2010). Only serendipitous diagnosis or the development of highly sensitive biomarkers can circumvent this issue. Fortunately, it remains common for IBM to be diagnosed prior to the onset of significant disability, meaning that arresting rather than reversing the condition would still represent a considerable advance in current treatment. Reflecting the greater spectrum of available drugs that target the immune system, all previous approaches to IBM treatment have focused on the inflammatory component of the pathology. No individual trials have been of sufficient size or duration to prove the presence or absence of treatment effect. However, the combination of the negative findings of these trials with a large body of anecdotal evidence on the failure of immunosuppressive medication, suggests current immunotherapies are unlikely to produce significant effects in IBM when used in isolation.

Therefore, an approach based on preclinical evaluation of novel therapeutic strategies appears justified. In establishing this, the starting position of this thesis was not to align the experiments strictly along either an inflammatory or degenerative hypothesis. Rather, they sought to recapitulate elements of downstream IBM pathology likely to be present at the current realistic point of diagnosis, and determine whether these were modifiable. Priority was given to those pathological elements that appear likely to represent points of interaction between inflammatory and degenerative mechanisms since these are the logical points of greatest therapeutic attraction. For example, the primary myositides, PM and DM, even in aggressive and necrotizing forms, are often successfully treated with immune therapies (Valiyil et al. 2010). Therefore to inhibit the communication between inflammation and degeneration, in whichever direction this occurs, could improve the effectiveness of existing drugs through combination therapy.

6.2 Development of a preclinical model of IBM

As no accepted animal model of IBM exists, it was felt that the advantages of higher throughput in cellular models made an *in vitro* approach more appropriate in this context. First, as described in Chapter 3, primary satellite cell cultures were established from neonatal rat pups and the culture conditions then optimised to ensure a consistent proportion of readily identifiable myotubes could be maintained and demonstrated. This involved modification of the culture medium, plating density and a variety of myogenic purification techniques, including pre-plating, differential centrifugation and fluorescence activated cell sorting. Rat satellite cells present several advantages over their human counterparts. They are readily available, with a high yield presented by neonatal pups meaning that a small number of animals can support a large number of cultures. The source can easily be standardised, with consistent age, genetic background and environmental conditions rather than the typically heterogeneous donor population represented by human cultures. Furthermore, each culture can be established afresh, without the need for multiple passages of subclones of the original cell population that is a necessity of human satellite cell work and, notably in the case of IBM, can reveal underlying biological changes of these precursors such as inherent tendency to amyloid accumulation (Morosetti et al. 2010).

Next, cultures cells were exposed to a variety of IBM-relevant stressors, including the over-expression of βAPP or exposure to cytokines IL1β, TNFα and IFNY. This panel represented a practical number of conditions for further testing, balancing degenerative and inflammatory stimuli. Furthermore, previous work on each stressor *in vitro* suggested associated with pathology that could feasibly be reproduced in this cellular model. The overexpression of βAPP in human myocytes has previously been shown to induce mitochondrial dysfunction, cytoplasmic inclusions and proteasomal inhibition (Askanas et al. 1997; Fratta et al. 2005). The exposure of human myocytes to cytokines appears to upregulate expression of βAPP (Schmidt et al. 2008). Therefore, it was first confirmed that these techniques are applicable to primary rat satellite cell cultures.

βAPP plasmid transfection with Lipofectamine™ was optimised through comparison of a number of DNA:Lipofectamine™ ratios, using immunocytochemistry and western blotting to examine the effect of each on culture myogenicity, differentiation and expression of βAPP and the amyloid oligomers Aβ40 and Aβ42. It was determine that overexpression of βAPP and consequent upregulation of Aβ40 and Aβ42 with transfection could be successfully achieved without compromising the overall suitability of the cultures for further experimentation. βAPP overexpression was associated with the formation of cytoplasmic proteinaceous aggregates and ubiquinated inclusions. In keeping with previous work on human satellite cells, exposure to cytokines also increased β-amyloid expression. These inflammatory stimuli, however, were not associated with consistent formation of aggregates, perhaps due to the relatively smaller effect on expression levels. This might reflect a threshold between the expression levels, or their rate of increase, observed after cytokine exposure and βAPP transfection beyond which normal cellular degradative machinery is overwhelmed. Surplus proteins would then misfold and aggregate. This is consistent with the inhibitory action of β-amyloid proteins on proteasomal function (Fratta et al. 2005).

MHCI was not only upregulated by cytokines, but also by βAPP transfection, indicating that the environment of insufficient protein breakdown extends to additional proteins beyond β-amyloid. This supports the hypothesis that MHCI expression might be a central interlinking feature of IBM pathogenesis, since it can be driven by both degenerative and inflammatory stimuli. Its downstream consequences include further inflammation and likely perpetuation of ER stress, thereby establishing a self-perpetuating cycle (Dalakas 2006). Notably, however, the MHCI upregulation demonstrated by PM and DM generally does not appear sufficient to induce downstream degenerative features in isolation. It remains unclear whether this distinction represents a fundamental disparity between IBM and these conditions, or whether the relatively aged cellular milieu characteristic of IBM confers particular susceptibility.

6.3 Evaluation of Arimoclomol on pathological outcome measures of IBM

Having determined that several features of IBM could be recapitulated in this *in vitro* model, the subsequent experiments described in Chapter 4 sought to characterise the model further, with the intention of developing IBM-relevant pathological outcome measures for the testing of potential drugs. Here, it was hypothesised that Arimoclomol, a coinducer of the cytoprotective HSR, could inhibit some of the pathological processes observed in IBM. Previous work demonstrated that augmentation of the HSR, including when achieved with Arimoclomol, translated to pathological and functional improvement in preclinical models of other diseases characterised by protein misfolding and aggregation, such as ALS and spinobulbar muscular atrophy (Kieran et al. 2004; Malik et al. 2013). Theoretically, there was additional evidence to support this strategy, including HSP70's inhibition of amyloidogenic aggregation (Evans et al. 2006) and anti-inflammatory effects, reflecting inhibition of NFκB (Feinstein et al. 1997).

It was first necessary to determine whether Arimoclomol affects overall cell viability in myogenic cultures exposed to IBM-like pathology and whether its described pharmacological effect to augment the expression of key heat shock protein HSP70 occurs here. MTT assays demonstrated that overexpression of βAPP is cytotoxic to myogenic cells, which progresses up to 96 hours after transfection. Similarly, exposure cytokines IL1β and TNFα produced a dose dependent cytotoxic effect. Arimoclomol treatment was associated with significant attenuation of the cytotoxic effects of these stimuli. By western blot, Arimoclomol increased the expression HSP70 that followed either or exposure to cytokines or βAPP overexpression by between 4 and 8 fold, implying this improvement in cytotoxicity could reflect increased chaperone activity.

Next, a panel of quantifiable measures was developed based on those pathological processes particularly distinctive of IBM, such as TDP-43 mislocalisation, or with potential interlinking roles between downstream degenerative and inflammatory processes, notably ER stress and NFκB activation.

6.3.1 TDP-43

TDP-43 histopathology, observed in a number of neurodegenerative conditions, is characterised by loss of normal nuclear staining and translocation to the cytoplasm, where it forms aggregates. This phenomenon appears to be the most common histopathological feature of IBM, affecting up to a quarter of fibres (Salajegheh et al. 2009) and, notably, is absent from cases of PM. Here, myotubes cultured under control conditions also demonstrated nuclear TDP-43 staining. Marked redistribution occurred under the IBM-relevant stressors of β-amyloid overexpression and exposure to cytokines, where non-nuclear TDP-43 was detected in the majority of cells. This was followed by loss of nuclear staining. There was significant contemporaneous increase in expression of TDP-43 which, although also a feature of IBM tissue, has not typically been a sufficient stimulus for TDP-43 aggregate formation when reproduced in isolation through over-expression in previous *in vitro* studies (Ash et al. 2010). Therefore, it appears more likely that the accumulation of TDP-43 in the cytoplasm is either its pathophysiological response to cellular stress or reflective of impaired protein degradative processes. Nevertheless, elevated TDP-43 does appear to be cytotoxic and sufficient to induce disease phenotypes, such as FTD (Tsai et al. 2010). Although evidently indicative of pathology, the downstream consequences of TDP-43 mislocalisation and increased expression can only be speculated since the protein's normal function is not fully understood. Here, its characteristic immunocytochemical changes lend themselves to being a quantitative indicator of IBM pathology. Therefore, it is notable that Arimoclomol treatment significantly attenuated TDP-43 mislocalisation and expression in primary myogenic cultures following over-expression of βAPP or exposure to cytokines. This effect is consistent with Arimoclomol's described anti-aggregation actions on other proteins and might reflect increased chaperone activity of HSP70, which has previously been found to influence the nuclear processing of TDP-43 (Udan-Johns et al. 2014). Reduced expression may succeed attenuation of cytoplasmic aggregation through restoration of TDP-43 auto-homeostatic mechanism (Lee et al. 2012). Further alleviation of TDP-43 pathology may occur indirectly through Arimoclomol's effect on ER stress, which were examined next.

6.3.2 Endoplasmic Reticulum Function

The broad functions of the ER link it with several other components of IBM pathology, particularly via its role in intracellular calcium homeostasis and excitation-contraction coupling by subspecialised SR of skeletal muscle. Indeed, ER dysfunction is widely implicated in neurodegenerative diseases in addition to IBM (Roussel et al. 2013) (Vattemi et al. 2004). Although several cytoprotective functions have evolved to constitute the initial phases of the ER stress response, post-mitotic tissues remain inherently vulnerable to conditions that overwhelm these defences since they cannot dilute the insult itself through cell division. This may be exacerbated by the 'ER handicap' of aged tissue, in which ER chaperone activity appears relatively reduced (Nuss et al. 2008). Diseases of protein aggregation, such as IBM, represent a vicious pathogenic cycle in which the capacity of cellular degradative machinery has been exceeded, with the resulting additional ER stress further stimulating the accumulation of these misfolded proteins and so on. Regards the proteins of particular interest here, β-amyloid and TDP-43 are well established as inducers of ER stress (LaFerla et al. 2007; Walker et al. 2013). In addition, MHCI upregulation has been proposed to exacerbate ER stress in myositis and IBM (Dalakas 2006; Li et al. 2009). The activation of NFκB by ER stress is perhaps the most direct link to explain how a secondary inflammatory response might be sustained by a primarily degenerative stimulus.

Therefore, ER function was examined in this model. Two aspects were investigated; cytosolic and ER calcium concentration using live cell confocal imaging and expression of proteins involved in ER stress using western blots. Cytosolic calcium concentration, $[Ca^{2+}]_{Cyto}$, was found to be significantly elevated in myogenic cells of cultures transfected with βAPP or exposed to IL1β or TNFα. This finding is consistent with established features of cellular stress is likely to reflect ER Ca^{2+} leak, with additional possibilities including store-operated uptake via increased cell membrane permeability or channel opening (Altamirano et al. 2012). It is in keeping with elevated $[Ca^{2+}]_{Cyto}$ observed in the MCK-BAPP transgenic mouse, where AB42 is proposed to modulate ryanodine

receptor opening, leading to impaired muscle force (Moussa et al. 2006). In relation to wider IBM pathogenesis, the numerous deleterious consequences of perturbed intracellular $[Ca^{2+}]_{Cyto}$ include activation of NFκB and, thereby increased expression of proinflammatory factors (Altamirano et al. 2012).

ER Stress was evidenced more directly through the observation that $[Ca^{2+}]_{ER}$, determined through the change in $[Ca^{2+}]_{Cyto}$ in response to SERCA inhibition with thapsigargin, was significantly reduced following βAPP over-expression or exposure to cytokines. This finding was supported by the observation of increased expression of ER stress markers BiP (following βAPP over-expression or IL1β exposure) and CHOP (following βAPP over-expression, or exposure to IL1β or TNFα). The demonstration of ER stress under these conditions is consistent with previous studies of βAPP and Aβ42, predominantly with respect to neurons in the context of Alzheimer's disease (Ghribi et al. 2001; Resende et al. 2008; Lee do et al. 2010). The mechanism through which cytokines perpetuate ER stress may differ, reflecting combined upregulation of βamyloid proteins and MHCI.

Arimoclomol treatment significantly attenuated disturbances of cytosolic and ER calcium, implying it has a protective function against the development or perpetuation of ER stress. This was corroborated by the reduction of CHOP expression following Arimoclomol treatment of cultures over-expressing βAPP or exposed to IL1β. The relative lack of effect of Arimoclomol on BiP and ATF expression in all culture conditions implies an action further downstream in the UPR pathway. The mechanism of this cytoprotective effect may reflect an increased chaperone effect associated with augmented HSP70 expression, consistent with previous studies that observed stabilisation of SERCA and calcium homeostasis, and increased cytoplasmic refolding of misfolded proteins (Nanasi et al. 2001; Liu et al. 2008).

6.3.3 NFκB activation

Next to ER stress, the pro-inflammatory transcription factor NFκB represents the most logical central pathogenic mechanism to link inflammation and degeneration in sporadic IBM, just as it appears fundamental to IBMPFD

(Nogalska et al. 2007; Custer et al. 2010). This mechanism would mirror that established in the secondary inflammation of Duchenne muscular dystrophy (Messina et al. 2011). An additional role in muscle atrophy further signifies its potential importance (Jackman et al. 2004).

In keeping with an established direct effect, cytokines activated NFκB, determined by translocation of the p65 subunit to the cell nucleus by immunocytochemistry. Interestingly, βAPP overexpression also significantly increased NFκB activation. This mechanism could reflect the influence of ER stress and upregulated MHCI, evidenced under the same conditions here, and demonstrated by previous studies (Nagaraju et al. 2005). The contribution of upregulated MHCI is likely to be small since Arimoclomol inhibited NFκB activation whilst not affecting MHCI expression.

Indeed, Arimoclomol inhibited NFκB activation whether stimulated by cytokines or βAPP over-expression. The mechanism of this effect is likely to be multifactorial, incorporating the consequences of attenuated ER stress, however since a direct stimulatory effect of cytokines on NFκB is also apparently inhibited, Arimoclomol or HSP70 may also have a direct inhibitory action on NFκB. This would be consistent with previous work on astroglial cultures, where HSP70 inhibits inflammatory signalling (Feinstein et al. 1996).

Next, it was determined whether Arimoclomol's cytoprotective effects were mediated through alteration of βAPP or MHCI expression. Specifically, it was possible that Arimoclomol could reduce the βAPP expression associated with transfection. In turn, this would have been expected to attenuate its pathogenic effects. In fact, no such effect was observed and Arimoclomol did not effect βAPP expression after either transfection or exposure to cytokines. This implies its effects lie downstream. This is important since the importance of βAPP specifically in the pathogenesis of IBM is contested and other degenerative proteins might have equal or greater importance (Greenberg 2009). Furthermore, it was not the central hypothesis of this work that βAPP is the primary upstream trigger of IBM. Rather, it was employed as a stimulus of other pathogenic elements. Arimoclomol did not affect MHCI expression either. Extrapolating the significance of this result to the *in vivo* pathogenesis requires

caution since, there, MHCI is influenced by a systemic immune system and, whereas cultured myotubes do demonstrate some constitutive expression of MHCI under control conditions, this does not appear to be the case in skeletal muscle *in vivo*. Nevertheless, the lack of effect of Arimoclomol on MHCI expression here implies its effects instead lie further downstream, consistent with the lack of influence on βAPP. This could be inferred as a positive finding since the features of TDP-43 translocation, ER stress and NFκB activation are present on muscle biopsy by the time of clinical presentation in IBM (Salajegheh et al. 2009). Therefore, it is unrealistic to prevent their onset. Rather, a reasonable therapeutic approach would be to inhibit them or limit their perpetuation. A pharmacological action that targets these processes more directly could be preferable to one that is dependent on a specific, as yet unidentified, upstream trigger.

6.4 Translating the effects of Arimoclomol to clinical treatment

To lay the required foundation to advance Arimoclomol along the translational research pathway of drug development, a small Phase IIa study was established in patients with IBM. The primary endpoint was safety and tolerability, determined by adverse events (AEs) and adherence to the medication. No significant difference in AEs between the Arimoclomol and placebo group was detected. No serious AEs deemed likely to be related to trial medication occurred in the Arimoclomol group. The trial subjects adhered tightly to the prescribed regimen, with a minimum of 96.5%, indicating excellent tolerability over the four-month treatment period. This is, in part, likely to reflect the lack of any significant detrimental impact on disease course suggested by the secondary outcome measures. These results were consistent with the findings of previous early phase human safety studies of Arimoclomol and the largest study of the drug to date, involving 84 patients (Cudkowicz et al. 2008). This length of evaluation is longer than the equivalent Phase II study of many other subsequently licensed medications. Therefore, the safety and tolerability data for Arimoclomol in IBM appear suitable to support its further evaluation in larger trials.

Additional challenges of such further studies were anticipated and this trial, therefore, took the opportunity to evaluate a number of secondary outcome measures to help inform a future trial's framework.

The measurement of muscle strength is an obvious candidate as an outcome measure in a study of myopathic disease. However, this trial evidenced the challenges presented by this. Even with consistency of evaluating personnel, the quantitative technique of maximal voluntary isometric contraction testing (MVICT) demonstrated high variability between subjects and did not change proportionately with time, meaning that the detection of a realistic treatment effect in a trial of realistic size and duration would be unlikely using this measure. However, improved correlation with time was observed in subgroup analysis of individual movements, notably handgrip, which is of particular relevance to IBM. Therefore, restricted MVICT testing might be reasonable. Manual muscle testing (MMT) sum score declined in close correlation with time in both treatment groups, meaning this technique could more effectively detect deviation from disease natural history through a treatment effect. However, as an ordinal scale, it is difficult to infer clinically meaningful effects from changes in MMT scores, even if numerically significant. Therefore, it is likely that patient reported outcome measures, such as functional rating scales, might form an important component of efficacy trials. Accordingly, it is reassuring that the validated IBM functional rating scale (IBMFRS) demonstrated a steady, closely correlated decline over the time course of this trial.

Finally, evidence for Arimoclomol's pharmacological actions to augment the expression of HSP70, inhibit inflammation and inhibit protein aggregation was sought using serial muscle biopsies. This approach was undermined by inherent limitations of the necessity to biopsy different anatomical sites in individual patients, combined with the apparent high variation in HSP70 concentration, of over 18 fold, between patients. The same limitation applied to comparison of a panel of histopathological markers. In the context of a safety and tolerability study, it is, however, useful to observe a lack of large potentially harmful effect on the affected tissue, such as exacerbation of inflammation. For future trials,

the evolution of MRI in neuromuscular diseases might provide a more practical outcome measure than direct muscle biopsy.

6.5 Limitations and Conclusion

Any preclinical cellular or animal model of sporadic disease is limited by the inherent complexity of aetiology that typically relies on multiple genetic and environmental factors. Recapitulating IBM is particularly difficult due to the opacity surrounding its fundamental cause, even to the extent that it remains unclear whether it is primarily an inflammatory or degenerative disease. Nevertheless, this does not preclude translational research on IBM. Indeed, even the identification of a disease trigger may not automatically yield a panacea. Instead, the logical approach is to identify, reproduce and seek to manipulate consistent and central pathogenic features. This is the underlying theme of this thesis and, therefore, it is important not to extrapolate the significance of certain results retrospectively as though they sought to characterise the mechanism of pathogenesis *in vivo*. For example, βAPP and inflammatory cytokines were *de facto* primary stimuli of IBM-like features in these experiments but they may not assume the same upstream position in the context of the human disease. Instead, the most promising conclusion of these experiments is that recapitulation and manipulation of established components of IBM pathology can be achieved *in vitro*.

This thesis demonstrates an alternative strategy in the development of treatment for IBM to that which has typically been used in the field. Rather than conduct sequential small clinical efficacy trials of drugs licensed for other conditions, this approach is based on a preclinical model that could be used to examine multiple new therapeutic strategies. Here, one such approach was investigated, using augmentation of the heat shock response with Arimoclomol. This was associated with significant effects on several aspects of IBM pathology and improved cell viability in a preclinical disease model, none of which were demonstrated by drugs previously studied on patients with the disease. To advance this *in vitro* work on Arimoclomol towards a study of clinical efficacy involves several more steps. The first of these, to demonstrate satisfactory

safety and tolerability in patients with IBM, was successfully achieved. Therefore, careful consideration of a larger efficacy trial of Arimoclomol in IBM is justified. Evaluation of other new therapeutic strategies on preclinical models should occur simultaneously and thereby maintain the translational research process that will accelerate the discovery of an effective treatment for this disabling disease.

Chapter 7: Appendix

7.1 Supplementary methods in clinical trial of Arimoclomol

To standardise clinical assessment as far as possible, thereby to reduce inter-observer variability, assessments were performed according to the following guidance provided to investigators.

7.1.1 Clinical examination of power

- Explain or demonstrate the movement that is required of the patient.

- Ask the patient to perform the movement through the full range against gravity.

- If the patient does not perform or is unable to perform the complete movement, check for these limiting factors:

    i) Understanding of the required task

    ii) Availability of the appropriate range of motion (limitations may be due to soft tissue tightness)

    iii) Weakness

- Based on the limiting factor(s):

    - Instruct and demonstrate again.

    - Decide if joint restriction is affecting the performance.

    - Repeat the test using the alternative gravity eliminated position.

If the patient experiences pain during the testing, the clinical evaluator must determine whether the patient feels that he/she is able to give his best effort in spite of his discomfort. If yes, continue the testing but note under comments that the patient complained of pain. If the patient feels that discomfort prohibits him from giving a maximal effort, do not test that muscle.

If the clinical evaluator is undecided between two muscle grades, he/she should always grade down. For example, if the left elbow flexors are to be graded as possibly a 4+ or a 4, the evaluator should record a 4.

The precise order of testing, in terms of whether the evaluator should test R/L, R/L or complete one side in each position is left to the discretion of the CE. However, it is important that the evaluator always be on the same side as the muscle being tested (for example, if testing right knee flexion prone, the evaluator should be on the right side of the patient. To test left knee flexion, the evaluator would move to the opposite side of the exam table, and thus be on the patient's left side).

Because this is a research protocol, family members or support people are not allowed in the room during testing. If the clinical evaluator needs the assistance of a second person, his first choice should always be a staff person. If it is absolutely necessary to "borrow" a family member, that person should only remain in the testing area during the actual transfer and/or positioning. It should be explained to anxious patients or family that it is imperative to maintain consistent and exact testing conditions and that for this reason, no visitors are allowed.

A firm testing surface is necessary to provide proper stability. An examination table is adequate, but a Hi-Lo table is preferred to provide ease of transfer and adequate height for the evaluator during different tests.

MRC Grade	**Degree of Strength**
5	Normal strength
5-	Uncertain muscle weakness
4+	Ability to resist against all but maximal pressure throughout range of motion
4	Ability to resist against moderate pressure throughout range of motion

4-	Ability to resist against minimal pressure throughout range of motion
3+	Ability to move through full range of motion against gravity and to resist against minimal pressure through partial range of motion, then the contraction breaks abruptly
3	Ability to move through full range of motion against gravity. If a patient has a contracture that limits joint movement, the mechanical range will be to the point at which the contracture causes joint restriction.
3-	Ability to move through partial range of motion against gravity.
2	Ability to move through full or partial range of motion with gravity eliminated
1	A flicker of movement is seen or felt in the muscle
0	No contraction

7.1.1.1 Manual muscle testing

Muscles are listed in the order and position of muscle testing. Certain muscles will be graded in one position only. For other muscles, the first testing position will indicate a grading ranged of 5 to 3-; if the muscle cannot be grade in this range, then it will be tested again in an alternate position.

A. POSITION I: SITTING

The patient is sitting comfortably on the edge of the examination table with the legs dangling. The edges of the examination table should support the patient's thigh to a level proximal to the knee joint. The patient's shoes are off.

The following are performed in this position:

Shoulder Abduction

The patient's arm is by his/her side. He is asked to abduct the shoulder to 90 degrees with the elbow flexed and the forearm pronated. Stabilization is provided at the opposite shoulder to prevent the patient from leaning away from the abducted arm. The examiner places his/her hand just proximal to the patient's elbow and pushes it downward. Enter grade 5 to 3-. If the patient is unable to raise the arm out from his side, no grade is entered. Retest the muscle when the patient is in the supine position.

Elbow Flexion

The patient starts in slight shoulder flexion with the forearm supinated and the elbow extended. He is asked to bring the hand to the level of his shoulder, flexing proximal to the patient's wrist and pressure is exerted to straighten the elbow. Resistance is given with the elbow flexed to 90 degrees. The examiner's other hand stabilizes under the elbow at the distal humerus or against the anterior surface of the proximal humerus. If the patient is unable to bend the elbow against gravity, the examiner raises the patient's upper arm so the motion becomes a horizontal movement of the forearm (i.e., with gravity eliminated). The patient's upper arm is supported passively during this maneuver.

Wrist Extension

The patient's forearm is pronated with the elbow at about 30 degrees from extension and the patient is asked to bring the wrist backwards. The examiner supports and stabilizes the forearm proximal to the wrist and presses the dorsum of the patient's hand with the wrist in an extended position. The fingers may be fully flexed or relaxed. If the patient is not able to extend the wrist against gravity, the examiner raises the patient's upper arm so the motion becomes a horizontal movement of the forearm (i.e., with gravity eliminated). The patient's upper arm is supported passively during this maneuver.

Wrist Flexion

The patient's forearm is supinated with the elbow at about 30 degrees from extension and the patient is asked to bend the hand upward, flexing the wrist. The fingers may be fully flexed or relaxed. The examiner supports and stabilizes the forearm proximal to the wrist and exerts pressure on the patient's palm to straighten out the wrist. If the patient cannot flex the wrist against gravity, the forearm is turned into a position midway between pronation and supination, and the patient attempts to flex the wrist in a horizontal plane.

Hip flexion

The patient should be asked to sit up straight. The hands must grasp the edge of the examining table. During this test, the patient should be discouraged from leaning backwards or sideways, or from flexing his knee to support the limb by pressing the belly of the gastrocnemius muscle on the edge of the examining table. In addition, the thigh should remain in neutral position. Pressure is exerted on the anterior distal surface of the thigh in the direction of hip extension. Enter grade 5 to 3-.

NOTE: For this test, resistance can be graded if the hip can be actively flexed to at least 30 degrees from the plane of the table. Full active range is not required. To achieve a grade of 3-, the patient should be able to flex the hip enough that the examiner can slide his hand cleanly under the distal thigh. If the patient can lift the thigh, but cannot maintain neutral rotation, grade as 3-. If the patient cannot lift the leg, do not grade. Test again in the alternate testing positions (i.e., side-lying gravity eliminated).

Knee Extension

The examiner may put his hand or a rolled towel under the distal end of the thigh to cushion that part against pressure. The patient is then asked to extend the knee. Once full active range of motion has been observed, the patient is asked to bend his knee to about 20 degrees from 0. The examiner places his other hand on the lower leg above the ankle, and exerts downward pressure.

Enter grade 5 to 3-. If the patient cannot straighten his leg against gravity, do not grade in this position. Retest in the side-lying position with gravity eliminated.

NOTE: For this test, resistance can be graded if the knee can be actively extended to within 10 degrees from 0.

Ankle Dorsiflexion

The examiner supports the leg just above the ankle joint. The patient is asked to bring the foot upwards. The examiner's hand is placed on the dorsum of the foot, and downward pressure is exerted. Enter grade 5 to 3-. If the patient is unable to dorsiflex the foot, do not grade in this position. Retest in the side-lying position with gravity eliminated.

NOTE: For this test, attempt to achieve dorsiflexion without inversion. If the patient can only dorsiflex with some inversion, it will be evaluator's decision whether to allow the motion.

B. POSITION 2: PRONE

The examiner should remove any pillows on the exam table prior to testing.

Neck Extension

The patient is asked to bring the head upward with his arms at his side while the examiner holds the shoulders stable. He should be able to do this so that his face is looking straight ahead for testing. One of the examiner's hands is then placed over the occiput and pressure is exerted in the direction of the neck flexion. As a safety measure, the examiner keeps his other hand just off the patient's chin. Enter grade 5 to 3-. If the patient cannot lift his eyes to the horizontal, the examiner must evaluate the passive range of motion available. If the patient cannot lift his head against gravity, retest in the side-lying position.

Hip Extension

The patient is asked to hyperextend the hip with the knee flexed to 90 degrees or more. The examiner stabilizes at the pelvis, and gives pressure against the distal thigh in the direction of hip flexion. Enter grade 5 to 3. If the patient is unable to lift the hip against gravity, or barely lifts it, retest with the patient leaning over the table so that his entire trunk is supported and his free leg is just touching the floor. The patient can stabilize by holding onto the table. Ask him to shift his weight onto one leg. The examiner then supports the opposite leg in 90 degrees of knee flexion, and asks the patient to lift that leg away from the table. Grade as 3- if the patient lifts the leg but not to the horizontal plane. If the patient cannot lift the thigh from the resting vertical position (with the examiner supporting the knee in flexion), do not grade. Retest in the side-lying position with gravity eliminated.

NOTE: To avoid having the patient change position more than necessary, assessing for a grade 3- can be done as the first or last muscle tested, as the patient gets on or off from the exam table.

Knee Flexion

The patient is asked to bend the knee 90 degrees. Once it has been shown that the patient has full range of motion, have him extend the knee to about 120 degrees so that the hamstring group is not too shortened. One of the examiner's hands stabilizes just proximal to the Achilles tendon, and pressure is exerted to straighten the knee. Enter grade 5 to 3-. If the patient cannot flex the knee, do not grade. Instead, re-test in the side-lying position with gravity eliminated.

Ankle Plantar Flexion

With the patient' knee flexed to 90 degrees, the patient is asked to plantar flex the ankle. The examiner grasps the calcaneus with one hand and pulls it upwards, towards the ceiling. At the same time, the other hand is placed over the ball of the foot and resistance is exerted in a downward fashion. Enter grade

5 to 3-. If the patient cannot plantar flex the ankle, do not grade. Re-test in the side-lying position with gravity eliminated.

C. POSITION 3: SIDE-LYING

Hip Abduction (emphasis on gluteus medius)

The patient is lying comfortably on his side. His bottom leg is slightly flexed to help stabilize the pelvis. In addition, he is holding onto the table edge, and the examiner (standing behind the patient) steadies the pelvis with one hand to prevent it rolling backward. With the top knee extended and with the hip *in slight extension and external rotation* the patient attempts to lift his leg towards the ceiling. Pressure is exerted downwards just proximal to the ankle in an angle of adduction and slight flexion. Enter grade 5 to 3-. If the patient cannot move the leg against gravity, do not grade. Re-test with gravity eliminated in the supine position. Again, be sure to passively evaluate what range of motion is available.

ALTERNATE TESTING POSITIONS:

Neck Extension (Alternate Testing)

With the examiner supporting the weight of the patient's head if necessary, the patient's neck is flexed and he is asked to extend it back. Enter grade 2-0.

NOTE: To avoid excessive positions changes, the clinical examiner may wish to test neck flexors in this position at this time. Also, if the evaluator has any uncertainty about a grade of 2, the use of a powder board is recommended.

Hip Flexion (Alternate Testing)

The leg, which is uppermost in this position, is supported by the examiner's hands under the patient's thigh and lower leg. The patient is then asked to flex the hip. Enter grade 2-0.

Hip Extension (Alternate Testing)

The leg that is uppermost in this position (side-lying) is supported by the examiner's hands/forearms under the patient's thigh and lower leg. The hip is positioned in flexion, and the patient is asked to extend the hip. Enter grade 2-0.

Knee Flexion (Alternate Testing)

The patient's uppermost limb is supported by the examiner's hands under the thigh and lower leg. The patient is then asked to bend the knee. Enter grade 2-0.

Knee Extension (Alternate Testing)

The patient's uppermost limb is supported by the examiner's hands under the thigh and lower leg. The patient is then asked to straighten the knee. Enter grade 2-0.

Ankle Dorsiflexion (Alternate Testing)

With the lower limb and foot supported by the examiner's hands, the patient is asked to move the foot cranially. Enter grade 2-0.

Ankle Plantar Flexion (Alternate Testing)

With the lower limb and foot supported by the examiner's hands, the patient is asked to move the foot caudally. Enter grade 2-0.

D. POSITION 4: SUPINE

The examiner should remove any pillows on the exam table prior to testing.

Neck Flexion

The patient is asked to flex the neck until the chin touches the chest, or whatever is full range for that patient. Pressure is exerted by the examiner with

the hand on the patient's forehead. For safety, the examiner's other hand should be held just under the patient's head. Enter grade 5 to 3-. If the patient cannot flex the cervical spine so that the chin moves toward the sternum, do not grade. Re-test in the alternate position with gravity eliminated (NOTE: Raising the head from the table even against pressure, without cervical flexion, **is** not graded as neck flexion).

Elbow Extension

The examiner supports the patient's upper arm in 90 degrees of shoulder flexion so that the elbow is pointing towards the ceiling. The forearm is in the neutral position and lies across the patient's chest. The patient is then asked to extend the elbow. Resistance is applied by the examiner's hand just proximal to the patient's wrist. The elbow must be flexed about 20 degrees from full extension when testing active strength. Enter grade 5 to 3-. If the patient is unable to move the forearm against gravity, do not grade. Re-test in the alternate position with gravity eliminated.

Shoulder Abduction (Alternate Testing)

The patient's elbow is flexed to 90 degrees and the examiner holds the patient's hand. In the way, the examiner can raise the elbow and upper arm just off the table (thus taking the weight off the patient's arm). The patient is asked to move the upper arm into abduction. Enter grade 2-0.

Hip Abduction (Alternate Testing)

The patient is asked to abduct his leg. The weight of the limb is taken by the examiner, usually under the knee and ankle.

NOTE: Do not allow extreme external rotation, hip flexion, or knee flexion. Enter grade 2-0.

E. POSITION 5: REPEAT SIDE-LYING

Neck Flexion (Alternate Testing):

With the examiner supporting the weight of the patient's head if necessary, the patient is asked to flex his neck forward. Enter grade 2-0.

F. POSITION 6: REPEAT SITTING

Elbow Extension (Alternate Testing)

The patient's shoulder is flexed to 90 degrees and the elbow is flexed towards his body in the horizontal plane. The forearm is in the neutral position. As the examiner supports the upper arm, the patient is asked to straighten his elbow. Enter grade 2-0.

7.1.1.2 Myometry protocols

The following protocols for quantitative myometry were followed:

Elbow Extension:

Subject is supine with arm resting on table, parallel with trunk (prop towel under elbow for maximum positioning) elbow at 90-degree angle. The trap is placed at distal end of forearm, two finger widths from the wrist, which is in neutral position with palm inward. The tester stabilises the arm by placing their hand over the biceps region so that the arm is unable to rise from the table and stabilises to avoid rotation of arm. The subject attempts maximal elbow extension in neutral forearm position.

Elbow Flexion:

This employs the same position as elbow extension. The tester secures the elbow joint to prevent change of arm position and prevents shoulder protraction by placing hand on anterior aspect of shoulder. The subject attempts maximal elbow flexion in neutral forearm position.

Ankle Dorsiflexion:

The subject is supine with the feet hanging off of the bed, not touching the bed. A small towel may need to be placed under the ankle to lift the heel off of the bed. The strap is placed on the top of the foot and enough tension must be applied so that when the subject dorsiflexes their foot, their ankle must be at 90-degrees of dorsiflexion with the strap taut.

Knee Flexion:

The subject sits at the end of the bed with a towel roll under the thigh at the knee. The strap is placed just above the ankle (no more than 1 finger width above the ankle). Enough tension must be applied, such that when the subject flexes the knee, they reach a 90-degree angle at the knee.

Knee Extension:

The same position as knee flexion is use, with the strap placed just above the ankle (no more than 1 finger width above the ankle). Enough tension must be applied, so that when the subject extends the knee, they must reach a 90-degree angle at the knee.

Grip Strength:

The subject sits with knees and hips at 90 degrees and feet flat on the floor. There is 0 degree of shoulder abduction, the arm is by the side and the elbow is flexed at 90 degrees. Subject holds the dynamometer in hand. Support dynamometer with a flat hand. The subject attempts maximal grip squeeze.

7.1.2 Instructions to investigators on interpretation of IBMFRS

All investigators were provided the following instructions on how to administer the IBM functional rating scale.

Testing Procedures and Methods

1) Advise the patient that he/she is to compare his/her current function with how he/she functioned prior to enquiring about any symptoms of IBM.

2) State to the patient, "I'm going to ask you some questions about how you're currently functioning at home". The intention of this scale is to have the patient rate their own function. During the consultation, the caregiver should not offer any comments.

3) Ask, "How are you doing with … ?" for each question in the IBMFRS. Even if you agree with the patient's answer, be sure to clarify the patient's choice by probing further. Ensure sure that the level below or above the number selected is not the more appropriate answer. If the patient is unable to volunteer a satisfactory response, or the response is clearly in conflict with observed function, the evaluator should prompt, using one of the available choices

4) Record the patient's response, to the closest available approximation from the 5-point list, on the case report form provided.

5) The order of questioning should be followed as written

6) It is important that the responses given by the patient reflect their actual abilities at the time of the visit not what the patient or caregiver thinks s/he "could" do. For example, if the caregiver normally dresses the patient, but the patient states that he could do it, given enough time, then the patient should be rated by his actual function which is "needs attendant for self care".

1. Swallowing

4 Normal eating habits

(No difficulty swallowing, can eat any foods of choice)

3 Early eating problems – occasional choking

(Ask whether patient avoids any foods because they get "caught" in his/her throat. If yes, then rate 3. This score indicates that the patient can still eat all foods of choice, but with occasional choking)

2 Dietary consistency changes

1 Frequent choking

0 Needs tube feeding

2. Handwriting (with dominant hand prior to IBM onset)

(This item inquires about handwriting without any assistive devices, such as foam tubing &/or mechanical aids due to finger weakness)

4 Normal

3 Slow or sloppy: all words are legible

2 Not all words are legible

1 Able to grip pen but unable to write

0 Unable to grip pen

3. Cutting food and handling utensils

4 Normal

(No difficulty cutting or handling utensils by methods used prior to disease onset)

3 Somewhat slow and clumsy, but no help needed

(Some difficulty cutting or handling utensils by methods used prior to disease onset, but patient continues to do so independently)

2 Can cut most foods (> 50%), although slow and clumsy; some help needed

(Some difficulty cutting or handling utensils by methods used prior to disease onset; patient requires assistance, but still tries to cut some foods, and still does >50% of the task successfully.)

1 Food must be cut by someone, but can still feed slowly

(Patient cannot cut foods by methods used prior to disease onset, but still tries to feed him/herself and succeeds at least occasionally)

0 Needs to be fed

4. Fine Motor Tasks (opening doors, using keys. Picking up small objects)

4. Independent

3. Slow or clumsy in completing task

(Does not use any assistive device to perform)

2. Independent but requires modified techniques or assistive devices

1. Frequently requires assistance from caregiver

0. Unable to perform

5. Dressing

4. Normal

3. Independent but with increased effort or decreased efficiency

2. Independent but requires assistive devices or modified techniques

(Velcro, shirts, without buttons, etc)

1. Requires assistance from caregiver for some clothing items

0. Total dependence

6. Hygiene

(If the patient chooses not to bathe self for whatever reason, he/she is rated as not able)

4 Normal function

Patient has no difficulty, and is still completely independent in dressing and hygiene by methods used prior to disease onset

3 Independent but with increased effort or decreased activity

Patient still completely independent in dressing but requires more effort to dress. No substitute methods are used to dress.

2 Independent but requires use of assistive devices

Patient requires occasional assistance or the use of assistive devices or substitute methods (e.g., pull-on clothes, velcro closures or shoes, pre-buttoned shirt, lying down to don pants) in dressing and hygiene. Methods used are now different than those used prior to disease onset.

1 Requires occasional assistance from caregiver

(Means patient needs daily caregiver assistance with dressing but patient has some level of function)

0 Completely dependent

7. Turning in bed and adjusting covers

(If the patient chooses not to turn in bed or adjust bedclothes for whatever reason, he/she is rated as not able. This item refers to the ability to do both activities (turning and adjusting bedclothes) to be marked 4 or 3. Performing one activity is 2)

4 Normal

3 Somewhat slow and clumsy, but no help needed

2 Can turn alone, or adjust sheets, but with great difficulty

(Patient can turn alone or adjust sheets, but completes task with great difficulty, no help needed.)

1 Can initiate, but not turn or adjust sheets alone

0 Unable or requires total assistance

8. Sit to stand

4. Independent (without use of the arms)

3. Performs with substitute motions (leaning forward, rocking) but without use of arms

2. Requires of use of arms

1. Requires assistance from a device or person

0. Unable to stand

9. Walking

4 Normal

3 Slow or mild unsteadiness

(Patient notes some difficulty, but walks without assistance)

2 Intermittent use of an assistive device (includes AFO, cane, walker, or a caregiver)

1 Dependent on assistive device (includes AFO's, cane, walker, or a caregiver)

0 Wheelchair dependent (includes scooters)

10. Climbing stairs (If the patient chooses not to climb stairs for whatever reason, he/she is rated as not able)

4 Normal

3 Slow with hesitation or increased effort; uses hand rail intermittently

2 Dependent on hand rail

1 Dependent on hand rail and additional support (cane or person)

0 Cannot climb stairs

References

1. Abuzakouk, M., C. Feighery, et al. (1996). "Collagenase and Dispase enzymes disrupt lymphocyte surface molecules." Journal of immunological methods **194**(2): 211-216.

2. Alfaro, L. A., S. A. Dick, et al. (2011). "CD34 promotes satellite cell motility and entry into proliferation to facilitate efficient skeletal muscle regeneration." Stem cells **29**(12): 2030-2041.

3. Altamirano, F., J. R. Lopez, et al. (2012). "Increased resting intracellular calcium modulates NF-kappaB-dependent inducible nitric-oxide synthase gene expression in dystrophic mdx skeletal myotubes." The Journal of biological chemistry **287**(25): 20876-20887.

4. Asakura, A., M. Komaki, et al. (2001). "Muscle satellite cells are multipotential stem cells that exhibit myogenic, osteogenic, and adipogenic differentiation." Differentiation; research in biological diversity **68**(4-5): 245-253.

5. Asakura, A., P. Seale, et al. (2002). "Myogenic specification of side population cells in skeletal muscle." The Journal of cell biology **159**(1): 123-134.

6. Ash, P. E., Y. J. Zhang, et al. (2010). "Neurotoxic effects of TDP-43 overexpression in C. elegans." Human molecular genetics **19**(16): 3206-3218.

7. Askanas, A. S., G; Engel, WK (1998). Inclusion Body Myositis and Myopathies, Cambridge University Press.

8. Askanas, V. and W. K. Engel (1975). "A new program for investigating adult human skeletal muscle grown aneurally in tissue culture." Neurology **25**(1): 58-67.

9. Askanas, V. and W. K. Engel (2003). "Proposed pathogenetic cascade of inclusion-body myositis: importance of amyloid-beta, misfolded proteins, predisposing genes, and aging." Current opinion in rheumatology **15**(6): 737-744.

10. Askanas, V. and W. K. Engel (2006). "Inclusion-body myositis: a myodegenerative conformational disorder associated with Abeta, protein misfolding, and proteasome inhibition." Neurology **66**(2 Suppl 1): S39-48.

11. Askanas, V., W. K. Engel, et al. (2012). "Pathogenic considerations in sporadic inclusion-body myositis, a degenerative muscle disease associated with aging and abnormalities of myoproteostasis." Journal of neuropathology and experimental neurology **71**(8): 680-693.

12. Askanas, V., J. McFerrin, et al. (1997). "Beta APP gene transfer into cultured human muscle induces inclusion-body myositis aspects." Neuroreport **8**(9-10): 2155-2158.

13. Askanas, V., J. McFerrin, et al. (1996). "Transfer of beta-amyloid precursor protein gene using adenovirus vector causes mitochondrial abnormalities in cultured normal human muscle." Proceedings of the National Academy of Sciences of the United States of America **93**(3): 1314-1319.

14. Atkin, J. D., R. L. Scott, et al. (2005). "Properties of slow- and fast-twitch muscle fibres in a mouse model of amyotrophic lateral sclerosis." Neuromuscular disorders : NMD **15**(5): 377-388.

15. Ayala, Y. M., P. Zago, et al. (2008). "Structural determinants of the cellular localization and shuttling of TDP-43." Journal of cell science **121**(Pt 22): 3778-3785.

16. Badrising, U. A., M. Maat-Schieman, et al. (2000). "Epidemiology of inclusion body myositis in the Netherlands: a nationwide study." Neurology **55**(9): 1385-1387.

17. Badrising, U. A., M. L. Maat-Schieman, et al. (2002). "Comparison of weakness progression in inclusion body myositis during treatment with methotrexate or placebo." Annals of neurology **51**(3): 369-372.

18. Badrising, U. A., M. L. Maat-Schieman, et al. (2005). "Inclusion body myositis. Clinical features and clinical course of the disease in 64 patients." Journal of neurology **252**(12): 1448-1454.

19. Badrising, U. A., G. M. Schreuder, et al. (2004). "Associations with autoimmune disorders and HLA class I and II antigens in inclusion body myositis." Neurology **63**(12): 2396-2398.

20. Banwell, B. L. and A. G. Engel (2000). "AlphaB-crystallin immunolocalization yields new insights into inclusion body myositis." Neurology **54**(5): 1033-1041.

21. Bao, S., N. J. C. King, et al. (1990). "Elevated Mhc Class-I and Class-Ii Antigens in Cultured Human Embryonic Myoblasts Following Stimulation with Gamma-Interferon." Immunology and Cell Biology **68**: 235-242.

22. Barnes, P. J. and M. Karin (1997). "Nuclear factor-kappaB: a pivotal transcription factor in chronic inflammatory diseases." The New England journal of medicine **336**(15): 1066-1071.

23. Barohn, R. J., A. A. Amato, et al. (1995). "Inclusion body myositis: explanation for poor response to immunosuppressive therapy." Neurology **45**(7): 1302-1304.

24. Barohn, R. J., L. Herbelin, et al. (2006). "Pilot trial of etanercept in the treatment of inclusion-body myositis." Neurology **66**(2 Suppl 1): S123-124.

25. Ben-Yair, R. and C. Kalcheim (2005). "Lineage analysis of the avian dermomyotome sheet reveals the existence of single cells with both dermal and muscle progenitor fates." Development **132**(4): 689-701.

26. Bence, N. F., R. M. Sampat, et al. (2001). "Impairment of the ubiquitin-proteasome system by protein aggregation." Science **292**(5521): 1552-1555.

27. Bischoff, R. (1997). "Chemotaxis of skeletal muscle satellite cells." Developmental dynamics : an official publication of the American Association of Anatomists **208**(4): 505-515.

28. Bohan, A. and J. B. Peter (1975). "Polymyositis and dermatomyositis (first of two parts)." The New England journal of medicine **292**(7): 344-347.

29. Brack, A. S., M. J. Conboy, et al. (2007). "Increased Wnt signaling during aging alters muscle stem cell fate and increases fibrosis." Science **317**(5839): 807-810.

30. Brady, O. A., P. Meng, et al. (2011). "Regulation of TDP-43 aggregation by phosphorylation and p62/SQSTM1." Journal of neurochemistry **116**(2): 248-259.

31. Brewer, G. J. (1997). "Effects of acidosis on the distribution of processing of the beta-amyloid precursor protein in cultured hippocampal neurons." Molecular and chemical neuropathology / sponsored by the International Society for Neurochemistry and the World Federation of Neurology and research groups on neurochemistry and cerebrospinal fluid **31**(2): 171-186.

32. Brown, E. G., L. Wood, et al. (1999). "The medical dictionary for regulatory activities (MedDRA)." Drug safety : an international journal of medical toxicology and drug experience **20**(2): 109-117.

33. Brustovetsky, N., T. Brustovetsky, et al. (2002). "Calcium-induced cytochrome c release from CNS mitochondria is associated with the permeability transition and rupture of the outer membrane." Journal of neurochemistry **80**(2): 207-218.

34. Bryson, J. B., C. Hobbs, et al. (2012). "Amyloid precursor protein (APP) contributes to pathology in the SOD1(G93A) mouse model of amyotrophic lateral sclerosis." Human molecular genetics **21**(17): 3871-3882.

35. Buratti, E., A. Brindisi, et al. (2005). "TDP-43 binds heterogeneous nuclear ribonucleoprotein A/B through its C-terminal tail: an important region for the inhibition of cystic fibrosis transmembrane conductance regulator exon 9 splicing." The Journal of biological chemistry **280**(45): 37572-37584.

36. Burdakov, D., O. H. Petersen, et al. (2005). "Intraluminal calcium as a primary regulator of endoplasmic reticulum function." Cell calcium **38**(3-4): 303-310.

37. Camello, C., R. Lomax, et al. (2002). "Calcium leak from intracellular stores--the enigma of calcium signalling." Cell calcium **32**(5-6): 355-361.

38. Cantwell, C., M. Ryan, et al. (2005). "A comparison of inflammatory myopathies at whole-body turbo STIR MRI." Clinical radiology **60**(2): 261-267.

39. Cardozo, A. K., F. Ortis, et al. (2005). "Cytokines downregulate the sarcoendoplasmic reticulum pump Ca2+ ATPase 2b and deplete endoplasmic reticulum Ca2+, leading to induction of endoplasmic reticulum stress in pancreatic beta-cells." Diabetes **54**(2): 452-461.

40. Chahin, N. and A. G. Engel (2008). "Correlation of muscle biopsy, clinical course, and outcome in PM and sporadic IBM." Neurology **70**(6): 418-424.

41. Chen, Y. R. and C. G. Glabe (2006). "Distinct early folding and aggregation properties of Alzheimer amyloid-beta peptides Abeta40 and Abeta42: stable trimer or tetramer formation by Abeta42." The Journal of biological chemistry **281**(34): 24414-24422.

42. Cheng, H. C., C. M. Ulane, et al. (2010). "Clinical progression in Parkinson disease and the neurobiology of axons." Annals of neurology **67**(6): 715-725.

43. Cherin, P., S. Pelletier, et al. (2002). "Intravenous immunoglobulin for dysphagia of inclusion body myositis." Neurology **58**(2): 326.

44. Chiang, P. M., J. Ling, et al. (2010). "Deletion of TDP-43 down-regulates Tbc1d1, a gene linked to obesity, and alters body fat metabolism." Proceedings of the National Academy of Sciences of the United States of America **107**(37): 16320-16324.

45. Choi, J., M. L. Costa, et al. (1990). "MyoD converts primary dermal fibroblasts, chondroblasts, smooth muscle, and retinal pigmented epithelial cells into striated mononucleated myoblasts and multinucleated myotubes." Proceedings of the National Academy of Sciences of the United States of America **87**(20): 7988-7992.

46. Chou, S. M. (1986). "Inclusion body myositis: a chronic persistent mumps myositis?" Human pathology **17**(8): 765-777.

47. Civatte, M., C. Bartoli, et al. (2005). "Expression of the beta chemokines CCL3, CCL4, CCL5 and their receptors in idiopathic inflammatory myopathies." Neuropathology and applied neurobiology **31**(1): 70-79.

48. Colombrita, C., E. Zennaro, et al. (2009). "TDP-43 is recruited to stress granules in conditions of oxidative insult." Journal of neurochemistry **111**(4): 1051-1061.

49. Confalonieri, P., P. Bernasconi, et al. (2000). "Increased expression of beta-chemokines in muscle of patients with inflammatory myopathies." Journal of neuropathology and experimental neurology **59**(2): 164-169.

50. Corbett, E. F. and M. Michalak (2000). "Calcium, a signaling molecule in the endoplasmic reticulum?" Trends in biochemical sciences **25**(7): 307-311.

51. Cornelison, D. D. and B. J. Wold (1997). "Single-cell analysis of regulatory gene expression in quiescent and activated mouse skeletal muscle satellite cells." Developmental biology **191**(2): 270-283.

52. Cortese, A., P. Machado, et al. (2013). "Longitudinal observational study of sporadic inclusion body myositis: implications for clinical trials." Neuromuscular disorders : NMD **23**(5): 404-412.

53. Cossu, G., B. Zani, et al. (1980). "In vitro differentiation of satellite cells isolated from normal and dystrophic mammalian muscles. A comparison with embryonic myogenic cells." Cell differentiation **9**(6): 357-368.

54. Covault, J. and J. R. Sanes (1986). "Distribution of N-CAM in synaptic and extrasynaptic portions of developing and adult skeletal muscle." The Journal of cell biology **102**(3): 716-730.

55. Cox, F. M., M. Reijnierse, et al. (2011). "Magnetic resonance imaging of skeletal muscles in sporadic inclusion body myositis." Rheumatology **50**(6): 1153-1161.

56. Cox, F. M., M. J. Titulaer, et al. (2011). "A 12-year follow-up in sporadic inclusion body myositis: an end stage with major disabilities." Brain : a journal of neurology **134**(Pt 11): 3167-3175.

57. Cudkowicz, M. E., J. M. Shefner, et al. (2008). "Arimoclomol at dosages up to 300 mg/day is well tolerated and safe in amyotrophic lateral sclerosis." Muscle & nerve **38**(1): 837-844.

58. Cupler, E. J., M. Leon-Monzon, et al. (1996). "Inclusion body myositis in HIV-1 and HTLV-1 infected patients." Brain : a journal of neurology **119 (Pt 6)**: 1887-1893.

59. Cushman, M., B. S. Johnson, et al. (2010). "Prion-like disorders: blurring the divide between transmissibility and infectivity." Journal of cell science **123**(Pt 8): 1191-1201.

60. Custer, S. K., M. Neumann, et al. (2010). "Transgenic mice expressing mutant forms VCP/p97 recapitulate the full spectrum of IBMPFD including degeneration in muscle, brain and bone." Human molecular genetics **19**(9): 1741-1755.

61. CytRxCorp (2009). CytRxCorp and UCL Biomedical Research Unit - Arimoclomol Investigational Medicinal Product Dossier Version 1.0 (Confidential unpublished document). London, UCL**:** 114.

62. Dalakas, M. C. (2006). "Inflammatory, immune, and viral aspects of inclusion-body myositis." Neurology **66**(2 Suppl 1): S33-38.

63. Dalakas, M. C. (2006). "Sporadic inclusion body myositis--diagnosis, pathogenesis and therapeutic strategies." Nature clinical practice. Neurology **2**(8): 437-447.

64. Dalakas, M. C., B. Koffman, et al. (2001). "A controlled study of intravenous immunoglobulin combined with prednisone in the treatment of IBM." Neurology **56**(3): 323-327.

65. Dalakas, M. C., G. Rakocevic, et al. (2009). "Effect of Alemtuzumab (CAMPATH 1-H) in patients with inclusion-body myositis." Brain : a journal of neurology **132**(Pt 6): 1536-1544.

66. Dalakas, M. C., G. Rakocevic, et al. (2007). "Inclusion body myositis with human immunodeficiency virus infection: four cases with clonal expansion of viral-specific T cells." Annals of neurology **61**(5): 466-475.

67. Dalakas, M. C., B. Sonies, et al. (1997). "Treatment of inclusion-body myositis with IVIg: a double-blind, placebo-controlled study." Neurology **48**(3): 712-716.

68. De Bleecker, J. L., B. De Paepe, et al. (2002). "Differential expression of chemokines in inflammatory myopathies." Neurology **58**(12): 1779-1785.

69. De Bleecker, J. L., V. I. Meire, et al. (1999). "Immunolocalization of tumor necrosis factor-alpha and its receptors in inflammatory myopathies." Neuromuscular disorders : NMD **9**(4): 239-246.

70. De Paepe, B., K. K. Creus, et al. (2007). "Chemokine profile of different inflammatory myopathies reflects humoral versus cytotoxic immune responses." Annals of the New York Academy of Sciences **1109**: 441-453.

71. De Paepe, B., K. K. Creus, et al. (2009). "Role of cytokines and chemokines in idiopathic inflammatory myopathies." Current opinion in rheumatology **21**(6): 610-616.

72. De Paepe, B., K. K. Creus, et al. (2012). "Upregulation of chemokines and their receptors in Duchenne muscular dystrophy: potential for attenuation of myofiber necrosis." Muscle & nerve **46**(6): 917-925.

73. Decary, S., V. Mouly, et al. (1997). "Replicative potential and telomere length in human skeletal muscle: implications for satellite cell-mediated gene therapy." Human gene therapy **8**(12): 1429-1438.

74. DiFiglia, M., E. Sapp, et al. (1997). "Aggregation of huntingtin in neuronal intranuclear inclusions and dystrophic neurites in brain." Science **277**(5334): 1990-1993.

75. Ding, X. Z., C. M. Fernandez-Prada, et al. (2001). "Over-expression of hsp-70 inhibits bacterial lipopolysaccharide-induced production of cytokines in human monocyte-derived macrophages." Cytokine **16**(6): 210-219.

76. Dion, E., P. Cherin, et al. (2002). "Magnetic resonance imaging criteria for distinguishing between inclusion body myositis and polymyositis." The Journal of rheumatology **29**(9): 1897-1906.

77. Dodd, S. L., B. Hain, et al. (2009). "Hsp27 inhibits IKKbeta-induced NF-kappaB activity and skeletal muscle atrophy." FASEB journal : official

publication of the Federation of American Societies for Experimental Biology **23**(10): 3415-3423.

78. Dul, J. L., D. P. Davis, et al. (2001). "Hsp70 and antifibrillogenic peptides promote degradation and inhibit intracellular aggregation of amyloidogenic light chains." The Journal of cell biology **152**(4): 705-716.

79. Evans, C. G., S. Wisen, et al. (2006). "Heat shock proteins 70 and 90 inhibit early stages of amyloid beta-(1-42) aggregation in vitro." The Journal of biological chemistry **281**(44): 33182-33191.

80. Feinstein, D. L., E. Galea, et al. (1996). "Heat shock protein 70 suppresses astroglial-inducible nitric-oxide synthase expression by decreasing NFkappaB activation." The Journal of biological chemistry **271**(30): 17724-17732.

81. Feinstein, D. L., E. Galea, et al. (1997). "Suppression of glial nitric oxide synthase induction by heat shock: effects on proteolytic degradation of IkappaB-alpha." Nitric oxide : biology and chemistry / official journal of the Nitric Oxide Society **1**(2): 167-176.

82. Feldmann, M., E. Andreakos, et al. (2002). "Is NF-kappaB a useful therapeutic target in rheumatoid arthritis?" Annals of the rheumatic diseases **61 Suppl 2**: ii13-18.

83. Felice, K. J. and W. A. North (2001). "Inclusion body myositis in Connecticut: observations in 35 patients during an 8-year period." Medicine **80**(5): 320-327.

84. Fratta, P., W. K. Engel, et al. (2005). "Proteasome inhibition and aggresome formation in sporadic inclusion-body myositis and in amyloid-beta precursor protein-overexpressing cultured human muscle fibers." The American journal of pathology **167**(2): 517-526.

85. FSH-DY-Group (1997). "A prospective, quantitative study of the natural history of facioscapulohumeral muscular dystrophy (FSHD): implications for therapeutic trials. The FSH-DY Group." Neurology **48**(1): 38-46.

86. Fulda, S., A. M. Gorman, et al. (2010). "Cellular stress responses: cell survival and cell death." International journal of cell biology **2010**: 214074.

87. Garcia, J. (2000). "MRI in inflammatory myopathies." Skeletal radiology **29**(8): 425-438.

88. Garlepp, M. J., H. Tabarias, et al. (1995). "Apolipoprotein E epsilon 4 in inclusion body myositis." Annals of neurology **38**(6): 957-959.

89. Ghribi, O., M. M. Herman, et al. (2001). "Abeta(1-42) and aluminum induce stress in the endoplasmic reticulum in rabbit hippocampus, involving nuclear translocation of gadd 153 and NF-kappaB." Brain research. Molecular brain research **96**(1-2): 30-38.

90. Gibson, M. C. and E. Schultz (1983). "Age-related differences in absolute numbers of skeletal muscle satellite cells." Muscle & nerve **6**(8): 574-580.

91. Gifondorwa, D. J., M. B. Robinson, et al. (2007). "Exogenous delivery of heat shock protein 70 increases lifespan in a mouse model of amyotrophic lateral sclerosis." The Journal of neuroscience : the official journal of the Society for Neuroscience **27**(48): 13173-13180.

92. Giordana, M. T., M. Piccinini, et al. (2010). "TDP-43 redistribution is an early event in sporadic amyotrophic lateral sclerosis." Brain pathology **20**(2): 351-360.

93. Glover, G. H. and E. Schneider (1991). "Three-point Dixon technique for true water/fat decomposition with B0 inhomogeneity correction." Magnetic resonance in medicine : official journal of the Society of Magnetic Resonance in Medicine / Society of Magnetic Resonance in Medicine **18**(2): 371-383.

94. Goldgaber, D., H. W. Harris, et al. (1989). "Interleukin 1 regulates synthesis of amyloid beta-protein precursor mRNA in human endothelial cells." Proceedings of the National Academy of Sciences of the United States of America **86**(19): 7606-7610.

95. Greenberg, S. A. (2009). "How citation distortions create unfounded authority: analysis of a citation network." BMJ **339**: b2680.

96. Greenberg, S. A., E. M. Bradshaw, et al. (2005). "Plasma cells in muscle in inclusion body myositis and polymyositis." Neurology **65**(11): 1782-1787.

97. Greenberg, S. A., G. S. Pinkus, et al. (2007). "Myeloid dendritic cells in inclusion-body myositis and polymyositis." Muscle & nerve **35**(1): 17-23.

98. Greenberg, S. A., J. L. Pinkus, et al. (2006). "Nuclear membrane proteins are present within rimmed vacuoles in inclusion-body myositis." Muscle & nerve **34**(4): 406-416.

99. Gregory, J. M., T. P. Barros, et al. (2012). "The aggregation and neurotoxicity of TDP-43 and its ALS-associated 25 kDa fragment are differentially affected by molecular chaperones in Drosophila." PloS one **7**(2): e31899.

100. Griggs, R. C., V. Askanas, et al. (1995). "Inclusion body myositis and myopathies." Annals of neurology **38**(5): 705-713.

101. Grilli, M., F. Goffi, et al. (1996). "Interleukin-1beta and glutamate activate the NF-kappaB/Rel binding site from the regulatory region of the amyloid precursor protein gene in primary neuronal cultures." The Journal of biological chemistry **271**(25): 15002-15007.

102. Hammadi, M., A. Oulidi, et al. (2013). "Modulation of ER stress and apoptosis by endoplasmic reticulum calcium leak via translocon during unfolded protein response: involvement of GRP78." FASEB journal : official publication of the Federation of American Societies for Experimental Biology **27**(4): 1600-1609.

103. Hardiman, O., L. H. van den Berg, et al. (2011). "Clinical diagnosis and management of amyotrophic lateral sclerosis." Nature reviews. Neurology **7**(11): 639-649.

104. Hawke, T. J. and D. J. Garry (2001). "Myogenic satellite cells: physiology to molecular biology." Journal of applied physiology **91**(2): 534-551.

105. Hayashi, Y., Y. Sawa, et al. (2002). "Preoperative glutamine administration induces heat-shock protein 70 expression and attenuates cardiopulmonary bypass-induced inflammatory response by regulating nitric oxide synthase activity." Circulation **106**(20): 2601-2607.

106. Herman, A. M., P. J. Khandelwal, et al. (2012). "Wild type TDP-43 induces neuro-inflammation and alters APP metabolism in lentiviral gene transfer models." Experimental neurology **235**(1): 297-305.

107. Hilton-Jones, D., A. Miller, et al. (2010). "Inclusion body myositis: MRC Centre for Neuromuscular Diseases, IBM workshop, London, 13 June 2008." Neuromuscular disorders : NMD **20**(2): 142-147.

108. Honda, H. and A. Rostami (1989). "Expression of major histocompatibility complex class I antigens in rat muscle cultures: the possible developmental role in myogenesis." Proceedings of the National Academy of Sciences of the United States of America **86**(18): 7007-7011.

109. Husmann, I., L. Soulet, et al. (1996). "Growth factors in skeletal muscle regeneration." Cytokine & growth factor reviews **7**(3): 249-258.

110. Hussain, S. G. and K. V. Ramaiah (2007). "Reduced eIF2alpha phosphorylation and increased proapoptotic proteins in aging." Biochemical and biophysical research communications **355**(2): 365-370.

111. Ieronimakis, N., G. Balasundaram, et al. (2010). "Absence of CD34 on murine skeletal muscle satellite cells marks a reversible state of activation during acute injury." PloS one **5**(6): e10920.

112. Igaz, L. M., L. K. Kwong, et al. (2011). "Dysregulation of the ALS-associated gene TDP-43 leads to neuronal death and degeneration in mice." The Journal of clinical investigation **121**(2): 726-738.

113. Jackman, R. W. and S. C. Kandarian (2004). "The molecular basis of skeletal muscle atrophy." American journal of physiology. Cell physiology **287**(4): C834-843.

114. Jackson, C. E., R. J. Barohn, et al. (2008). "Inclusion body myositis functional rating scale: a reliable and valid measure of disease severity." Muscle & nerve **37**(4): 473-476.

115. Jain, M., M. Smith, et al. (2006). "Intra-rater and inter-rater reliability of the 10-point Manual Muscle Test (MMT) of strength in children with juvenile idiopathic inflammatory myopathies (JIIM)." Physical & occupational therapy in pediatrics **26**(3): 5-17.

116. Janssens, J. and C. Van Broeckhoven (2013). "Pathological mechanisms underlying TDP-43 driven neurodegeneration in FTLD-ALS spectrum disorders." Human molecular genetics **22**(R1): R77-87.

117. Joffe, M. M., L. A. Love, et al. (1993). "Drug therapy of the idiopathic inflammatory myopathies: predictors of response to prednisone, azathioprine, and methotrexate and a comparison of their efficacy." The American journal of medicine **94**(4): 379-387.

118. Johnson, B. S., D. Snead, et al. (2009). "TDP-43 is intrinsically aggregation-prone, and amyotrophic lateral sclerosis-linked mutations accelerate aggregation and increase toxicity." The Journal of biological chemistry **284**(30): 20329-20339.

119. Johnston, J. A., C. L. Ward, et al. (1998). "Aggresomes: a cellular response to misfolded proteins." The Journal of cell biology **143**(7): 1883-1898.

120. Kadi, F., N. Charifi, et al. (2006). "The number of satellite cells in slow and fast fibres from human vastus lateralis muscle." Histochemistry and cell biology **126**(1): 83-87.

121. Kalmar, B. and L. Greensmith (2009). "Activation of the heat shock response in a primary cellular model of motoneuron neurodegeneration-evidence for neuroprotective and neurotoxic effects." Cellular & molecular biology letters **14**(2): 319-335.

122. Kalmar, B., C. H. Lu, et al. (2014). "The role of heat shock proteins in Amyotrophic Lateral Sclerosis: The therapeutic potential of Arimoclomol." Pharmacology & therapeutics **141**(1): 40-54.

123. Kampman, M. T., S. L. Benestad, et al. (1999). "Denervation enhances spontaneous inflammatory myopathy in SJL mice." Muscle & nerve **22**(7): 883-888.

124. Kaspers, G. J., J. J. Wijnands, et al. (2005). "Immunophenotypic cell lineage and in vitro cellular drug resistance in childhood relapsed acute lymphoblastic leukaemia." European journal of cancer **41**(9): 1300-1303.

125. Kaufman, R. J. (1999). "Stress signaling from the lumen of the endoplasmic reticulum: coordination of gene transcriptional and translational controls." Genes & development **13**(10): 1211-1233.

126. Kieran, D., B. Kalmar, et al. (2004). "Treatment with arimoclomol, a coinducer of heat shock proteins, delays disease progression in ALS mice." Nature medicine **10**(4): 402-405.

127. Kim, I., W. Xu, et al. (2008). "Cell death and endoplasmic reticulum stress: disease relevance and therapeutic opportunities." Nature reviews. Drug discovery **7**(12): 1013-1030.

128. Kimonis, V. E., M. J. Kovach, et al. (2000). "Clinical and molecular studies in a unique family with autosomal dominant limb-girdle muscular dystrophy and Paget disease of bone." Genetics in medicine : official journal of the American College of Medical Genetics **2**(4): 232-241.

129. Kissel, J. T., M. P. McDermott, et al. (1998). "Pilot trial of albuterol in facioscapulohumeral muscular dystrophy. FSH-DY Group." Neurology **50**(5): 1402-1406.

130. Kitazawa, M., K. N. Green, et al. (2006). "Genetically augmenting Abeta42 levels in skeletal muscle exacerbates inclusion body myositis-like pathology and motor deficits in transgenic mice." The American journal of pathology **168**(6): 1986-1997.

131. Kitazawa, M., S. Oddo, et al. (2005). "Lipopolysaccharide-induced inflammation exacerbates tau pathology by a cyclin-dependent kinase 5-mediated pathway in a transgenic model of Alzheimer's disease." The Journal of neuroscience : the official journal of the Society for Neuroscience **25**(39): 8843-8853.

132. Koffman, B. M., K. Sivakumar, et al. (1998). "HLA allele distribution distinguishes sporadic inclusion body myositis from hereditary inclusion body myopathies." Journal of neuroimmunology **84**(2): 139-142.

133. Koistinen, H., R. Prinjha, et al. (2006). "Elevated levels of amyloid precursor protein in muscle of patients with amyotrophic lateral sclerosis and a mouse model of the disease." Muscle & nerve **34**(4): 444-450.

134. Kovach, M. J., B. Waggoner, et al. (2001). "Clinical delineation and localization to chromosome 9p13.3-p12 of a unique dominant disorder in four families: hereditary inclusion body myopathy, Paget disease of bone, and frontotemporal dementia." Molecular genetics and metabolism **74**(4): 458-475.

135. Kuang, S., K. Kuroda, et al. (2007). "Asymmetric self-renewal and commitment of satellite stem cells in muscle." Cell **129**(5): 999-1010.

136. LaFerla, F. M., K. N. Green, et al. (2007). "Intracellular amyloid-beta in Alzheimer's disease." Nature reviews. Neuroscience **8**(7): 499-509.

137. Larman, H. B., M. Salajegheh, et al. (2013). "Cytosolic 5'-nucleotidase 1A autoimmunity in sporadic inclusion body myositis." Annals of neurology **73**(3): 408-418.

138. Layzer, R., H. S. Lee, et al. (2009). "Dermatomyositis with inclusion body myositis pathology." Muscle & nerve **40**(3): 469-471.

139. Le Grand, F. and M. A. Rudnicki (2007). "Skeletal muscle satellite cells and adult myogenesis." Current opinion in cell biology **19**(6): 628-633.

140. Le Moigne, A., I. Martelly, et al. (1990). "Characterization of myogenesis from adult satellite cells cultured in vitro." The International journal of developmental biology **34**(1): 171-180.

141. Lee do, Y., K. S. Lee, et al. (2010). "Activation of PERK signaling attenuates Abeta-mediated ER stress." PloS one **5**(5): e10489.

142. Lee, E. B., V. M. Lee, et al. (2012). "Gains or losses: molecular mechanisms of TDP43-mediated neurodegeneration." Nature reviews. Neuroscience **13**(1): 38-50.

143. Lee, J. E., Y. J. Kim, et al. (2004). "The 70 kDa heat shock protein suppresses matrix metalloproteinases in astrocytes." Neuroreport **15**(3): 499-502.

144. Leff, R. L., F. W. Miller, et al. (1993). "The treatment of inclusion body myositis: a retrospective review and a randomized, prospective trial of immunosuppressive therapy." Medicine **72**(4): 225-235.

145. Li, C. K., P. Knopp, et al. (2009). "Overexpression of MHC class I heavy chain protein in young skeletal muscle leads to severe myositis: implications for juvenile myositis." The American journal of pathology **175**(3): 1030-1040.

146. Li, Y., P. Ray, et al. (2010). "A Drosophila model for TDP-43 proteinopathy." Proceedings of the National Academy of Sciences of the United States of America **107**(7): 3169-3174.

147. Lienhard, K., S. P. Lauermann, et al. (2013). "Validity and reliability of isometric, isokinetic and isoinertial modalities for the assessment of quadriceps muscle strength in patients with total knee arthroplasty." Journal of electromyography and kinesiology : official journal of the International Society of Electrophysiological Kinesiology **23**(6): 1283-1288.

148. Lindberg, C., E. Trysberg, et al. (2003). "Anti-T-lymphocyte globulin treatment in inclusion body myositis: a randomized pilot study." Neurology **61**(2): 260-262.

149. Lindquist, S. and E. A. Craig (1988). "The heat-shock proteins." Annual review of genetics **22**: 631-677.

150. Liu, J., L. A. Shinobu, et al. (2005). "Elevation of the Hsp70 chaperone does not effect toxicity in mouse models of familial amyotrophic lateral sclerosis." Journal of neurochemistry **93**(4): 875-882.

151. Liu, Y. and A. Chang (2008). "Heat shock response relieves ER stress." The EMBO journal **27**(7): 1049-1059.

152. Lodi, R., D. J. Taylor, et al. (1998). "Normal in vivo skeletal muscle oxidative metabolism in sporadic inclusion body myositis assessed by 31P-magnetic resonance spectroscopy." Brain : a journal of neurology **121 (Pt 11)**: 2119-2126.

153. Lotz, B. P., A. G. Engel, et al. (1989). "Inclusion body myositis. Observations in 40 patients." Brain : a journal of neurology **112 (Pt 3)**: 727-747.

154. Lundberg, I., A. K. Ulfgren, et al. (1997). "Cytokine production in muscle tissue of patients with idiopathic inflammatory myopathies." Arthritis and rheumatism **40**(5): 865-874.

155. Lunemann, J. D., J. Schmidt, et al. (2007). "Macroautophagy as a pathomechanism in sporadic inclusion body myositis." Autophagy **3**(4): 384-386.

156. Machado, P., A. Miller, et al. (2009). "Sporadic inclusion body myositis: an unsolved mystery." Acta reumatologica portuguesa **34**(2A): 161-182.

157. Machado, P. M., M. Ahmed, et al. (2014). "Ongoing developments in sporadic inclusion body myositis." Current rheumatology reports **16**(12): 477.

158. Mackey, A. L., M. Kjaer, et al. (2009). "Assessment of satellite cell number and activity status in human skeletal muscle biopsies." Muscle & nerve **40**(3): 455-465.

159. Maehlen, J., I. Nennesmo, et al. (1989). "Peripheral nerve injury causes transient expression of MHC class I antigens in rat motor neurons and skeletal muscles." Brain research **481**(2): 368-372.

160. Malicdan, M. C., S. Noguchi, et al. (2007). "Perspectives on distal myopathy with rimmed vacuoles or hereditary inclusion body myopathy: contributions from an animal model. Lack of sialic acid, a central determinant in sugar chains, causes myopathy?" Acta myologica : myopathies and cardiomyopathies : official journal of the Mediterranean Society of Myology / edited by the Gaetano Conte Academy for the study of striated muscle diseases **26**(3): 171-175.

161. Malik, B., N. Nirmalananthan, et al. (2013). "Co-induction of the heat shock response ameliorates disease progression in a mouse model of human spinal and bulbar muscular atrophy: implications for therapy." Brain : a journal of neurology **136**(Pt 3): 926-943.

162. Maravall, M., Z. F. Mainen, et al. (2000). "Estimating intracellular calcium concentrations and buffering without wavelength ratioing." Biophysical journal **78**(5): 2655-2667.

163. Marciniak, S. J., C. Y. Yun, et al. (2004). "CHOP induces death by promoting protein synthesis and oxidation in the stressed endoplasmic reticulum." Genes & development **18**(24): 3066-3077.

164. Martins, S. M., D. J. Frosoni, et al. (2006). "Formation of soluble oligomers and amyloid fibrils with physical properties of the scrapie isoform of the prion protein from the C-terminal domain of recombinant murine prion protein mPrP-(121-231)." The Journal of biological chemistry **281**(36): 26121-26128.

165. Mau, M., N. Oksbjerg, et al. (2008). "Establishment and conditions for growth and differentiation of a myoblast cell line derived from the semimembranosus muscle of newborn piglets." In vitro cellular & developmental biology. Animal **44**(1-2): 1-5.

166. Mauro, A. (1961). "Satellite cell of skeletal muscle fibers." The Journal of biophysical and biochemical cytology **9**: 493-495.

167. McDonald, K. K., A. Aulas, et al. (2011). "TAR DNA-binding protein 43 (TDP-43) regulates stress granule dynamics via differential regulation of G3BP and TIA-1." Human molecular genetics **20**(7): 1400-1410.

168. Mendell, J. R., Z. Sahenk, et al. (1991). "Amyloid filaments in inclusion body myositis. Novel findings provide insight into nature of filaments." Archives of neurology **48**(12): 1229-1234.

169. Messina, S., A. Bitto, et al. (2006). "Nuclear factor kappa-B blockade reduces skeletal muscle degeneration and enhances muscle function in Mdx mice." Experimental neurology **198**(1): 234-241.

170. Messina, S., G. L. Vita, et al. (2011). "Activation of NF-kappaB pathway in Duchenne muscular dystrophy: relation to age." Acta myologica : myopathies and cardiomyopathies : official journal of the Mediterranean Society of Myology / edited by the Gaetano Conte Academy for the study of striated muscle diseases **30**(1): 16-23.

171. Meusser, B., C. Hirsch, et al. (2005). "ERAD: the long road to destruction." Nature cell biology **7**(8): 766-772.

172. Mhiri, C. and R. Gherardi (1990). "Inclusion body myositis in French patients. A clinicopathological evaluation." Neuropathology and applied neurobiology **16**(4): 333-344.

173. Michaelis, D., N. Goebels, et al. (1993). "Constitutive and cytokine-induced expression of human leukocyte antigens and cell adhesion molecules by human myotubes." The American journal of pathology **143**(4): 1142-1149.

174. Michalak, M., J. M. Robert Parker, et al. (2002). "Ca2+ signaling and calcium binding chaperones of the endoplasmic reticulum." Cell calcium **32**(5-6): 269-278.

175. Mikol, J., A. Felten-Papaiconomou, et al. (1982). "Inclusion-body myositis: clinicopathological studies and isolation of an adenovirus type 2 from muscle biopsy specimen." Annals of neurology **11**(6): 576-581.

176. Millay, D. P., M. A. Sargent, et al. (2008). "Genetic and pharmacologic inhibition of mitochondrial-dependent necrosis attenuates muscular dystrophy." Nature medicine **14**(4): 442-447.

177. Miller, Z. A., K. P. Rankin, et al. (2013). "TDP-43 frontotemporal lobar degeneration and autoimmune disease." Journal of neurology, neurosurgery, and psychiatry **84**(9): 956-962.

178. Minta, A., J. P. Kao, et al. (1989). "Fluorescent indicators for cytosolic calcium based on rhodamine and fluorescein chromophores." The Journal of biological chemistry **264**(14): 8171-8178.

179. Moisse, K., J. Mepham, et al. (2009). "Cytosolic TDP-43 expression following axotomy is associated with caspase 3 activation in NFL-/- mice: support for a role for TDP-43 in the physiological response to neuronal injury." Brain research **1296**: 176-186.

180. Molnar, G., M. L. Ho, et al. (1996). "Evidence for multiple satellite cell populations and a non-myogenic cell type that is regulated differently in regenerating and growing skeletal muscle." Tissue & cell **28**(5): 547-556.

181. Momma, K., S. Noguchi, et al. (2012). "Rimmed vacuoles in Becker muscular dystrophy have similar features with inclusion myopathies." PloS one **7**(12): e52002.

182. Morgan, J. E. and T. A. Partridge (2003). "Muscle satellite cells." The international journal of biochemistry & cell biology **35**(8): 1151-1156.

183. Morosetti, R., A. Broccolini, et al. (2010). "Increased aging in primary muscle cultures of sporadic inclusion-body myositis." Neurobiology of aging **31**(7): 1205-1214.

184. Morrow, J. M., C. D. Sinclair, et al. (2014). "Reproducibility, and age, body-weight and gender dependency of candidate skeletal muscle MRI outcome measures in healthy volunteers." European radiology **24**(7): 1610-1620.

185. Morrow, J. S. C. F. A. (2011). "MRI quantification of lower limb muscle fatty atrophy: a potential outcome measure in chronic neuromuscular diseases." J Neurol Neurosurg Psychiatry **83**.

186. Moss, F. P. and C. P. Leblond (1971). "Satellite cells as the source of nuclei in muscles of growing rats." The Anatomical record **170**(4): 421-435.

187. Moussa, C. E., Q. Fu, et al. (2006). "Transgenic expression of beta-APP in fast-twitch skeletal muscle leads to calcium dyshomeostasis and IBM-like pathology." FASEB journal : official publication of the Federation of American Societies for Experimental Biology **20**(12): 2165-2167.

188. Muchowski, P. J. and J. L. Wacker (2005). "Modulation of neurodegeneration by molecular chaperones." Nature reviews. Neuroscience **6**(1): 11-22.

189. Muir, A. R., A. H. Kanji, et al. (1965). "The structure of the satellite cells in skeletal muscle." Journal of anatomy **99**(Pt 3): 435-444.

190. Muntzing, K., C. Lindberg, et al. (2003). "Inclusion body myositis: clonal expansions of muscle-infiltrating T cells persist over time." Scandinavian journal of immunology **58**(2): 195-200.

191. Murata, K. and M. C. Dalakas (1999). "Expression of the costimulatory molecule BB-1, the ligands CTLA-4 and CD28, and their mRNA in inflammatory myopathies." The American journal of pathology **155**(2): 453-460.

192. MuscleStudyGroup (2001). "Randomized pilot trial of betaINF1a (Avonex) in patients with inclusion body myositis." Neurology **57**(9): 1566-1570.

193. MuscleStudyGroup (2004). "Randomized pilot trial of high-dose betaINF-1a in patients with inclusion body myositis." Neurology **63**(4): 718-720.

194. Nagaraju, K., L. Casciola-Rosen, et al. (2005). "Activation of the endoplasmic reticulum stress response in autoimmune myositis: potential role in muscle fiber damage and dysfunction." Arthritis and rheumatism **52**(6): 1824-1835.

195. Nagaraju, K., N. Raben, et al. (2000). "Conditional up-regulation of MHC class I in skeletal muscle leads to self-sustaining autoimmune myositis and myositis-specific autoantibodies." Proceedings of the National Academy of Sciences of the United States of America **97**(16): 9209-9214.

196. Naidoo, N., M. Ferber, et al. (2008). "Aging impairs the unfolded protein response to sleep deprivation and leads to proapoptotic signaling." The Journal of neuroscience : the official journal of the Society for Neuroscience **28**(26): 6539-6548.

197. Nanasi, P. P. and A. Jednakovits (2001). "Multilateral in vivo and in vitro protective effects of the novel heat shock protein coinducer, bimoclomol: results of preclinical studies." Cardiovascular drug reviews **19**(2): 133-151.

198. Narhi, L. O., J. Schmit, et al. (2012). "Classification of protein aggregates." Journal of pharmaceutical sciences **101**(2): 493-498.

199. Nogalska, A., W. K. Engel, et al. (2010). "Increased BACE1 mRNA and noncoding BACE1-antisense transcript in sporadic inclusion-body myositis muscle fibers--possibly caused by endoplasmic reticulum stress." Neuroscience letters **474**(3): 140-143.

200. Nogalska, A., C. Terracciano, et al. (2009). "p62/SQSTM1 is overexpressed and prominently accumulated in inclusions of sporadic inclusion-body myositis muscle fibers, and can help differentiating it from polymyositis and dermatomyositis." Acta neuropathologica **118**(3): 407-413.

201. Nogalska, A., S. Wojcik, et al. (2007). "Endoplasmic reticulum stress induces myostatin precursor protein and NF-kappaB in cultured human muscle fibers: relevance to inclusion body myositis." Experimental neurology **204**(2): 610-618.

202. Nonaka, T., M. Masuda-Suzukake, et al. (2013). "Prion-like properties of pathological TDP-43 aggregates from diseased brains." Cell reports **4**(1): 124-134.

203. Nuss, J. E., K. B. Choksi, et al. (2008). "Decreased enzyme activities of chaperones PDI and BiP in aged mouse livers." Biochemical and biophysical research communications **365**(2): 355-361.

204. Oddo, S., A. Caccamo, et al. (2008). "Blocking Abeta42 accumulation delays the onset and progression of tau pathology via the C terminus of heat shock protein70-interacting protein: a mechanistic link between Abeta and tau pathology." The Journal of neuroscience : the official journal of the Society for Neuroscience **28**(47): 12163-12175.

205. Oldfors, A., N. G. Larsson, et al. (1993). "Mitochondrial DNA deletions in inclusion body myositis." Brain : a journal of neurology **116 (Pt 2)**: 325-336.

206. Oldfors, A., A. R. Moslemi, et al. (2006). "Mitochondrial abnormalities in inclusion-body myositis." Neurology **66**(2 Suppl 1): S49-55.

207. Olive, M., A. Janue, et al. (2009). "TAR DNA-Binding protein 43 accumulation in protein aggregate myopathies." Journal of neuropathology and experimental neurology **68**(3): 262-273.

208. Ozden, S., A. Gessain, et al. (2001). "Sporadic inclusion body myositis in a patient with human T cell leukemia virus type 1-associated myelopathy." Clinical infectious diseases : an official publication of the Infectious Diseases Society of America **32**(3): 510-514.

209. Paradas, C., C. Marquez, et al. (2005). "X-linked Emery-Dreifuss muscular dystrophy and vacuoles: an immunohistochemical characterization." Muscle & nerve **32**(1): 61-65.

210. Parfitt, D. A., M. Aguila, et al. (2014). "The heat-shock response co-inducer arimoclomol protects against retinal degeneration in rhodopsin retinitis pigmentosa." Cell death & disease **5**: e1236.

211. Park, Y. G., J. H. Moon, et al. (2006). "A comparative study of magnetic-activated cell sorting, cytotoxicity and preplating for the purification of human myoblasts." Yonsei medical journal **47**(2): 179-183.

212. Parker, K. C., S. W. Kong, et al. (2009). "Fast-twitch sarcomeric and glycolytic enzyme protein loss in inclusion body myositis." Muscle & nerve **39**(6): 739-753.

213. Paz Gavilan, M., J. Vela, et al. (2006). "Cellular environment facilitates protein accumulation in aged rat hippocampus." Neurobiology of aging **27**(7): 973-982.

214. Perez, C. A., R. F. Margolskee, et al. (2003). "Making sense with TRP channels: store-operated calcium entry and the ion channel Trpm5 in taste receptor cells." Cell calcium **33**(5-6): 541-549.

215. Phillips, B. A., L. A. Cala, et al. (2001). "Patterns of muscle involvement in inclusion body myositis: clinical and magnetic resonance imaging study." Muscle & nerve **24**(11): 1526-1534.

216. Phillips, B. A., P. J. Zilko, et al. (2000). "Prevalence of sporadic inclusion body myositis in Western Australia." Muscle & nerve **23**(6): 970-972.

217. Polesskaya, A., P. Seale, et al. (2003). "Wnt signaling induces the myogenic specification of resident CD45+ adult stem cells during muscle regeneration." Cell **113**(7): 841-852.

218. Prakriya, M., S. Feske, et al. (2006). "Orai1 is an essential pore subunit of the CRAC channel." Nature **443**(7108): 230-233.

219. Quartuccio, L., G. De Marchi, et al. (2007). "Treatment of inclusion body myositis with cyclosporin-A or tacrolimus: successful long-term management in patients with earlier active disease and concomitant autoimmune features." Clinical and experimental rheumatology **25**(2): 246-251.

220. Raju, R. and M. C. Dalakas (2005). "Gene expression profile in the muscles of patients with inflammatory myopathies: effect of therapy with IVIg and biological validation of clinically relevant genes." Brain : a journal of neurology **128**(Pt 8): 1887-1896.

221. Raju, R., O. Vasconcelos, et al. (2003). "Expression of IFN-gamma-inducible chemokines in inclusion body myositis." Journal of neuroimmunology **141**(1-2): 125-131.

222. Ran, R., A. Lu, et al. (2004). "Hsp70 promotes TNF-mediated apoptosis by binding IKK gamma and impairing NF-kappa B survival signaling." Genes & development **18**(12): 1466-1481.

223. Rehfeldt, C., K. Walther, et al. (2002). "Intrinsic properties of muscle satellite cells are changed in response to long-term selection of mice for different growth traits." Cell and tissue research **310**(3): 339-348.

224. Resende, R., E. Ferreiro, et al. (2008). "ER stress is involved in Abeta-induced GSK-3beta activation and tau phosphorylation." Journal of neuroscience research **86**(9): 2091-2099.

225. Reynaud, E. (2010). "Protein Misfolding and Degenerative Diseases. ." Nature Education **3**.

226. Riedel, M., O. Goldbaum, et al. (2010). "17-AAG induces cytoplasmic alpha-synuclein aggregate clearance by induction of autophagy." PloS one **5**(1): e8753.

227. Romisch, K. (2004). "A cure for traffic jams: small molecule chaperones in the endoplasmic reticulum." Traffic **5**(11): 815-820.

228. Rose, M. R. (2013). "188th ENMC International Workshop: Inclusion Body Myositis, 2-4 December 2011, Naarden, The Netherlands." Neuromuscular disorders : NMD **23**(12): 1044-1055.

229. Roussel, B. D., A. J. Kruppa, et al. (2013). "Endoplasmic reticulum dysfunction in neurological disease." Lancet neurology **12**(1): 105-118.

230. Rutkove, S. B., R. A. Parker, et al. (2002). "A pilot randomized trial of oxandrolone in inclusion body myositis." Neurology **58**(7): 1081-1087.

231. Salajegheh, M., J. L. Pinkus, et al. (2009). "Sarcoplasmic redistribution of nuclear TDP-43 in inclusion body myositis." Muscle & nerve **40**(1): 19-31.

232. Santorelli, F. M., M. Sciacco, et al. (1996). "Multiple mitochondrial DNA deletions in sporadic inclusion body myositis: a study of 56 patients." Annals of neurology **39**(6): 789-795.

233. Schmidt, J., K. Barthel, et al. (2008). "Interrelation of inflammation and APP in sIBM: IL-1 beta induces accumulation of beta-amyloid in skeletal muscle." Brain : a journal of neurology **131**(Pt 5): 1228-1240.

234. Schmidt, J. and M. C. Dalakas (2013). "Inclusion body myositis: from immunopathology and degenerative mechanisms to treatment perspectives." Expert review of clinical immunology **9**(11): 1125-1133.

235. Schmidt, J., G. Rakocevic, et al. (2004). "Upregulated inducible co-stimulator (ICOS) and ICOS-ligand in inclusion body myositis muscle: significance for CD8+ T cell cytotoxicity." Brain : a journal of neurology **127**(Pt 5): 1182-1190.

236. Seale, P., L. A. Sabourin, et al. (2000). "Pax7 is required for the specification of myogenic satellite cells." Cell **102**(6): 777-786.

237. Sekul, E. A., C. Chow, et al. (1997). "Magnetic resonance imaging of the forearm as a diagnostic aid in patients with sporadic inclusion body myositis." Neurology **48**(4): 863-866.

238. Semino-Mora, C. and M. C. Dalakas (1998). "Rimmed vacuoles with beta-amyloid and ubiquitinated filamentous deposits in the muscles of patients with long-standing denervation (postpoliomyelitis muscular atrophy): similarities with inclusion body myositis." Human pathology **29**(10): 1128-1133.

239. Sherman, M. Y. and A. L. Goldberg (2001). "Cellular defenses against unfolded proteins: a cell biologist thinks about neurodegenerative diseases." Neuron **29**(1): 15-32.

240. Shtifman, A., C. W. Ward, et al. (2010). "Amyloid-beta protein impairs Ca2+ release and contractility in skeletal muscle." Neurobiology of aging **31**(12): 2080-2090.

241. Sinclair, C. D., J. M. Morrow, et al. (2012). "Skeletal muscle MRI magnetisation transfer ratio reflects clinical severity in peripheral neuropathies." Journal of neurology, neurosurgery, and psychiatry **83**(1): 29-32.

242. Stadelmann, C., C. Wegner, et al. (2011). "Inflammation, demyelination, and degeneration - recent insights from MS pathology." Biochimica et biophysica acta **1812**(2): 275-282.

243. Stevens, J. C., R. Chia, et al. (2010). "Modification of superoxide dismutase 1 (SOD1) properties by a GFP tag--implications for research into amyotrophic lateral sclerosis (ALS)." PloS one **5**(3): e9541.

244. Stiber, J., A. Hawkins, et al. (2008). "STIM1 signalling controls store-operated calcium entry required for development and contractile function in skeletal muscle." Nature cell biology **10**(6): 688-697.

245. Sugarman, M. C., T. R. Yamasaki, et al. (2002). "Inclusion body myositis-like phenotype induced by transgenic overexpression of beta APP in skeletal muscle." Proceedings of the National Academy of Sciences of the United States of America **99**(9): 6334-6339.

246. Szegezdi, E., S. E. Logue, et al. (2006). "Mediators of endoplasmic reticulum stress-induced apoptosis." EMBO reports **7**(9): 880-885.

247. Takahashi, A., P. Camacho, et al. (1999). "Measurement of intracellular calcium." Physiological reviews **79**(4): 1089-1125.

248. Tawil, R. and R. C. Griggs (2002). "Inclusion body myositis." Current opinion in rheumatology **14**(6): 653-657.

249. Tawil R, H. B., Moxley RT, et al. (1994). " Dual energy x-ray absorptiometry:
quantifying muscle mass in therapeutic trials. ." Annals of neurology **36:320. Abstract.**

250. Temiz, P., C. C. Weihl, et al. (2009). "Inflammatory myopathies with mitochondrial pathology and protein aggregates." Journal of the neurological sciences **278**(1-2): 25-29.

251. Tews, D. S. and H. H. Goebel (1996). "Cytokine expression profile in idiopathic inflammatory myopathies." Journal of neuropathology and experimental neurology **55**(3): 342-347.

252. Tollervey, J. R., T. Curk, et al. (2011). "Characterizing the RNA targets and position-dependent splicing regulation by TDP-43." Nature neuroscience **14**(4): 452-458.

253. Tournadre, A. and P. Miossec (2007). "Cytokine response in inflammatory myopathies." Current rheumatology reports **9**(4): 286-290.

254. Treiman, M., C. Caspersen, et al. (1998). "A tool coming of age: thapsigargin as an inhibitor of sarco-endoplasmic reticulum Ca(2+)-ATPases." Trends in pharmacological sciences **19**(4): 131-135.

255. Troost, D., P. K. Das, et al. (1992). "Immunohistological alterations in muscle of patients with amyotrophic lateral sclerosis: mononuclear cell phenotypes and expression of MHC products." Clinical neuropathology **11**(3): 115-120.

256. Tsai, K. J., C. H. Yang, et al. (2010). "Elevated expression of TDP-43 in the forebrain of mice is sufficient to cause neurological and pathological phenotypes mimicking FTLD-U." The Journal of experimental medicine **207**(8): 1661-1673.

257. Tupling, A. R., A. O. Gramolini, et al. (2004). "HSP70 binds to the fast-twitch skeletal muscle sarco(endo)plasmic reticulum Ca2+ -ATPase (SERCA1a) and prevents thermal inactivation." The Journal of biological chemistry **279**(50): 52382-52389.

258. Turk, M., G. Haaker, et al. (2014). "C9ORF72-ALS: P62- and ubiquitin-aggregation pathology in skeletal muscle." Muscle & nerve **50**(3): 454-455.

259. Udan-Johns, M., R. Bengoechea, et al. (2014). "Prion-like nuclear aggregation of TDP-43 during heat shock is regulated by HSP40/70 chaperones." Human molecular genetics **23**(1): 157-170.

260. Ulianich, L., G. Terrazzano, et al. (2011). "ER stress impairs MHC Class I surface expression and increases susceptibility of thyroid cells to NK-mediated cytotoxicity." Biochimica et biophysica acta **1812**(4): 431-438.

261. Valiyil, R., L. Casciola-Rosen, et al. (2010). "Rituximab therapy for myopathy associated with anti-signal recognition particle antibodies: a case series." Arthritis care & research **62**(9): 1328-1334.

262. van der Pas, J., G. J. Hengstman, et al. (2004). "Diagnostic value of MHC class I staining in idiopathic inflammatory myopathies." Journal of neurology, neurosurgery, and psychiatry **75**(1): 136-139.

263. van Meerloo, J., G. J. Kaspers, et al. (2011). "Cell sensitivity assays: the MTT assay." Methods in molecular biology **731**: 237-245.

264. Vattemi, G., W. K. Engel, et al. (2004). "Endoplasmic reticulum stress and unfolded protein response in inclusion body myositis muscle." The American journal of pathology **164**(1): 1-7.

265. Vattemi, G., W. K. Engel, et al. (2001). "Presence of BACE1 and BACE2 in muscle fibres of patients with sporadic inclusion-body myositis." Lancet **358**(9297): 1962-1964.

266. Vattemi, G., W. K. Engel, et al. (2003). "BACE1 and BACE2 in pathologic and normal human muscle." Experimental neurology **179**(2): 150-158.

267. Verma, A., D. J. Hirsch, et al. (1990). "Inositol trisphosphate and thapsigargin discriminate endoplasmic reticulum stores of calcium in rat brain." Biochemical and biophysical research communications **172**(2): 811-816.

268. Villanova, M., M. Kawai, et al. (1993). "Rimmed vacuoles of inclusion body myositis and oculopharyngeal muscular dystrophy contain amyloid precursor protein and lysosomal markers." Brain research **603**(2): 343-347.

269. Walker, A. K., K. Y. Soo, et al. (2013). "ALS-associated TDP-43 induces endoplasmic reticulum stress, which drives cytoplasmic TDP-43 accumulation and stress granule formation." PloS one **8**(11): e81170.

270. Wallace, D. C. (1992). "Mitochondrial genetics: a paradigm for aging and degenerative diseases?" Science **256**(5057): 628-632.

271. Walsh, D. M. and D. J. Selkoe (2007). "A beta oligomers - a decade of discovery." Journal of neurochemistry **101**(5): 1172-1184.

272. Walter, M. C., H. Lochmuller, et al. (2000). "High-dose immunoglobulin therapy in sporadic inclusion body myositis: a double-blind, placebo-controlled study." Journal of neurology **247**(1): 22-28.

273. Wang, I. F., L. S. Wu, et al. (2008). "TDP-43, the signature protein of FTLD-U, is a neuronal activity-responsive factor." Journal of neurochemistry **105**(3): 797-806.

274. Wattjes, M. P., R. A. Kley, et al. (2010). "Neuromuscular imaging in inherited muscle diseases." European radiology **20**(10): 2447-2460.

275. Watts, G. D., D. Thomasova, et al. (2007). "Novel VCP mutations in inclusion body myopathy associated with Paget disease of bone and frontotemporal dementia." Clinical genetics **72**(5): 420-426.

276. Waza, M., H. Adachi, et al. (2006). "Alleviating neurodegeneration by an anticancer agent: an Hsp90 inhibitor (17-AAG)." Annals of the New York Academy of Sciences **1086**: 21-34.

277. Wedderburn, L. R., H. Varsani, et al. (2007). "International consensus on a proposed score system for muscle biopsy evaluation in patients with juvenile dermatomyositis: a tool for potential use in clinical trials." Arthritis and rheumatism **57**(7): 1192-1201.

278. Weiss, Y. G., A. Maloyan, et al. (2002). "Adenoviral transfer of HSP-70 into pulmonary epithelium ameliorates experimental acute respiratory distress syndrome." The Journal of clinical investigation **110**(6): 801-806.

279. Wetmore, D. R. and K. D. Hardman (1996). "Roles of the propeptide and metal ions in the folding and stability of the catalytic domain of stromelysin (matrix metalloproteinase 3)." Biochemistry **35**(21): 6549-6558.

280. Wilson, F. C., S. R. Ytterberg, et al. (2008). "Epidemiology of sporadic inclusion body myositis and polymyositis in Olmsted County, Minnesota." The Journal of rheumatology **35**(3): 445-447.

281. Winton, M. J., L. M. Igaz, et al. (2008). "Disturbance of nuclear and cytoplasmic TAR DNA-binding protein (TDP-43) induces disease-like redistribution, sequestration, and aggregate formation." The Journal of biological chemistry **283**(19): 13302-13309.

282. Wojcik, S., A. Nogalska, et al. (2008). "Myostatin and its precursor protein are increased in the skeletal muscle of patients with Type-II muscle fibre atrophy." Folia morphologica **67**(1): 6-12.

283. Wojcik, S., A. Nogalska, et al. (2007). "Myostatin precursor protein is increased and associates with amyloid-beta precursor protein in inclusion-body myositis culture model." Neuropathology and applied neurobiology **33**(2): 238-242.

284. Wood, H. (2011). "A hexanucleotide repeat expansion in C9ORF72 links amyotrophic lateral sclerosis and frontotemporal dementia." Nature reviews. Neurology **7**(11): 595.

285. Wu, K. D., D. Bungard, et al. (2001). "Regulation of SERCA Ca2+ pump expression by cytoplasmic Ca2+ in vascular smooth muscle cells." American journal of physiology. Cell physiology **280**(4): C843-851.

286. Yamazaki, H., N. Hiramatsu, et al. (2009). "Activation of the Akt-NF-kappaB pathway by subtilase cytotoxin through the ATF6 branch of the unfolded protein response." Journal of immunology **183**(2): 1480-1487.